

**Isolation and Structural Elucidation of
Bioactive Secondary Metabolites from
Marine Organisms**

**Isolierung und Strukturaufklärung von
bioaktiven Sekundärmetaboliten aus
marinen Organismen**

**Inaugural-Dissertation
zur
Erlangung des Doktorgrades
der Mathematisch-Naturwissenschaftlichen Fakultät
der Heinrich-Heine-Universität Düsseldorf**

**vorgelegt von
Sherif S. E. Elsayed
aus Kairo, Ägypten**

Düsseldorf, 2010

Aus dem Institut für Pharmazeutische Biologie und Biotechnologie
der Heinrich-Heine-Universität Düsseldorf

Gedruckt mit der Genehmigung der
Mathematisch-Naturwissenschaftlichen Fakultät der
Heinrich-Heine-Universität Düsseldorf

Gedruckt mit der Unterstützung der
Kulturabteilung und Studienmission der Botschaft der Arabischen Republik Ägypten

Referent: Prof. Dr. Peter Proksch

Koreferent: Dr. Wim Wätjen

Tag der mündlichen Prüfung: 16.12.2010

Erklärung

Hiermit erkläre ich ehrenwörtlich, dass ich die vorliegende Dissertation mit dem Titel „Isolierung und Strukturaufklärung von bioaktiven Sekundärmetaboliten aus marinen Organismen“ selbst angefertigt habe. Außer den angegebenen Quellen und Hilfsmitteln wurden keine weiteren verwendet. Diese Dissertation wurde weder in gleicher noch in abgewandelter Form in einem anderen Prüfungsverfahren vorgelegt. Weiterhin erkläre ich, dass ich früher weder akademische Grade erworben habe, noch dies versucht habe.

Düsseldorf, den 29.10.2010

Sherif Elsayed

Acknowledgement

First and foremost thanks to the Almighty God “ALLAH” who has granted me all these graces to fulfill this work and blessed me by His power, mercy and patience during my life. To Him I extend my heartfelt thanks.

It is a great pleasure to get this opportunity to express my deepest appreciation and sincere gratitude to Prof. Dr. rer. nat. Peter Proksch for setting an example to what a sincere professor, scientist, and advisor should be. I am deeply grateful to him for giving me this valuable chance to pursue my predoctoral research and for the excellent work facilities at the Institute of Pharmaceutical Biology and Biotechnology, Heinrich-Heine University, Düsseldorf. I would like to express my sincere thanks and gratitude to him for supervising this study, suggesting the research project, his unforgettable support, his direct guidance, his generous considerations, his admirable supervision, his fruitful discussions, and his valuable suggestions in both work and life issues.

I would like to express my cordial thanks and all my regards to Dr. RuAngelie Edrada-Ebel for her constructive advices, NMR courses, her help in NMR data interpretation, supplying the echinoderm specimen as well as for hosting some HR-MS measurement by the facility at Strathclyde Institute of Pharmacy and Biomedical Science, University of Strathclyde, Glasgow, United Kingdom.

My special thanks to Prof. Dr. rer. nat. Werner E. G. Müller and Mrs. Renate Steffen, Institute of Physiological Chemistry and Pathobiochemistry, University of Mainz, for carrying out the cytotoxicity assays, Dr. Laurent Meijer, National Centre for Scientific Research, Biological Station, Roscoff, France, and Dr. Michael Kubbutat, ProQinase GmbH, Freiburg, Germany for conducting the protein kinase inhibition assays.

My deep thanks and gratitude to Prof. Dr. rer. nat. Wim Wätjen, Institute of Toxicology, Heinrich-Heine University, Düsseldorf, for his guidance, conducting cytotoxicity assays and for accepting the co-supervision.

My appreciation to the sincere collaboration of Dr. W. Peters and Mr. P. Behm, Institute of Inorganic and Structure Chemistry, Heinrich-Heine University, Düsseldorf, for conducting 500 MHz NMR measurements, Dr. H. Keck and Dr. P. Tommes, Institute of Inorganic and Structure Chemistry, Heinrich-Heine University, Düsseldorf, for carrying out EI- and FAB-MS experiments, and my cordial thanks to Dr. Victor Wray, Helmholtz Centre for Infection Research, Braunschweig and Mrs. C. Kakoschke for 600 MHz NMR measurements, HR-MS experiments, and his generous help and his fruitful discussions by interpreting NMR data.

Acknowledgement

I would like to extend my deep thanks and gratitude to Dr. Nicole J. de Voogd, National Museum of Natural History, Leiden, Netherlands, for help and support in supplying the three sponge specimens explored in this study.

I would like to express my profound gratitude to my professors and colleagues from the Department of Pharmacognosy and Phytochemistry, Ain-Shams University, Cairo, Egypt, especially Prof. Dr. M. M. Al-Azizi, and Prof. Dr. A. Singab for their guidance, supervision, their continuous encouragement, and their kind advices. To whom I owe so much is Ass. Prof. Dr. N. A. Ayoub, Acting Head of the Department of Pharmacognosy and Phytochemistry, Ain-Shams University, Cairo, Egypt, for her extensive efforts and help to solve the daily problems during my master studies and her guidance and support thereafter.

I would like to extend my thanks to my past and present colleagues and labmates Dr. M. Abdelgawwad, Dr. M. Ashour, Dr. Tu N. Duong, Dr. S. Ortlepp, Dr. T. Hertiani, Dr. A. Hassan, Dr. N. Weber, Dr. A. Debbab, Dr. I. D. Indriani, Dr. A. Hamed, Dr. A. Putz, Dr. M. Bayer, Dr. E. Moustafa, Dr. S. Younes, Dr. A. Diesel, Dr. Y. Wang, Dr. F. Riebe, Dr. J. Kjer, Dr. S. Ruhl, Dr. J. Xu, W. Döring, Y. Zhou, M. ElAmrani, W. Ebrahim, B. Lipowicz, D. Rösberg, A. Marmann, and all the others for the nice multicultural time I spent with them, for their help and assistance whenever I needed it. My deep thanks to my colleagues Mustapha ElAmrani and David Rösberg for their help in writing and revising the German summary in this study.

Special thanks to Mrs. M. Thiel and Mrs. C. Eckelskemper for their administrative help whenever needed, as well as Mrs. K. Rohde, Mrs. W. Schlag, Mrs. S. Miljanovic, Mrs. H. Goldbach-Gecke, and Mrs. K. Friedrich for their kind help in any technical problem encountered during the work.

My profound appreciation to the Egyptian Ministry of Higher Education, Missions Office for the predoctoral fellowship and for the financial support during my stay in Germany.

Last but not least, my gratitude, thankfulness, and my grand indebtedness to my family, my wife Mona, my mother, brothers and sisters for their unfailing love, spiritual support and everlasting prayers.

At the end, my heartily thanks and prayers to my father, who passed away, and I will never forget that he was the first mentor in my life who inspired me how to set my own goals in life and to carry on to reach them. May Almighty ALLAH bless him.

To All of You, Thank You Very Much!

Zusammenfassung

Marine Schwämme sind wegen der Vielfalt an Sekundärmetaboliten eine große Quelle von Naturstoffen. Ein Drittel aller natürlichen Produkte der Meerestiere wurden aus Schwämmen gewonnen. Sie haben sich als wichtige Quelle für neue Verbindungen etabliert (Whitehead, 1999). Darüber hinaus gelten sie auch als eine Quelle für bioaktive Substanzen, ihre Wirkstoffe sind interessante Kandidaten für neue Medikamente, vor allem in den Bereichen: Krebs, anti-inflammatorische, und anti-infektiöse Substanzen so wie Schmerzmittel (Proksch *et al.*, 2002).

Vor kurzem wurden zwei marine Naturstoffe als neue Medikamente eingeführt: Prialt[®] (Wirkstoff: Ziconotid) als potentes Analgetikum gegen schwere chronische Schmerzen und Yondelis[®] (Wirkstoff: Trabectedin [ET-743]) als Antitumor-Mittel zur Behandlung von fortgeschrittenem Weichteilsarkomen. Darüber hinaus befinden sich die Präparate Aplidin[®] (Plitidepsin), Kahalalide F und Zalypsis[®] (Jorumycin-Derivat) in der klinischen Testphase zur Behandlung von soliden Tumoren und hämatologischen Malignomen.

In vielen erfolgreichen Fällen, wie oben gezeigt, haben sich aus marinen Organismen gewonnene Substanzen als pharmazeutisch bedeutend erwiesen, sie haben präklinische oder klinische Phasen der Arzneimittelprüfung zur Behandlung von schweren Krankheiten wie der Alzheimer-Krankheit, Diabetes Typ 2, Krebs und Infektionskrankheiten erreicht, daneben werden schmerzstillende und entzündungshemmende Aktivitäten untersucht.

Daher bestand das Ziel dieser Studie in der Isolierung und Strukturaufklärung von marinen Naturstoffen, entweder bekannt oder bevorzugt neu, in Mengen, die die Durchführung verschiedener Tests zur biologischen Aktivität ermöglichen.

Die Isolierung von Sekundärmetaboliten und die Strukturaufklärung wurden durch wichtige analytische Techniken wie Massenspektrometrie und Kernresonanzspektroskopie durchgeführt. Darüber hinaus wurden die absolute Konfiguration der ausgewählten optisch aktiven Naturstoffe auf der Grundlage der chiralen Derivatisierung mit der Mosher-Analyse bestimmt. Für die Bestimmung der biologischen Aktivität, wurde eine Vielzahl von Tests wie Messung der Zytotoxizität (MTT), Bestimmung der antibakteriellen, antimykotischen, antiviralen Aktivität, Protein-Kinase-Hemmung und antioxidativen Aktivität (DPPH) durchgeführt.

Verschiedene Arten von Meerestieren wurden in dieser Studie untersucht, darunter befinden sich Schwämme, Stachelhäuter und Seegrass, sie wurden aus verschiedenen geografischen Standorten gesammelt, nämlich Indonesien, den Philippinen und Thailand.

Zusammenfassung

1. *Acanthostylotella* sp.

Sechs neue Dibromopyrrolalkaloide wurden aus dem methanolischen Extrakt des indonesischen Schwamms *Acanthostylotella* sp. (Indonesien) isoliert. Dazu gehören die vier neuen Acanthamide (A-D) sowie die Substanzen Methyl-3,4-dibromo-1*H*-pyrrol-2-carboxylat und 3,5-Dibromo-1*H*-pyrrol-2-carbonsäure. Darüber hinaus wurden acht bekannte Dibromopyrrolalkaloide aus demselben Extrakt gewonnen. Unter den isolierten Verbindungen ergab Mukanadin D moderate Zytotoxizität gegen Maus-Lymphom (L5178Y) Zellen. Methyl-3,4-dibromo-1*H*-pyrrol-2-carboxylat zeigte moderate antimikrobielle und antivirale Aktivitäten.

2. *Stylissa massa*

Aus dem methanolischen Auszug des Schwamms *Stylissa massa* (Indonesien) wurden 22 Bromopyrrolalkaloide isoliert, darunter zwei neue natürliche Dibromopyrrolalkaloide, Ethyl-3,4-dibromo-1*H*-pyrrol-2-carboxylat und Dispacamid E. Die isolierten Verbindungen wiesen interessante Bioaktivitätsergebnisse in verschiedenen Bioassays wie z.B. dem Zytotoxizitätsassay (MTT), der Prüfung der antimikrobiellen, antimykotischen und antiviralen Aktivität sowie der In-vitro-Protein-Kinase-hemmenden Wirkung auf.

3. *Jaspis splendens*

Acht Verbindungen wurden durch eine bioaktivitätsgeführte Isolierung (sog. „bioguided isolation“) aus dem in Ethylacetat löslichen Anteil des methanolischen Extraktes von *Jaspis splendens* (Indonesien) gewonnen. Neben drei bekannten Ketosteroiden, einem Derivat des Diketopiperazins Cyclo-L-Pro-L-Tyr und dem Nukleosid-Derivat Sangivamycin wurden zwei neue Jaspamidderivate, zusammen mit der bekannten Verbindung Jaspamid isoliert.

Alle isolierten Verbindungen zeigten starke Zytotoxizität gegen Maus-Lymphom (L5178Y)-Zellen, insbesondere die neuen Jaspamid-Derivate zusammen mit Jaspamid, Cyclo-L-Pro-L-Tyr und Sangivamycin wiesen die höchste Zytotoxizität mit IC₅₀-Werten im Bereich von <0,1 bis 0,28 µg/ml, aufverglichen mit Kahalalid F (IC₅₀ = 6,3 µg/ml) sind dies relativ niedrige Konzentrationsbereiche.

4. *Thalassia testudinum*

Eine genaue chemische Untersuchung des methanolischen Extrakts von *T. testudinum* (Thailand) wurde durchgeführt und führte zur Isolierung von der beiden sulfatierten Flavonoidglycoside, Thalassiolin A und Thalassiolin C. Luteolin-3'-*O*-glucuronid wurde

Zusammenfassung

zum ersten Mal, aus einen marinen Organismen isoliert. Schließlich wurden alle isolierten Flavonglycoside auf ihre antioxidative (DPPH) Aktivität getestet.

5. Comanthus sp.

Eine bioaktivitätsgeführte Fraktionierung des *Comanthus sp.* (Philippinen) – Extraktes wurde durchgeführt. Dies führte zur Isolierung von sechzehn Verbindungen, fünf von ihnen waren Anthrachinone, einer davon ein neuer Naturstoff, fünf weitere sind Naphthopyrone, ein Nukleosid-, 2'-desoxythymidin und fünf steroidale Sekundärmetabolite. Die absolute Konfiguration der beiden optisch aktiven Anthrachinonderivaten Rhodoptilometrin und seinem 6-*O*-Sulfat-Derivat wurde zum ersten Mal durch die Mosher-Analyse vermittelt, und zeigte, dass beide von ihnen (*S*)-(-) Enantiomere sind.

Alle isolierten Verbindungen wurden verschiedenen Tests unterzogen, um Aufschlüsse über die antioxidative (DPPH), zytotoxische (MTT-Assay gegen die Maus-Lymphom-Zell-Linie L5178Y), Protein-Kinasen inhibierende (In-vitro-Untersuchung auf 24 verschiedene Proteinkinasen), antimikrobielle, antimykotische und antivirale Aktivität zu erhalten. Anthrachinone und Naphthopyrone zeigten besondersinteressante Ergebnisse.

Table of Contents

1. Introduction	1
1.1. Significance of the study	1
1.2. The biological importance of marine natural products	2
1.2.1. Antiviral and antitumor marine natural products	2
1.2.2. Protein kinase inhibitory activity of marine natural products	4
1.2.3. Antimalarial marine natural products	4
1.2.4. Anthelmintic activity of marine natural products	5
1.2.5. Reversing multi-drug resistance (MDR) activity	6
1.2.6. Immunosuppressive activity of marine natural products	7
1.3. The importance of marine natural products to the source organism	7
1.3.1. Chemical defense against fouling and spatial competition	7
1.3.2. Chemical defense against predators	7
1.4. The current status of marine natural products to research	8
1.5. Aim of the study	11
2. Material and methods	12
2.1. Marine organism materials	12
2.1.1. Sponges	12
2.1.1.1. <i>Acanthostylotella</i> sp.	13
2.1.1.2. <i>Stylissa massa</i>	14
2.1.1.3. <i>Jaspis splendens</i>	14
2.1.2. Seagrasses	15
2.1.2.1. <i>Thalassia testudinum</i>	15
2.1.3. Echinoderms	15
2.1.3.1. <i>Comanthus</i> sp.	17
2.2. Chemicals	18
2.2.1. General laboratory chemicals	18
2.2.2. Chromatography	18
2.2.2.1. Stationary phases	18
2.2.2.2. Spray reagents	18
2.2.3. Solvents	19
2.2.3.1. General solvents	19
2.2.3.2. Solvents for HPLC	19

Contents

2.2.3.3. Solvents for optical rotation	19
2.2.3.4. Solvents for NMR	20
2.3. Methods	21
2.3.1. Isolation and purification of secondary metabolites	21
2.3.1.1. Isolation of secondary metabolites from <i>Acanthostylotella</i> sp.	21
2.3.1.2. Isolation of secondary metabolites from <i>Stylissa massa</i>	22
2.3.1.3. Isolation of secondary metabolites from <i>Jaspis splendens</i>	23
2.3.1.4. Isolation of secondary metabolites from <i>Thalassia testudinum</i>	23
2.3.1.5. Isolation of secondary metabolites from <i>Comanthus</i> sp.	24
2.3.2. Chromatographic methods	25
2.3.2.1. Thin layer chromatography (TLC)	25
2.3.2.2. Vacuum liquid chromatography (VLC)	25
2.3.2.3. Column chromatography	26
2.3.2.4. Flash chromatography	26
2.3.2.5. Preparative high pressure liquid chromatography (HPLC)	27
2.3.2.6. Semi-preparative high pressure liquid chromatography (HPLC)	27
2.3.2.7. Analytical high pressure liquid chromatography (HPLC)	28
2.3.3. Structure elucidation of the isolated secondary metabolites	28
2.3.3.1. Mass spectrometry	28
2.3.3.1.1. Electrospray ionization mass spectrometry (ESI-MS)	29
2.3.3.1.2. Electron impact mass spectrometry (EI-MS)	29
2.3.3.1.3. Fast atom bombardment mass spectrometry (FAB-MS)	30
2.3.3.1.4. High resolution mass spectrometry (HR-MS)	30
2.3.3.2. Nuclear magnetic resonance spectroscopy (NMR)	30
2.3.3.3. Optical activity	31
2.3.3.4. Determination of absolute stereochemistry by Mosher reaction	32
2.3.4. Testing the biological activity(ies)	32
2.3.4.1. Antimicrobial serial dilution assay	32
2.3.4.2. Cytotoxicity assay	34
2.3.4.2.1. Microculture tetrazolium (MTT) assay	34
2.3.4.2.2. Protein kinase assay	35
2.3.4.2.3. Radical scavenging (DPPH) assay	36
2.3.5. General laboratory equipment	39

3. Results	40
3.1. Secondary metabolites isolated from <i>Acanthostylorella</i> sp.	40
3.1.1. Acanthamide A (1 , new natural product)	41
3.1.2. Acanthamide B (2 , new natural product)	43
3.1.3. Acanthamide C (3 , new natural product)	44
3.1.4. Acanthamide D (4 , new natural product)	46
3.1.5. Methyl 3,4-dibromo-1 <i>H</i> -pyrrole-2-carboxylate (5 , new natural product)	49
3.1.6. 3,5-Dibromo-1 <i>H</i> -pyrrole-2-carboxylic acid (6 , new natural product)	51
3.1.7. 4,5-Dibromo- <i>N</i> -(methoxymethyl)-1 <i>H</i> -pyrrole-2-carboxamide (7 , known)	53
3.1.8. 4,5-Dibromo-1 <i>H</i> -pyrrole-2-carboxamide (8 , known)	54
3.1.9. Mukanadin D (9 , known)	57
3.1.10. (±)-Longamide B methyl ester (10 , known)	59
3.1.11. (±)-Longamide B (11 , known)	61
3.1.12. (±)-Longamide (12 , known)	63
3.1.13. 3,4-Dibromo-1 <i>H</i> -pyrrole-2-carboxamide (13 , known)	66
3.1.14. 2-Cyano-4,5-dibromo-1 <i>H</i> -pyrrole (14 , known)	67
3.1.15. Bioactivity assay results of compounds isolated from marine sponge <i>Acanthostylorella</i> sp.	68
3.2. Secondary metabolites isolated from <i>Stylissa massa</i>	69
3.2.1. Ethyl 3,4-dibromo-1 <i>H</i> -pyrrole-2-carboxylate (15 , new natural product)	70
3.2.2. 4-Bromo-1 <i>H</i> -pyrrole-3-carboxamide (16 , known)	72
3.2.3. 3,4-Dibromo-1 <i>H</i> -pyrrole-2-carboxamide (17 , known)	74
3.2.4. (-)-Longamide B methyl ester (18 , known)	74
3.2.5. (-)-Longamide B ethyl ester, Hanishsin (19 , known)	75
3.2.6. (-)-Longamide B (31 , known)	76
3.2.7. Aldisine (20 , known)	79
3.2.8. 2,3-Dibromoaldisine (21 , known)	81
3.2.9. 2-Bromoaldisine (22 , known)	83
3.2.10. 3-Bromoaldisine (23 , known)	84
3.2.11. (-)-Mukanadin C (24 , known)	87
3.2.12. (-)-Longamide (25 , known)	88
3.2.13. Latonduine A (26 , known)	91
3.2.14. (-)-Dibromophakellin H ⁺ Cl ⁻ (27 , known)	93
3.2.15. (-)-Monobromoisophakellin (28 , known)	94

Contents

3.2.16. (-)-Dibromocantharelline (32 , known)	95
3.2.17. (-)-Hymenine (29 , known)	99
3.2.18. Dispacamide E (30 , new natural product)	100
3.2.19. (10Z)-Debromohymenialdisine (33 , known)	104
3.2.20. Spongiacidin B (34 , known)	105
3.2.21. (10Z)-Hymenialdisine (35 , known)	108
3.2.22. (10E)-3-Bromohymenialdisine (36 , known)	109
3.2.23. Biological activity of bromopyrrole alkaloids isolated from Indonesian marine sponge <i>Stylissa massa</i> .	112
3.3. Secondary metabolites isolated from <i>Jaspis splendens</i>	114
3.3.1. Jaspamide (37 , known)	115
3.3.2. Jaspamide Q (38 , new natural product)	117
3.3.3. Jaspamide R (39 , new natural product)	119
3.3.4. 6 β -hydroxy-24-methylcholesta-4,22-dien-3-one (40 , known)	123
3.3.5. 6 β -hydroxy-24-methylcholesta-4-en-3-one (41 , known)	124
3.3.6. 6 β -hydroxy-24-ethylcholesta-4-en-3-one (42 , known)	125
3.3.7. Maculosin-1, <i>cyclo</i> -(L-Pro-L-Tyr) (43 , known)	127
3.3.8. Sangivamycin (44 , known)	128
3.3.9. Biological activity of compounds isolated from <i>Jaspis splendens</i> collected in Kalimantan (Indonesia)	131
3.4. Secondary metabolites isolated from <i>Thalassia testudinum</i>	132
3.4.1. Thalassiolin A (45 , known)	133
3.4.2. Thalassiolin C (46 , known)	134
3.4.3. Luteolin-3'-O-glucuronide (47 , known)	136
3.4.4. Biological activity of compounds isolated from <i>Thalassia testudinum</i>	139
3.5. Secondary metabolites isolated from <i>Comanthus</i> sp.	140
3.5.1. 1'-Deoxyrhodoptilometrene (48 , new natural product)	141
3.5.2. 1'-Deoxyrhodoptilometrin (49 , known)	144
3.5.3. (<i>S</i>)-(-) Rhodoptilometrin (50 , known)	148
3.5.4. 1'-Deoxyrhodoptilometrin-6-O-sulfate (51 , known)	151
3.5.5. Rhodoptilometrin-6-O-sulfate (52 , known)	152
3.5.6. Comaparvin (53 , known)	156
3.5.7. 6-Methoxycomaparvin (54 , known)	156

	<i>Contents</i>
3.5.8. 6-Methoxycomaparvin-5-methyl ether (55 , known)	160
3.5.9. 6-Methoxycomaparvin-5-methyl ether-8- <i>O</i> -sulfate (56 , known)	163
3.5.10. 6-Hydroxycomaparvin-8- <i>O</i> -sulfate (57 , known)	164
3.5.11. 2'-Deoxythymidine (58 , known)	167
3.5.12. Biological activity of anthraquinones and naphthopyrones isolated from the marine Echinoderm <i>Comanthus</i> sp.	169
4. Discussion	172
4.1. Methods for natural products tracing	172
4.2. Bromopyrroles: a typical class of marine alkaloids	173
4.3. Biological activity of bromopyrrole alkaloids	177
4.4. Jaspamides: a unique group of cyclodepsipeptides	179
4.5. Thalassiolins: sulfated flavonoids from <i>Thalassia testudinum</i>	181
4.6. Anthraquinones and naphthopyrones from <i>Comanthus</i> sp.	182
4.6.1. Biosynthesis of anthraquinones and naphthopyrones	182
4.6.2. Biological activity of anthraquinones and naphthopyrones	185
4.7. Sulfated secondary metabolites: occurrence and influence	186
5. Summary	188
6. References	191
7. List of abbreviations	205
8. Attachments	207
Resume	236

1. Introduction

Marine environment has represented the greatest biodiversity compared to the terrestrial one; with 34 of the 36 phyla of life exist. More than 70% of our planet's surface is covered by oceans, and life on Earth has its origin in the sea. In certain marine ecosystems, such as coral reefs or the deep sea floor, experts estimate that the biological diversity is even higher than in tropical rain forests, around 1000 species per m² in some areas. This outstanding biological diversity imparted an extraordinary chemical library of marine natural products with a diverse array of bioactivities. Consequently, marine environment offers a new frontier for research and attracts scientists from different disciplines, such as pharmacology, biology, ecology, organic and bioorganic chemistry. Although the field of marine natural products is a relatively new research area and the difficulties involved in collecting samples, it proved to be a productive source for bioactive natural products. The development of SCUBA in 1960s and more recently submersible vehicles have allowed easy access of both shallow and deep-water marine organisms for studies by natural products chemists.

1.1. Significance of the study

The deep habitats of marine invertebrates and the sedentary lifestyle together with the soft body necessitate a chemical means of defense from predators. Therefore, they have evolved the ability to synthesize toxic and/or deterrent compounds, or to obtain them from the symbiotic marine micro-organisms.

Many marine-derived compounds show strong biological activities as any natural product released into the water is rapidly diluted and, therefore, needs to be highly potent to exert a significant biological effect. Marine natural products have attracted the attention of scientists from different disciplines, such as chemistry, pharmacology, biology and ecology (Newman *et al.*, 2000; König and Wright, 1996; Claeson and Bohlin, 1997). This notion is supported by the fact that, before 1995, ~ 6,500 marine natural products had been isolated, whereas this figure has now escalated to more than 19,000 compounds (Marinlit: a database of the marine natural products literature, 2009. Contact address: John W. Blunt, Christchurch, New Zealand).

The interest in the marine environment has been stimulated by the array of biological activities of marine natural products and hence their potential biomedical applications (Pawlik, 1993). For this reason, and because of the immense biological diversity in the sea as a whole, it is increasingly recognized that a huge number of natural products and novel chemical entities exist in the oceans, with some of them exhibiting biological activities that

Introduction

may also be useful in the quest for finding new drugs with greater efficacy and specificity for the treatment of human diseases (Bhakuni and Rawat, 2005; Proksch *et al.*, 2002). This was exemplified by the newly admitted marine-derived medicaments: Prialt[®] (also known as ziconotide) as a potent analgesic for severe chronic pain and Yondelis[®] (known also as trabectedin or E-743) as antitumor agent for the treatment of advanced soft tissue sarcoma. Moreover, Aplidin[®] (plitidepsin), kahalalide F, and Zalypsis[®] (jorumycin derivative) are in clinical trials for treatment of solid tumors and haematological malignancies. Therefore, marine ecosystem is considered as a valuable treasure of useful substances that could be used, for example, to develop new treatments for infectious diseases or cancer (Proksch *et al.*, 2002).

1.2. The biological importance of marine natural products

1.2.1. Antiviral and antitumor marine natural products

Viruses have remained resistant to treatment or prophylaxis longer than any other infectious organism and cancers are the second leading cause of death in the first world, but, it is estimated that 60% of all illnesses in the developed countries is a consequence of viral infections. The search for viral chemotherapeutic agents from marine sources has yielded several promising therapeutic leads reported to display notable antiviral activity. The leading work of Bergmann and Feeny in 1951, which reports the presence of the unusual arabinosyl nucleosides, spongothymidine, spongosine and spongouridine (Fig. 1.1) from the sponge *Cryptotethia crypta* (Bergmann and Feeney, 1951; Bergmann and Burke 1955; Bergmann *et al.*, 1957), have provided the lead compounds for the development of the therapeutically used Ara-C (cytarabine) for treatment of leukemia, in addition to the virustatic agent Ara-A (vidarabine), azidothymidine (AZT), and acyclovir which was introduced to the market and used therapeutically against *Herpes encephalitis* since the late of 1970s (Miller *et al.*, 1968; Whitley *et al.*, 1977).

The didemnins (Fig. 1.1) are a family of closely related cyclic depsipeptides obtained from *Trididemnum solidum*, a Caribbean tunicate, or sea squirt, of the family Didemnidae (Rinehart *et al.*, 1981). The didemnins inhibit the growth of both RNA and DNA viruses and are highly cytotoxic to L1210 leukaemic cells and P388 leukaemia (Martin *et al.*, 1986). Didemnin A inhibits *Coxsackie A21* virus and *Herpes simplex* virus. Didemnin B shows cytotoxicity to L1210, P388 leukaemic cells and B-16 melanoma (Rinehart *et al.*, 1981).

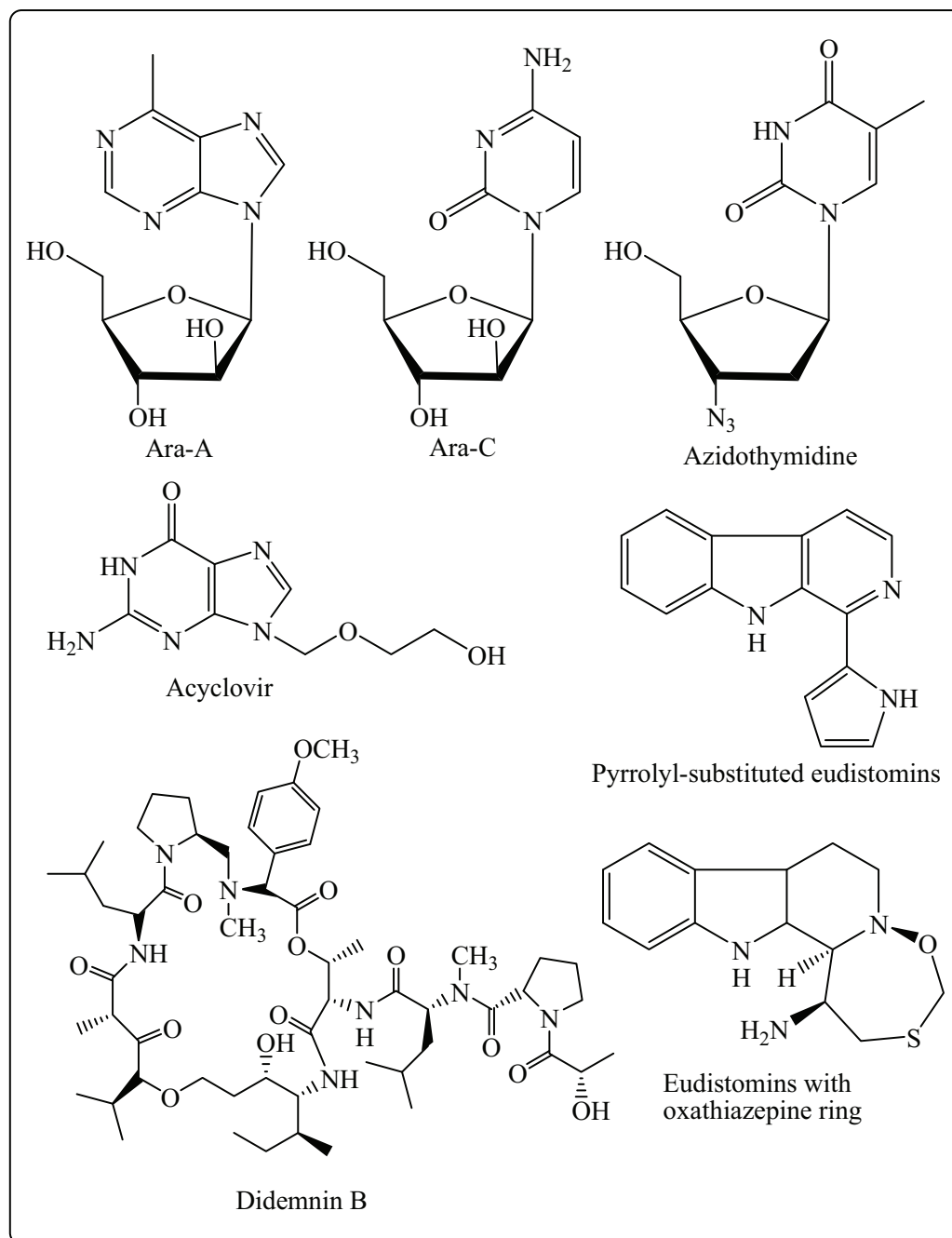


Fig. 1.1. Biologically important marine natural products.

Eudistomins (Fig. 1.1) were isolated in 1981 from colonial tunicate *Eudistoma olivaceum* (Rinehart *et al.*, 1981). There are four distinct structural categories of eudistomins, namely unsubstituted, pyrrolyl-substituted, pyrrolinyl-substituted and tetrahydro- β -carboline containing a uniquely condensed oxathiazepine ring system. The oxathiazepine-containing eudistomins possess a pronounced antiviral activity toward the DNA virus HSV-1 (Rinehart *et al.*, 1984).

Bryostatins are macrocyclic lactones isolated from the marine bryozoan *Bugula neritica*. Bryostatin 1 (Fig. 1.2) was one of the most promising anticancer agents and the

Introduction

most abundant of this group. This compound was first known to inhibit the growth of murine P388 leukemia cells at subnanomolar concentrations (Pettit *et al.*, 1982; Pettit *et al.*, 1993). Presently, there are more than 20 bryostatin derivatives have been reported (Wender *et al.*, 1999). The MOA of bryostatins were determined. These compounds are thought to bind to protein kinase C (PKC), a tumor promoting receptor. As a result, the PKC enzyme is significantly down-regulated, leading to inhibition of growth and cell death. However, the positive effects of bryostatin are obtained only when combined with other chemotherapies such as taxol and cisplatin. According to an independent research, Haygood and coworker demonstrated the hypothesis that bryostatins are symbiotic origin. Bryostatins were isolated from the symbiotic microbes (*Candidatus Endobugula sertula*) (Davidson *et al.*, 2001).

1.2.2. Protein kinase inhibitory activity of marine natural products

Kinases are ATP-dependent enzymes that add phosphate groups to proteins. Protein phosphorylation is the key regulatory mechanism that is utilised to regulate the activity of enzymes and transcription factors (Meijer *et al.*, 2000). Therefore, protein kinases play an essential role in virtually all cellular processes and are involved in most diseases. Hymenialdisine (Fig. 1.2) is a marine constituent which has been isolated from many marine sponges belonging to the genera *Acanthella*, *Axinella* and *Hymeniacidon* (Mattia *et al.*, 1982; Cimino *et al.*, 1982; Kitagawa *et al.*, 1983). Hymenialdisine and its derivatives have caught the scientific interest of several research groups particularly due to their biological activity profile, namely being nanomolar kinase inhibitors against CDKs, GSK-3 β , CK1 and Chk1 which are necessary parts regulating several vital cellular functions such as gene expression, cellular proliferation, membrane transport and apoptosis as well (Meijer *et al.*, 2000) and targeting these kinases has been appealing for the treatment of diseases like Alzheimer's disease, type II diabetes and cancer (Nikoulina *et al.*, 2000; Martinez *et al.*, 2002). In addition, hymenialdisines inhibited several pro-inflammatory cytokines (IL-1, IL-2, IL-6, and NO) through inhibition of the NF- κ B signalling pathway which is potentially valuable for treatment of serious inflammatory diseases such as rheumatoid arthritis and osteoarthritis (Sharma *et al.*, 2004).

1.2.3. Antimalarial marine natural products

Malaria is a particularly serious disease in sub-Saharan Africa, but it is also a serious public-health issue in certain regions of south East Asia and South America. Most malaria cases and deaths are caused by the parasite *Plasmodium falciparum* (Mishra *et al.*, 1999). Since

removal of the vector of transmission (the anopheles mosquito) is almost impossible, new antimalarial agents providing novel mechanisms of action will always be needed to combat resistance to drugs such as chloroquine, mefloquine, quinine, and sulfadoxine-pyrimethamine. Manzamine A (Fig. 1.2) exhibits potent *in vitro* activity against *P. falciparum* (D6 clone), with an MIC of 0.0045 $\mu\text{g/mL}$, compared with control drug (chloroquine and artemisinin) MICs of 0.0155 $\mu\text{g/mL}$ and 0.010 $\mu\text{g/mL}$, respectively (Ang *et al.*, 2000). *In vivo*, manzamine A inhibits the growth of the rodent malaria parasite *Plasmodium berghei*, with more than 90% of the asexual erythrocytic stages of *P. berghei* inhibited after one intraperitoneal injection of 50 or 100 $\mu\text{mol/kg}$ manzamine A into infected mice (Ang *et al.*, 2000). Therefore, manzamine A and its analogues are clearly valuable candidates for further investigation and development as promising leads against malaria and perhaps other serious infectious diseases.

1.2.4. Anthelmintic activity of marine natural products

Anthelmintics are drugs used to rid host organisms of helminth parasites. Parasitism by nematodes (unsegmented worms that constitute the phylum Nematoda) represents a major issue in the commercial livestock industry and contributes substantially to malnutrition and disease in human beings. Particularly difficult to eradicate is *Ascaris lumbricoides*, the large gut worm, which causes malnutrition and obstructive bowel disease, and the soil transmitted blood sucking hookworms *Ancylostoma duodenale* and *Necator americanus*, which lead to severe blood loss and iron-deficiency anaemia, decreased food intake, impaired digestion, malabsorption and poor growth rate (Crompton and Nesheim, 2002). Despite the availability of excellent commercial anthelmintics, growing resistance to key structural classes (benzimidazoles and macrolides) necessitates the search for new bioactive agents (Crompton and Nesheim, 2002).

Jaspamide (=jasplakinolide, Fig. 1.2) is a cyclodepsipeptide was isolated firstly in 1986 from the sponge *Jaspis cf. johnstoni* by Ireland and Crews. It exhibited an *in vitro* 50% effective dose of less than 1 $\mu\text{g/mL}$ against the nematode *Nippostrongylus braziliensis* (Nagai *et al.*, 1992). In addition to being a potent antiparasitic (Zabrisikie *et al.*, 1986; Crews *et al.*, 1986), jaspamide is known for other pronounced bioactivities including antifungal (Scott *et al.*, 1988), insecticidal (Zabrisikie *et al.*, 1986; Crews *et al.*, 1986), and antiproliferative activities (Inman and Crews, 1989).

Introduction

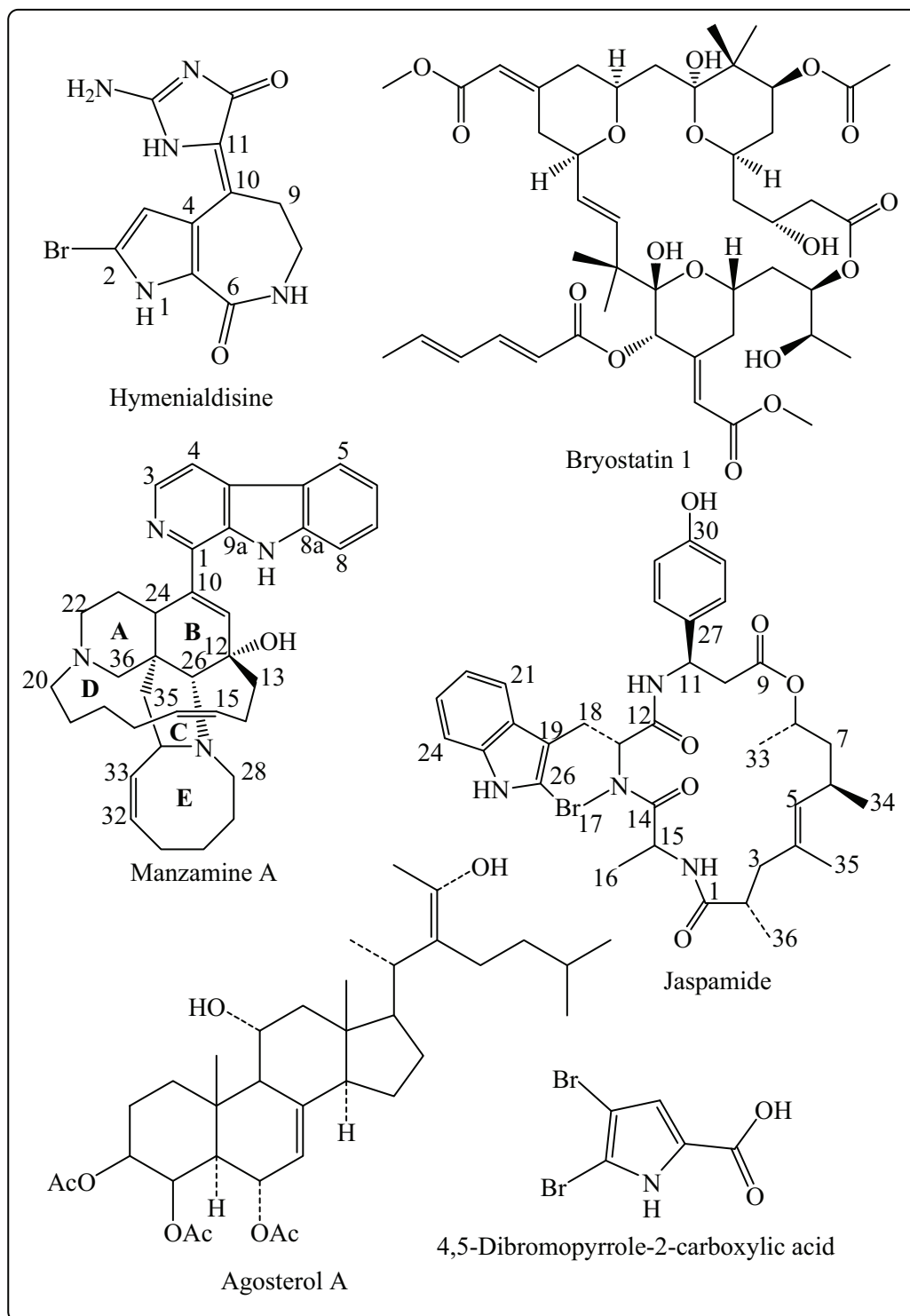


Fig. 1.2. Biologically important marine natural products.

1.2.5. Reversing multi-drug resistance (MDR) activity

Multidrug resistance (MDR) in tumour cells has been recognised as a major obstacle to successful cancer chemotherapy. Overexpression of certain membrane glycoproteins has

been observed in MDR tumour cell lines. The substance which inhibits the action of these membrane glycoproteins would have high possibility for solving the MDR problems in cancer chemotherapy. Agosterol A (Fig. 1.2) completely reversed the resistance to colchicine in KB-C2 cells and also the resistance to vincristine in KB-CV60 cells. Agosterol A is a polyhydroxylated sterol acetate and was isolated from a marine sponge of genus *Spongia*. It reverses MDR caused by overexpression of multi-drug resistance associated protein (MRP). It may be a pharmaceutical candidate for reversing MDR (Aoki *et al.*, 1998).

1.2.6. Immunosuppressive activity of marine natural products

There are also other marine natural products which show *in vitro* immunosuppressive activity such as 4 α -methyl-5 α -cholest-8-en-3 β -ol (Fig. 1.3) and 4,5-dibromopyrrole-2-carboxylic acid (Fig. 1.2). Both compounds were highly active in suppression of murine splenocytes in the two-way mixed lymphocyte reaction (MLR) with little or no demonstrable cytotoxicity. Both compounds were isolated from the marine sponge *Agelas flabelliformis* and could be useful in organ transplantations (Gunasekera *et al.*, 1989).

1.3. The importance of marine natural products to the source organism

Marine natural products play an important role to the source organism. Some of them are beneficial as chemical defense means including:

1.3.1. Chemical defense against fouling and spatial competition

Aerophobin-2 and isofistularin-3 (Fig. 1.3) are secondary metabolites produced by the marine sponge *Aplysina aerophoba* that were found to be enzymatically converted after injury into dienone and aeroplysinin-1, respectively, which was found to protect the sponge from invasion of pathogenic microorganisms (Proksch and Ebel, 1998; Ebel *et al.*, 1997).

1.3.2. Chemical defense against predators

Latrunculins A and B (Fig. 1.3) protect the sponge *Latrunculina magnifica* from fishes (e.g. *Gambusia affinis*) (Neeman *et al.*, 1975). The unpalatability of the ascidian *Trididemnum solidum* was shown to be due to alkaloids of didemnin B and nor-didemnin which inhibited the reef fishes from feeding (Lindquist *et al.*, 1992).

Introduction

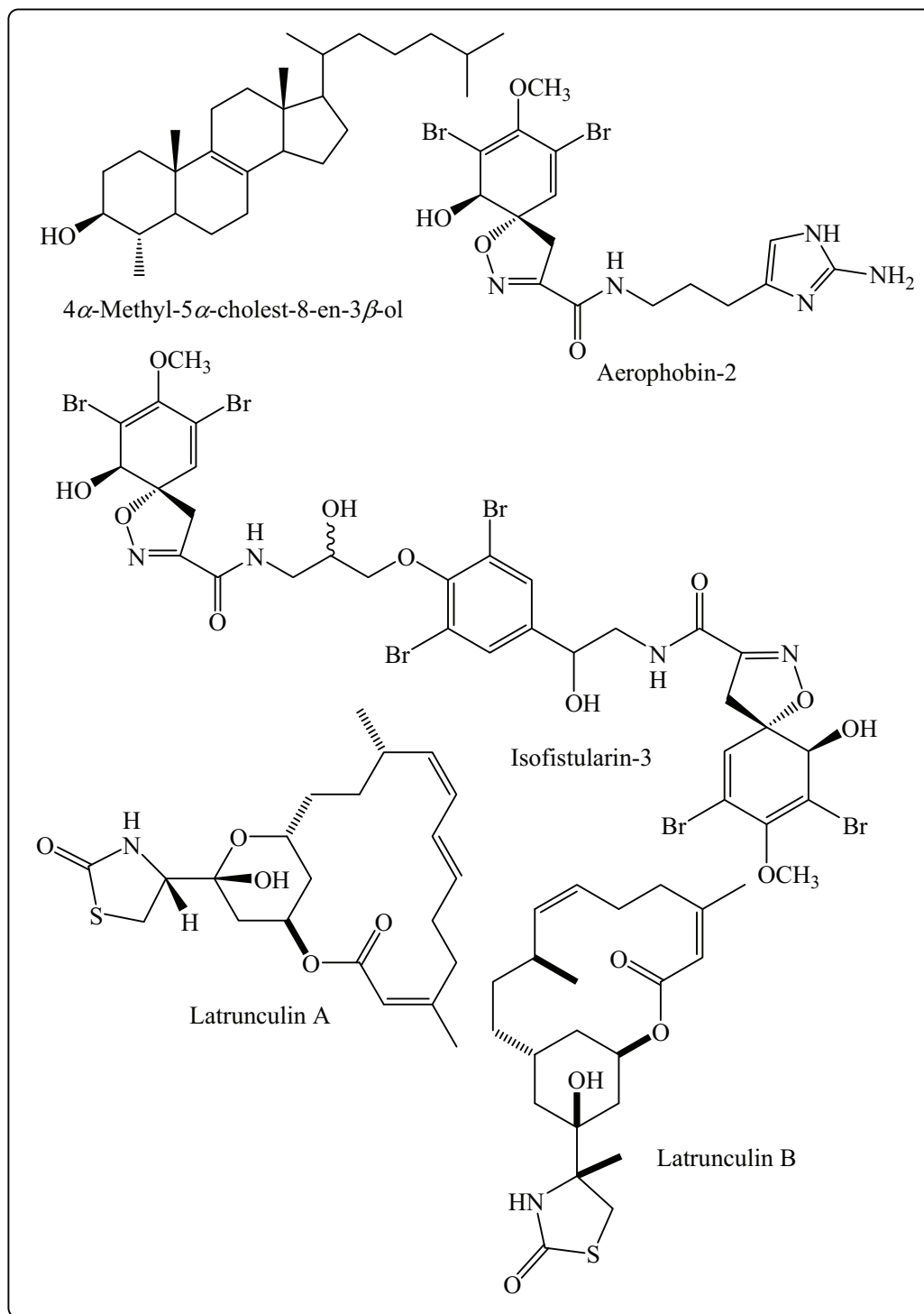


Fig. 1.3. Biologically important marine natural products.

1.4. The current status of marine natural products research

Marine natural products proved appealing for scientific interests. Consequently, this led to the discovery of potentially active metabolites considered valuable for further preclinical or clinical trials. As successful examples for medical remedies from marine resources,

Prialt[®] (also known as ziconotide) as a potent analgesic for severe chronic pain and Yondelis[®] (known also as trabectedin or ET-743) as antitumor agent for the treatment of advanced soft tissue sarcoma. In addition Aplidin[®] (plitidepsin), kahalalide F, and Zalypsis[®] (jorumycin derivative) are in clinical trials for treatment of solid tumors and haematological malignancies.

In 2004, Newman and Cragg summarized the natural products and related compounds from marine sources which are in advanced preclinical or clinical trials (Table 1.1) (Newman and Cragg, 2004).

Table 1.1. Current status of marine natural products in clinical and preclinical trials.

Name	Source	Status (Disease)
Didemnin B	<i>Trididemnum solidum</i>	Phase II (Cancer)
Bryostatin 1	<i>Bugula neritina</i>	Phase II (Cancer)
Dolastatin 10	<i>Dolabella auricularia</i> (Marine microbe derived; cyanophyte)	Phase II (Cancer)
Cematodin	Synthetic derivative of Dolastatin 15 (Marine microbe derived; cyanophyte)	Phase II (Cancer)
TZT-1027	Synthetic Dolasatatin	Phase II (Cancer)
Girolline	<i>Pseudaxinyssa cantharella</i>	Phase I (Cancer)
Aplidine	<i>Aplidium albicans</i>	Phase III (Cancer) EC COMP/EMEA approved orphan drug status for ALL (07/2003)
E7389	<i>Lissodendoryx</i> sp.	Phase I (Cancer)
Discodermolide	<i>Discodermia dissoluta</i>	Phase I (Cancer)
Kahalalide F	<i>Elysia rufescens</i> / <i>Bryopsis</i> sp.	Phase II (Cancer)
ES-285 (Spisulosine)	<i>Spisula polynyma</i>	Phase I (Cancer)
HTI-286	<i>Cymbastella</i> sp.	Phase I (Cancer)
Bengamide derivative	<i>Jaspis</i> sp.	Phase I (Cancer)
Cryptophycins (also Arenastatin A)	<i>Nostoc</i> sp. <i>Dysidea arenaria</i>	Phase I (Cancer)

Introduction

Name	Source	Status (Disease)
KRN-7000	<i>Agelas mauritianus</i>	Phase I (Cancer)
Squalamine	<i>Squalus acanthias</i>	Phase II (Cancer)
AE-941 (Neovastat)	Shark	Phase III (Cancer)
Laulimalide	<i>Cacospongia mycofijiensis</i>	Preclinical (Cancer)
Curacin A	<i>Lyngbya majuscula</i>	Preclinical (Cancer)
Vitilevuamide	<i>Didemnum cucliferum</i> <i>Polysyncraton lithostrotum</i>	Preclinical (Cancer)
Diazonamide	<i>Diazona angulata</i>	Preclinical (Cancer)
Eleutherobin	<i>Eleutherobia</i> sp.	Preclinical (Cancer)
Sarcodictyin	<i>Sarcodictyon roseum</i>	Preclinical (Cancer)
Peloruside A	<i>Mycale hentscheli</i>	Preclinical (Cancer)
Salicylhalimides A&B	<i>Haliclona</i> sp.	Preclinical (Cancer)
Thiocoraline	<i>Micromonospora marina</i>	Preclinical (Cancer)
Neoamphimedine	<i>Xestospongia</i> sp.	Preclinical (Cancer)
Aplyronine A	<i>Aplysia kurodai</i>	Preclinical (Cancer)
DMBX (aka GTS-21)	<i>Amphiporus lactifloreus</i>	Phase I (Alzheimer's)
Manoalide	<i>Luffariaella variabilis</i>	Phase II (Anti-psoriatic)
IPL-576092 (aka HMR-4011 A)	<i>Petrosia contignata</i>	Phase II (Anti-asthmatic)
IPL-512602	<i>Petrosia contignata</i>	Phase II (Anti-inflammatory)
IPL-550260	<i>Petrosia contignata</i>	Phase I (Anti-inflammatory)
CGX-1160	<i>Conus geographus</i>	Preclinical (Pain)
CGX-1007	<i>Conus geographus</i>	Preclinical (Epilepsy)
AMM336	<i>Conus catus</i>	Preclinical (Pain)
Chi-conotoxin	<i>Conus</i> sp.	Preclinical (Pain)
ACV1	<i>Conus victoriae</i>	Preclinical (Pain)

In addition, other elegant reviews have recently been published discussing the actual clinical status of marine natural products (Molinski *et al.*, 2009; Mayer *et al.*, 2010).

1.5. Aim of the study

Chemistry and biological activities of marine natural products have been an attractive investment for massive research efforts. Many successful cases, as shown above, proved to have various pharmaceutical significances, which have been developed to preclinical or clinical trial phases for treatment of serious diseases such as Alzheimer's disease, type II diabetes, cancer and infectious diseases in addition to pain killing and anti-inflammatory activities.

Based on the previous findings, this study has been concerned with the isolation and structural elucidation of marine secondary metabolites, either known or preferentially new ones, of the bioactive extracts from different marine resources including sponges, seagrasses and echinoderms collected off different locations namely Indonesia, Philippines, and Thailand. Beyond that the main target was to get as much as possible from each substance so as to enable further assessment of various bioactivities to find out every possible potential bioactivity. Various biological assays have been incorporated in this study including cytotoxicity (MTT), antibacterial, antifungal, antiviral, protein kinase inhibitory and antioxidant (DPPH) activities.

Materials and Methods

2. Materials and Methods

2.1. Marine organism materials

Biological materials involved in this work were all marine organisms including three sponges, one echinoderm, and one plant. They were collected in different locations. Regarding sponges, the unidentified *Acanthostylotella* sp., *Jaspis splendens*, and *Stylissa massa*, they were collected off the Pacific Ocean (Indonesia), the unidentified echinoderm *Comanthus* sp. was collected off the South China Sea (Phillipines), and turtle grass *Thalassia testudinum* was collected off the Mediterranean Sea (Turkey).

2.1.1. Sponges

Sponges are animals constituting the phylum Porifera “Pore bearer” (Kingdom Animalia). Their bodies consist of jelly-like mesohyl sandwiched between two thin layers of cells. Unlike other animals, sponges are unique in having some specialized cells that can transform into other types. Sponges lack nervous, digestive, or circulatory systems. Instead they rely on maintaining a continuous water flow through their bodies to obtain food, oxygen, and to remove wastes. They are defined as sessile metazoans, and however there are freshwater species, the great majority are marine species, ranging from tidal zones to depths exceeding 8,800 meters. While most of the 9,000 known species feed on bacteria and other food particles, some sponges host photosynthesizing microorganisms as endosymbionts which often produce more food and oxygen than their consumption. On the contrary, sponges that live in poor food environments have become carnivores.

Sponges use various materials to reinforce their mesohyl and in some cases to produce skeletons, and this forms the main basis for classifying sponges. Calcareous sponges produce spicules made of calcium carbonate. Demosponges reinforce the mesohyl with fibers of a special form of collagen called spongin, most also produce spicules of silica, and a few secrete massive external frameworks of calcium carbonate.

A sponge’s body is hollow and is held in shape by mesohyl, a jelly-like substance made of collagen, and reinforced by a dense network of fibers also made of collagen. The inner surface is covered with choanocytes, cells with conical or collars surrounding one flagellum per choanocytes. The wave-like motion of the whip-like porocytes that form closable inlet valves. Pinacocytes, plate-like cells, form a single layered skin over all other parts of the mesohyl that are not covered by choanocytes, and the external pinacocytes also digest food particles that are too large to enter the ostia, while those at the base are responsible for anchoring the animal.

Other types of cell live and move within the mesohyl:

- **Lophocytes** are amoeba-like cells that move slowly through the mesohyl and secrete collagen fibers.
- **Collencytes** are another type of collagen-producing cell.
- **Rhabdiferous cells** secrete polysaccharides that also form part of the mesohyl.
- **Oocytes** and **spermatocytes** are reproductive cells.
- **Sclerocytes** secrete the mineralized spicules "little spines" that form the skeletons of many sponges and in some species provide some defense against predators.
- In addition to or instead of sclerocytes, demosponges have **spongocytes** that secrete a form of collagen that polymerizes into spongin, a thick fibrous material that stiffens the mesohyl.
- **Myocytes** ("muscle cells") conduct signals and cause parts of the animal to contract.
- **Grey cells** act as sponges' equivalent of an immune system.
- **Archaeocytes** (or amoebocytes) are amoeba-like cells that are totipotent, in other words each is capable of transformation into any other type of cell. They also have important roles in feeding and in clearing debris that block the ostia.

For a long time sponges were assigned to a separate subkingdom, Parazoa "beside the animals". They are now classified as a phylum within the Animalia, and divided into classes mainly according to the composition of their skeletons:

- Hexactinellida (glass sponges) have silicate spicules, the largest of which have six rays and may be individual or fused. The main components of their bodies are syncytia in which large numbers of cell share a single external membrane.
- Calcarea have skeletons made of calcite, a form of calcium carbonate, which may form separate spicules or large masses. All the cells have a single nucleus and membrane.
- Most Demospongiae have silicate spicules or spongin fibers or both within their soft tissues. However a few also have massive external skeletons made of aragonite, another form of calcium carbonate. All the cells have a single nucleus and membrane.
- Archeocyatha are known only as fossils from the Cambrian period.

2.1.1.1. *Acanthostylotella* sp.

The sponge *Acanthostylotella* sp. (class Demospongiae, order Poecilosclerida, family Raspailiidae) (Fig. 2.1) was collected at a depth of 3 m in a shallow sandy channel with sea grasses at the East side of Nusa Lembongan, Selat Ceningan (08°41'03"S115°27'43"E, off the island Bali, Indonesia) in 2001. The sponge material was immersed in ethanol

Materials and Methods

immediately after collection. A voucher specimen is kept in ethanol under the registration number RMNH POR. 2264 at the National Museum of Natural History, Leiden, Netherlands.

2.1.1.2. *Stylissa massa*

The sponge *Stylissa massa* (class Demospongiae, order Halichondrida, family Dictyonellidae) (Fig. 2.2) was collected off the shores of Papoea Island (Indonesia) in January 2008, identified, and supplied by Dr. Nicole de Voogd, National Museum of Natural History, Leiden, Netherlands.

2.1.1.3. *Jaspis splendens*

In August 2008, specimens of the sponge *Jaspis splendens* (Fig. 2.3) were collected on two neighboring Islands from East Kalimantan (Indonesia), namely Samama, Panjang, and a submerged reef shoal, at 10 meter depths. Numbers of voucher specimens are RMNH Por. 4234, 4266 and 4299, respectively. They were taxonomically identified as *Jaspis splendens* (order Astrophorida, family Ancorinidae) at the National Museum of Natural History, Leiden, Netherlands. HPLC and LCMS analyses of the three samples revealed that they were identical with regard to their peptide derivatives. Hence, the material was combined in order to obtain sufficient amounts of compounds for subsequent structure elucidation.



Fig. 2.1. *Acanthostylotella* sp.



Fig. 2.2. *Stylissa massa*



Fig. 2.3. *Jaspis splendens*



Fig. 2.4. *Thalassia testudinum*

2.1.2. Seagrasses

Seagrasses are flowering plants from one of four plant families, Posidoniaceae, Zosteraceae, Hydrocharitaceae, or Cymodoceaceae, all in the order Alismatales, the class of monocotyledons, which grow in marine environments. These marine flowering plants were called seagrasses because the leaves are long, narrow, very often green, and grow in large meadows which look like grassland, resembling terrestrial grasses of the family Poaceae. Since these plants must photosynthesize, they are limited to growing submerged in the photic zone, and most occur in shallow and sheltered coastal waters anchored in sand or mud bottoms. They undergo pollination while submerged and complete their entire life cycle underwater. There are about sixty species worldwide, although the taxonomy is still disputed.

Seagrasses form extensive beds or meadows, which can be either monospecific, one species, or multispecific, more than one species coexist. Seagrass beds are highly diverse and productive ecosystems, and can harbor hundreds of associated species from all phyla, for example juvenile and adult fish, epiphytic and free-living macroalgae and microalgae, mollusks, bristle worms, and nematodes.

Seagrasses are sometimes labeled ecosystem engineers, because they partly create their own habitat, the leaves slow down water-currents increasing sedimentation, and the seagrass roots and rhizomes stabilize the seabed. Their importance for associated species is mainly due to provision of shelter and for their extraordinarily high rate of primary production. As a result, seagrasses provide coastal zones with a number of ecosystem goods and ecosystem services, for instance fishing grounds, wave protection, oxygen production and protection against coastal erosion.

2.1.2.1. *Thalassia testudinum*

The seagrass *Thalassia testudinum* (Fig. 2.4) was collected by snorkeling at 2 m depth off Muk Island, Trang Province, Thailand in July, 2007.

2.1.3. Echinoderms

Echinoderms (Phylum Echinodermata) are a phylum of marine animals. Echinoderms are found at every ocean depth, from the intertidal zone to the abyssal zone (4,000 to 6,000 meters depth). The phylum contains about 7,000 living species, making it the second-largest grouping of deuterostomes, after the chordates; they are also the largest phylum that has no freshwater or terrestrial representatives.

Materials and Methods

The word (Echinoderm) was derived from the Greek word (echinodermata), "spiny skin", that came from (echinos), "sea-urchin", and (derma), "skin". Echinoderms are important both biologically and geologically: biologically because few other groupings are so abundant in the biotic desert of the deep sea, as well as the shallower oceans, and geologically as their ossified skeletons are major contributors to many limestone formations, and can provide valuable clues as to the geological environment. Further, it is held by some that the radiation of echinoderms was responsible for the Mesozoic revolution of marine life.

Two main subdivisions of Echinoderms are traditionally recognized: the more familiar, motile Eleutherozoa, which encompasses the Asterozoa (starfish), Ophiurozoa (brittle stars), Echinozoa (sea urchins and sand dollars) and Holothurozoa (sea cucumbers); and the sessile Pelmatzoa, which consists of the crinoids and extinct Paracrinozoa. Some crinoids, the feather stars, have secondarily re-evolved a free-living lifestyle.

Echinoderms evolved from animals with bilateral symmetry; although adult echinoderms possess radial symmetry, echinoderm larvae are ciliated, free-swimming organisms that organize in a bilaterally symmetric fashion that makes them look like embryonic chordates. Later, the left side of the body grows at the expense of the right side, which is eventually exploded. The left side then grows in a pentaradially symmetric fashion, in which the body is arranged in five parts around a central axis. All echinoderms exhibit fivefold radial symmetry in portions of their body at some stage of life, even if they have secondary bilateral symmetry. Many crinoids and some starfish exhibit symmetry in multiples of the basic five, with starfish such as *Helicoplaster* sp. known to possess up to 50 arms, and the sea-lily *Comanthina schlegelii* boasting 200.

They have mesodermal skeleton made up of calcareous plates or ossicles, despite the robustness of the individual skeletal modules, complete echinoderm skeletons are rare in the fossil record. This is because they quickly disarticulate once the encompassing skin rots away, and in the absence of tissue there is nothing to hold the plates together. The modular construction is a result of the growth system employed by echinoderms, which adds new segments at the centre of the radial limbs, pushing the existing plates outwards in the fashion of a conveyor belt. The spines of sea urchins are most readily lost, as they are not even attached to the main skeleton in life. Each spine can be moved individually and is thus only loosely attached in life; a walk above a rocky shore will often reveal a large number of spineless but otherwise complete sea urchin skeletons. The epidermis of echinoderms consists of cells responsible for the support and maintenance of the skeleton,

as well as pigment cells, mechanoreceptor cells, which detect motion on the animal's surface, and sometimes gland cells which secrete sticky fluids or even toxins.

Although echinoderms possess a complete digestive tube (tubular gut), it is very simple, often simply leading directly from mouth to anus. It can generally be divided into a pharynx, stomach, intestine and rectum, or cloaca. There are present haemal and perihemal systems which are of coelomic region, thus so possess an open and reduced circulatory system consisting of a central ring and five radial vessels, but often without heart or blood. Gaseous exchange occurs by dermal branchiae or papulae in star fishes, peristomal gills in sea urchins, genital bursae in brittle stars and cloacal trees in holothurians. Exchange of gases also takes place through tube feet. They lack specialized excretory organs and so nitrogenous wastes are diffused out via gills or terminal branchia. Ammonia is the chief excretory matter. They have a simple radial nervous system that consists of a modified nerve net, interconnected neurons with no central brain, although some do possess ganglia. Nerves radiate from central rings around the mouth into each arm and the branches of these nerves coordinate the movements of the organism.

The gonads of the organisms occupy the entire body cavities of sea urchins and sea cucumbers; the less voluminous crinoids, brittle stars and starfish having two gonads per arm. While the primitive condition is considered to be one genital aperture, many organisms have multiple holes through which eggs or sperm may be released.

Echinoderms become sexually mature after approximately two to three years, depending on the species and the environmental conditions. The eggs and sperm cells are released into open water, where fertilization takes place. However, internal fertilization has currently been observed in three species of starfish, three brittle stars and a deep water sea cucumber. In some species of feather star, the embryos develop in special breeding bags, where the eggs are held until sperm released by a male happen to find them and fertilize the contents.

Many echinoderms have remarkable powers of regeneration. Some sea stars are capable of regenerating lost arms. In some cases, lost arms have been observed to regenerate a second complete sea star. Sea cucumbers often discharge parts of their internal organs if they perceive danger. The discharged organs and tissues are quickly regenerated.

2.1.3.1. *Comanthus* sp.

The echinoderm *Comanthus* sp. (Fig. 2.5) was collected off the northern shores of Mindoro Island along the so-called Manila Channel in April 1994. The echinoderm was frozen directly after collection, freeze-dried, ground, and stored at -20°C.

Materials and Methods



Fig. 2.5. *Comanthus* sp.

2.2. Chemicals

2.2.1. General laboratory chemicals

(-)-2-Butanol	Merk
(<i>R</i>)-(-)-Methoxy- α -trifluoromethylphenylacetyl chloride	Aldrich
(<i>S</i>)-(-)-Methoxy- α -trifluoromethylphenylacetyl chloride	Aldrich
2,2-Diphenyl-1-picryl-hydrazyl (DPPH)	Sigma
2-Aminoethyl diphenylboronate	Fluka
Anisaldehyde (4-methoxybenzaldehyde)	Merk
Concentrated ammonia solution	Fluka
Dimethylsulfoxide	Merk
Formic acid	Gruessing
Ninhydrin	Riedel-deHaen
Trifluoroacetic acid (TFA)	Merk

2.2.2. Chromatography

2.2.2.1. Stationary phases

Pre-coated TLC plates, Silica Gel 60 F ₂₅₄ , layer thickness 0.2 mm	Merk
Silica Gel 60, 0.04 – 0.063 mm mesh size	Merk
Pre-coated TLC plates, RP-18, F ₂₅₄ S, layer thickness 0.25 mm	Merk
RP-18, 0.04 – 0.063 mm mesh size	Merk
Sephadex LH-20, 0.25 – 0.1 mm mesh size	Merk
Diaion HP20	Supelco

2.2.2.2. Spray reagents

The reagents were stored in amber-colored bottles and kept refrigerated until being used. TLC was used to monitor the identity of each of the fractions and the qualitative purity of

the isolated compounds. It was also utilized to optimize the solvent system that would be applied for column chromatography.

Anisaldehyde/H₂SO₄ spray Reagent

Methanol	85 mL
Glacial acetic acid	10 mL
Conc. H ₂ SO ₄	5 mL (added slowly)
Anisaldehyde	0.5 mL

Flavone reagent

Flavone Reagent A:		Flavone Reagent B:	
2-Aminoethyl diphenylborionate	1 g	Polyethylene glycol 400	5 mL
Methanol upto	100 mL	Ethanol	95 mL

2.2.3. Solvents

2.2.3.1. General solvents

Acetone, acetonitrile, dichloromethane, ethanol, ethyl acetate, *n*-hexane, and methanol were used. The solvents were purchased from the Institut of Chemistry, University of Duesseldorf. They were distilled before use and special grades were used for spectroscopic measurements.

2.2.3.2. Solvents for HPLC

Acetonitrile	LiChroSolv HPLC grade (Merk)
Methanol	LiChroSolv HPLC grade (Merk)
Nanopure water	distilled and heavy metals free water obtained by passing distilled water through nano- and ion-exchange filter cells (Barnstead, France).

2.2.3.3. Solvents for optical rotation

Chloroform	Special grade (Sigma)
Ethanol	Special grade (Sigma)
Methanol	Special grade (Sigma)
Water	Special grade (Fluka)

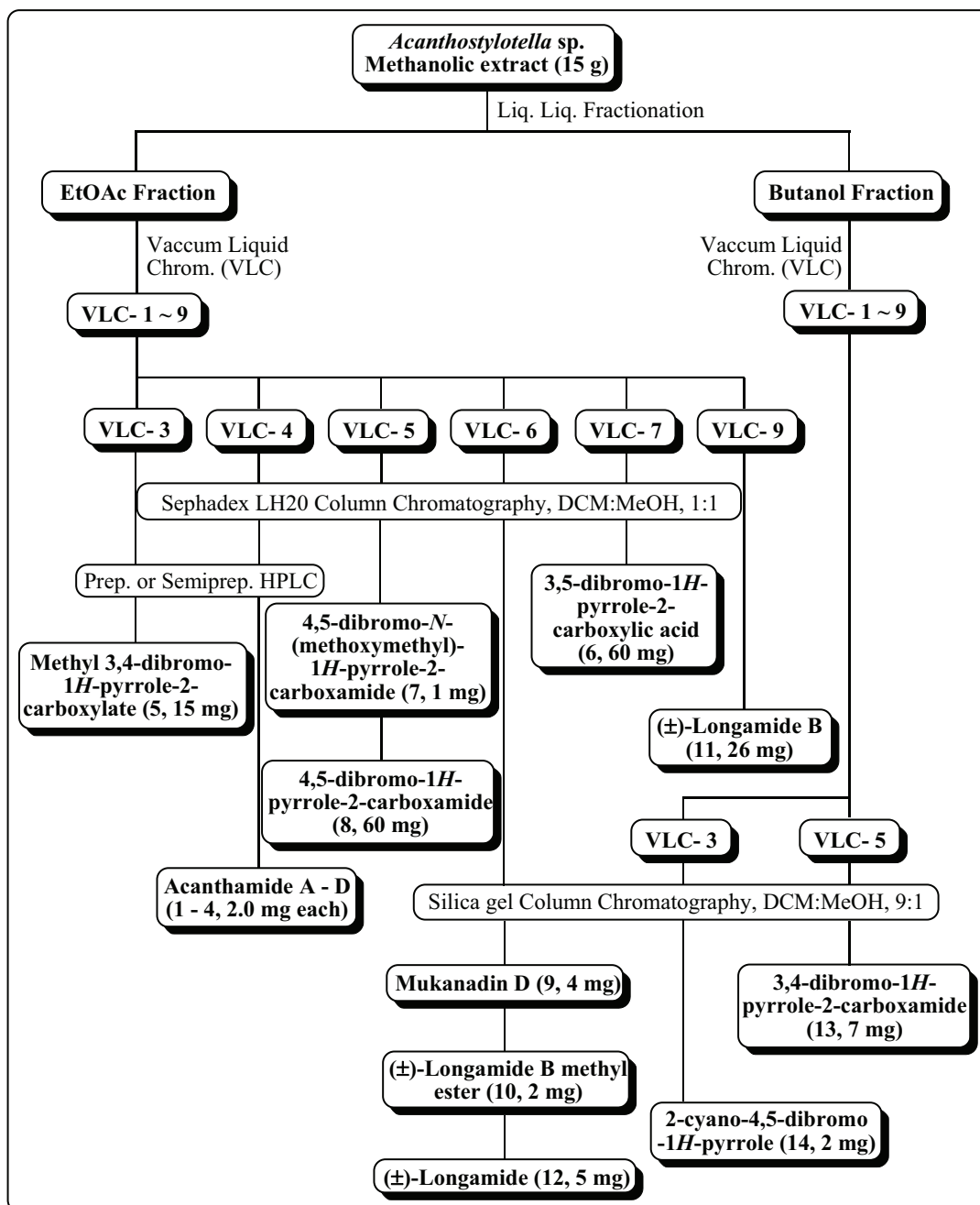
Materials and Methods

2.2.3.4. Solvents for NMR

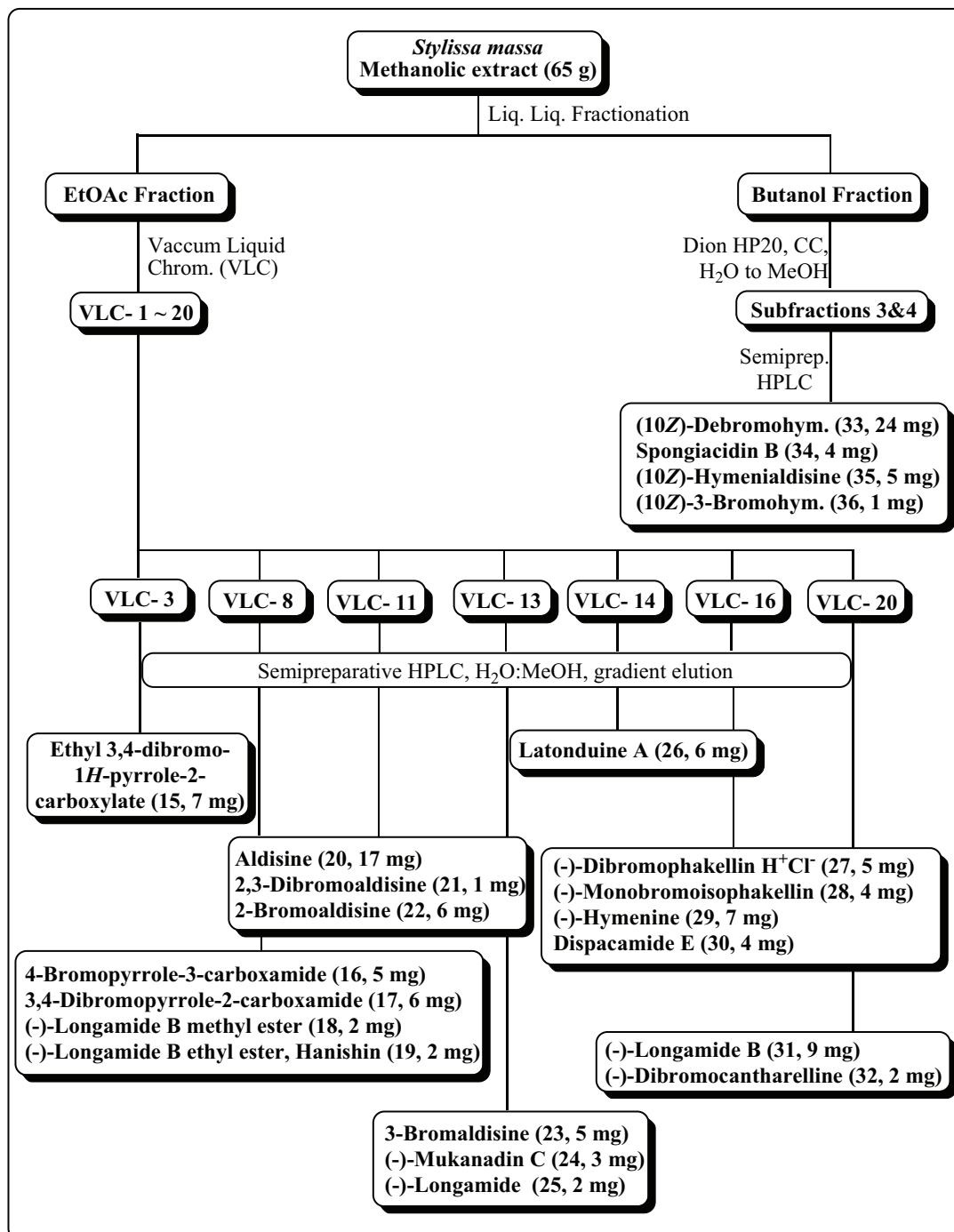
Chloroform- <i>d</i>	Uvasol, Merk
DMSO- <i>d</i> ₆	Uvasol, Merk
Methanol- <i>d</i> ₄	Uvasol, Merk
Pyridine- <i>d</i> ₅	Uvasol, Merk

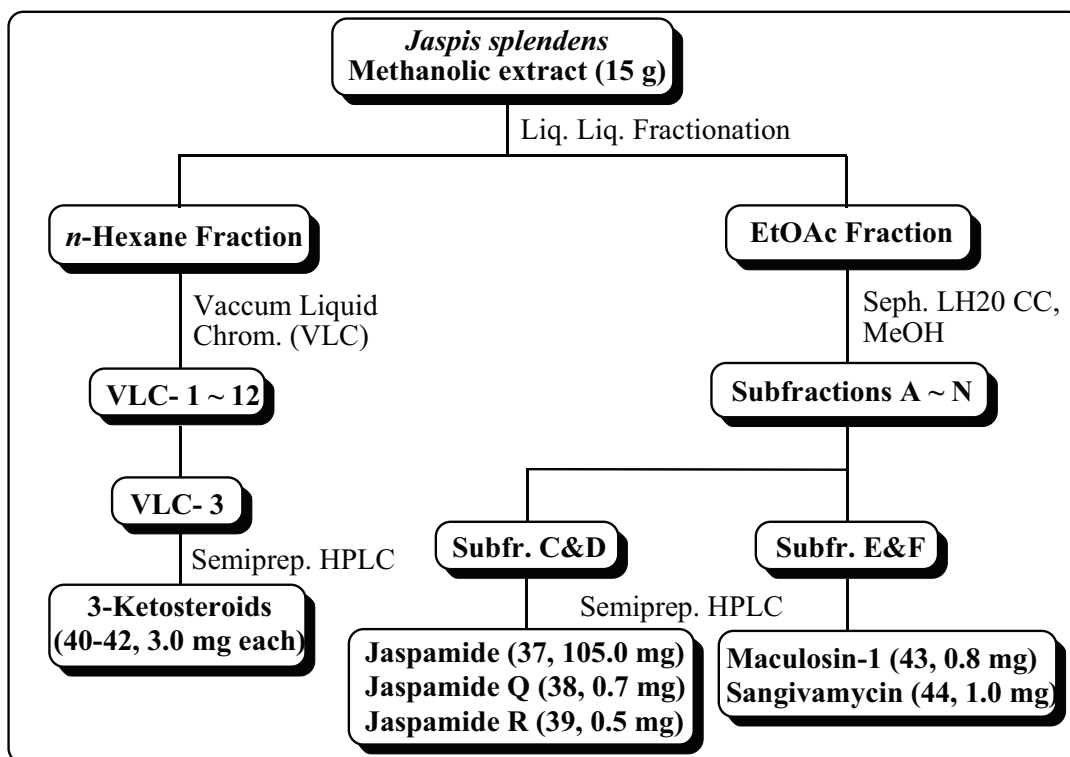
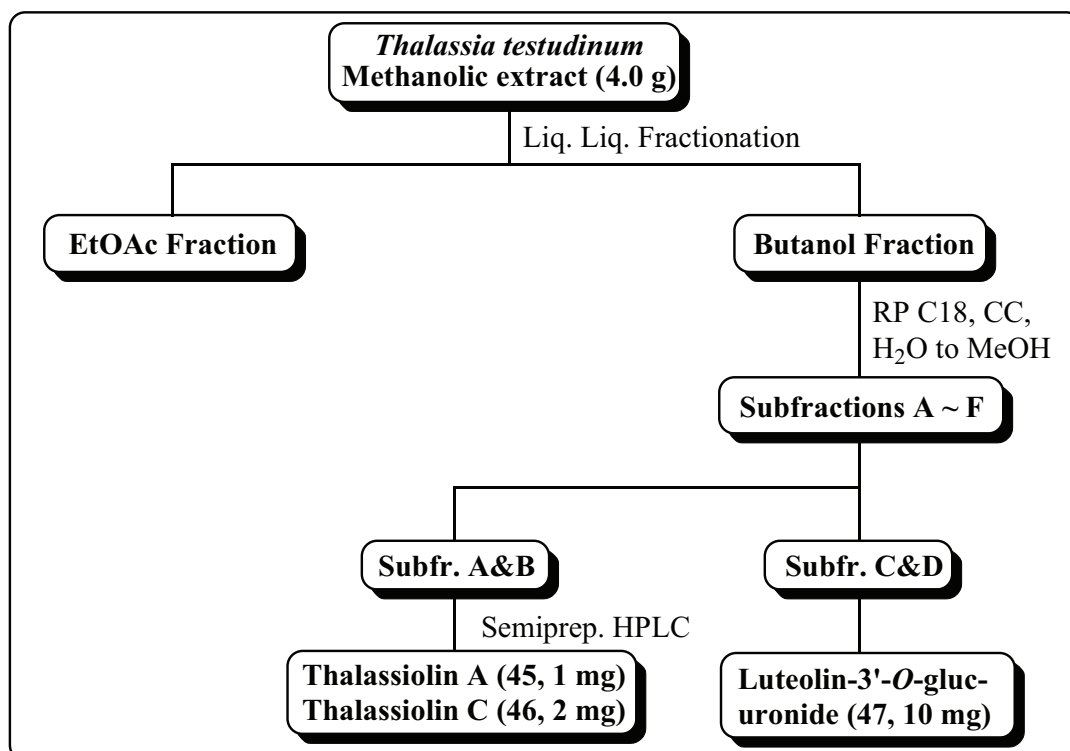
2.3. Methods

2.3.1. Isolation and purification of secondary metabolites

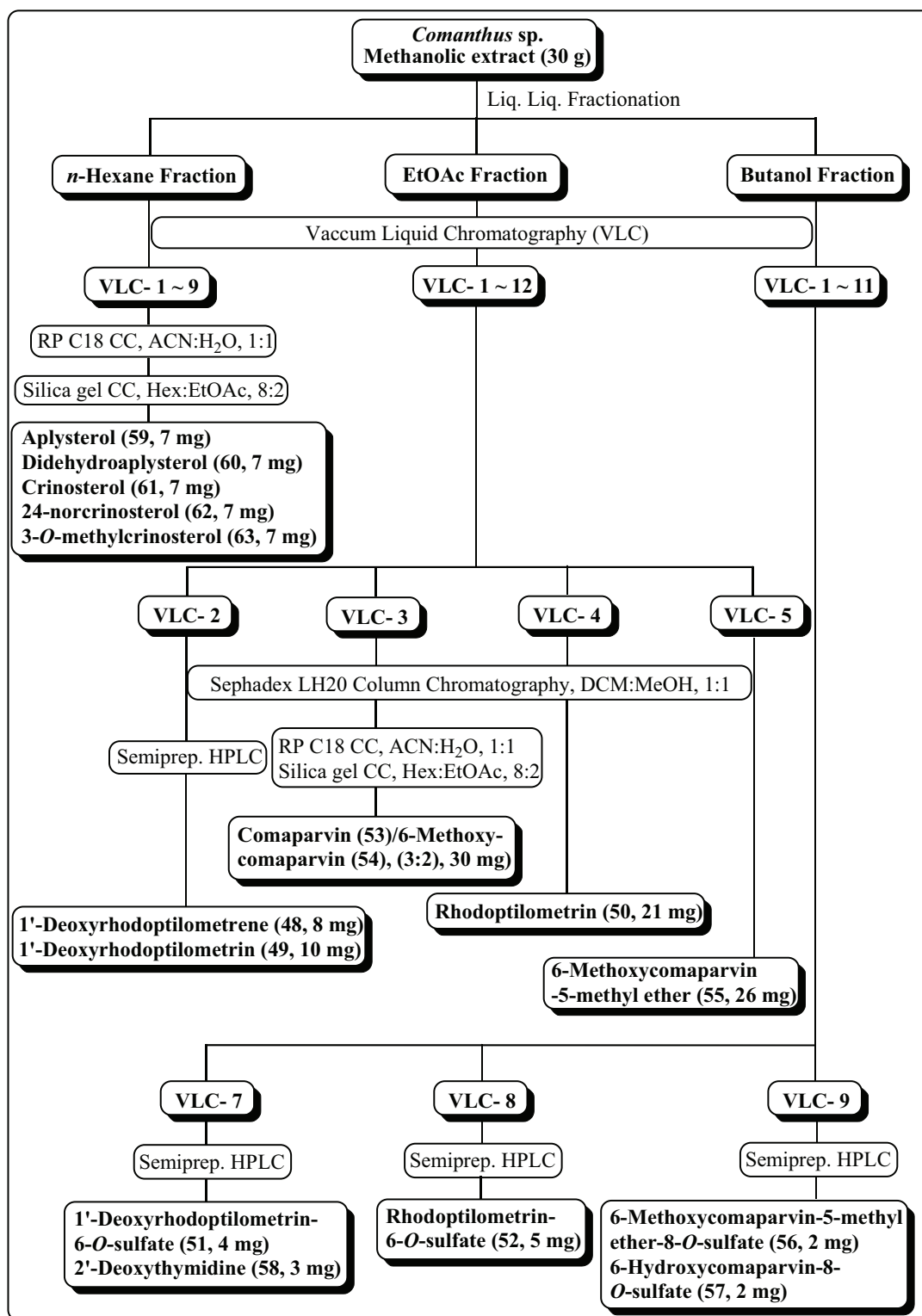
2.3.1.1. Isolation of secondary metabolites from *Acanthostylotella* sp.

2.3.1.2. Isolation of secondary metabolites from *Stylissa massa*



2.3.1.3. Isolation of secondary metabolites from *Jaspis splendens*2.3.1.4. Isolation of secondary metabolites from *Thalassia testudinum*

2.3.1.5. Isolation of secondary metabolites from *Comanthus* sp.



2.3.2. Chromatographic methods

2.3.2.1. Thin layer chromatography (TLC)

Chromatography refers to any separation method in which the components are distributed between two different phases, stationary phase and mobile phase. The components separate because of having different affinities for these two phases. Therefore, they move at different rates along the TLC plates and the column. TLC was performed on pre-coated TLC plates with silica gel 60 F₂₅₄ (layer thickness 0.2 mm, E. Merk, Darmstadt, Germany) using the following eluents:

For polar compounds	EtOAc:MeOH:H ₂ O (30:5:4, 30:6:5, and 30:7:6)
For semi-polar compounds	DCM:MeOH (95:5, 90:10, 85:15, 80:20, and 70:30) DCM:MeOH:EtOAc (90:10:5, and 80:20:10)
For non-polar compounds	<i>n</i> -Hexane:EtOAc (95:5, 90:10, 85:15, 80:20, and 70:30) <i>n</i> -Hexane:MeOH (95:5, and 90:10)

TLC on reversed phase RP18 F₂₅₄ (layer thickness 0.25 mm, Merk, Darmstadt, Germany) was used for polar substances and using different solvent systems of MeOH:H₂O (90:10, 80:20, 70:30, and 60:40). The band separation on TLC was detected under UV lamp at 254 and 366 nm, followed by spraying TLC plates with anisaldehyde/H₂SO₄ or vanillin/H₂SO₄ reagent and they were heated subsequently at 110°C.

2.3.2.2. Vacuum liquid chromatography (VLC)

Vacuum liquid chromatography is a useful method as an initial isolation procedure for samples having relatively large weights. The apparatus consists of a 500 cm sintered glass filter funnel with an inner diameter of 12 cm. Silica gel 60 was packed to a hard cake at a height of 5–10 cm under applied vacuum. The sample used as adsorbed onto a small amount of silica gel using volatile solvents. The resulting sample mixture was then packed onto top of the column. Using step gradient elution with non-polar solvent (e.g. *n*-Hexane or DCM) and increasing amounts of polar solvents (e.g. EtOAc or MeOH) successive fractions were collected. The flow was produced by vacuum and the column was allowed to run dry after each fraction collected.

Materials and Methods

2.3.2.3. Column chromatography

Fractions derived from VLC were subjected to repeated separation through column chromatography using appropriate stationary and mobile phase solvent systems previously determined by TLC. The following separation systems were used:

- I. Normal phase chromatography using a polar stationary phase, typically silica gel, in conjunction with a non-polar mobile phase (e.g. *n*-Hexane, DCM) with gradually increasing amount of a polar solvent (e.g. EtOAc or MeOH). Thus, hydrophobic compounds elute quicker than hydrophilic compounds.
- II. Reversed phase (RP) chromatography using a non-polar stationary phase and a polar mobile phase (e.g. H₂O, MeOH). The stationary phase consists of silica packed with *n*-alkyl chains covalently bound. For instance, C-8 signifies an octanyl chain and C-18 an octadecyl ligand in the matrix. The more hydrophobic the matrix on each ligand, the greater the tendency of the column to retain hydrophobic moieties. Thus, hydrophilic compounds elute more quickly than do hydrophobic compounds. Elution was performed using H₂O with gradually increasing amount of MeOH.
- III. Size exclusion chromatography involves separations based on molecular size of compounds being analyzed. The stationary phase consists of porous beads (Sephadex LH-20). Compounds having larger molecular size will be excluded from the interior of the bead and thus will firstly elute, while compounds with smaller molecular size will enter the beads and elute according to their ability to exit from the small sized pores where they were trapped. Elution was performed using MeOH or MeOH:DCM (1:1).
- IV. Ion exclusion chromatography uses ion exchange resin beds (Diaion HP-20) that acts as a charged solid separation medium. The components of the processed sample have different electrical affinities to his medium and consequently they differently retained by the resin according to their different affinities.

2.3.2.4. Flash chromatography

Flash chromatography is a preparative column chromatography based on optimized pre-packed columns and an air pressure driven eluent at a high flow rate. It is a simple and quick technique widely used to separate a variety of organic compounds. Normally, the columns are dry Silica Gel 60 GF₂₅₄ pre-packed, of 18 cm height, vertically clamped and assembled in the system. The column is filled and saturated with the desired mobile phase just prior to sample loading. Samples are dissolved in a small volume of the initial solvent used and the resulting mixture was then packed onto the top of the column using special

syringe. The mobile phase (isocratic or gradient elution) is then pumped through the column with the help of air pressure resulting in sample separation. This technique is considered as a low to medium pressure technique and is applied to samples from few milligrams to some gram of sample.

2.3.2.5. Preparative high pressure liquid chromatography (HPLC)

This technique was used for isolation and purification of compounds from fractions previously separated using column chromatographic separation. The most appropriate solvent systems were determined before running the HPLC separation. The mobile phase combination was MeOH or acetonitrile and nanopure H₂O with or without 0.01% TFA or 0.1% formic acid, pumped in gradient or isocratic manner depending on the compounds retention time. Each injection consisted of 20–80 mg of the fraction dissolved in 400 mL of the solvent system. The solvent system was pumped through the column at a rate of 20 mL/min. The eluted peaks were detected by the online UV detector and collected separately in Erlenmeyer flasks.

Preparative HPLC system specifications are described as follows:

Pump	Varian, PrepStar 218
Detector	Varian, ProStar 320 UV-Vis detector
HPLC Program	Varian Star (V.6)
Column	Varian Dynamax (250 × 4.6 mm, ID and 250 × 21.4 mm, ID), pre-packed with Microsorb 60-8 C-18, with integrated pre-column

2.3.2.6. Semi-preparative high pressure liquid chromatography (HPLC)

This process is used for purification of compounds from fractions previously separated using column chromatography separation. The most appropriate solvent system was determined before running the HPLC separation. The mobile phase combination was MeOH and nanopure H₂O with or without 0.01% TFA or 0.1% formic acid, pumped in gradient or isocratic manner depending on the compounds retention time. Each injection consisted of 1–3 mg of the fraction dissolved in 1 mL of the solvent system. The solvent system was pumped through the column at a rate of 5 mL/min. The eluted peaks were detected by the online UV detector and collected separately in Erlenmeyer flasks. The separation column (125 × 4 mm, ID) was pre-filled with Eurosphere C18 (Knauer, Berlin, Germany).

Materials and Methods

Semi-preparative HPLC system specifications are described as follows:

Pump	Merk Hitachi L-7100
Detector	Merk Hitachi UV detector L-7400
Column	Knauer (300 × 8 mm, ID), pre-packed with Eurosphere 100–10 C18, with integrated pre-column

2.3.2.7. Analytical high pressure liquid chromatography (HPLC)

Analytical HPLC was used to identify the distribution of peaks either from extracts or fractions, as well as to evaluate the purity of isolated compounds. The solvent gradient used started with MeOH:Nanopure H₂O (10:90), adjusted to pH 2 with phosphoric acid, and reaches 100% MeOH in 35 minutes as a standard gradient, or in 25.5 minutes as a half-time gradient. The autosampler injected 20 μL sample. All peaks were detected by UV-VIS photodiode array detector. In some cases, special programs were used. HPLC instrument consists of the pump, the detector, the injector, the separation column, and the reservoir of mobile phase. The separation column (125 × 2 mm, ID) was pre-filled with Eurosphere-100 C18 (5 μm), with integrated pre-column (Knauer, Berlin, Germany).

LC/UV system specifications are described as follows:

Pump	Dionex P580A LPG
Detector	Dionex Photodiode Array Detector UVD 340S
Column thermostat	STH 585
Autosampler	ASI-100T
HPLC Program	Chromleon (V. 6.3)
Column	Knauer (125 × 4 mm, ID), pre-packed with Eurosphere 100–5 C18, with integrated pre-column

2.3.3. Structure elucidation of the isolated secondary metabolites

2.3.3.1. Mass spectrometry (MS)

Mass spectrometers use the difference in mass-to-charge ratio (m/z) of ionized molecules to separate them from each other. Mass spectrometry is therefore useful for quantification of atoms or molecules and also for determination of chemical and structural information of molecules. A mass spectrometer consists of an ion source, ion detector, and mass-selective

analyzer. The output of mass spectrometers shows a plot of relative intensity vs. the mass-to-charge ratio (m/z).

2.3.3.1.1. Electrospray ionization mass spectrometry (ESI-MS)

A mass spectrometer is an analytical instrument used to determine the molecular weight of a compound. Principally, mass spectrometers are divided into three parts; ionization source, analyzer, and detector, which should be maintained under high vacuum conditions in order to maintain the ions travel through the instrument without any hindrance from air molecules. Once a sample was injected into ionization source, the molecules are ionized. The ions were then passed and extracted into the analyzer. In the analyzer, the ions were separated according to their mass (m) to charge (z) ratio (m/z). Once the separated ions flow into the detector, the signals are transmitted to the data system where the mass spectrum is recorded.

Liquid chromatography / Mass spectrometry (LC/MS)

High pressure liquid chromatography is a powerful method for the separation of complex mixtures, especially when many of the components may have similar polarities. If a mass spectrum of each component can be recorded as it elutes from the LC column, quick characterization of the components is greatly facilitated. Usually, ESI-MS is interfaced with LC to make an effective online LC/MS. HPLC/ESI-MS was carried out using a Finnigan LCQ-DECA mass spectrometer connected to a UV detector. The samples were dissolved in H₂O/MeOH mixtures and injected to HPLC/ESI-MS set-up. For standard LC/MS measurements, a solvent gradient that started with acetonitrile:nanopure H₂O (10:90), adjusted with 0.1 % HCOOH, and reached to 100 % acetonitrile in 35 minutes was used.

LC/UV/MS system specifications are described as follows:

HPLC system	Agilent 1100 series (pump, detector, and autosampler)
MS spectrometer	Finnigan LC Q-DECA
Column	Knauer, (250 × 2 mm, ID), pre-packed with Eurosphere 100-5 C18, with integrated pre-column

2.3.3.1.2. Electron impact mass spectrometry (EI-MS)

Analysis involves vaporizing a compound in an evacuated chamber and then bombarding it with electrons having 25.80 eV (2.4–7.6 MJ/mol) of energy. The high energy electron

Materials and Methods

stream not only ionizes an organic molecule (requiring about 7–10 eV) but also causes extensive fragmentation (the strongest single bonds in organic molecules have strengths of about 4 eV). The advantage is that fragmentation is extensive, giving rise to a pattern of fragment ions which can help to characterize the compound. The disadvantage is the frequent absence of a molecular ion.

Low resolution EI-MS was measured on a Finnigan MAT 8430 mass spectrometer. Measurements were done by Dr. Peter Tommes, Institute for Inorganic and Structural Chemistry, Heinrich-Heine University, Duesseldorf.

2.3.3.1.3. Fast atom bombardment mass spectrometry (FAB-MS)

This was the first widely accepted method that employs energy sudden ionization. FAB is useful for compounds, especially polar molecules, unresponsive to either EI or CI mass spectrometry. It enables both non-volatile and high molecular weight compounds to be analyzed. In this technique, a sample is dissolved or dispersed in a polar and relatively non-volatile liquid matrix, introduced into the source on a copper probe tip. Then, this matrix is bombarded with a beam of atoms of about 8 Kev. It uses a beam of neutral gas (Ar or Xe atoms) and both positive and negative ion FAB spectra can be obtained.

Low resolution FAB-MS was measured by a Finnigan MAT 8430 mass spectrometer. Measurements were done by Dr. Peter Tommes, Institute for Inorganic and Structural Chemistry, Heinrich-Heine University, Duesseldorf.

2.3.3.1.4. High resolution mass spectrometry (HR-MS)

High resolution is achieved by passing the ion beam through an electrostatic analyzer before it enters the magnetic sector. In such a double focusing mass spectrometer, ion masses can be measured with an accuracy of about 1 ppm. With measurement of this accuracy, the atomic composition of the molecular ions can be determined.

HRESI-MS was measured on a Micromass Qtof 2 mass spectrometer at Helmholtz Centre for Infection Research, Braunschweig. The time-to-flight analyzer separates ions according to their mass-to-charge ratios (m/z) by measuring the time it takes for ions to travel through a field free region known as the flight.

2.3.3.2. Nuclear magnetic resonance spectroscopy (NMR)

Nuclear magnetic resonance is a phenomenon which occurs when the nuclei of certain atoms are immersed in a static magnetic field and exposed to a second oscillating magnetic field. Some nuclei experience this phenomenon, and others do not, dependent upon

whether they possess a property called spin. It is used to study physical, chemical, and biological properties of matter. As a consequence, NMR spectroscopy finds applications in several areas of science. NMR spectroscopy is routinely used by chemists to study chemical structure using simple one dimensional technique. Two dimensional techniques were used to determine and confirm the structure of more complicated molecules.

NMR spectra were recorded at 300° K on a Bruker ARX-500 by Dr. Peter Tommes, Institute for Inorganic and Structural Chemistry, Heinrich-Heine University, Duesseldorf. Some measurements were also performed at the Helmholtz Centre for Infection Research, Braunschweig, by Dr. Victor Wray using an AVANCE DMX-600 NMR spectrometer. All 1D and 2D spectra were obtained using the standard Bruker software. The samples were dissolved in different solvents, the choice of which was dependent on the solubility of the samples. Residual solvent signals were used as internal standards (reference signal). The observed chemical shift (δ) values were given in ppm and the coupling constants (J) in Hz.

2.3.3.3. Optical activity

Optically active compounds contain at least one chiral centre. Optical activity is a microscopic property of a collection of these molecules that arises from the way they interact with light. Optical rotation was determined on a Perkin-Elmer-241 MC polarimeter. The substance was stored in a 0.5 mL cuvette with 0.1 dm length. The angle of rotation was measured at the wavelength at 546 and 579 nm of a mercury vapour lamp at room temperature (25°C). The specific optical rotation was calculated using the expression:

$$[\alpha]_D^T = \frac{[\alpha]_{579} \times 3.199}{4.199 - \frac{[\alpha]_{579}}{[\alpha]_{546}}}$$

with $[\alpha]_D^T$ = Specific rotation at the wavelength of Sodium D-line, 589 nm, at certain temperature T.

$[\alpha]_{579}$ and $[\alpha]_{546}$ = Optical rotation at wavelengths 579 and 546 nm, respectively, calculated using the formula:

$$[\alpha]_\lambda = \frac{100\alpha}{l \times c}$$

where α = the measured angle of rotation in degrees,

l = the length in dm of the polarimeter tube,

c = the concentration of the substance expressed in g/100 mL.

Materials and Methods

2.3.3.4. Determination of absolute stereochemistry by Mosher reaction

The reaction was performed according to a modified Mosher ester procedure described by Su *et al.* (Ohtani *et al.*, 1991; Su *et al.*, 2002).

Reaction with (*R*)-(-)- α -(trifluoromethyl) phenylacetyl chloride

The compounds (1 mg of each) were transferred into NMR tubes and were dried under vacuum. Deuterated pyridine (0.5 mL) and (*R*)-MTPA chloride were added into NMR immediately under a N₂ gas stream. The reagent was added in the ratio of 0.14 mM reagent to 0.10 mM of the compound (Dale and Mosher, 1973). The NMR tubes were shaken carefully to mix the samples and MTPA chloride evenly. The reaction NMR tubes were permitted to stand at room temperature and monitored by ¹H-NMR until the reaction was completed. ¹H-¹H COSY was measured to confirm the assignment of the signals.

Reaction with (*S*)-(-)- α -(trifluoromethyl) phenylacetyl chloride

Another portion of each compound (1 mg) was transferred into NMR tube. The reaction was performed in the same manner as described before to yield the (*S*)-MTPA ester.

2.3.4. Testing the biological activity(ies)

Finding the biologically important compounds from the marine sources is only achieved if, and when, assay systems have been devised that will allow for successful biologically guided fractionation of the culture extracts.

2.3.4.1. Antimicrobial serial dilution assay

This test was conducted under aseptic conditions using microtiter 96 well plates.

Microorganisms

Crude extracts and isolated pure compounds were tested for activity against the following standard strains:

Gram-positive bacteria	<i>Streptococcus pneumonia</i>
	Multi resistant <i>Staphylococcus aureus</i> (MRSA)
	<i>Enterococcus faecalis</i>
Gram-negative bacteria	<i>Klebsiella, pneumonia</i>
	<i>Esherichia coli</i>
	<i>Pseudomonas aeruginosa</i>

Fungi	<i>Aspergillus fumigatus</i>
	<i>Aspergillus faecalis</i>
	<i>Candida albicans</i>
	<i>Candida krusei</i>
Viruses	Human Rhino Virus (HRV2)
	Human Rhino Virus (HRV8)
	Human Rhino Virus (HRV39)
	Respiratory Syncytial Virus A (RSVA)

Antimicrobial screening assay

Test samples were dissolved in 0.2 mL DMSO followed by dilution in 800 μ L cell culture water. For further use, pure compounds were diluted from 250 to 62.5 μ g/mL and extracts from 1250 to 312 μ g/mL in MHB medium for bacterial screening and in Sabouroud medium, for fungal screening. Afterwards the substance/extract solution was overlaid with the microbes (10^4 CFU/mL). Then plates were incubated at 35°C for 24 h and 48 h to allow bacterial and fungal growth, respectively. As negative control an antibiotic/antimycotic mix was used in addition to a non treated infected control (positive). The test was analysed by checking the microbial growth with the visible eye and by measurement of the turbidity at 650 nm. All procedures were done under aseptic conditions in a sterile laminar air flow according to good laboratory practice.

Antiviral screening assay

Test samples were serially diluted in DMSO with concentrations declining from 50 to 0.39 μ g/mL. Afterwards, the substances were mixed with a viral solution in a concentration of 10^4 CFU/mL. Then, the mixture was incubated for 15 minutes and then transferred on to the HeLa cells. Cell growth was checked firstly with visible inspection under the microscope after 24 h at 35°C. After 72 h incubation period, the plates were stained with crystal violet to control cell growth. Evaluation was done with a multiple-plate reader.

Determination of minimum inhibitory concentration (MIC)

Minimum inhibitory concentration is defined as the least concentration of an antimicrobial required to inhibit or control the growth of a micro-organism.

Substances with an activity around 125 μ g/ml and extracts with 625 μ g/ml were considered as possible candidates for further antimicrobial screening. With these positive

Materials and Methods

candidates, MIC assays were performed to determine their exact values. Therefore the substances/extracts were diluted from 125 $\mu\text{g/mL}$ to 0.24 $\mu\text{g/mL}$ and screened in the same manner as in the primary screening. MICs were distinguished as the least dilutions of the substances/extracts that revealed no microbial growth visibly or by measurement of the turbidity at 650 nm.

2.3.4.2. Cytotoxicity assay

2.3.4.2.1. Microculture tetrazolium (MTT) Assay

Cytotoxicity assays were carried out by Prof. Dr. W. E. G. Müller, Institute for Physiological Chemistry and Pathobiochemistry, University of Mainz, Mainz. Cytotoxicity was tested against L5178Y mouse lymphoma cells using microculture tetrazolium (MTT) assay, and compared to that of untreated controls (Carmichael *et al.*, 1987).

Cell cultures

L5178Y mouse lymphoma cells were grown in Eagle's minimal essential medium supplement with 10 % horse serum in roller tube culture. The medium contained 100 units/mL penicillin and 100 $\mu\text{g/mL}$ streptomycin. The cells were maintained in a humidified atmosphere at 37°C with 5% CO₂.

MTT colorimetric assay

Of the test samples, stock solutions in ethanol 96% (v/v) were prepared. Exponentially, growing cells were harvested, counted, and diluted appropriately. Of the cell suspension, 50 μL containing 3750 cells were pipetted into 96-well microtiter plates. Subsequently, 50 μL of a solution of the test samples containing the appropriate concentration was added to each well. The concentration range was 3 and 10 $\mu\text{g/mL}$. The small amount of ethanol present in the wells did not affect the experiments. The test plates were incubated at 37°C with 5% CO₂ for 72 h. A solution of 3-(4,5-dimethylthiazol-2-yl)-2,5-diphenyltetrazolium bromide (MTT) was prepared at 5 mg/mL in phosphate buffered saline (PBS; 1.5 mM KH₂PO₄, 6.5 mM Na₂HPO₄, 137 mM NaCl, 2.7 mM KCl; pH 7.4) and from the solution, 20 μL was pipetted into each well. The yellow MTT penetrates the healthy living cells and in the presence of mitochondrial reductase, MTT is transformed to its blue formazan complex. After an incubation period of 3 h 45 min at 37°C in a humidified incubator with 5% CO₂, the medium was centrifuged (15 min, 20°C, 210 x g) with 200 μL DMSO, the cells were lysed to liberate the formed formazan product. After thorough mixing, the absorbance was measured at 520 nm using a scanning microtiter-well spectrophotometer.

The colour intensity is correlated with the number of healthy living cells. Cell survival was calculated using the formula:

$$\text{Survival \%} = 100 \times \frac{\text{Absorbance of treated cells} - \text{Absorbance of culture medium}}{\text{Absorbance of untreated cells} - \text{Absorbance of culture medium}}$$

All experiments were carried out in triplicates and repeated three times. As controls, media with 0.1% EGMME/DMSO were included in the experiments.

2.3.4.2.2. Protein kinase assay

Protein kinase assays were carried out by Dr. Michael Kubbutat (ProQinase GmbH, Freiburg, Germany).

Protein kinase enzymes are integral components of numerous signal transduction pathways involved in the regulation of cell growth, differentiation, and response to changes in the extracellular environment. Consequently, kinases are major targets for potentially developing novel drugs to treat diseases such as cancer and various inflammatory disorders. The inhibitory potency of the samples was determined using 24 protein kinases (Table 2.1).

The IC₅₀ profile of the compounds and/or fractions showing an inhibitory potency of ≥ 40 % with at least one of the 24 kinases at an assay concentration of 1×10⁻⁰⁶ g/mL was determined. IC₅₀ values were measured by testing 10 concentrations of each sample in singlicate (n=1).

Sample preparation

The compounds/fractions were provided as 1×10⁻⁰³ g/mL stock solutions in 100% DMSO (1000 or 500 μL) in micronic boxes. The boxes stored at -20°C. Prior to the assays, 100 μL of the stock solutions was transferred into separate microtiter plates. Subsequently, they were subjected to serial, semi-logarithmic dilution using 100% DMSO as a solvent resulting in 100 different concentrations, using 100% DMSO as control. Then, 7 × 5 μL of each concentration were aliquoted and diluted with 45 μL H₂O only a few minutes before being transferred into the assay plate to minimize precipitation. The plates were shaken thoroughly and then used for the transfer of 5 μL compound solution into the assay plates.

Recombinant protein kinases

All protein kinases were expressed in Sf9 insect cells as human recombinant GST-fusion proteins or His-tagged proteins by means of the baculovirus expression system. Kinases were purified by affinity chromatography using either GSH-agarose (Sigma) or Ni-NTH-agarose (Qiagen). Purity was checked by SDS-PAGE/silver staining and the

Materials and Methods

identity of each kinase was verified by western blot analysis with kinase specific antibodies or by mass spectrometry.

Protein kinase assay

A proprietary protein kinase assay (³³PanQinase[®] Activity Assay) was used for measuring the kinase activity of the protein kinases. All kinase assays were performed in 96-well FlashPlates[™] from Perkin Elmer/NEN (Boston, MA, USA) in a 50 μ L reaction volume. The reaction mixture was pipetted in the following order: 20 μ L assay buffer, 5 μ L ATP solution in H₂O, 5 μ L test compound in 10% DMSO and 10 μ L substrate / 10 μ L enzyme solution (premixed). The assay for all enzymes contained 60 mM HEPES-NaOH (pH 7.5), 3 mM MgCl₂, 3 mM MnCl₂, 3 μ M Na-orhtovanadate, 1.2 mM DTT, 50 μ g/mL PEG₂₀₀₀₀, 1 μ M [γ -³³P]-ATP. The reaction mixtures were incubated at 30°C for 80 minutes and stopped with 50 μ L 2% (v/v) H₃PO₄. The plates were aspirated and washed two times with 200 μ L of 0.9% (w/v) NaCl or 200 μ L H₂O. Incorporation of ³³P_i was determined with a microplate scintillation counter (Microbeta Trilux, Wallac). All assays were performed with a Beckman Coulter/Sagian robotic system.

2.3.4.2.3. Radical scavenging (DPPH) assay

Extracts, fractions and/or pure compounds were evaluated for their ability to function as free radical scavengers. The qualitative test was performed with a rapid TLC screening method using the 2,2-diphenyl-1-picrylhydrazyl radical (DPPH). Analytical TLC on Silica gel 60 F₂₅₄ plates were developed under appropriate conditions after application of 10 μ L of each test compound solution (1 mg/mL), dried and sprayed with DPPH solution (0.2% w/v, MeOH); 5 min later active compounds appeared as yellow spots against a purple background. The purple stable free radical 2,2-diphenyl-1-picrylhydrazyl was reduced to the yellow colored diphenylpicryl hydrazine. Quercetin was used as a standard antioxidant.

The quantitative assay was carried out at room temperature as described in 2007 by Tsevegsuren *et al.*: 10 μ L of a methanolic solution of the test compound(s) were added to 490 μ L of a 100 μ M DPPH solution in MeOH. Serial concentrations, ranging from 1.56 to 200 μ M, were prepared and analyzed in triplicate. 490 μ L of 100 μ M DPPH solution in MeOH plus 10 μ L of propyl gallate, 100 μ M solution were used as positive control. 490 μ L of 100 μ M DPPH solution plus 10 μ L of MeOH were used as blank. The absorbance at 517 nm was determined after 30 min incubation and the percentage of DPPH reduction was calculated. The difference between a DPPH blank solution and the positive control

Materials and Methods

was taken as 100% antioxidative activity. The percent antioxidative activity was then calculated from the difference in absorption between the test sample and the DPPH blank as follows:

$$a_A (\%) = [(A_B - A_P) / (A_B - A_{Pos})] \times 100$$

where a_A = % antioxidative activity in comparison with the positive control, A_B = absorption of DPPH solution as blank, A_P = absorption of test sample, and A_{Pos} = absorption of positive control (propylgallate). IC_{50} values were calculated by linear regression (Tsevegsuren *et al.*, 2007). Quercetin was taken as reference compound under the same experimental conditions.

Table 2.1. List of tested protein kinases, their substrates and diseases induced.

Family	Kinase	Substrate	Oncologically relevant mechanism	Disease
Serine/Threonine kinases	AKTI/PKB alpha	GCS3(14-27)	Apoptosis	Gastric cancer (Staal, 1987)
	ARK5	Autophos.	Apoptosis	Colorectal cancer (Kusakai <i>et al.</i> , 2004)
	Aurora A	tetra(LRRWSLG)	Proliferation	Pancreatic cancer (Li <i>et al.</i> , 2003)
	Aurora B	tetra(LRRWSLG)	Proliferation	Breast cancer (Keen and Taylor, 2004)
	CDK2/Cyclin A	Histone H1	Proliferation	Pancreatic cancer (Iseki <i>et al.</i> , 1998)
	CDK4/Cyclin D1	Rb-CTF	Proliferation	Breast cancer (Yu <i>et al.</i> , 2006)
	CK2-alpha 1	P53-CTM	Proliferation	Rhabdomyosarcoma (Izeradjene <i>et al.</i> , 2004)
	COT	Autophos.	Proliferation	Breast cancer (Sourvinos, 1999)
	PLK-1	Casein	Proliferation	Prostate cancer (Weichert <i>et al.</i> , 2004)

Materials and Methods

Family	Kinase	Substrate	Oncologically relevant mechanism	Disease
	B-RAF-VE	MEK1-KM	Proliferation	Thyroid cancer (Ouyang <i>et al.</i> , 2006)
	SAK	Autophos.	Proliferation	Colorectal cancer (Macmillan <i>et al.</i> , 2001)
Soluble Tyrosine kinase	FAK	Poly(Glu,Tyr) _{4:1}	Metastasis	Breast cancer (Schmitz <i>et al.</i> , 2005)
	SRC	Poly(Glu,Tyr) _{4:1}	Metastasis	Colon cancer (Dehm <i>et al.</i> , 2001)
Receptor Tyrosine kinase	EGFR	Poly(Glu,Tyr) _{4:1}	Proliferation	Glioblastoma multiform (National Cancer Institute, 2005)
	EPHB4	Poly(Glu,Tyr) _{4:1}	Angiogenesis	Prostate cancer (Xia <i>et al.</i> , 2005)
	ERBB2	Poly(Glu,Tyr) _{4:1}	Proliferation	Gastric carcinoma (Lee <i>et al.</i> , 2005)
	FLT3	Poly (Ala,Glu,Lys,Tyr) _{6:2:4:1}	Proliferation	Leukemia (Menezes <i>et al.</i> , 2005)
	IGF1-R	Poly(Glu,Tyr) _{4:1}	Apoptosis	Breast cancer (Zhang and Yee, 2000)
	INS-R	Poly (Ala,Glu,Lys,Tyr) _{6:2:4:1}	“Counter Kinase”	Ovarian cancer (Kalli <i>et al.</i> , 2002)
	MET	Poly (Ala,Glu,Lys,Tyr) _{6:2:4:1}	Metastasis	Lung cancer (Qiao, 2002)
	PDGFR-beta	Poly (Ala,Glu,Lys,Tyr) _{6:2:4:1}	Proliferation	Prostate cancer (Hofer <i>et al.</i> , 2004)

Family	Kinase	Substrate	Oncologically relevant mechanism	Disease
	TIE-2	Poly(Glu,Tyr) _{4:1}	Angiogenesis	Rheumatoid arthrititis (DeBusk <i>et al.</i> , 2003)
	VEGF-R2	Poly(Glu,Tyr) _{4:1}	Angiogenesis	Pancreatic cancer (Li <i>et al.</i> , 2003)
	VEGF-R3	Poly(Glu,Tyr) _{4:1}	Angiogenesis	Breast cancer (Garces <i>et al.</i> , 2006)

2.3.5. General laboratory equipment

Balances	Mettler 200, Mettler AT 250, Mettler PE 1600, Sartorius MCI AC210S
Centrifuge	Biofuge pico, Heraeus
Cleanbench	HERAsafe, Heraeus
Digital pH meter	420Aplus, Orion
Drying Ovens	Kelvitront, Heraeus
Fraction collector	Cygnnet, ISCO
Freeze dryer	Lyovac GT2, Steris
-80°C Freezer	Forma Scientific, 86-Freezer
Hot plate	Camag
Magnetic stirrer	Combi Mag, IKA
Rotary evaporator	Vacuubrand, IKA
Sonicator	Sonorex RK 102, Bandelin
Syringes	Hamilton
Ultra Turrax	T18 basic, IKA
UV lamp	Camag (254 and 366)
Vacuum centrifuge	SpeedVac SPD 111V, Savant

Results

3. Results

3.1. Secondary metabolites isolated from *Acanthostylotella* sp.

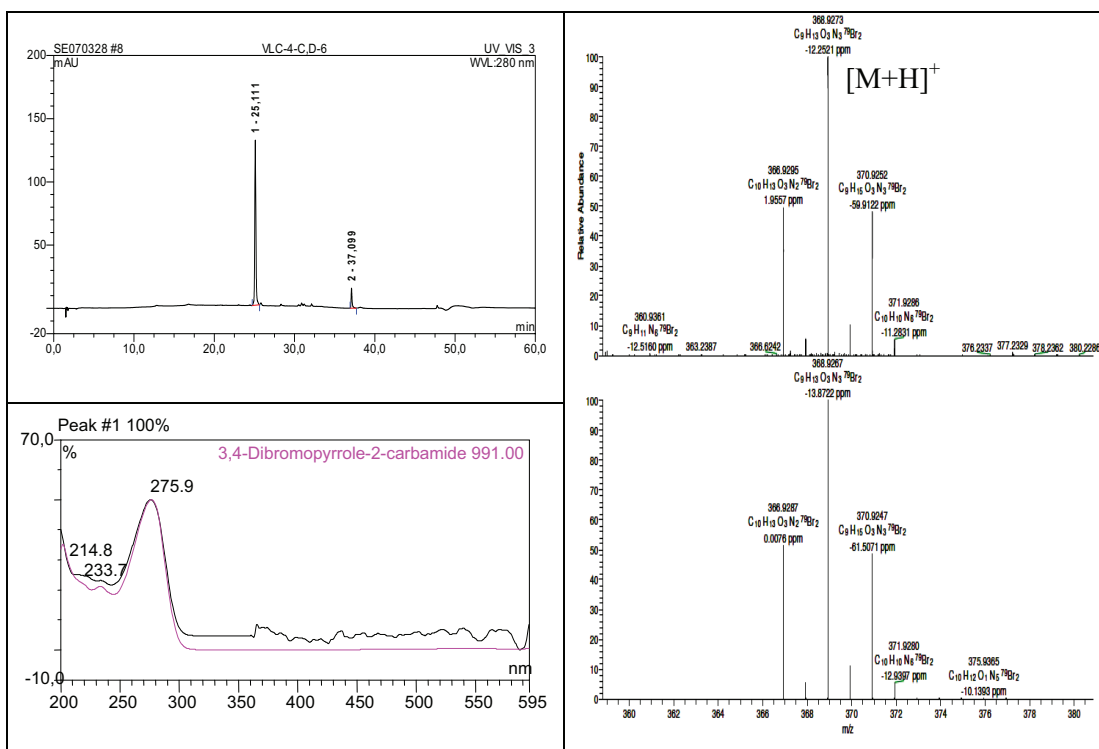
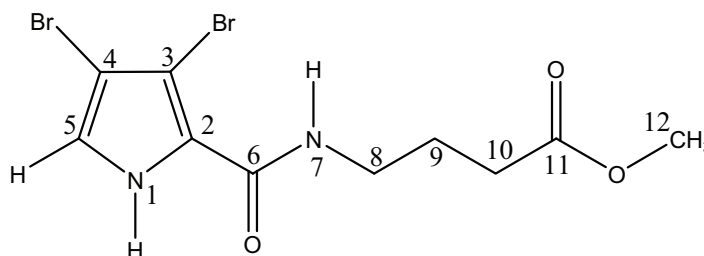
In this study, we investigated an undescribed species of the genus *Acanthostylotella* (class Demospongiae, order Poecilosclerida, family Raspailiidae), collected at the East side of Nusa Lembongan, Selat Ceningan, Bali, Indonesia in 2001. Total methanolic extract of the sponge was subjected to liquid-liquid partition technique against *n*-Hexane, EtOAc, and BuOH. The EtOAc soluble fraction was then subjected to VLC and eluted using a stepwise gradient system from 100% *n*-Hexane to 100% EtOAc, and from 100% DCM to 100% MeOH. Each fraction was purified by column chromatography using Sephadex LH-20 as a stationary phase and either MeOH or DCM:MeOH (1:1) as a mobile phase followed by either preparative or semi-preparative reversed phase HPLC (C18 Eurosphere 100) when required using the appropriate gradient elution of MeOH:H₂O.

This afforded six new dibromopyrrole alkaloids (**1–6**) in addition to eight known compounds (**9–14**). The optical rotations of compounds **10**, **11**, and **12** were determined which indicated that they were all racemate mixtures. Isolated compounds were tested for different bioactivities, including cytotoxicity, antimicrobial, protein kinase, and radical scavenging activities.

In this part, we would present the results of the chemical investigation of the natural products produced by *Acanthostylotella* sp.

3.1.1. Acanthamide A (1, new natural product)

Acanthamide A	
Synonym(s)	Methyl 4-(3,4-dibromo-1 <i>H</i> -pyrrole-2-carboxamido) butanoate
Sample code	VLC-4-C,D-6
Biological source	<i>Acanthostylotella</i> sp.
Sample amount	2.0 mg
Physical description	White amorphous solid
Molecular formula	C ₁₀ H ₁₂ ⁷⁹ Br ₂ N ₂ O ₃
Molecular weight	368 g/mol
Retention time (HPLC)	25.1 min (standard gradient)



Results

Compound (**1**) was obtained as a white amorphous solid. The molecular formula of **1** was revealed to be $C_{10}H_{12}^{79}Br_2N_2O_3$ by HRESIMS (m/z 366.9296 $[M+H]^+$, Δ +2.4 ppm), and the existence of two bromine atoms in the compound was supported by ESI mass spectrum which exhibited pseudomolecular ion peaks at m/z 366, 368, and 370 in a ratio of 1:2:1. The UV absorption [λ_{max} 276 nm] was indicative of a substituted pyrrole chromophore (Forenza *et al.*, 1971; Garcia *et al.*, 1973). Structural elucidation of **1** was based on results of 1D and 2D NMR spectral analyses including 1H NMR, 1H — 1H COSY, and HMBC (Table 3.1), (Fig. 3.1). The position of the aromatic proton [δ_H 6.90 (*d*, 2.2 Hz)] at C-5 of the pyrrole ring was established based on the 1H — 1H COSY spectrum that showed a clear correlation between the aromatic proton and *NH* proton of the pyrrole ring. In addition to 1H — 1H COSY, the HMBC spectra confirmed the nature of the side chain and its attachment to C-2 of the pyrrole ring. The 1H — 1H COSY spectrum further disclosed the presence of one spin system extending from *NH*-7 to the methylene group at C-10 passing over two other methylene groups at positions 8 and 9. The HMBC spectrum (Fig. 3.1) unambiguously proved the attachment of the side chain to the carbonyl group C-6 by exhibiting correlations between both the amide proton (*NH*-7) [δ_H 8.12 (*t*, 6.3 Hz)] and the methylene protons at C-8 [δ_H 3.20 (*q*, 6.3 Hz)] to the carbonyl carbon C-6 (δ_C 159.7). Also, the HMBC spectrum confirmed the presence of a methyl ester group (CH_3 -12) whose protons [δ_H 4.00 (*s*, 3 H)] showed correlations with the methylene protons at C-9 and C-10 to the carbonyl carbon C-11 (δ_C 173.9). From these data, compound **1** was identified as methyl 4-(3,4-dibromo-1*H*-pyrrole-2-carboxamido) butanoate which was named acanthamide A.

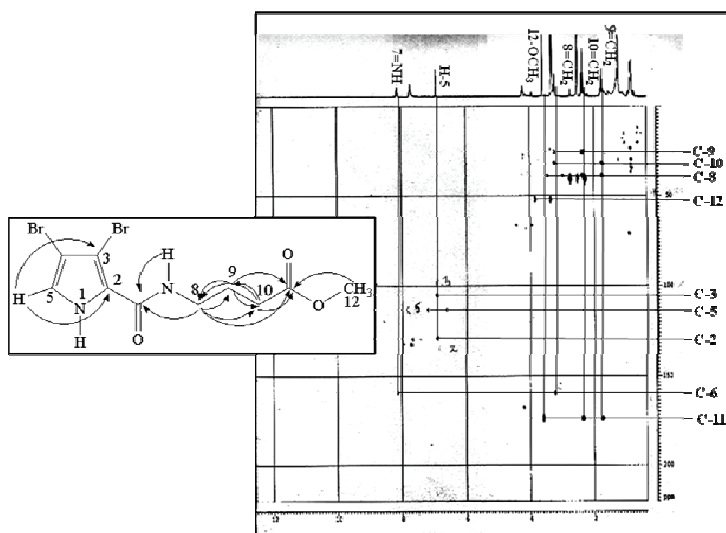
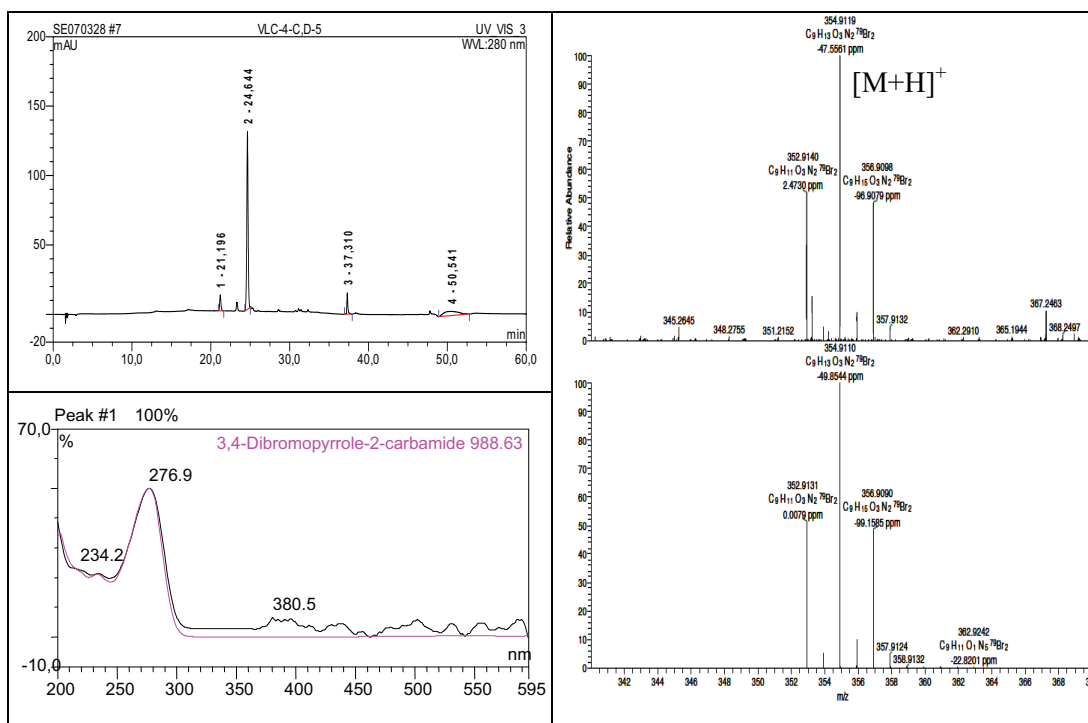
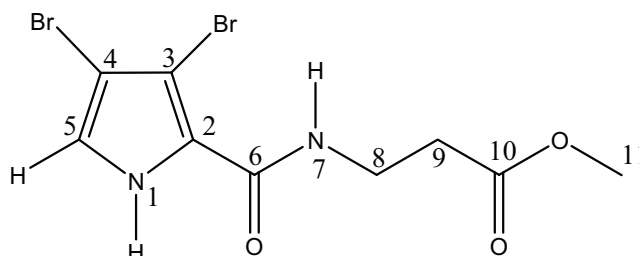


Fig. 3.1. HMBC spectrum and key correlations of acanthamide A (**1**).

3.1.2. Acanthamide B (2, new natural product)

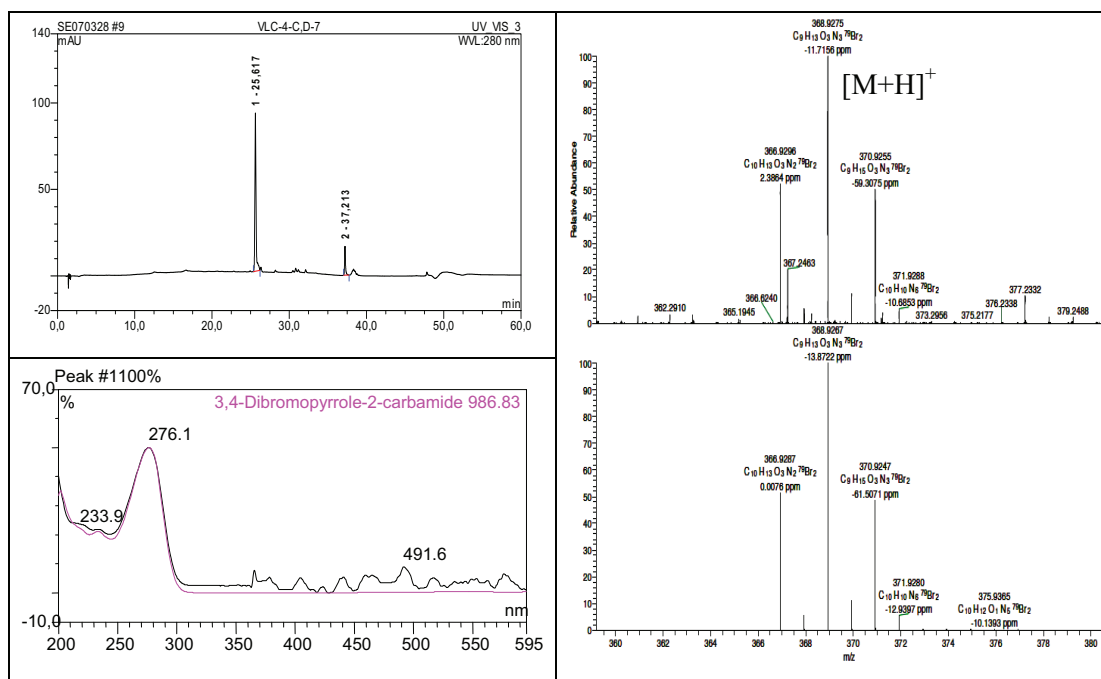
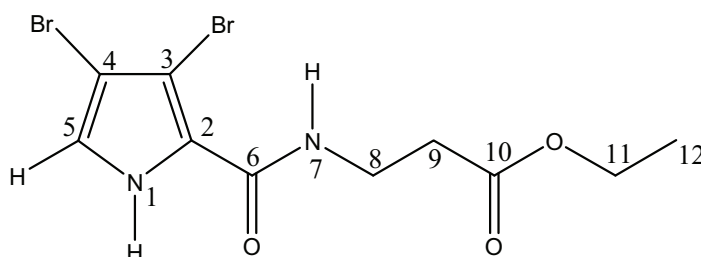
Acanthamide B	
Synonym(s)	Methyl 3-(3,4-dibromo-1 <i>H</i> -pyrrole-2-carboxamido)propanoate
Sample code	VLC-4-C,D-5
Biological source	<i>Acanthostylotella</i> sp.
Sample amount	2.0 mg
Physical description	White amorphous solid
Molecular formula	C ₉ H ₁₀ ⁷⁹ Br ₂ N ₂ O ₃
Molecular weight	354 g/mol
Retention time (HPLC)	24.64 min (standard gradient)



Results

3.1.3. Acanthamide C (3, new natural product)

Acanthamide C	
Synonym(s)	Ethyl 3-(3,4-dibromo-1 <i>H</i> -pyrrole-2-carboxamido) propanoate
Sample code	VLC-4-C,D-7
Biological source	<i>Acanthostylotella</i> sp.
Sample amount	2.0 mg
Physical description	White amorphous solid
Molecular formula	C ₁₀ H ₁₂ ⁷⁹ Br ₂ N ₂ O ₃
Molecular weight	368 g/mol
Retention time (HPLC)	25.62 min (standard gradient)



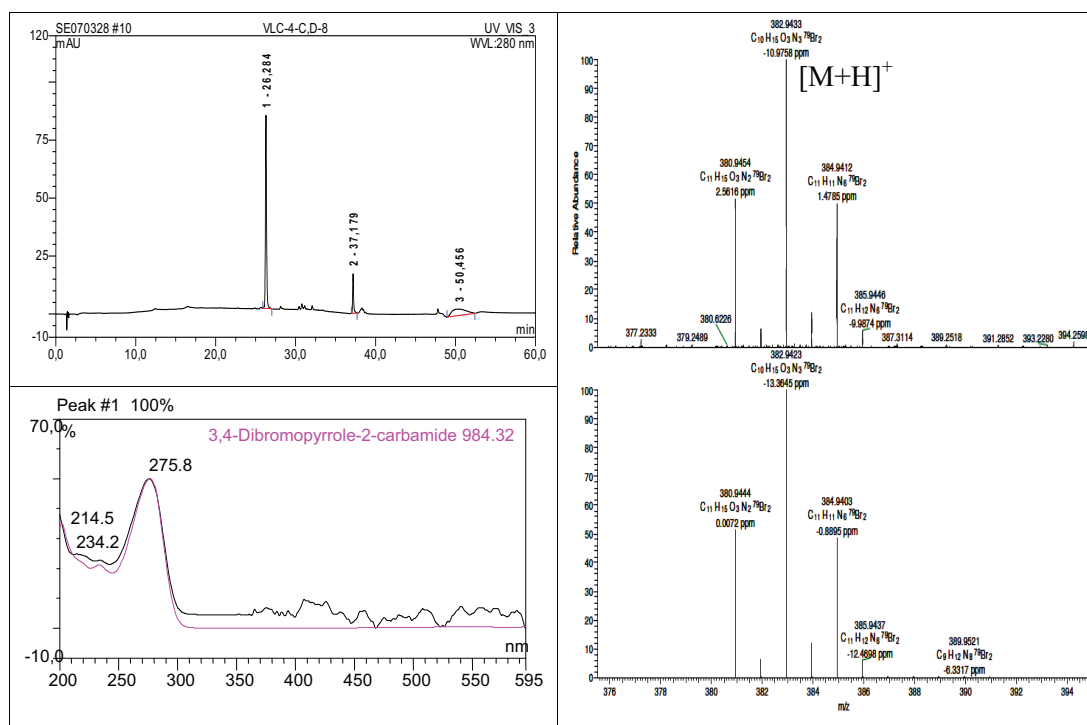
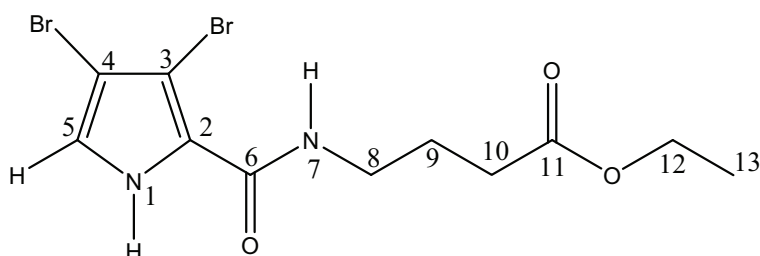
Compound (**2**) was obtained as a white amorphous solid. The ESI mass spectrum of **2** revealed a pseudomolecular ion peaks at m/z 352, 354, and 356, in a ratio of 1:2:1, supporting the presence of two bromine atoms in the compound. The molecular formula was determined as $C_9H_{11}^{79}Br_2N_2O_3$ by HRESIMS (m/z 352.9140 $[M+H]^+$, Δ +2.5 ppm) which differs from that of **1** by the lack of 14 amu. In the 1H -NMR spectrum of **2**, one methylene group present in the spectrum of **1** [δ_H 1.70 (*m*, 2H)] is missing. The structure of **2** was unambiguously established based on 1D and 2D NMR including 1H NMR and 1H — 1H COSY (Table 3.2). The 1H — 1H COSY spectrum exhibited an aromatic proton [δ_H 6.86 (*d*, 2.5 Hz)] at C-5 next to the *NH* proton as observed for compound **1**. The nature of the side chain attached at C-2 of the pyrrole ring was deduced based on the 1H — 1H COSY spectrum which revealed the presence of a CO(NH)—(CH₂)₂— unit thus confirming the connectivity from the amide (*NH*-7) to the methylene group (CH₂-9) through the methylene group at position 8. Thus, the structure of **2** was assigned as methyl 3-(3,4-dibromo-1*H*-pyrrole-2-carboxamido) propanoate; acanthamide B which differs from acanthamide A by lack of one methylene group in the side chain.

Compound (**3**) was isolated from EtOAc soluble fraction as a white amorphous solid. Its molecular formula was established as $C_{10}H_{12}^{79}Br_2N_2O_3$ by HRESIMS (m/z 366.9295 $[M+H]^+$, Δ +2.0 ppm). It exhibited pseudomolecular ion peaks at m/z 367, 369, and 371 in its ESI mass spectrum, in a ratio of 1:2:1, indicating that **3** was a dibrominated compound exhibiting the same molecular formula like compound **1**. Structural confirmation was based on results of 1H NMR and 1H — 1H COSY spectra (Table 3.2). The 1H — 1H COSY spectrum revealed the aromatic proton [δ_H 6.86 (*d*, 2.8 Hz)] at C-5 *ortho* to the *NH* group. The 1H — 1H COSY spectrum further confirmed the connectivity between the amide proton at (*NH*-7) and the methylene group at C-9. It also proved the presence of an ethyl ester group. Compound **3** revealed to be ethyl 3-(3,4-dibromo-1*H*-pyrrole-2-carboxamido) propanoate and it was given the name acanthamide C.

Results

3.1.4. Acanthamide D (4, new natural product)

Acanthamide D	
Synonym(s)	Ethyl 4-(3,4-dibromo-1 <i>H</i> -pyrrole-2-carboxamido) butanoate
Sample code	VLC-4-C,D-8
Biological source	<i>Acanthostylotella</i> sp.
Sample amount	2.0 mg
Physical description	White amorphous solid
Molecular formula	C ₁₁ H ₁₄ ⁷⁹ Br ₂ N ₂ O ₃
Molecular weight	382 g/mol
Retention time (HPLC)	26.28 min (standard gradient)



Compound (**4**) was isolated as a white amorphous solid from EtOAc soluble fraction. Based on HRESIMS, it was shown to have the molecular formula $C_{11}H_{14}^{79}Br_2N_2O_3$ (m/z 380.9454 $[M+H]^+$, Δ +2.5 ppm) which is 14 mass units larger than the molecular weights of **1** and **3**. Moreover, its ESI mass spectrum gave pseudomolecular ion peaks at m/z 380, 382, and 384 confirming the presence of two bromine substituents in the structure of **3**. The structure was confirmed based on 1H NMR and 1H — 1H COSY spectra (Table 3.2) (Fig. 3.2). As for compound **4**, the 1H — 1H COSY spectrum (Fig. 3.2) proved the presence of an ethyl ester group (positions 12 [δ_H 4.00 (*q*, 7.0 Hz, 2H)] and 13 [δ_H 1.20 (*t*, 7.0 Hz, 3H)]). Also, it confirmed the position of the aromatic proton [δ_H 6.90 (*d*, 2.8 Hz)] at C-5 of the pyrrole ring and the position of the side chain at C-2 by establishing the connectivity from the amide proton (NH-7) to the methylene group at C-10. Thus, the structure of **4** was established as ethyl 4-(3,4-dibromo-1*H*-pyrrole-2-carboxamido) butanoate, acanthamide D.

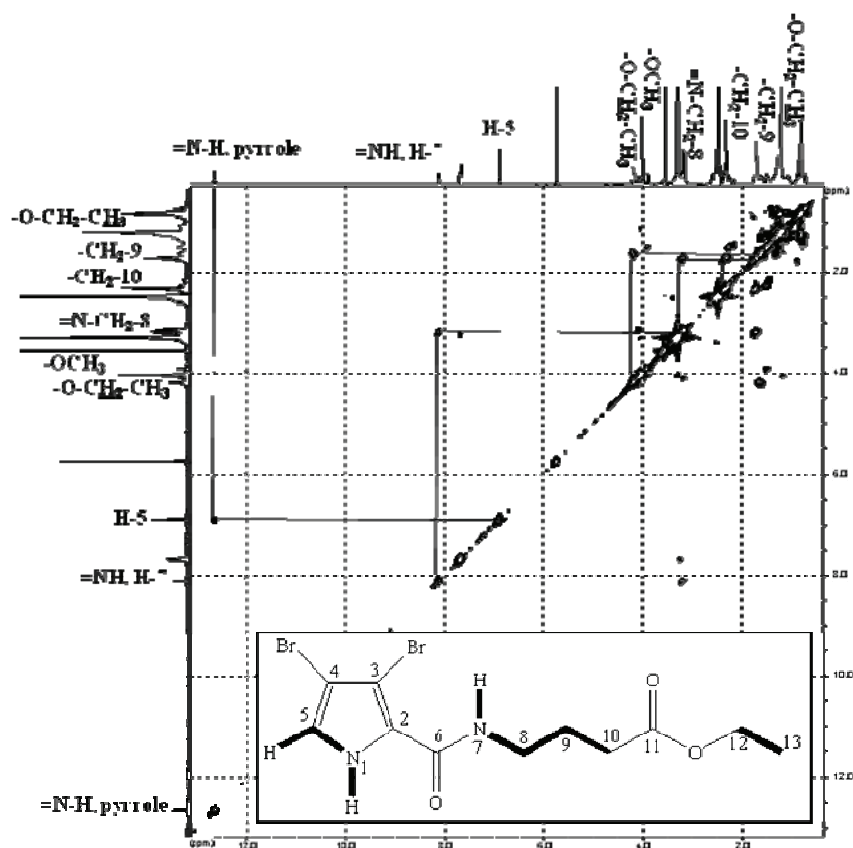


Fig. 3.2. 1H — 1H COSY spectrum of acanthamide D (**4**).

Results

Table 3.1. NMR data of acanthamides A (**1**), measured in DMSO-*d*₆.

H no.	1			
	δ_{H}	COSY	δ_{C}^a	HMBC (C to H)
1-NH	12.65 (1H, br s)	H-1/H-5		
2			128.8	
3			104.9	
4			<i>n.d.</i>	
5	6.90 (1H, <i>d</i> , 2.2 Hz)	H-5/H-1	113.1	CH-2 CH-5
6			159.7	
7-NH	8.12 (1H, <i>t</i> , 6.0 Hz)	H-7/H-8		NH-6 CH ₂ -6
8	3.20 (2H, <i>q</i> , 6.0 Hz)	H-8/H-9	38.7	CH ₂ -10 CH ₂ -10
9	1.70 (2H, <i>m</i>)	H-9/H-10	25.1	CH ₂ -10 CH ₂ -11
10	2.30 (2H, <i>t</i> , 7.0 Hz)	H-10/H-9	31.4	CH ₂ -8 CH ₂ -11
11			173.9	
12	4.00 (3H, <i>s</i>)		51.7	OCH ₃ -11
13				

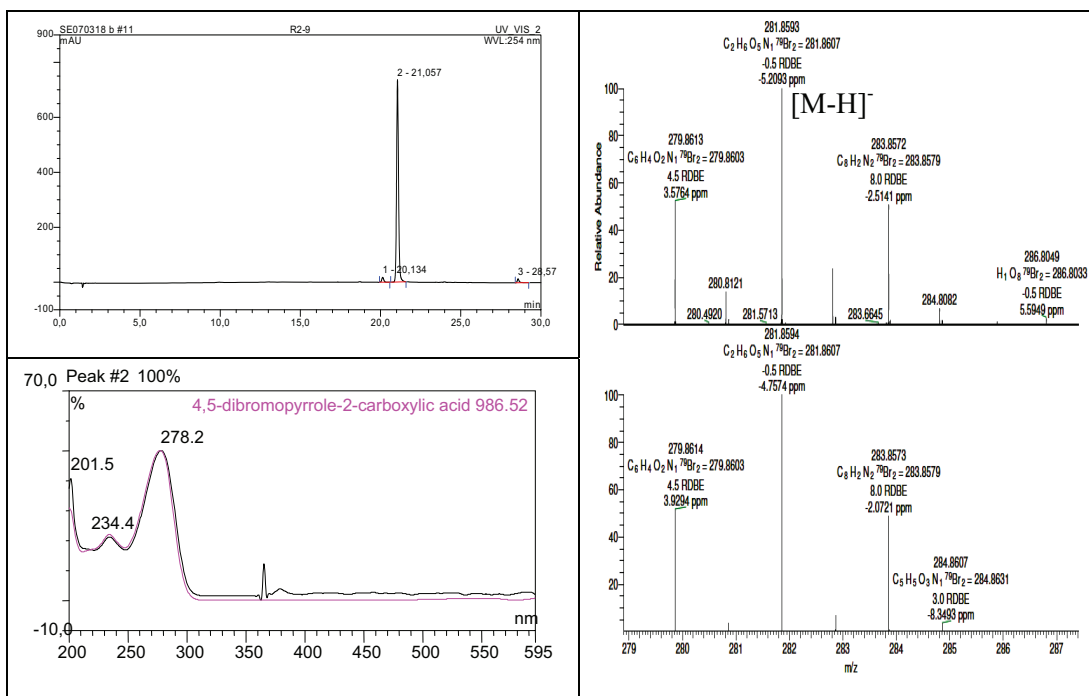
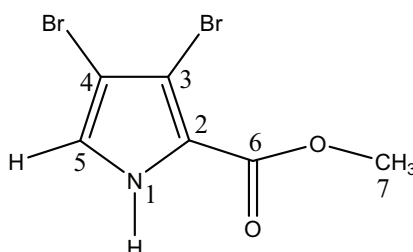
^a ¹³C NMR data were obtained from HMBC spectra. *n.d.* not detected.

Table 3.2. NMR data of acanthamides B–D (**2–4**), measured in DMSO-*d*₆.

H no.	2		3		4	
	δ_{H}	COSY	δ_{H}	COSY	δ_{H}	COSY
1-NH	12.7 (1H, br s)	H-1/H-5	12.68 (1H, br s)	H-1/H-5	12.65 (1H, br s)	H-1/H-5
2						
3						
4						
5	6.86 (1H, <i>d</i> , 2.5 Hz)	H-5/H-1	6.88 (1H, <i>d</i> , 2.8 Hz)	H-5/H-1	6.90 (1H, <i>d</i> , 2.8 Hz)	H-5/H-1
6						
7-NH	8.20 (1H, <i>t</i> , 5.5 Hz)	H-7/H-8	8.20 (1H, <i>t</i> , 5.0 Hz)	H-7/H-8	8.10 (1H, <i>t</i> , 5.0 Hz)	H-7/H-8
8	3.40 (2H, <i>q</i> , 6.0 Hz)	H-8/H-9	3.40 (2H, <i>q</i> , 6.0 Hz)	H-8/H-9	3.20 (2H, <i>q</i> , 6.0 Hz)	H-8/H-9
9	2.60 (2H, <i>t</i> , 6.6 Hz)	H-9/H-8	2.60 (2H, <i>t</i> , 6.6 Hz)	H-9/H-8	1.70 (2H, <i>m</i>)	H-9/H-10
10					2.30 (2H, <i>t</i> , 7.0 Hz)	H-10/H-9
11	3.60 (3H, <i>s</i>)		4.00 (2H, <i>q</i> , 7.0 Hz)	H-11/H-12		
12			1.20 (3H, <i>t</i> , 7.0 Hz)	H-12/H-11	4.00 (2H, <i>q</i> , 7.0 Hz)	H-12/H-13
13					1.20 (3H, <i>t</i> , 7.0 Hz)	H-13/H-12

3.1.5. Methyl 3,4-dibromo-1*H*-pyrrole-2-carboxylate (5, new natural product)

Methyl 3,4-dibromo-1 <i>H</i> -pyrrole-2-carboxylate	
Synonym(s)	Methyl 3,4-dibromo-1 <i>H</i> -pyrrole-2-carboxylate
Sample code	R2-9, Ac-3
Biological source	<i>Acanthostylotella</i> sp.
Sample amount	15.0 mg
Physical description	Pale Pink needle crystals
Molecular formula	C ₆ H ₅ ⁷⁹ Br ₂ NO ₂
Molecular weight	283 g/mol
Retention time (HPLC)	21.06 min (half-time gradient)



Results

Compound (**5**) was isolated as pale pink needle crystals. It showed pseudomolecular ion peaks at m/z 281, 283, and 285 at a 1:2:1 ratio in its ESI mass spectrum indicating that it was a dibrominated compound. The molecular formula of $C_6H_5^{79}Br_2NO_2$ was confirmed by HRESIMS (m/z 279.8613 [M-H]⁻, Δ +3.6 ppm). Derivatives of compound (**5**) exhibiting either a triisopropylsilyl or a methoxycarbonyl group as substituents of the pyrrole nitrogen atom had been reported as synthetic products (Handy and Zhang, 2006). In our study, **5** was obtained for the first time as a naturally-occurring bromopyrrole alkaloid. The ^{13}C NMR spectrum showed 6 signals representing one methoxy group and five sp^2 carbons including one methine group and four fully substituted carbons. 1H and ^{13}C NMR data of **5** (Table 3.3) were similar to those of the known related compounds methyl 4,5-dibromo-1*H*-pyrrole-2-carboxylate (**5A**) (König *et al.*, 1998; Forenza *et al.*, 1971), and methyl N-methyl-4,5-dibromopyrrole-2-carboxylate (Fathi-Afshar and Allen, 1988). The structure of **5** was further confirmed by interpretation of 1H — 1H COSY, and HMBC spectra. The 1H — 1H COSY spectrum showed a cross peak between the *NH* proton and the aromatic proton H-5 [δ_H 6.88 (*d*, 2.8 Hz); δ_C 117.9]. The HMBC spectrum (Fig. 3.3) supported the presence of the aromatic proton at C-5 and also revealed correlations between H-5 to C-2 (δ_C 123.7) and C-3 (δ_C 107.1). The presence of a methyl ester group [δ_H 3.87 (3H, *s*)] was deduced from correlation of the methyl protons to the carbonyl group C-6 (δ_C 160.2). Moreover, the methyl ester protons showed a HMQC correlation to C-7 (δ_C 52.0). Therefore, **5** was confirmed to be methyl 3,4-dibromo-1*H*-pyrrole-2-carboxylate.

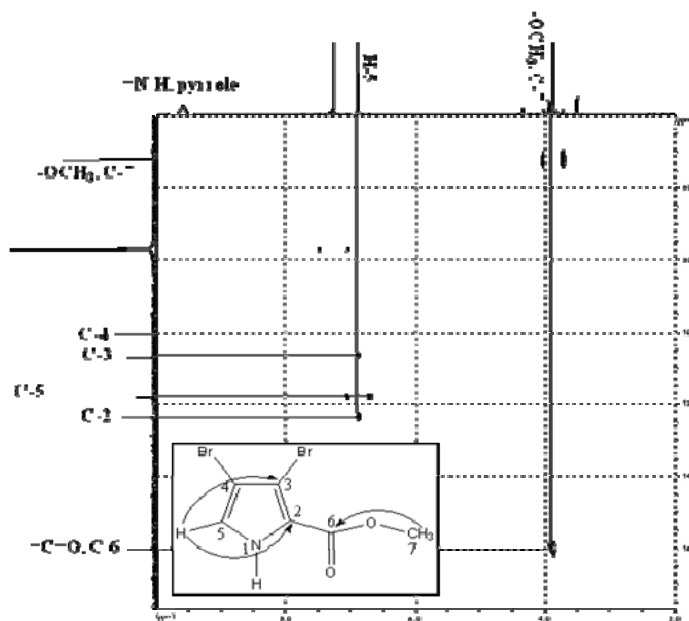
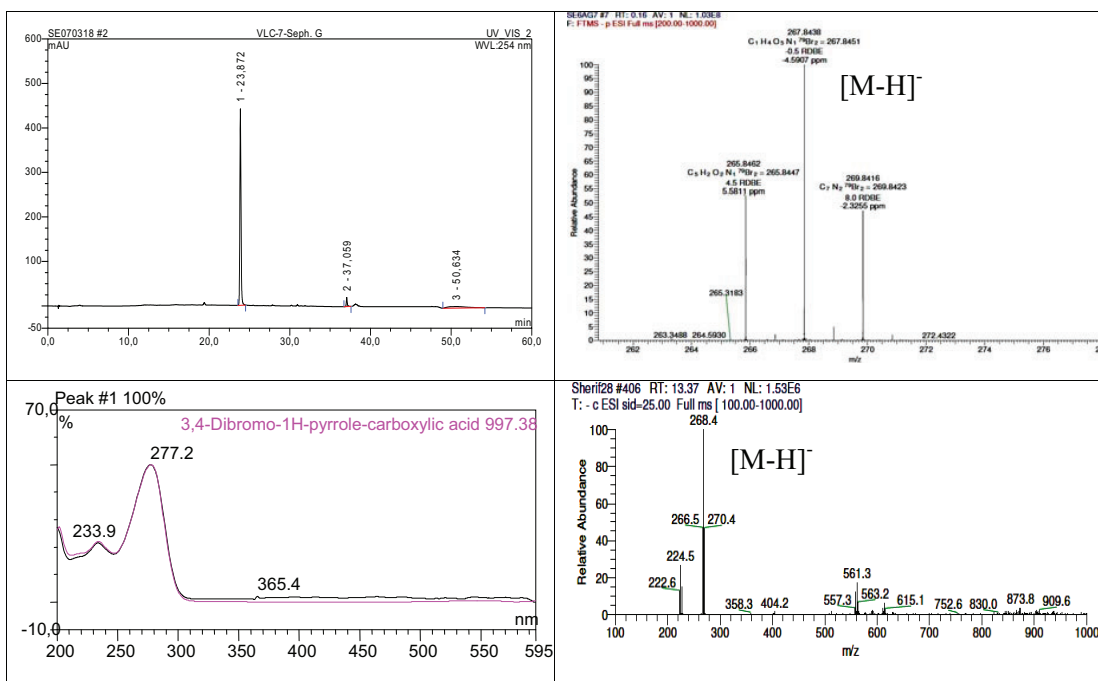
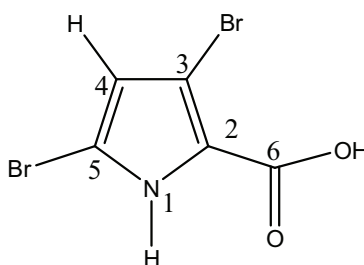


Fig. 3.3. HMBC spectrum and key correlations of methyl 3,4-dibromo-1*H*-pyrrole-2-carboxylate (**5**).

3.1.6. 3,5-Dibromo-1*H*-pyrrole-2-carboxylic acid (6, new natural product)

3,5-Dibromo-1 <i>H</i> -pyrrole-2-carboxylic acid	
Synonym(s)	3,5-Dibromo-1 <i>H</i> -pyrrole-2-carboxylic acid
Sample code	VLC-7-Seph. G
Biological source	<i>Acanthostylotella</i> sp.
Sample amount	60.0 mg
Physical description	White powder
Molecular formula	C ₅ H ₃ ⁷⁹ Br ₂ NO ₂
Molecular weight	269 g/mol
Retention time (HPLC)	23.87 min (standard gradient)



Results

Compound (**6**) was isolated as a white powder. The molecular formula of **6** was suggested to be $C_5H_3^{79}Br_2NO_2$ by HRESIMS (m/z 265.8462 $[M-H]^-$, Δ +5.6 ppm). The structure was completely elucidated by 1D and 2D NMR spectral analyses including 1H , ^{13}C NMR, and HMBC (Table 3.3), in addition to comparison of the data with those of structurally related compounds which are dibrominated at positions 4 and 5 or 3 and 4 of the pyrrole ring, like in the known compounds **8** and **13**, respectively. The ^{13}C -NMR spectrum of **6** was similar to those of **8** and **13**. It revealed the presence of five sp^2 carbons including one methine carbon (δ_C 114.4) and four fully substituted carbons including one carbonyl carbon (δ_C 161.9). Also the 1H NMR spectrum showed one aromatic proton [δ_H 6.60 (s)] attached to C-4 (δ_C 114.4) while no signals for the NH_2 between 7 to 8 ppm were observed as found in the known congeners **8** and **13**. Both 1H and ^{13}C NMR values of C-4 were similar to those observed in related compounds as in hymenialdisine (Cimino *et al.*, 1982; Kitagawa *et al.*, 1983), axinohydantoin (Pettit *et al.*, 1990), and spongiacidin D (Inaba *et al.*, 1998). The HMBC spectrum (Fig. 3.4) exhibited correlations between H-4 to carbons C-2 (δ_C 129.6) and C-5 (δ_C 103.3). Accordingly, **6** was deduced to be 3,5-dibromo-1H-pyrrole-2- carboxylic acid.

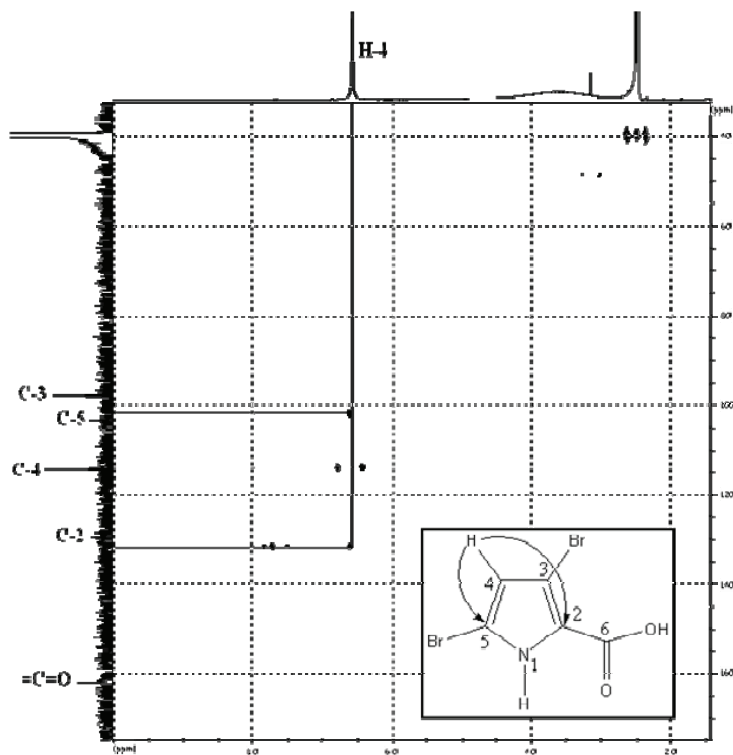
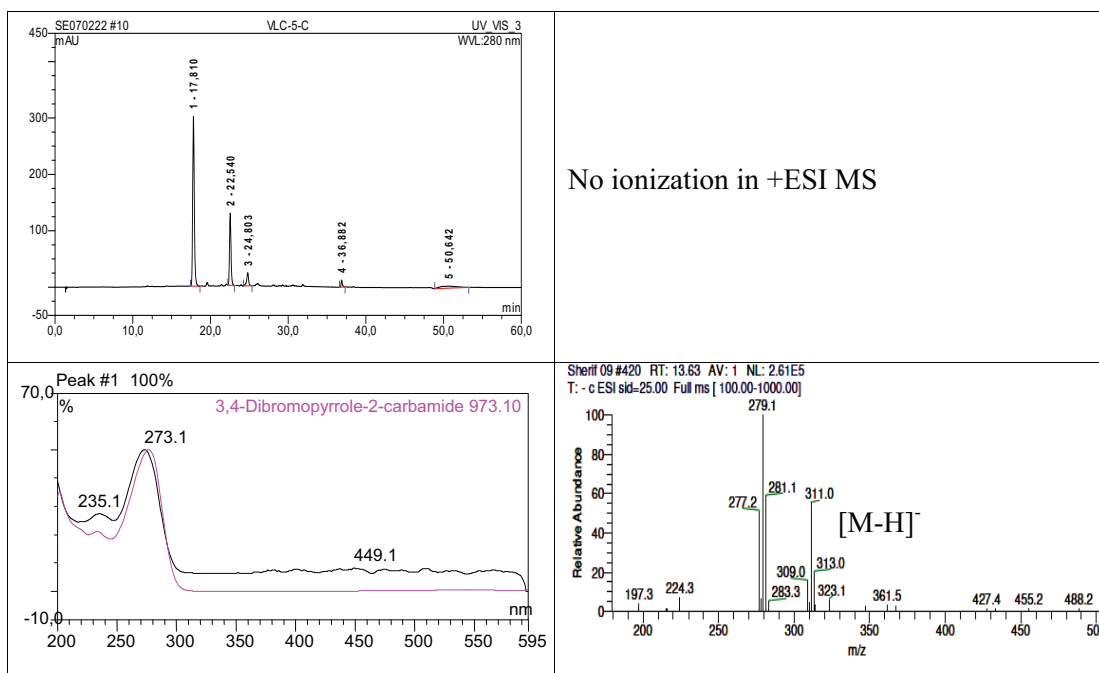
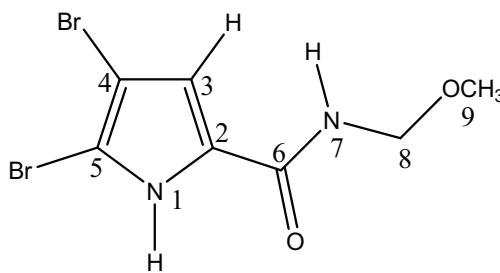


Fig. 3.4. HMBC spectrum and key correlations of 3,5-dibromo-1H-pyrrole-2-carboxylic acid (**6**).

3.1.7. 4,5-Dibromo-*N*-(methoxymethyl)-1*H*-pyrrole-2-carboxamide (7, known compound)

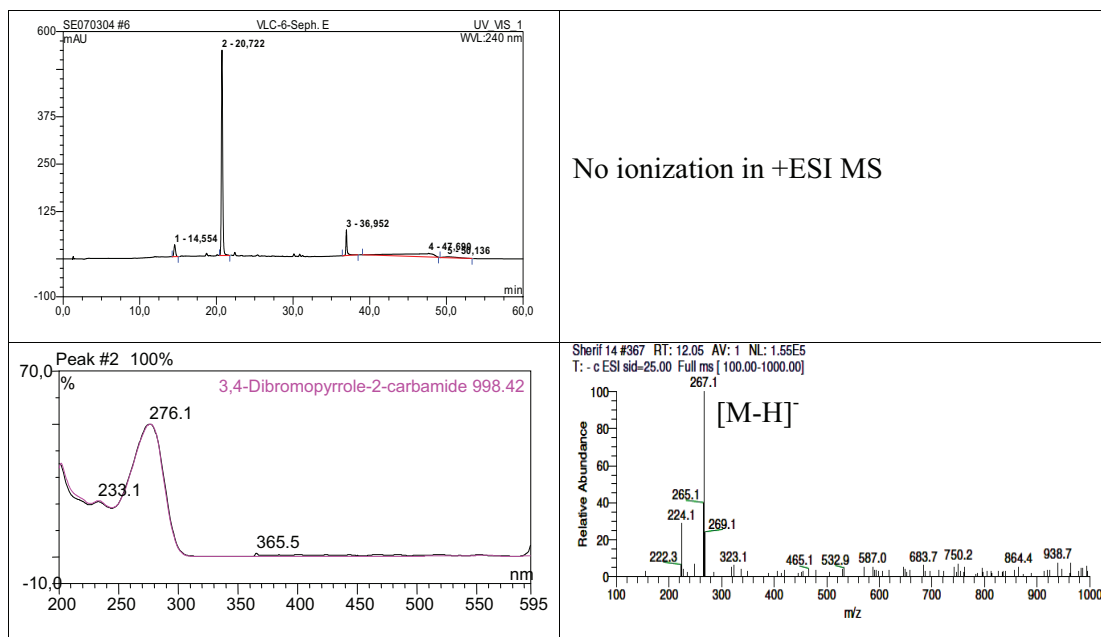
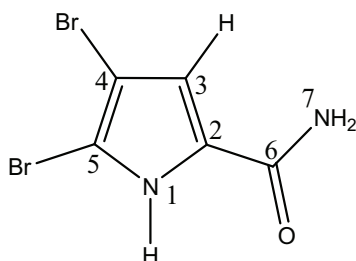
4,5-Dibromo- <i>N</i> -(methoxymethyl)-1 <i>H</i> -pyrrole-2-carboxamide	
Synonym(s)	4,5-Dibromo- <i>N</i> -(methoxymethyl)-1 <i>H</i> -pyrrole-2-carboxamide
Sample code	VLC-5-C
Biological source	<i>Acanthostylotella</i> sp.
Sample amount	1.0 mg
Physical description	White amorphous solid
Molecular formula	C ₇ H ₈ ⁷⁹ Br ₂ N ₂ O ₂
Molecular weight	312 g/mol
Retention time (HPLC)	17.81 min (standard gradient)



Results

3.1.8. 4,5-Dibromo-1*H*-pyrrole-2-carboxamide (8, known compound)

4,5-Dibromo-1 <i>H</i> -pyrrole-2-carboxamide	
Synonym(s)	4,5-Dibromo-1 <i>H</i> -pyrrole-2-carboxamide
Sample code	VLC-6-Seph. E
Biological source	<i>Acanthostylotella</i> sp.
Sample amount	60.0 mg
Physical description	White amorphous solid
Molecular formula	C ₅ H ₄ ⁷⁹ Br ₂ N ₂ O
Molecular weight	268 g/mol
Retention time (HPLC)	20.72 min (standard gradient)



Compound (**7**) was isolated as an amorphous white solid. In ESI mass spectrum, it revealed pseudomolecular ion peaks at m/z 309, 311, and 313 $[M-H]^-$, in a ratio of 1:2:1, confirming the existence of two bromine substituents in **7**. The structure was further confirmed by 1H NMR and $^1H-^1H$ COSY. According to these data (Table 3.4) and the reported literature (Umeyama *et al.*, 1998), compound (**7**) was deduced to be 4,5-dibromo-*N*-(methoxymethyl)-1*H*-pyrrole-2-carboxamide.

Compound (**8**) was isolated as an amorphous white solid. In ESI mass spectrum, it revealed pseudomolecular ion peaks at m/z 265, 267, and 269 $[M-H]^-$, in a ratio of 1:2:1, confirming the existence of two bromine substituents in **8**. The structure was further confirmed by 1D and 2D NMR including 1H , ^{13}C NMR, $^1H-^1H$ COSY, and HMBC (Fig. 3.5). According to these data (Table 3.4) and the reported literature (Forenza *et al.*, 1971), compound (**8**) was revealed to be 4,5-dibromo-1*H*-pyrrole-2-carboxamide.

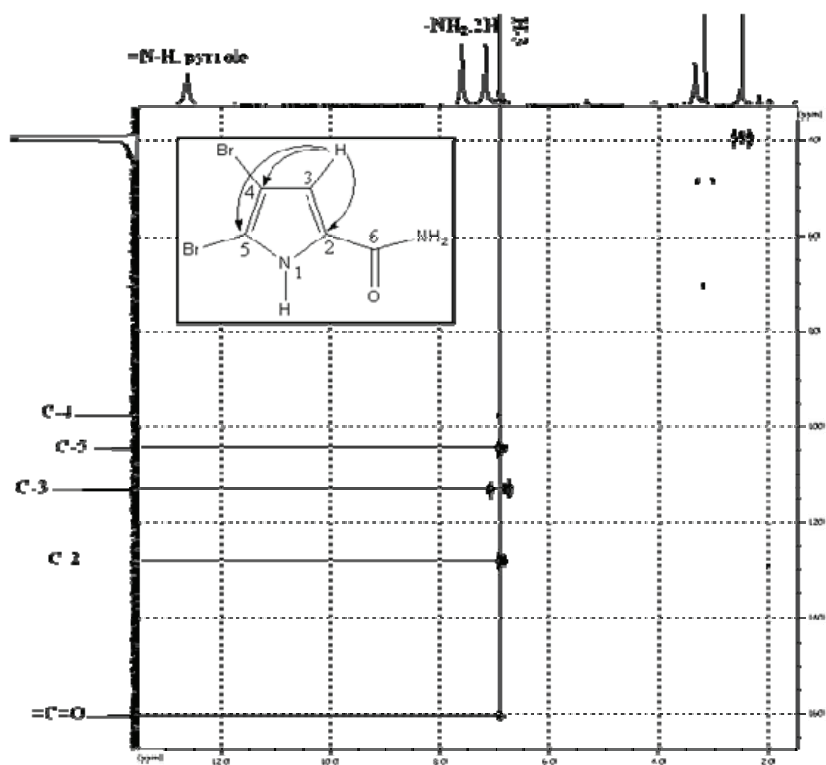


Fig. 3.5. HMBC spectrum and key correlations of 4,5-dibromo-1*H*-pyrrole-2-carboxamide (**8**).

Results

Table 3.3. NMR data of compounds **5**, and **6**.

H no.	5^a		5A (König <i>et al.</i>, 1998)		6^b	
	δ_{H}	δ_{C}	δ_{H}	δ_{C}	δ_{H}	δ_{C}
1	9.50 (1H, br s)		9.32 (1H, br s)			
2		123.7		123.8		129.6
3		107.1	6.90 (1H, s)	117.9		97.7
4		100.6		100.8	6.60 (1H, br s)	114.4
5	6.90 (1H, <i>d</i> , 2.5 Hz)	118.0		106.7		103.3
6		160.2		159.9		161.9
7	3.87 (3H, s)	52.0	3.80 (3H, s)	52.0		

^aNMR data measured in CDCl₃. ^bNMR data in DMSO-*d*₆.

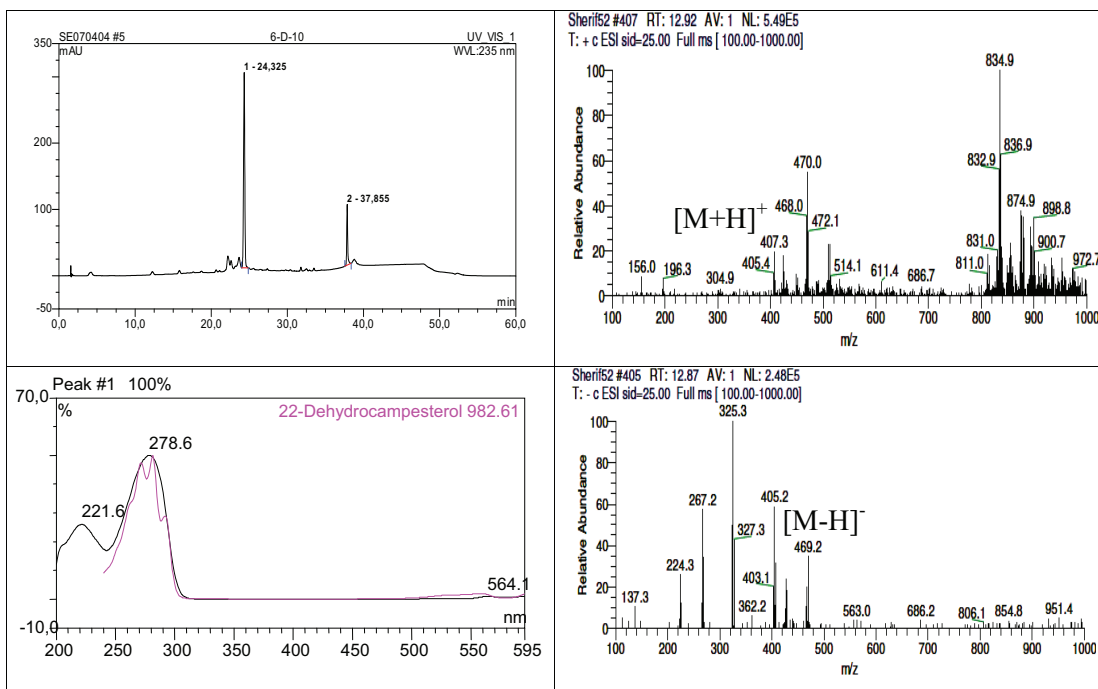
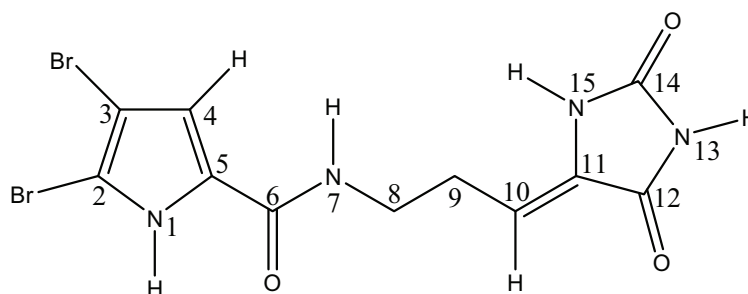
Table 3.4. NMR data of compounds **7**, **8**, **13**, and **14**.

H no.	7^a	8^b		13^b		14^a
	δ_{H}	δ_{H}	δ_{C}	δ_{H}	$\delta_{\text{C}}^{\text{c}}$	δ_{H}
1	9.37 (1H, br s)	12.63 (1H, br s)		12.63 (1H, br s)		9.15 (1H, br s)
2			128.2		125.0	
3	6.60 (1H, br s)	6.90 (1H, s)	113.1		104.6	
4			97.7		97.7	
5			104.6	6.90 (1H, <i>d</i> , 2.50 Hz)	113.1	6.87 (1H, <i>d</i> , 2.85 Hz)
6			160.4		160.2	
7		7.17 (1H, br s)		7.17 (1H, br s)		
		7.58 (1H, br s)		7.59 (1H, br s)		
8	4.84 (2H, <i>d</i> , 6.60 Hz)					
9	3.38 (3H, s)					

^aNMR data measured in CDCl₃. ^bNMR data in DMSO-*d*₆. ^c¹³C-NMR values were obtained from HMBC spectra.

3.1.9. Mukanadin D (9, known compound)

Mukanadin D	
Synonym(s)	4,5-Dibromo- <i>N</i> -(3-(2,5-dioximidazolidin-4-ylidene) propyl)-1 <i>H</i> -pyrrole-2-carboxamide
Sample code	VLC-6-D-10
Biological source	<i>Acanthostylotella</i> sp.
Sample amount	4.0 mg
Physical description	White needle crystals
Molecular formula	C ₁₁ H ₁₀ ⁷⁹ Br ₂ N ₄ O ₃
Molecular weight	406 g/mol
Retention time (HPLC)	24.33 min (standard gradient)



Results

Compound (**9**) was isolated as a white needle crystals. In ESI mass spectrum, it revealed pseudomolecular ion peaks at m/z 403, 405, and 407 $[M-H]^-$, in a ratio of 1:2:1, confirming the existence of two bromine substituents in **9**. The structure was further confirmed by 1D and 2D NMR including 1H NMR, and $^1H-^1H$ COSY (Fig. 3.6). According to these data (Table 3.5) and the reported literature (Hu *et al.*, 2005), compound (**9**) was proven to be mukanadin D.

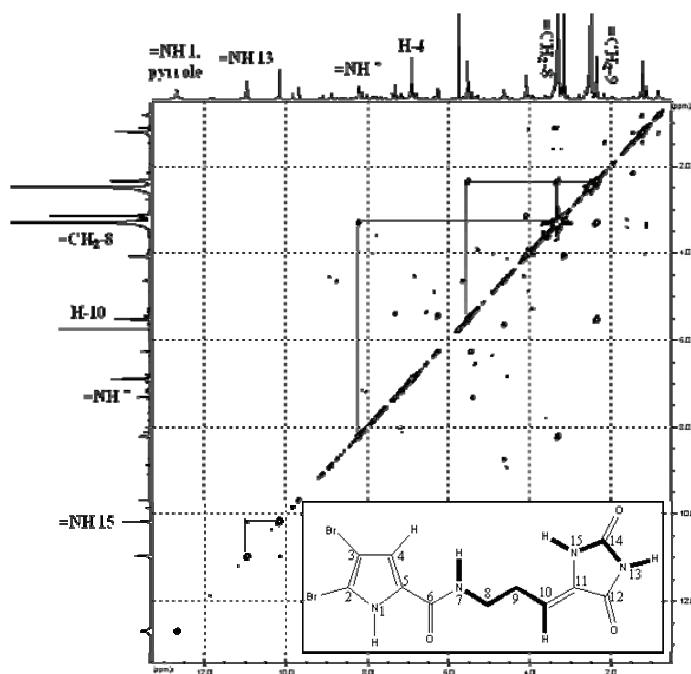


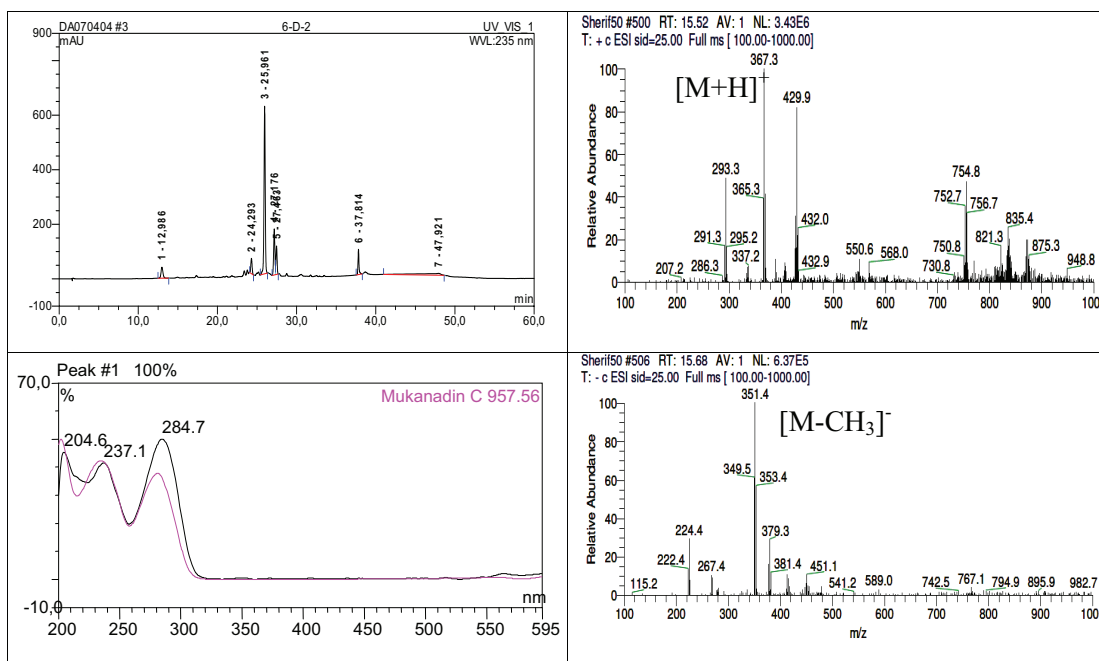
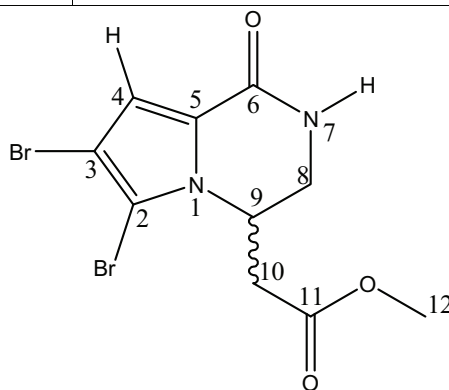
Fig. 3.6. $^1H-^1H$ COSY of mukanadin D (**9**).

Table 3.5. NMR data of mukanadin D (**9**), measured in $DMSO-d_6$.

H no.	9		
	δ_H	H no.	δ_H
1	12.70 (1H, br s)	9	2.35 (2H, m)
2		10	5.52 (1H, t, 7.6 Hz)
3		11	
4	6.89 (1H, s)	12	
5		13	10.16 (1H, br s)
6		14	
7	8.20 (1H, br s)	15	10.95 (1H, br s)
8	3.30 (2H, m)		

3.1.10. (±)-Longamide B methyl ester (10, known compound)

(±)-Longamide B methyl ester	
Synonym(s)	Methyl 2-(6,7-dibromo-1,2,3,4-tetrahydro-1-oxopyrrolo[1,2-a]pyrazin-4-yl) acetate
Sample code	6-D-2
Biological source	<i>Acanthostylotella</i> sp.
Sample amount	2.0 mg
Physical description	White amorphous solid
Molecular formula	C ₁₀ H ₁₀ ⁷⁹ Br ₂ N ₂ O ₃
Molecular weight	366 g/mol
Optical rotation c	0°C (c 0.1, CH ₃ OH)
Retention time (HPLC)	25.96 min (standard gradient)



Results

Compound (**10**) was isolated as a white amorphous solid. In ESI mass spectrum, it revealed pseudomolecular ion peaks at m/z 365, 367, and 369 $[M+H]^+$, in a ratio of 1:2:1, confirming the existence of two bromine substituents in **10**. The structure was further confirmed by 1D and 2D NMR including ^1H NMR, ^1H - ^1H COSY, and HMBC (Fig. 3.7). According to these data (Table 3.6) and the reported literature (Patel *et al.*, 2005; Umeyama *et al.*, 1998), compound (**10**) was proven to be (\pm)-Longamide B methyl ester.

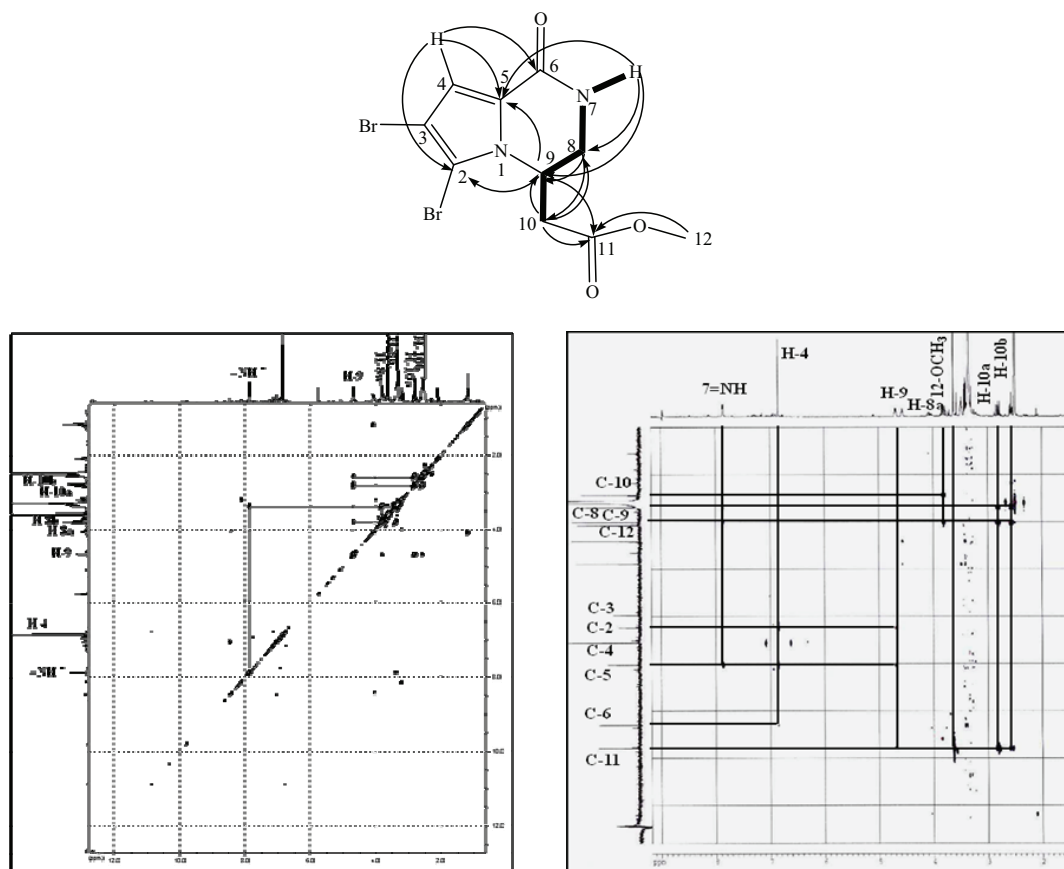
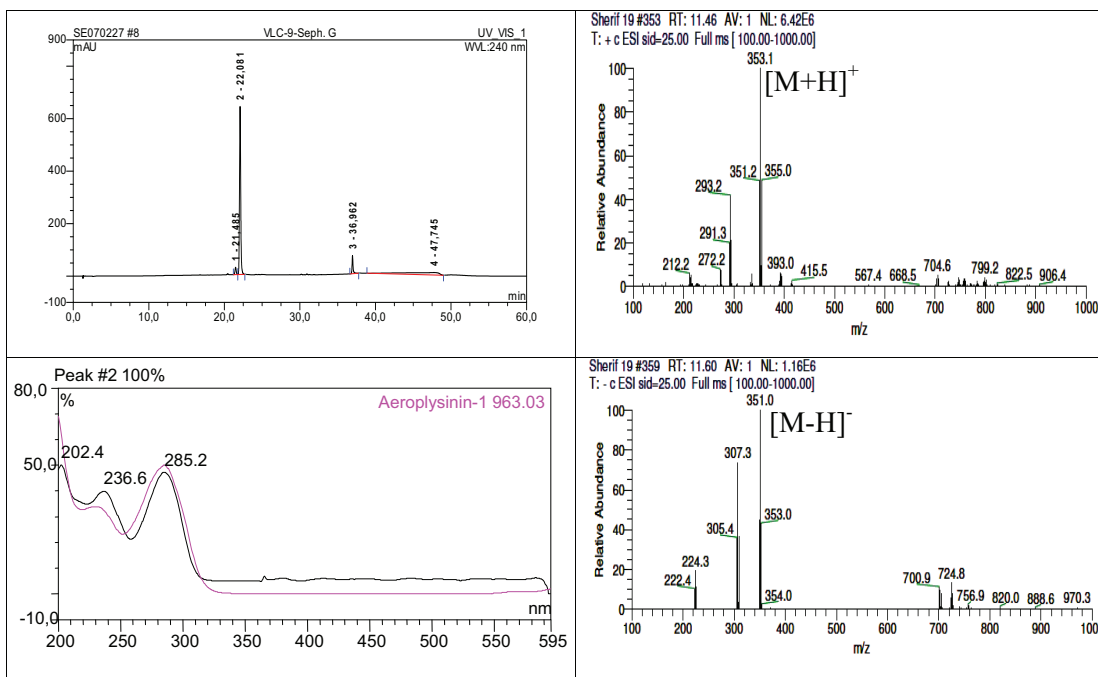
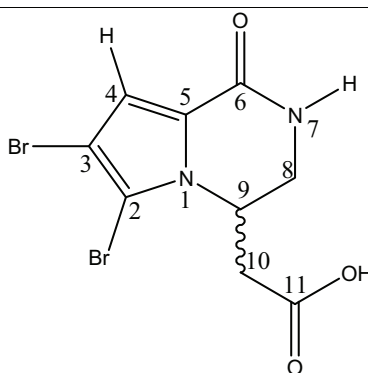


Fig. 3.7. ^1H - ^1H COSY and HMBC spectra of (\pm)-longamide B methyl ester (**10**).

3.1.11. (±)-Longamide B (11, known compound)

(±)-Longamide B	
Synonym(s)	2-(6,7-Dibromo-1,2,3,4-tetrahydro-1-oxopyrrolo[1,2-a]pyrazin-4-yl)acetic acid
Sample code	VLC-9-Seph. G
Biological source	<i>Acanthostylotella</i> sp.
Sample amount	26.0 mg
Physical description	White amorphous solid
Molecular formula	C ₉ H ₈ ⁷⁹ Br ₂ N ₂ O ₃
Molecular weight	352 g/mol
Optical rotation [α] _D ²⁰	0°C (c 0.14, CH ₃ OH)
Retention time (HPLC)	22.08 min (standard gradient)



Results

Compound (**11**) was isolated as a dark brown amorphous solid. In ESI mass spectrum, it revealed pseudomolecular ion peaks at m/z 351, 353, and 355 $[M+H]^+$, in a ratio of 1:2:1, confirming the existence of two bromine substituents in **11**. The structure was further confirmed by 1D and 2D NMR including 1H , ^{13}C NMR, DEPT, 1H - 1H COSY, and HMBC (Fig. 3.8). According to these data (Table 3.6) and the reported literature (Cafieri *et al.*, 1998; Patel *et al.*, 2005), compound (**11**) was proven to be (\pm)-Longamide B.

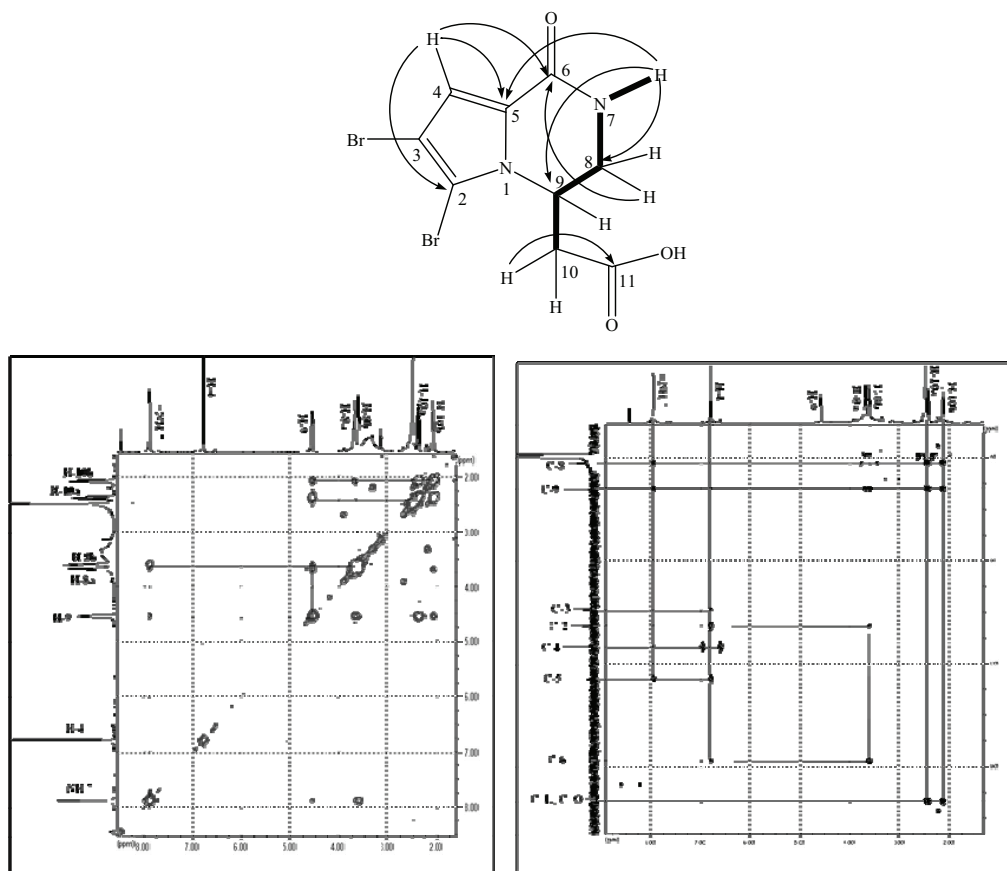
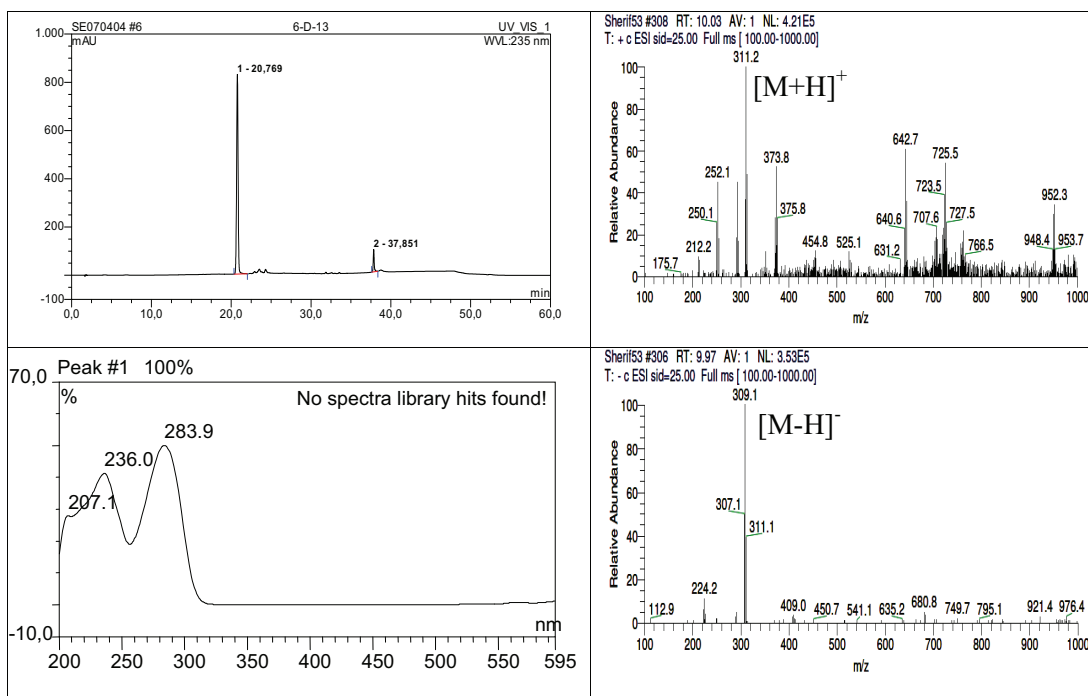
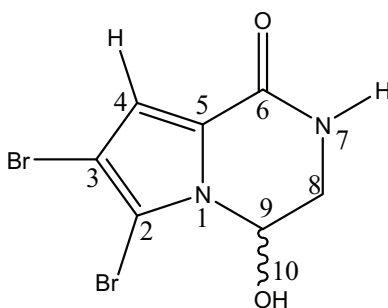


Fig. 3.8. 1H - 1H COSY and HMBC spectra of (\pm)-longamide B (**11**).

3.1.12. (±)-Longamide (12, known compound)

(±)-Longamide	
Synonym(s)	6,7-dibromo-3,4-dihydro-4-hydroxypyrrolo[1,2-a]pyrazin-1(2 <i>H</i>)-one
Sample code	6-D-13
Biological source	<i>Acanthostylotella</i> sp.
Sample amount	5.0 mg
Physical description	White amorphous solid
Molecular formula	C ₇ H ₆ ⁷⁹ Br ₂ N ₂ O ₂
Molecular weight	310 g/mol
Optical rotation [α]_D²⁰	0°C (c 0.2, CH ₃ OH)
Retention time (HPLC)	20.77 min (standard gradient)



Results

Compound (**12**) was isolated as a white amorphous solid. In ESI mass spectrum, it revealed pseudomolecular ion peaks at m/z 307, 309, and 311 $[M-H]^-$, in a ratio of 1:2:1, confirming the existence of two bromine substituents in **12**. The structure was further confirmed by 1D and 2D NMR including 1H , ^{13}C NMR, 1H - 1H COSY, and HMBC (Fig. 3.9). According to these data (Table 3.7) and the reported literature (Cafieri *et al.*, 1995), compound (**12**) was proven to be (\pm)-Longamide.

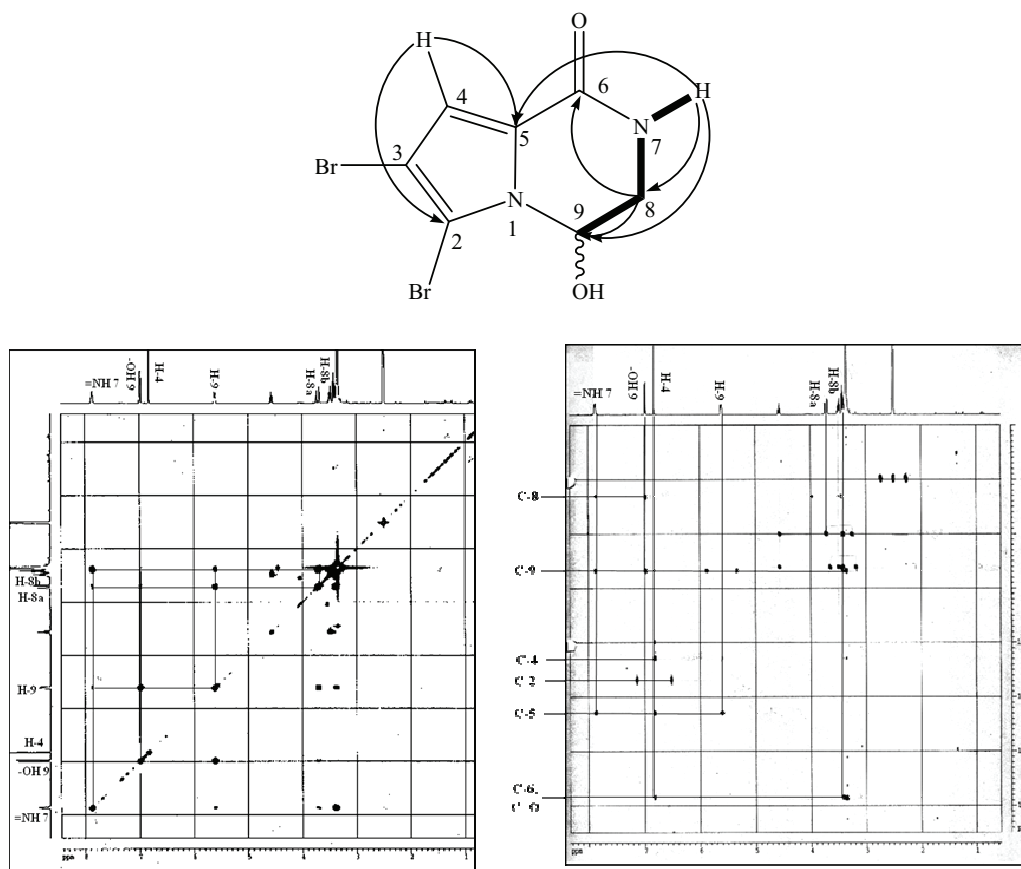


Fig. 3.9. 1H - 1H COSY and HMBC spectra of (\pm)-longamide (**12**).

Table 3.6. NMR data of compounds (**10** and **11**), measured in DMSO-*d*₆.

H no.	10		11	
	δ_{H}	δ_{C}	δ_{H}	δ_{C}
1				
2		106.0		105.3
3		99.5		98.8
4	6.84 (1H, <i>s</i>)	114.0	6.77 (1H, <i>s</i>)	113.4
5		125.7		125.8
6		157.6		156.8
7	7.80 (1H, <i>d</i> , 5.0 Hz)		7.87 (1H, <i>d</i> , 5.0 Hz)	
8	A: 3.80 (1H, <i>dd</i> , 13.7, 4.0 Hz) B: 3.37 (1H, <i>dd</i> , 12.7, 5.4 Hz)	42.4	A: 3.68 (1H, <i>dd</i> , 13.2, 3.6 Hz) B: 3.58 (1H, <i>dd</i> , 13.2, 5.0 Hz)	42.2
9	4.67 (1H, <i>m</i>)	50.2	4.55 (1H, <i>d</i> , 11.7 Hz)	52.1
10	A: 2.80 (1H, <i>dd</i> , 15.0, 6.0 Hz) B: 2.50 (1H, <i>dd</i> , 14.3, 6.0 Hz)	36.0	A: 2.38 (1H, <i>dd</i> , 15.1, 11.7 Hz) B: 2.08 (1H, <i>dd</i> , 15.1 Hz)	38.3
11		170.0		172.6
12-OCH ₃	3.56 (3H, <i>s</i>)	52.0		

Table 3.7. NMR data of (\pm)-longamide (**12**).

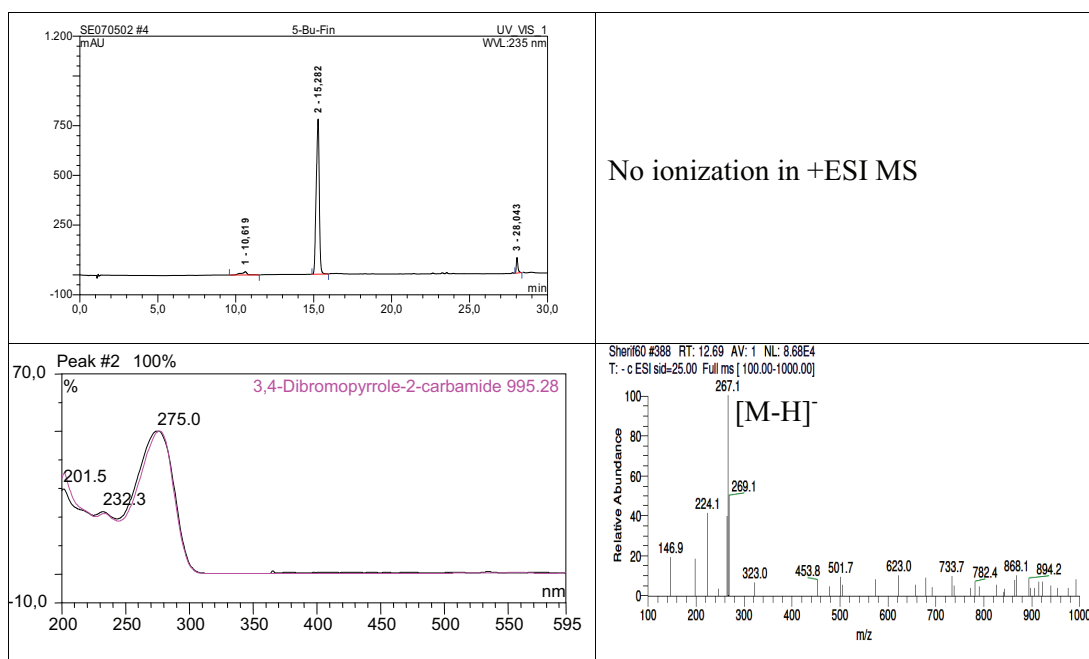
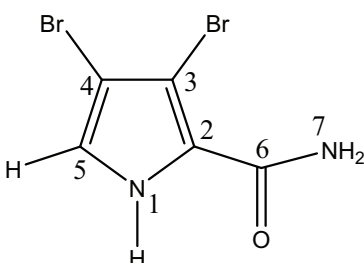
H no.	12	
	$\delta_{\text{H}}^{\text{a}}$	$\delta_{\text{C}}^{\text{b}}$
1		
2		108.1
3		102.2
4	6.80 (1H, <i>br s</i>)	116.6
5		126.2
6		160.6
7	7.8 (1H, <i>br d</i> , 5.0 Hz)	
8	A: 3.70 (1H, <i>dd</i> , 13.8, 2.8 Hz) B: 3.36 (1H, <i>dd</i> , 13.5, 5.3 Hz)	47.9
9	5.60 (1H, <i>br d</i>)	75.2
9-OH	6.97 (1H, <i>br d</i> , 2.8 Hz)	

^aNMR data measured in DMSO-*d*₆. ^bNMR data in CD₃OD.

Results

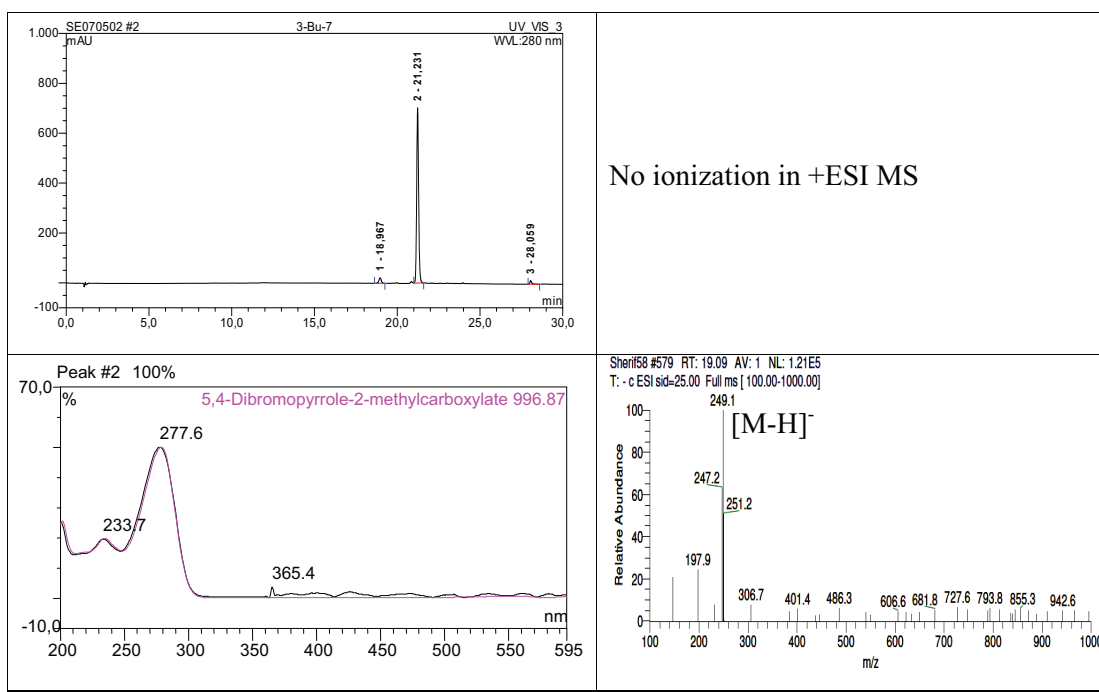
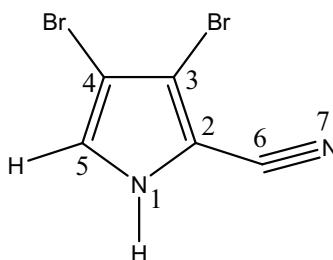
3.1.13. 3,4-Dibromo-1*H*-pyrrole-2-carboxamide (13, known compound)

3,4-Dibromo-1 <i>H</i> -pyrrole-2-carboxamide	
Synonym(s)	3,4-Dibromo-1 <i>H</i> -pyrrole-2-carboxamide
Sample code	5-Bu-Fin
Biological source	<i>Acanthostylotella</i> sp.
Sample amount	7.0 mg
Physical description	White amorphous solid
Molecular formula	C ₅ H ₄ ⁷⁹ Br ₂ N ₂ O
Molecular weight	268 g/mol
Retention time (HPLC)	15.28 min (half-time gradient)



3.1.14. 2-Cyano-4,5-dibromo-1*H*-pyrrole (14, known compound)

2-Cyano-4,5-dibromo-1 <i>H</i> -pyrrole	
Synonym(s)	2-Cyano-4,5-dibromo-1 <i>H</i> -pyrrole
Sample code	3-Bu-7
Biological source	<i>Acanthostylotella</i> sp.
Sample amount	2.0 mg
Physical description	White amorphous solid
Molecular formula	C ₅ H ₂ ⁷⁹ Br ₂ N ₂
Molecular weight	250 g/mol
Retention time (HPLC)	21.23 min (half-time gradient)



No ionization in +ESI MS

Results

Compound (**13**) was isolated as a greyish white amorphous solid. In ESI mass spectrum, it revealed pseudomolecular ion peaks at m/z 265, 267, and 269 [M-H]⁻, in a ratio of 1:2:1, confirming the existence of two bromine substituents in **13**. The structure was further confirmed by 1D and 2D NMR including ¹H, and ¹H-¹H COSY. According to these data (Table 3.4) and the reported literature (Hassan *et al.*, 2007; Supriyono *et al.*, 1995), compound (**13**) was proven to be 3,4-dibromo-1*H*-pyrrole-2-carboxamide.

Compound (**14**) was isolated as a white amorphous solid. In ESI mass spectrum, it revealed pseudomolecular ion peaks at m/z 247, 249, and 251 [M-H]⁻, in a ratio of 1:2:1, confirming the existence of two bromine substituents in **14**. The structure was further confirmed by 1D and 2D NMR including ¹H, and ¹H-¹H COSY. According to these data (Table 3.4) and the reported literature (König *et al.*, 1998; Forenza *et al.*, 1971), compound (**14**) was proven to be 2-cyano-4,5-dibromo-1*H*-pyrrole.

3.1.15. Bioactivity assay results of compounds isolated from marine sponge *Acanthostylorella* sp.

All isolated compounds from *Acanthostylorella* sp. were dibromopyrrole derivatives. They were subjected to vast array of biological activity assays. In cytotoxicity (MTT) assay against mouse lymphoma (L5178Y) cell line, only mukonadin D (**9**) showed moderate activity with an IC₅₀ of 8.7 µg/mL (21.7 µM).

In protein kinase inhibitory activity against 24 different enzymes and antioxidant activities, none of the isolated compounds proved to be of potential activity. In the *in vitro* antimicrobial and antiviral activity assays, methyl 3,4-dibromo-1*H*-pyrrole-2-carboxylate (**5**) revealed antibacterial activity with MIC values of 31.25 µg/mL against both multi resistant *Staphylococcus aureus* (MRSA), and *Streptococcus pneumoniae*. In addition it showed antifungal activity with MIC values of 62.5, and 125 µg/mL against *Aspergillus faecalis*, and *Aspergillus fumigatus*, respectively.

3.2. Secondary metabolites isolated from *Stylissa massa*

In this study, we investigated a specimen of *Stylissa massa* (class Demospongiae, order Halichondrida, family Dictyonellidae), collected off the shores of Papua Island (Indonesia) in January 2008, identified, and supplied by Dr. Nicole de Voogd, National Museum of Natural History, Leiden, Netherlands.

Total methanolic extract of the sponge was subjected to liquid liquid partition technique against *n*-Hexane, EtOAc, and BuOH. The EtOAc soluble fraction was then subjected to VLC and eluted using a stepwise gradient system from 100% *n*-Hexane to 100 % EtOAc, and from 100% DCM to 100% MeOH. Each fraction was purified by column chromatography using Sephadex LH-20 as a stationary phase and either MeOH or DCM:MeOH (1:1) as a mobile phase followed by either semi-preparative reversed phase HPLC (C18 Eurosphere 100) when required using the appropriate gradient elution of MeOH:H₂O.

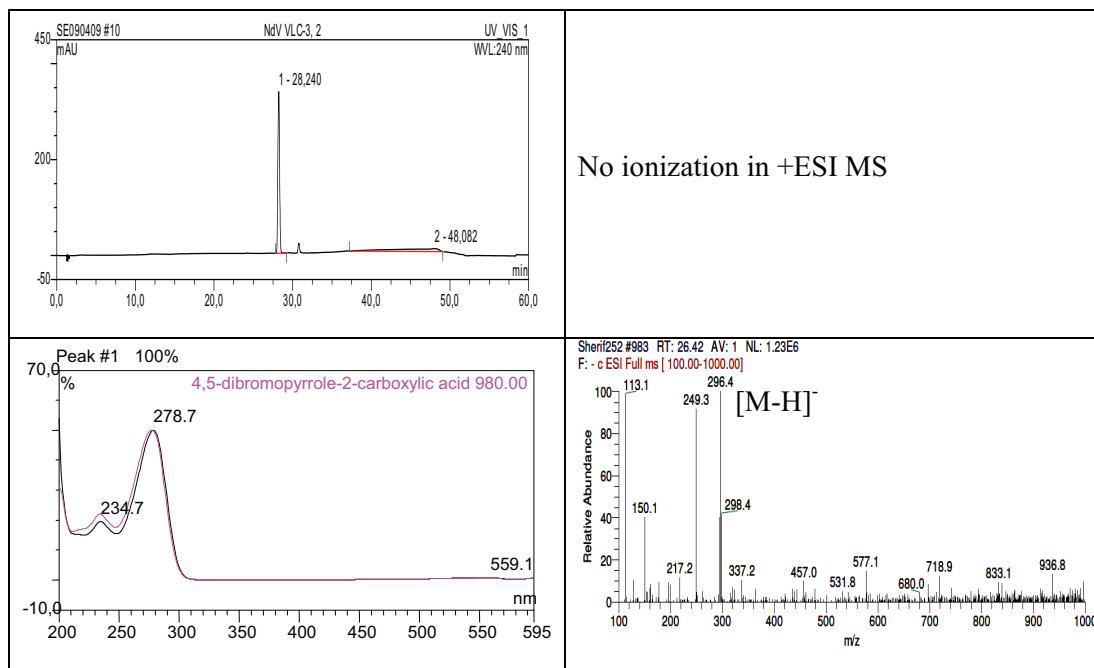
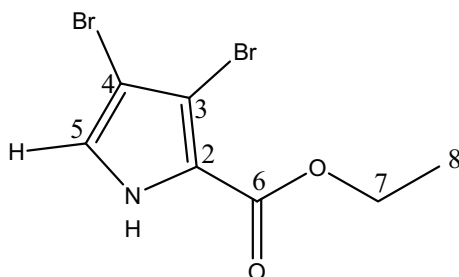
This afforded two new dibromopyrrole alkaloids (**15** and **30**) in addition to twenty known bromopyrrole alkaloids (**16–29** and **31–36**). Isolated compounds were tested for different bioactivities, including cytotoxicity, antibacterial, antifungal, antiviral and protein kinase inhibitory activities.

In this part, we would present the results of the chemical investigation of the natural products produced by *Stylissa massa*.

Results

3.2.1. Ethyl 3,4-dibromo-1*H*-pyrrole-2-carboxylate (15, new natural product)

Ethyl 3,4-dibromo-1 <i>H</i> -pyrrole-2-carboxylate	
Synonym(s)	Ethyl 3,4-dibromo-1 <i>H</i> -pyrrole-2-carboxylate
Sample code	NdV VLC-3,2
Biological source	<i>Stylissa massa</i>
Sample amount	7.0 mg
Physical description	White needle crystals
Molecular formula	C ₇ H ₇ ⁷⁹ Br ₂ NO ₂
Molecular weight	297 g/mol
Retention time (HPLC)	28.24 min (standard gradient)



Compound (**15**) was isolated as white needle crystals. It showed pseudomolecular ion peaks at m/z 294, 296, and 298 $[M-H]^-$ at a 1:2:1 ratio in its ESI mass spectrum indicating that it was a dibrominated compound. The molecular formula of $C_7H_7^{79}Br_2NO_2$ was confirmed by HRESIMS. In our study, **15** was obtained for the first time as a naturally-occurring bromopyrrole alkaloid. The ^{13}C NMR spectrum (Table 3.8) showed 7 signals representing one methyl, and one methylene group in addition to five sp^2 carbons including one methine group and four fully substituted carbons. The structure of **15** was further confirmed by interpretation of $^1H-^1H$ COSY, and HMBC spectra (Fig. 3.10). The $^1H-^1H$ COSY spectrum showed a cross peak between NH proton (δ_H 9.74, br s) and the aromatic proton H-5 [δ_H 6.89 (*d*, 2.8 Hz); δ_C 117.8]. The HMBC spectrum (Fig. 3.10) supported the presence of the aromatic proton at C-5 and also revealed correlations between H-5 to C-2 (δ_C 124.1) and C-3 (δ_C 106.7). The presence of an ethyl ester group was deduced from $^1H-^1H$ COSY that revealed a clear correlation between methylene group [δ_H 4.34 (*q*, 7.3 Hz); δ_C 61.1], and methyl group [δ_H 1.36 (*t*, 7.3 Hz); δ_C 14.3]; and HMBC spectra showed a correlation of the methylene protons to the carbonyl group C-6 (δ_C 159.7). Moreover, the methylene and methyl protons showed a HMQC correlation to C-7 (δ_C 61.1), and C-8 (δ_C 14.3), respectively. Therefore, **15** was confirmed to be ethyl 3,4-dibromo-1*H*-pyrrole-2-carboxylate.

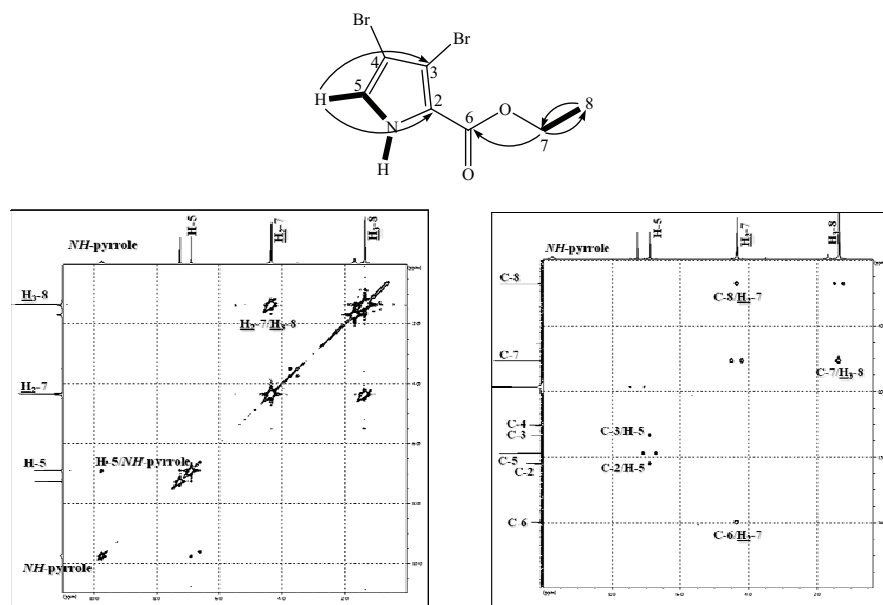
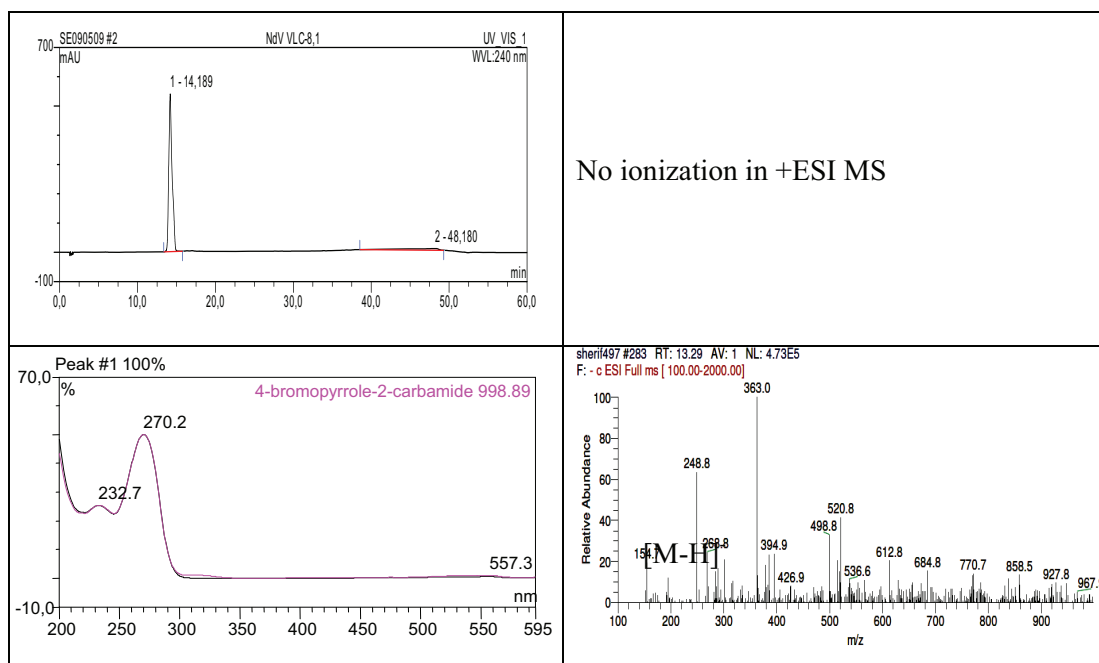
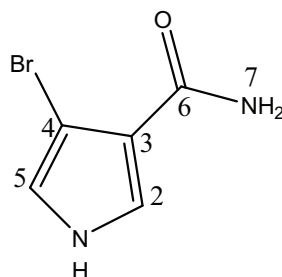


Fig. 3.10. $^1H-^1H$ COSY and HMBC spectra of ethyl 3,4-dibromo-1*H*-pyrrole-2-carboxylate (**15**).

Results

3.2.2. 4-Bromo-1*H*-pyrrole-3-carboxamide (16, known compound)

4-Bromo-1 <i>H</i> -pyrrole-3-carboxamide	
Synonym(s)	4-Bromo-1 <i>H</i> -pyrrole-3-carboxamide
Sample code	NdV VLC-8,1
Biological source	<i>Stylissa massa</i>
Sample amount	5.0 mg
Physical description	White amorphous solid
Molecular formula	C ₅ H ₅ ⁷⁹ BrN ₂ O
Molecular weight	189 g/mol
Retention time (HPLC)	14.19 min (standard gradient)



Compound (**16**) was isolated as a white amorphous solid. It showed pseudomolecular ion peaks at m/z 186, and 188 $[M-H]^-$ at a 1:1 ratio in its ESI mass spectrum indicating that it was a monobrominated compound. The structure of **16** was further confirmed by interpretation of ^1H — ^1H COSY, and HMBC spectra. The ^1H — ^1H COSY spectrum (Fig. 3.11) showed a cross peak between NH proton (δ_{H} 11.76, br *s*) and the aromatic protons H-2 [δ_{H} 6.95 (*dd*, 1.6, 2.9 Hz); δ_{C} 121.0], and H-5 [δ_{H} 6.83 (*dd*, 1.6, 2.9 Hz); δ_{C} 111.8]. The HMBC spectrum (Fig. 3.11) supported the proposed structure and revealed correlations between H-5 to C-2 (δ_{C} 121.0), and C-3 (δ_{C} 126.7); and H-2 to C-3 (δ_{C} 126.7), C-4 (δ_{C} 94.7), and C-5 (δ_{C} 111.8). Therefore, **16** was confirmed to be 4-bromo-1*H*-pyrrole-3-carboxamide that was firstly reported from the marine sponges *Axinella damicornis* and *Stylissa flabelliformis* by Hassan *et al.* in 2007.

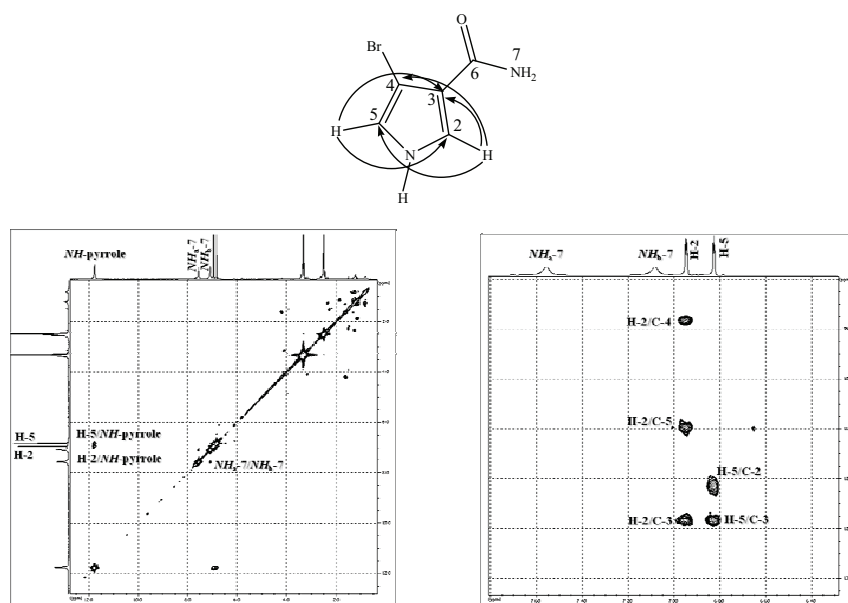


Fig. 3.11. ^1H — ^1H COSY and HMBC spectra of 4-bromo-1*H*-pyrrole-3-carboxamide (**16**).

Table 3.8. NMR data of compounds (**15** and **16**).

#	15, CDCl_3 , 500 MHz		16, $\text{DMSO}-d_6$, 500 MHz	
	δ_{H}	δ_{C}	δ_{H}	δ_{C}^*
1	9.74 (1H, br <i>s</i> , <i>NH</i> -pyrrole)		11.76 (1H, br <i>s</i> , <i>NH</i> -pyrrole)	
2		124.1, C	6.95 (1H, <i>dd</i> , 1.6, 2.9 Hz)	121.0
3		106.7, C		126.7
4		100.6, C		94.7
5	6.89 (1H, <i>d</i> , 2.8 Hz)	117.8, CH	6.83 (1H, <i>dd</i> , 1.6, 2.9 Hz)	111.8
6		159.7, C		
7	4.34 (2H, <i>q</i> , 7.3 Hz)	61.1, CH_2	7.56 (1H, br <i>s</i> , <i>NHa</i>) 7.08 (1H, br <i>s</i> , <i>NHb</i>)	
8	1.36 (3H, <i>t</i> , 7.3 Hz)	14.3, CH_3		

* ^{13}C NMR values obtained from HMBC spectrum.

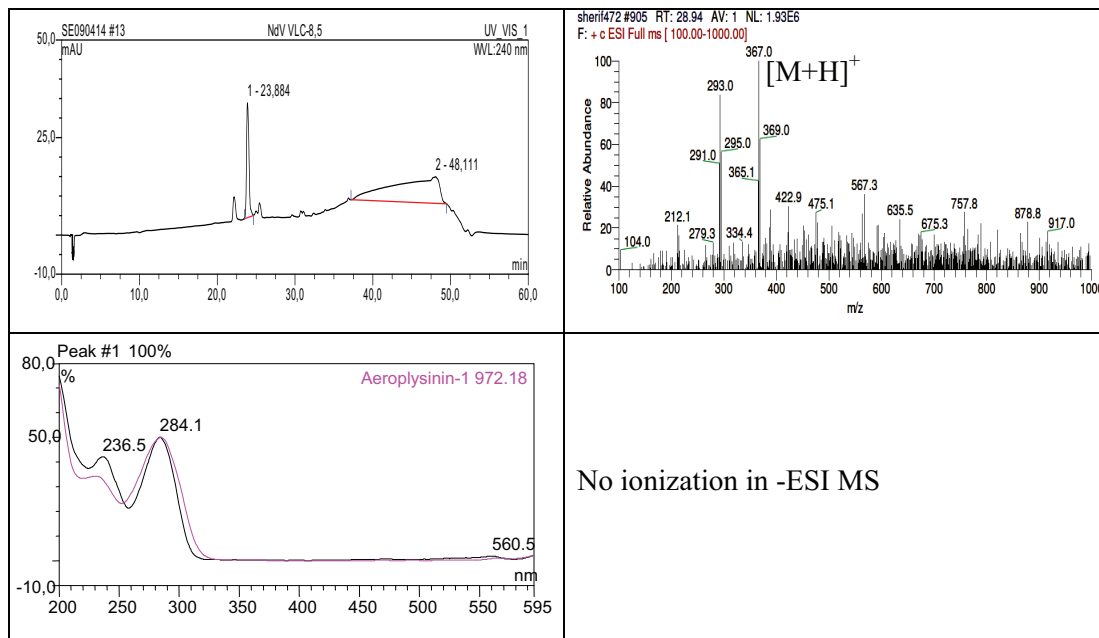
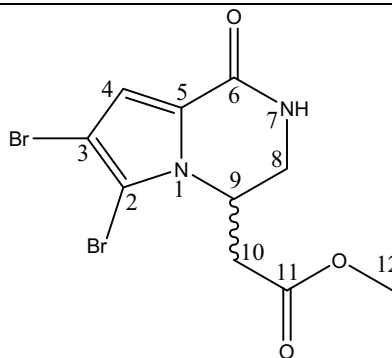
Results

3.2.3. 3,4-Dibromo-1*H*-pyrrole-2-carboxamide (17, known compound)

Please see 3.1.13. data included therein.

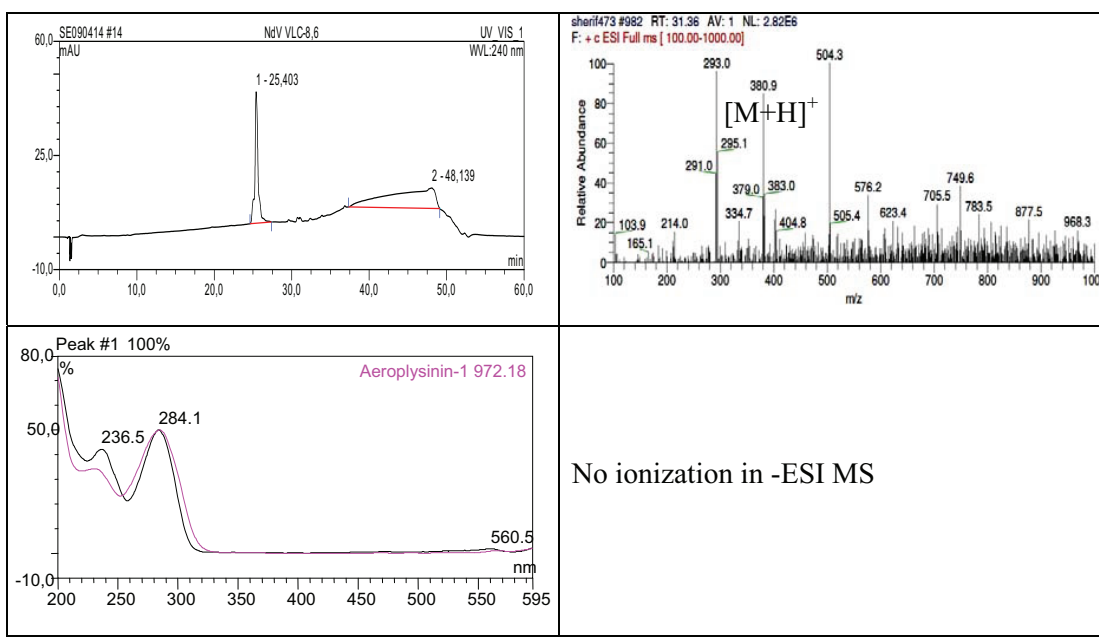
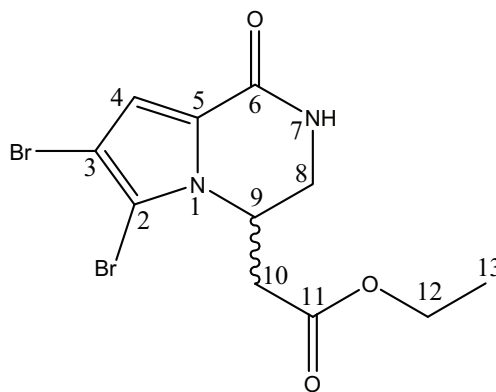
3.2.4. (-)-Longamide B methyl ester (18, known compound)

(-)-Longamide B methyl ester	
Synonym(s)	(-)-6,7-Dibromo-1,2,3,4-tetrahydro-1-oxopyrrolo[1,2-a]pyrazine-4-acetic acid methyl ester
Sample code	NdV VLC-8,5
Biological source	<i>Stylissa massa</i>
Sample amount	2.0 mg
Physical description	White amorphous solid
Molecular formula	C ₁₀ H ₁₀ ⁷⁹ Br ₂ N ₂ O ₃
Molecular weight	366 g/mol
Optical rotation [α] _D ²⁰	-9.0°C (c 0.02, CH ₃ OH)
Retention time (HPLC)	23.88 min (standard gradient)



3.2.5. (-)-Longamide B ethyl ester, Hanishsin (19, known compound)

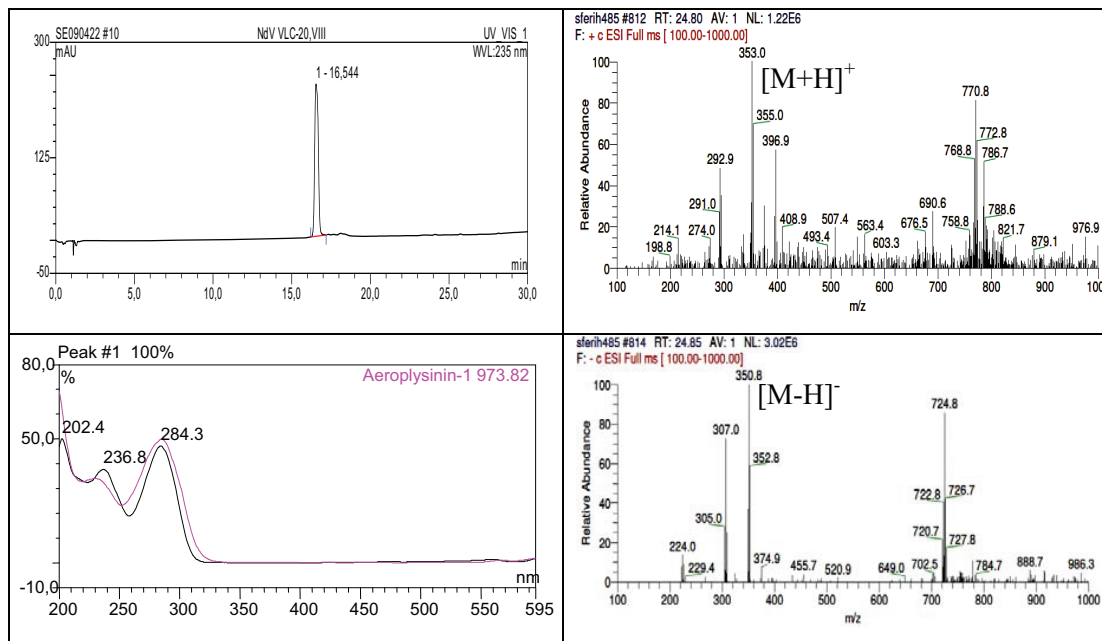
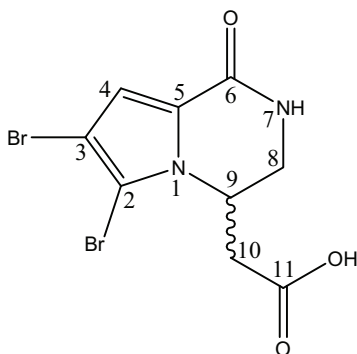
(-)-Longamide B ethyl ester, Hanishsin	
Synonym(s)	(-)-6,7-Dibromo-1,2,3,4-tetrahydro-1-oxopyrrolo[1,2-a]pyrazine-4-acetic acid ethyl ester
Sample code	NdV VLC-8,6
Biological source	<i>Stylissa massa</i>
Sample amount	2.0 mg
Physical description	White amorphous solid
Molecular formula	C ₁₁ H ₁₂ ⁷⁹ Br ₂ N ₂ O ₃
Molecular weight	380 g/mol
Optical rotation [α] _D ²⁰	-13.0°C (c 0.02, CH ₃ OH)
Retention time (HPLC)	25.40 min (standard gradient)



Results

3.2.6. (-)-Longamide B (31, known compound)

(-)-Longamide B	
Synonym(s)	(-)-6,7-Dibromo-1,2,3,4-tetrahydro-1-oxopyrrolo[1,2-a]pyrazine-4-acetic acid
Sample code	NdV VLC-20,VIII
Biological source	<i>Stylissa massa</i>
Sample amount	9.0 mg
Physical description	White amorphous solid
Molecular formula	C ₉ H ₈ ⁷⁹ Br ₂ N ₂ O ₃
Molecular weight	352 g/mol
Optical rotation $[\alpha]_D^{20}$	-5.0°C (c 0.04, CH ₃ OH)
Retention time (HPLC)	16.54 min (half-time gradient)



Compound (**18**) was isolated as a white amorphous solid. It showed pseudomolecular ion peaks at m/z 365, 367, and 369 $[M+H]^+$ at a 1:2:1 ratio in its ESI mass spectrum indicating the existence of two bromine substituents in **18**. The structure of **18** was further confirmed by interpretation of $^1H-^1H$ COSY. The $^1H-^1H$ COSY spectrum showed an extended spin system between $NH-7$ (δ_H 7.86, *d*, 5.1 Hz), $H-8_A$ [δ_H 3.80 (*dd*, 4.1, 13.6 Hz)], $H-8_B$ [δ_H 3.38 (*dd*, 5.4, 13.6 Hz)], then to $H-9$ [δ_H 4.68 (*m*)], $H-10_A$ [δ_H 2.80 (*dd*, 9.5, 15.5 Hz)], and $H-10_B$ [δ_H 2.57 (*dd*, 5.1, 15.5 Hz)]. Moreover, 1H NMR spectra of **18** revealed a singlet methyl resonance at δ_H 3.62 that was assigned to methyl ester group (CH_3-12). The optical rotation of **18** gave a value of $[\alpha]_D^{20}$ -9.0° (*c* 0.02, CH_3OH). Based on the preceding data (Table 3.9) and the reported literature (Patel *et al.*, 2006), **18** was confirmed to be (-)-longamide B methyl ester.

Compound (**19**) was isolated as a white amorphous solid. It showed pseudomolecular ion peaks at m/z 379, 381, and 383 $[M+H]^+$, (1:2:1) in its ESI mass spectrum which differed from **18** by more 14 amu. This difference in molecular weight was explained by the presence of methylene, and methyl groups at [δ_H 4.07 (*m*)], and [δ_H 1.17 (*t*, 7.3 Hz)], respectively in **19** instead of methyl group at [δ_H 3.62 (*s*)] in **18**. Apart from this difference, the spectral data of **19** and **18** were quite similar. The structure of **19** was further confirmed by interpretation of $^1H-^1H$ COSY. The $^1H-^1H$ COSY spectrum (Fig. 3.12) showed similarly an extended spin system between $NH-7$ (δ_H 7.86, *d*, 5.1 Hz), $H-8_A$ [δ_H 3.80 (*dd*, 4.4, 13.6 Hz)], $H-8_B$ [δ_H 3.36 (*dd*, 5.4, 13.6 Hz)], then to $H-9$ [δ_H 4.68 (*m*)], $H-10_A$ [δ_H 2.77 (*dd*, 9.5, 15.5 Hz)], and $H-10_B$ [δ_H 2.50 (*dd*, 5.1, 15.5 Hz)]. Moreover, it revealed a clear correlation between methylene group [δ_H 4.07 (*m*)], and methyl group [δ_H 1.17 (*t*, 7.3 Hz)] indicating the existence of an ethyl ester group. The optical rotation of **19** gave a value of $[\alpha]_D^{20}$ -13.0° (*c* 0.02, CH_3OH). According to the previous data (Table 3.9) and comparing to the reported literature (Mancini *et al.*, 1997), **19** was confirmed to be (-)-longamide B ethyl ester, hanishin.

Compound (**31**) was isolated as a faint yellow amorphous solid. It showed pseudomolecular ion peaks at m/z 351, 353, and 355 $[M+H]^+$, (1:2:1) in its ESI mass spectrum which differed from **18** by the lack of 14 amu. This difference in molecular weight was explained by the absence of the singlet methyl resonance at δ_H 3.62 was assigned to methyl ester group (CH_3-12) in **18**. Apart from this difference, the spectral data of **31** and **18** were quite similar. The structure of **31** was further confirmed by interpretation of $^1H-^1H$ COSY. The $^1H-^1H$ COSY spectrum showed as in **18** an extended spin system between $NH-7$ (δ_H 7.84, *d*, 5.1 Hz), $H-8_A$ [δ_H 3.80 (*dd*, 3.8, 13.3

Results

Hz)], H-8_B [δ_{H} 3.37 (*dd*, 5.4, 13.3 Hz)], then to H-9 [δ_{H} 4.64 (*m*)], H-10_A [δ_{H} 2.71 (*dd*, 10.8, 16.1 Hz)], and H-10_B [δ_{H} 2.50 (*dd*, 5.1, 16.1 Hz)]. The optical rotation of **31** gave a value of $[\alpha]_{\text{D}}^{20}$ -5.0° (*c* 0.04, CH₃OH). According to these data (Table 3.9) and by comparison to the reported literature (Cafieri *et al.*, 1998; Petal *et al.*, 2005), **31** was confirmed to be (-)-longamide B that was first isolated from the sponge *Agelas dispar*.

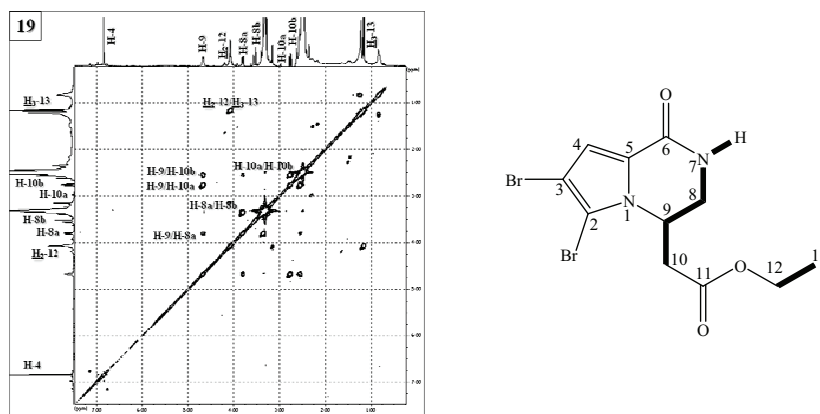


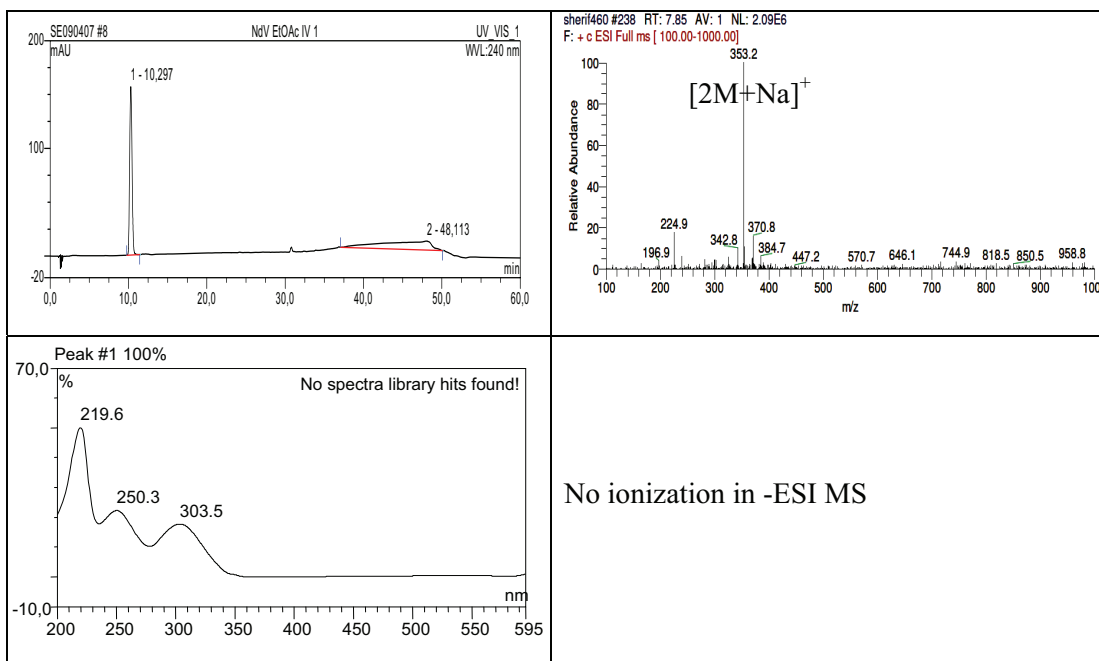
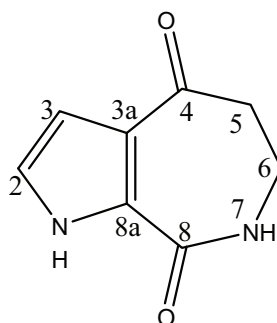
Fig. 3.12. ¹H-¹H COSY of (-)-longamide B ethyl ester, hanishin (**19**).

Table 3.9. NMR data of compounds (**18**, **19**, and **31**), measured in DMSO-*d*₆.

#	18	19	31
	δ_{H}	δ_{H}	δ_{H}
2			
3			
4	6.84 (1H, <i>s</i>)	6.84 (1H, <i>s</i>)	6.84 (1H, <i>s</i>)
5			
6			
7	7.86 (1H, <i>d</i> , 5.1 Hz, <i>NH</i>)	7.86 (1H, <i>d</i> , 5.1 Hz, <i>NH</i>)	7.84 (1H, <i>d</i> , 5.1 Hz, <i>NH</i>)
8	A: 3.80 (1H, <i>dd</i> , 4.1, 13.6 Hz) B: 3.38 (1H, <i>dd</i> , 5.4, 13.6 Hz)	A: 3.80 (1H, <i>dd</i> , 4.4, 13.6 Hz) B: 3.36 (1H, <i>dd</i> , 5.4, 13.6 Hz)	A: 3.80 (1H, <i>dd</i> , 3.8, 13.3 Hz) B: 3.37 (1H, <i>dd</i> , 5.4, 13.3 Hz)
9	4.68 (1H, <i>m</i>)	4.68 (1H, <i>m</i>)	4.64 (1H, <i>m</i>)
10	A: 2.80 (1H, <i>dd</i> , 9.5, 15.5 Hz) B: 2.57 (1H, <i>dd</i> , 5.1, 15.5 Hz)	A: 2.77 (1H, <i>dd</i> , 9.5, 15.5 Hz) B: 2.50 (1H, <i>dd</i> , 5.1, 15.5 Hz)	A: 2.71 (1H, <i>dd</i> , 10.8, 16.1 Hz) B: 2.50 (1H, <i>dd</i> , 5.1, 16.1 Hz)
12	OCH ₃ : 3.62 (3H, <i>s</i>)	=CH ₂ : 4.07 (2H, <i>m</i>)	OH: 12.75 (1H, <i>br s</i>)
13		-CH ₃ : 1.17 (3H, <i>t</i> , 7.3 Hz)	

3.2.7. Aldisine (20, known compound)

Aldisine	
Synonym(s)	6,7-Dihydropyrrolo[2,3-c]azepine-4,8(1 <i>H</i> ,5 <i>H</i>)-dione
Sample code	NdV EtOAc IV 1
Biological source	<i>Stylissa massa</i>
Sample amount	17.0 mg
Physical description	White amorphous solid
Molecular formula	C ₈ H ₈ N ₂ O ₂
Molecular weight	164 g/mol
Retention time (HPLC)	10.30 min (standard gradient)



Results

Compound (**20**) was isolated as a white amorphous solid. It showed pseudomolecular ion peaks at m/z 353 $[2M+Na]^+$ in its ESI mass spectrum. The structure of **20** was further confirmed by interpretation of $^1H-^1H$ COSY and HMBC spectra (Fig. 3.13). The $^1H-^1H$ COSY spectrum two extended spin systems. The first spin system existed between NH -pyrrole [δ_H 12.14 (br s)], H-2 [δ_H 6.97 (d , 2.5 Hz)], and H-3 [δ_H 6.54 (d , 2.5 Hz)]; and the second one was between NH -7 [δ_H 8.30 (t , 4.8 Hz)], $=CH_2$ -6 [δ_H 3.34 (m)], and $=CH_2$ -5 [δ_H 2.69 (m)]. The HMBC spectrum (Fig. 3.13) of **20** gave more evidences by revealing correlations from H-2 to C-3 (δ_C 109.1), C-3a (δ_C 123.5), and C-8a (δ_C 127.8); H-3 to C-2 (δ_C 122.1), C-3, and C-8a; from $=CH_2$ -6 to two carbonyl carbons at δ_C 194.0, and δ_C 161.8 that were ascribed to C-4, and C-8, respectively. Based on the aforementioned data (Table 3.10) and by comparison to the reported literature (Schmitz *et al.*, 1985), **20** was confirmed to be aldisine.

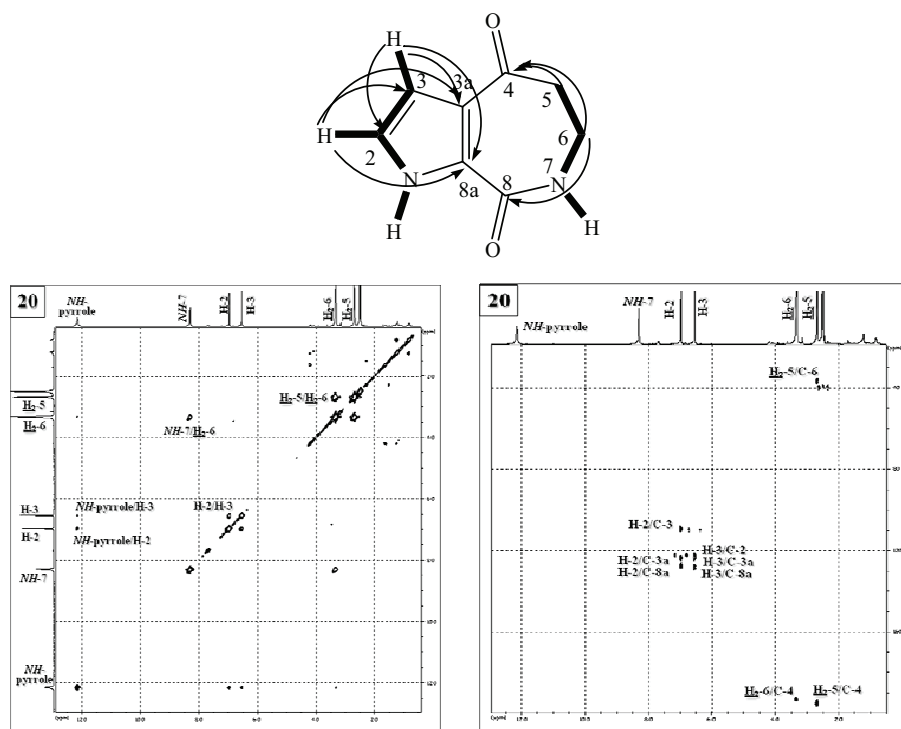
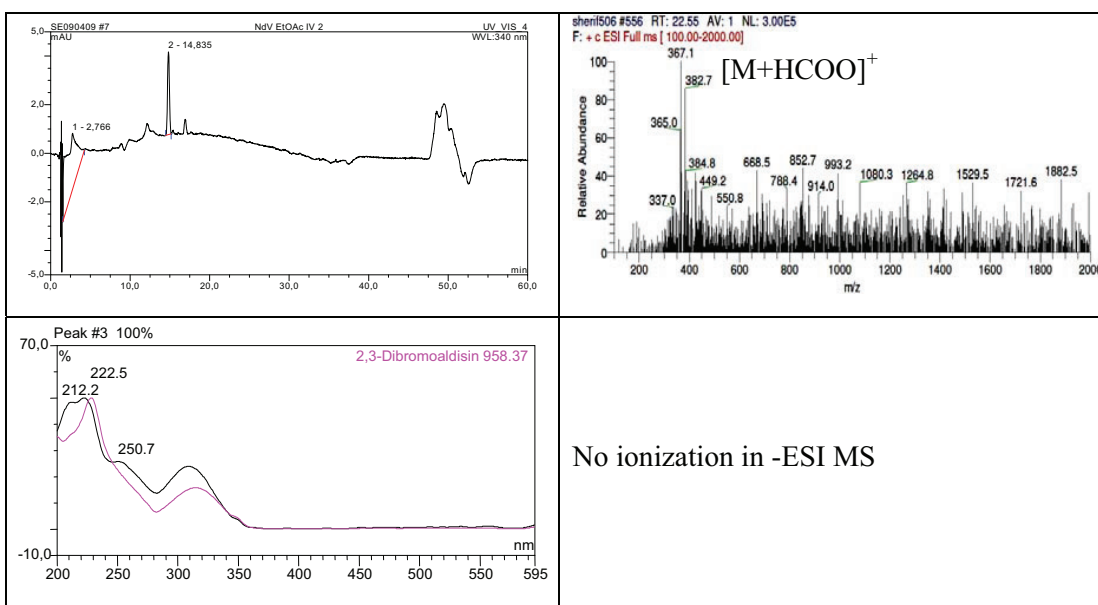
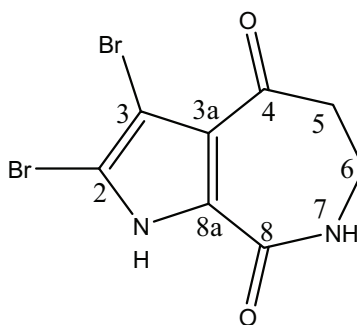


Fig. 3.13. $^1H-^1H$ COSY and HMBC spectra of aldisine (**20**).

3.2.8. 2,3-Dibromoaldisine (21, known compound)

2,3-Dibromoaldisine	
Synonym(s)	2,3-Dibromo-6,7-dihydropyrrolo[2,3-c]azepine-4,8(1 <i>H</i> ,5 <i>H</i>)-dione
Sample code	NdV EtOAc IV 2
Biological source	<i>Stylissa massa</i>
Sample amount	1.0 mg
Physical description	White amorphous solid
Molecular formula	C ₈ H ₆ ⁷⁹ Br ₂ N ₂ O ₂
Molecular weight	322 g/mol
Retention time (HPLC)	14.84 min (standard gradient)



Results

Compound (**21**) was isolated as a white amorphous solid. It showed pseudomolecular ion peaks at m/z 365, 367, 369 $[M+HCOO]^+$, (1:2:1) in its ESI mass spectrum indicating that **21** is dibrominated. 1H NMR spectra of **21** was similar to that of **20** with the only difference by the lack of two aromatic protons at $[\delta_H$ 6.97 (*d*, 2.5 Hz)], and $[\delta_H$ 6.54 (*d*, 2.5 Hz)] that were assigned for H-2, and H-3, respectively. Accordingly, **21** was supposed to be a 2,3-dibrominated derivative of **20**. The structure of **21** was further confirmed by interpretation of 1H — 1H COSY that showed an extended spin system between *NH*-7 $[\delta_H$ 8.52 (*t*, 5.1 Hz)], = \underline{CH}_2 -6 $[\delta_H$ 3.33 (*m*)], and = \underline{CH}_2 -5 $[\delta_H$ 2.74 (*m*)]. Based on the preceding findings (Table 3.10) and by comparing to the reported literature (Hassan *et al.*, 2007), **21** was confirmed to be 2,3-dibromoaldisine.

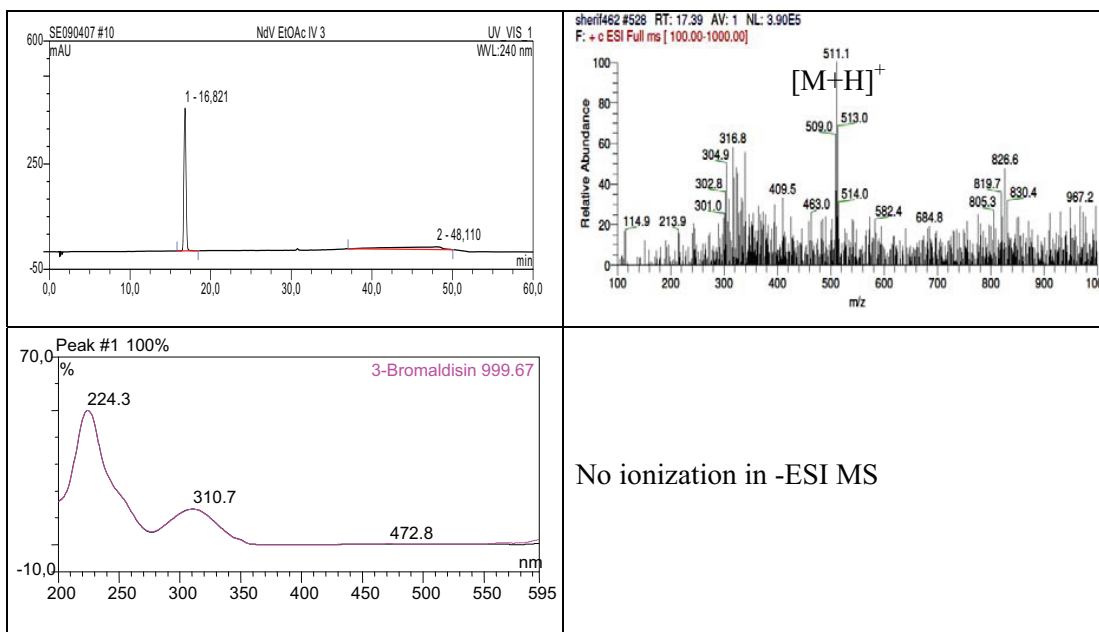
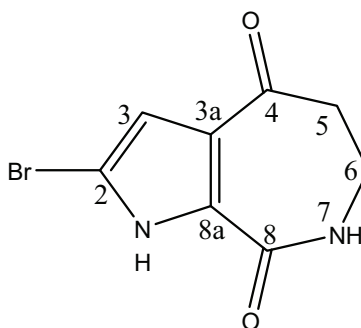
Table 3.10. NMR data of compounds (**20** and **21**), measured in DMSO- d_6 .

#	20		21
	δ_H	δ_C^*	δ_H
1	12.14 (1H, br <i>s</i>)		13.44 (1H, br <i>s</i>)
2	6.97 (1H, <i>d</i> , 2.5 Hz)	122.1	
3	6.54 (1H, <i>d</i> , 2.5 Hz)	109.1	
3a		123.5	
4		194.0	
5	2.69 (2H, <i>m</i>)		2.74 (2H, <i>m</i>)
6	3.34 (2H, <i>m</i>)	36.3	3.33 (2H, <i>m</i>)
7	8.30 (1H, <i>t</i> , 4.8 Hz, <i>NH</i>)		8.52 (1H, <i>t</i> , 5.1 Hz, <i>NH</i>)
8		161.8	
8a		127.8	

* ^{13}C NMR values obtained from HMBC spectrum.

3.2.9. 2-Bromoaldisine (22, known compound)

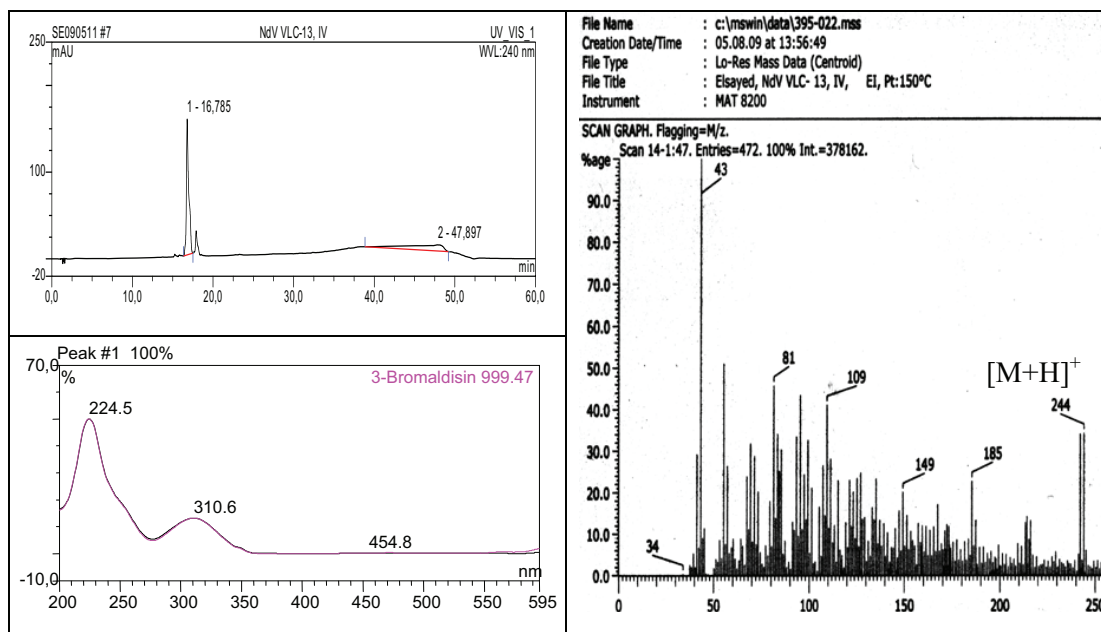
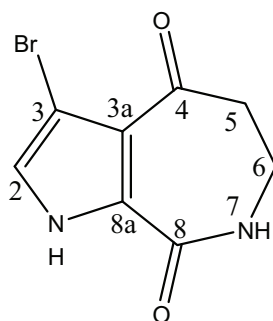
2-Bromoaldisine	
Synonym(s)	2-Bromo-6,7-dihydropyrrolo[2,3-c]azepine-4,8(1 <i>H</i> ,5 <i>H</i>)-dione
Sample code	NdV EtOAc IV 3
Biological source	<i>Stylissa massa</i>
Sample amount	6.0 mg
Physical description	White amorphous solid
Molecular formula	C ₈ H ₇ ⁷⁹ BrN ₂ O ₂
Molecular weight	243 g/mol
Retention time (HPLC)	16.82 min (standard gradient)



Results

3.2.10. 3-Bromoaldisine (23, known compound)

3-Bromoaldisine	
Synonym(s)	3-Bromo-6,7-dihydropyrrolo[2,3-c]azepine-4,8(1 <i>H</i> ,5 <i>H</i>)-dione
Sample code	NdV VLC-13,IV
Biological source	<i>Stylissa massa</i>
Sample amount	5.0 mg
Physical description	White amorphous solid
Molecular formula	C ₈ H ₇ ⁷⁹ BrN ₂ O ₂
Molecular weight	243 g/mol
Retention time (HPLC)	16.79 min (standard gradient)



Compound (**22**) was isolated as a white amorphous solid. It showed pseudomolecular ion peaks at m/z 509, 511, 513 $[2M+Na]^+$. 1H NMR spectra of **22** resembled that of **20** except in the presence of one aromatic proton at $[\delta_H 6.55 (s)]$ ascribed to H-3 in **22** instead of two aromatic protons at $[\delta_H 6.97 (d, 2.5 \text{ Hz})]$, and $[\delta_H 6.54 (d, 2.5 \text{ Hz})]$ that were assigned for H-2, and H-3 in **20**, respectively. Accordingly, **22** was supposed to be a 2-brominated derivative of **20**. The structure of **22** was further confirmed by interpretation of 1H — 1H COSY (Fig. 3.14) that showed one extended spin system between $NH-7$ $[\delta_H 8.38 (t, 5.1 \text{ Hz})]$, $=CH_2-6$ $[\delta_H 3.34 (m)]$, and $=CH_2-5$ $[\delta_H 2.69 (m)]$. 1H NMR of C-3 was similar to those observed in related compounds as in hymenialdisine (Cimino *et al.*, 1982; Kitagawa *et al.*, 1983), axinohydantoin (Pettit *et al.*, 1990), and spongiacidin D (Inaba *et al.*, 1998). According to the preceding findings (Table 3.11) and by comparing to the reported literature (Schmitz *et al.*, 1985; Hassan *et al.*, 2007), **22** was confirmed to be 2-bromoaldisine.

Compound (**23**) was isolated as a white amorphous solid. It showed pseudomolecular ion peaks at m/z 242, and 244 $[M+H]^+$ in its EI mass spectrum. The structure of **23** was further confirmed by interpretation of 1H — 1H COSY and HMBC spectra. The 1H — 1H COSY spectrum (Fig. 3.14) two extended spin systems. The first spin system existed between NH -pyrrole $[\delta_H 12.95 (br s)]$, and H-2 $[\delta_H 6.54 (d, 2.5 \text{ Hz})]$, and the second one was between $NH-7$ $[\delta_H 8.38 (t, 5.1 \text{ Hz})]$, $=CH_2-6$ $[\delta_H 3.34 (m)]$, and $=CH_2-5$ $[\delta_H 2.69 (m)]$. The HMBC spectrum of **23** gave more clues by revealing correlations from H-2 to C-3 (δ_C 104.9), and C-8a (δ_C 129.1); from both $=CH_2-5$, and $=CH_2-6$ to a carbonyl carbons at δ_C 193.8 that was ascribed to C-4. Based on the aforementioned data (Table 3.11) and by comparison to the reported literature (Hassan *et al.*, 2007), **23** was confirmed to be 3-bromoaldisine.

Results

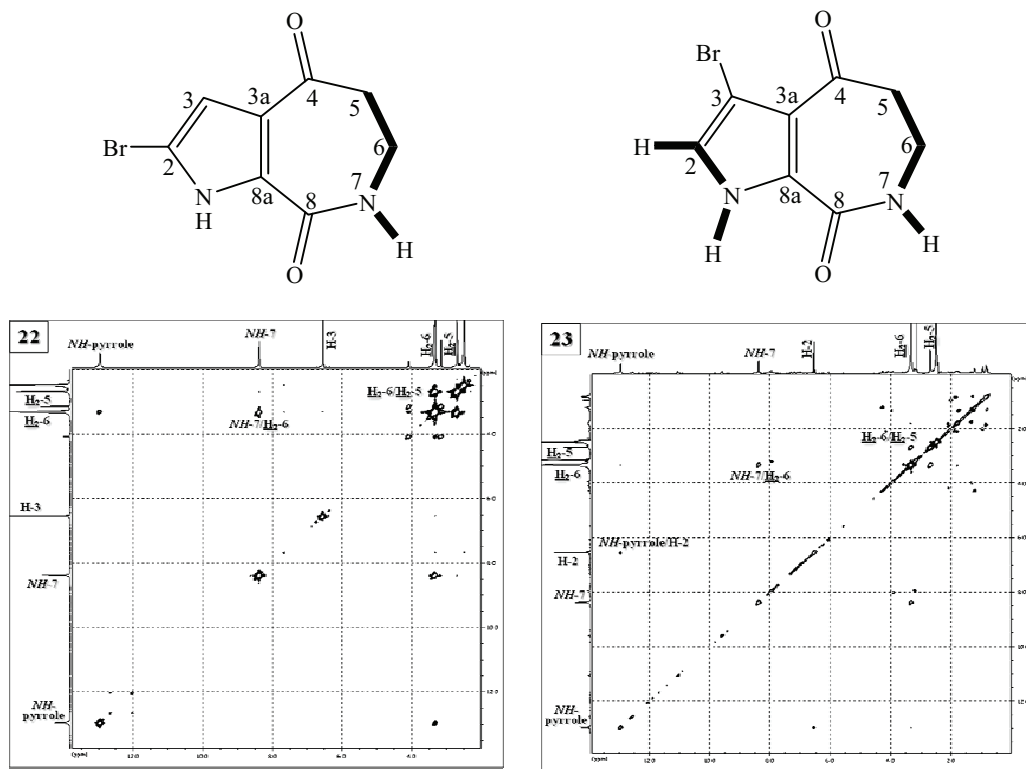


Fig. 3.14. ^1H - ^1H COSY spectra of 2-bromoaldisine (22) and 3-bromoaldisine (23).

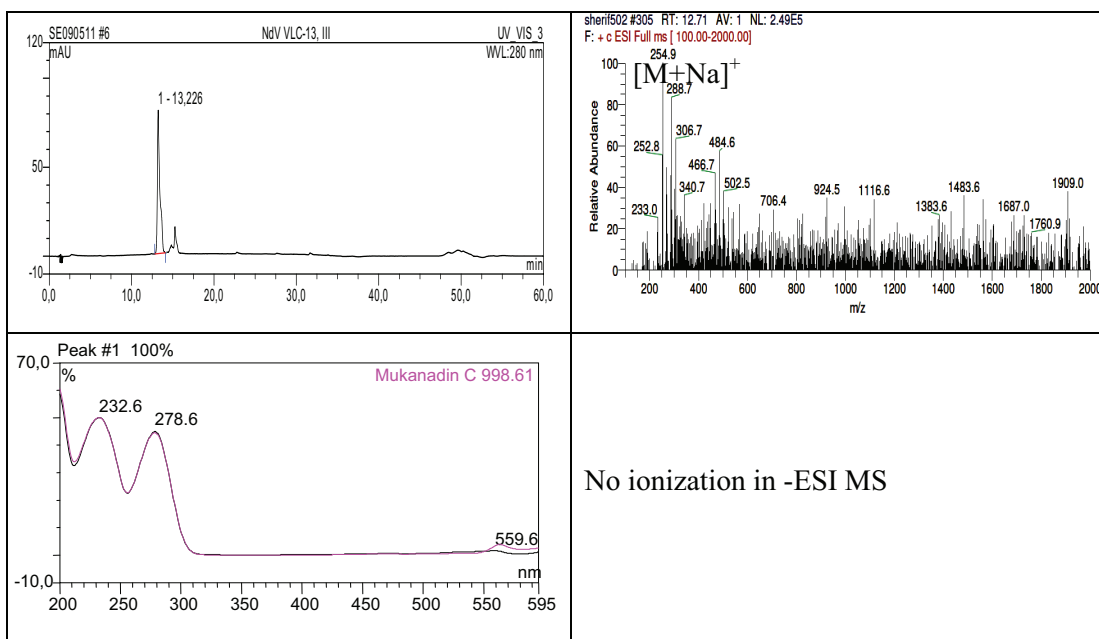
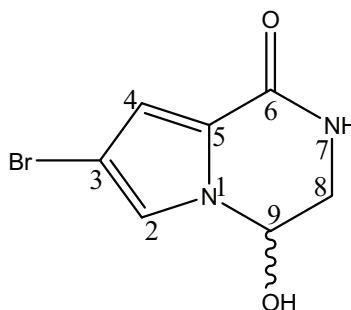
Table 3.11. NMR data of compounds (22 and 23), measured in $\text{DMSO}-d_6$.

#	22	23	
	δ_{H}	δ_{H}	δ_{C}^*
1	12.95 (1H, br s)	12.95 (1H, br s)	
2		6.54 (1H, d, 2.5 Hz)	111.0
3	6.55 (1H, s)		104.9
3a			
4			193.8
5	2.69 (2H, m)	2.69 (2H, m)	
6	3.34 (2H, m)	3.34 (2H, m)	36.3
7	8.38 (1H, t, 5.1 Hz, NH)	8.38 (1H, t, 5.1 Hz, NH)	
8			
8a			129.1

* ^{13}C NMR values obtained from HMBC spectrum.

3.2.11. (-)-Mukanadin C (24, known compound)

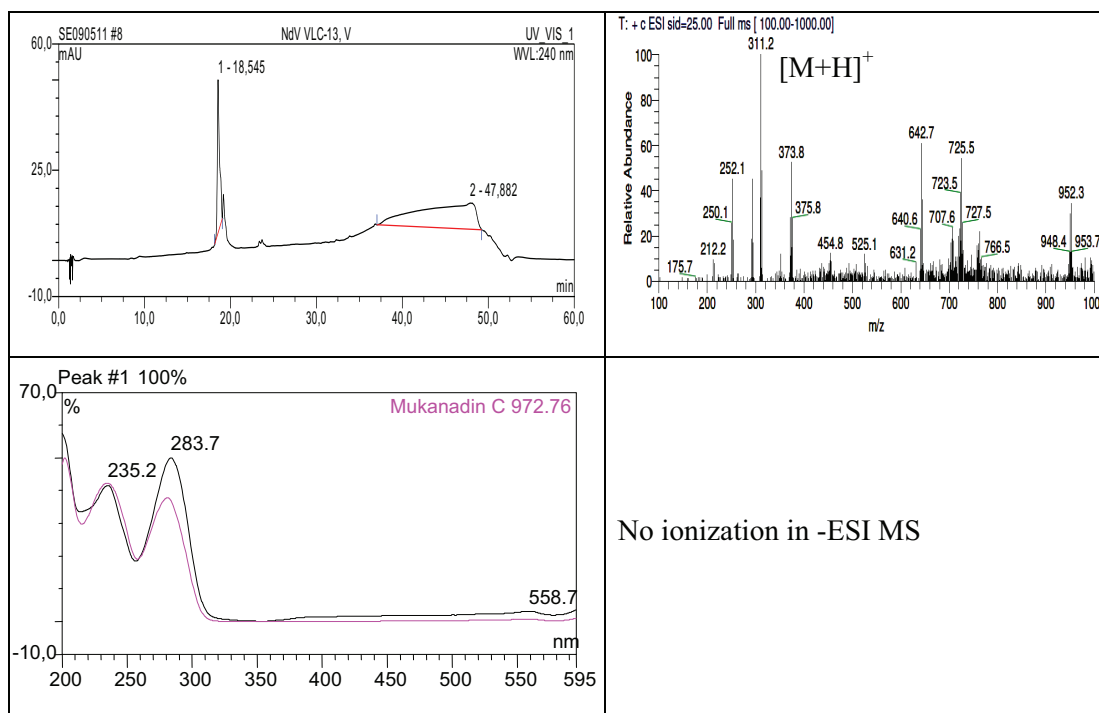
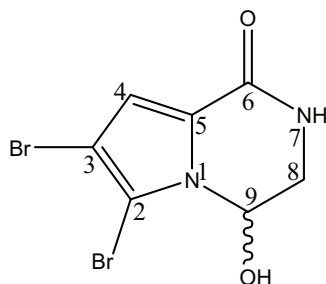
(-)-Mukanadin C	
Synonym(s)	6-Debromolongamide A
Sample code	NdV VLC-13,III
Biological source	<i>Stylissa massa</i>
Sample amount	3.0 mg
Physical description	White amorphous solid
Molecular formula	C ₇ H ₇ ⁷⁹ BrN ₂ O ₂
Molecular weight	231 g/mol
Optical rotation [α] _D ²⁰	-2.0°C (c 0.04, CH ₃ OH)
Retention time (HPLC)	13.23 min (standard gradient)



Results

3.2.12. (-)-Longamide (25, known compound)

(-)-Longamide	
Synonym(s)	6,7-Dibromo-3,4-dihydro-4-hydroxypyrrolo[1,2-a]pyrazin-1(2H)-one
Sample code	NdV VLC-13,V
Biological source	<i>Stylissa massa</i>
Sample amount	2.0 mg
Physical description	White amorphous solid
Molecular formula	C ₇ H ₆ ⁷⁹ Br ₂ N ₂ O ₂
Molecular weight	310 g/mol
Optical rotation [α] _D ²⁰	-18.0°C (c 0.04, CH ₃ OH)
Retention time (HPLC)	18.55 min (standard gradient)



Compound (**24**) was isolated as a white amorphous solid. It showed pseudomolecular ion peaks at m/z 253, and 255 $[M+Na]^+$, (1:1) in its EI mass spectrum revealing that **24** is a monobrominated compound. The structure of **24** was further confirmed by interpretation of $^1H-^1H$ COSY. The $^1H-^1H$ COSY spectrum (Fig. 3.15) showed two extended spin systems. The first spin system existed between H-2 [δ_H 7.16 (*d*, 1.9 Hz)], and H-4 [δ_H 6.63(*d*, 1.9 Hz)], and the second one was between NH-7 [δ_H 7.74 (*br s*)], H-8_A [δ_H 3.58 (*dd*, 3.2, 11.7 Hz)], H-8_B [δ_H 3.31 (*m*)], and H-9 [δ_H 5.57 (*d*, 4.8 Hz)]. The optical rotation of **24** gave a value of $[\alpha]_D^{20}$ -2.0° (*c* 0.04, CH₃OH). According to the aforementioned data (Table 3.12) and by comparison to the reported literature (Li *et al.*, 1998; Uemoto *et al.*, 1999), **24** was found to be (-)-mukanadin C.

Compound (**25**) was isolated as a white amorphous solid. It showed pseudomolecular ion peaks at m/z 309, 311, and 313 $[M+H]^+$, (1:2:1) in its EI mass spectrum revealing that **25** is a dibrominated compound. Compound (**25**) differed from **24** by more 79 amu. This difference was explained by the existence of one more bromine substituent in **25** than in **24**. This also was accompanied by disappearance of one proton resonance at [δ_H 7.16 (*d*, 1.9 Hz)] that was assigned to H-2 in **24**. The structure of **25** was further confirmed by interpretation of $^1H-^1H$ COSY spectrum (Fig. 3.15) that revealed one extended spin system between NH-7 [δ_H 7.87 (*d*, 4.7 Hz)], H-8_A [δ_H 3.70 (*dd*, 2.9, 13.9 Hz)], H-8_B [δ_H 3.38 (*m*)], and H-9 [δ_H 5.60 (*d*, 6.3 Hz)]. The optical rotation of **25** gave a value of $[\alpha]_D^{20}$ -18.0° (*c* 0.04, CH₃OH). According to the preceding data (Table 3.12) and by comparison to the reported literature (Cafieri *et al.*, 1995), **25** was found to be (-)-longamide that was first isolated from the marine sponge *Agelas longissima*.

Results

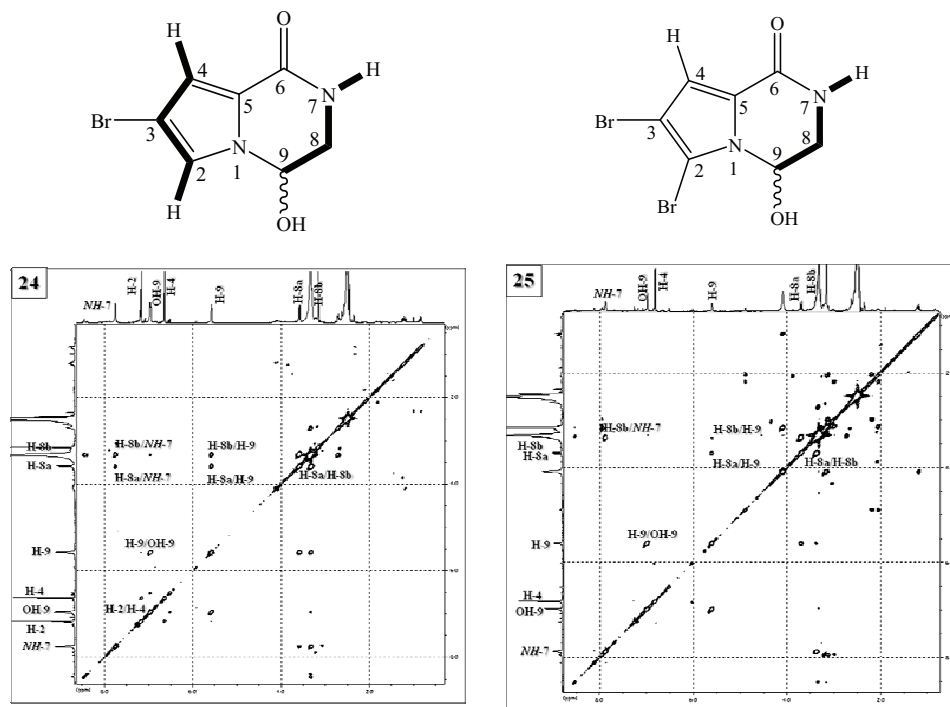


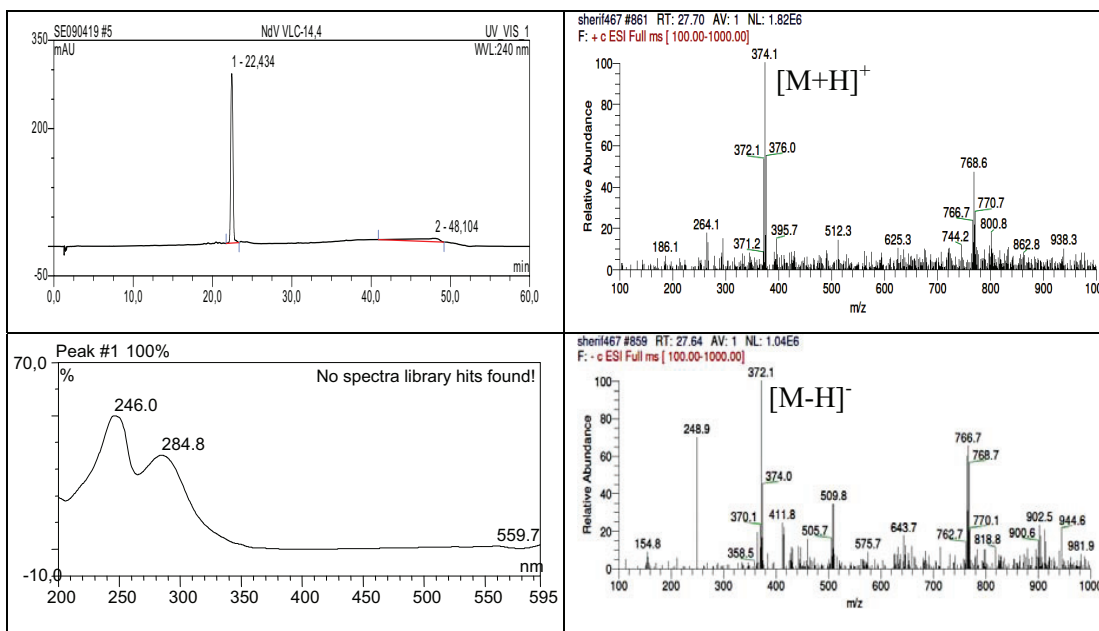
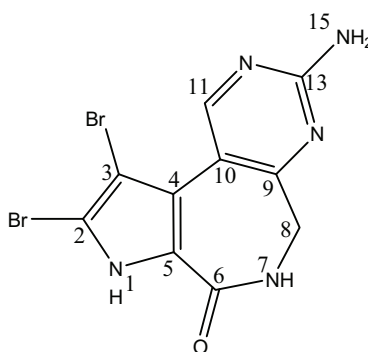
Fig. 3.15. ¹H-¹H COSY spectra of (-)-mukanadin C (24) and (-)-longamide (25).

Table 3.12. NMR data of compounds (24 and 25), measured in DMSO-*d*₆.

#	24	25
	δ _H	δ _H
2	7.16 (1H, <i>d</i> , 1.9 Hz)	
3		
4	6.63 (1H, <i>d</i> , 1.9 Hz)	6.81 (1H, <i>s</i>)
5		
6		
7	7.74 (1H, <i>br s</i>)	7.87 (1H, <i>d</i> , 4.7 Hz)
8	A: 3.58 (1H, <i>dd</i> , 3.2, 11.7 Hz) B: 3.31 (1H, <i>m</i>)	A: 3.70 (1H, <i>dd</i> , 2.9, 13.9 Hz) B: 3.38 (1H, <i>m</i>)
9	5.57 (1H, <i>d</i> , 4.8 Hz)	5.60 (1H, <i>d</i> , 6.3 Hz)
OH-9	6.95 (1H, <i>d</i> , 6.3 Hz)	6.98 (1H, <i>d</i> , 6.7 Hz)

3.2.13. Latonduine A (26, known compound)

Latonduine A	
Sample code	NdV VLC-14,4
Biological source	<i>Stylissa massa</i>
Sample amount	6.0 mg
Physical description	Yellow powder
Molecular formula	C ₁₀ H ₇ ⁷⁹ Br ₂ N ₅ O
Molecular weight	373 g/mol
Retention time (HPLC)	22.43 min (standard gradient)



Results

Compound (**26**) was isolated as a brownish yellow powder. It showed pseudomolecular ion peaks at m/z 372, 374, and 376 $[M+H]^+$, (1:2:1) in its EI mass spectrum revealing that **26** is a dibrominated compound. The structure of **26** was further confirmed by interpretation of ^1H — ^1H COSY, and HMBC spectra (Fig. 3.16). The ^1H — ^1H COSY spectrum (Fig. 3.16) revealed one spin system between NH -7 [δ_{H} 8.16 (d , 5.1 Hz)], and $=\text{CH}_2$ -8 [δ_{H} 3.90 (d , 5.1 Hz)]. Moreover, the HMBC spectrum (Fig. 3.16) revealed clear correlations from H-11 [δ_{H} 8.76 (s)] to C-10 (δ_{C} 113.0), C-13 (δ_{C} 162.2), and C-9 (δ_{C} 163.4); and from $=\text{CH}_2$ -8 [δ_{H} 3.90 (d , 5.1 Hz)] to C-6 (δ_{C} 164.0). Based on the previous data (Table 3.13) and by comparison to the reported literature (Linington *et al.*, 2003), **26** was found to be latonduine A that was first isolated from the marine sponge *Stylissa carteri*.

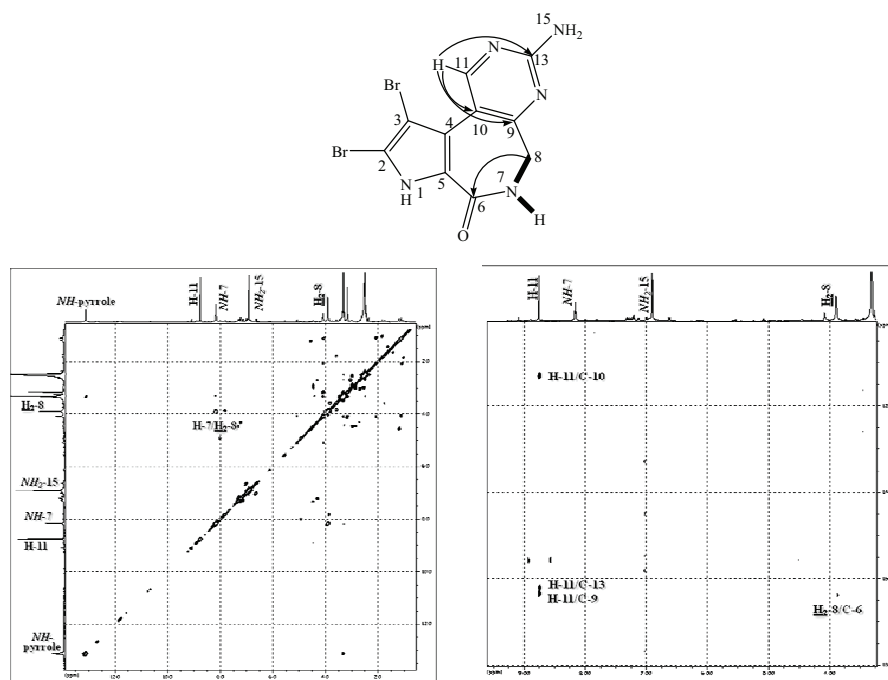


Fig. 3.16. ^1H — ^1H COSY and HMBC spectra of latonduine A (**26**).

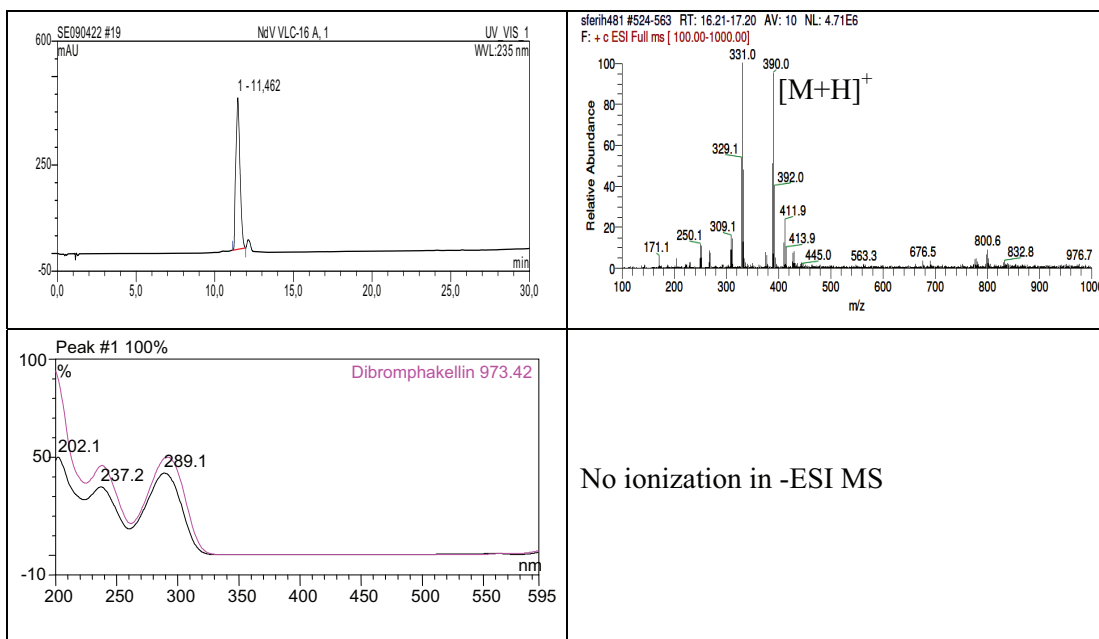
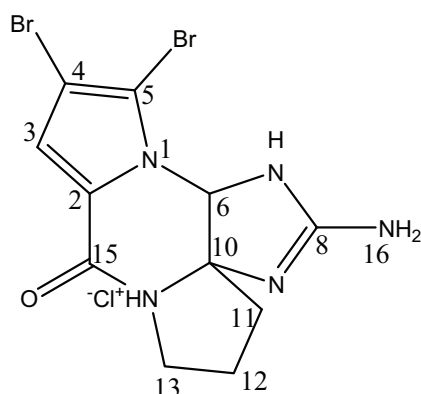
Table 3.13. NMR data of latonduine A (**26**), measured in $\text{DMSO}-d_6$.

26					
#	δ_{H}	δ_{C}^*	#	δ_{H}	δ_{C}^*
1	13.11 (1H, br s, <i>NH</i> -pyrrole)		10		113.0
6		164.0	11	8.76 (1H, <i>s</i>)	155.7
7	8.16 (1H, <i>d</i> , 5.1 Hz, <i>NH</i>)		13		162.2
8	3.90 (2H, <i>d</i> , 5.1 Hz)		15	6.90 (2H, <i>s</i> , <i>NH</i> ₂ -15)	
9		163.4			

* ^{13}C NMR values obtained from HMBC spectrum.

3.2.14. (-)-Dibromophakellin H⁺Cl⁻ (27, known compound)

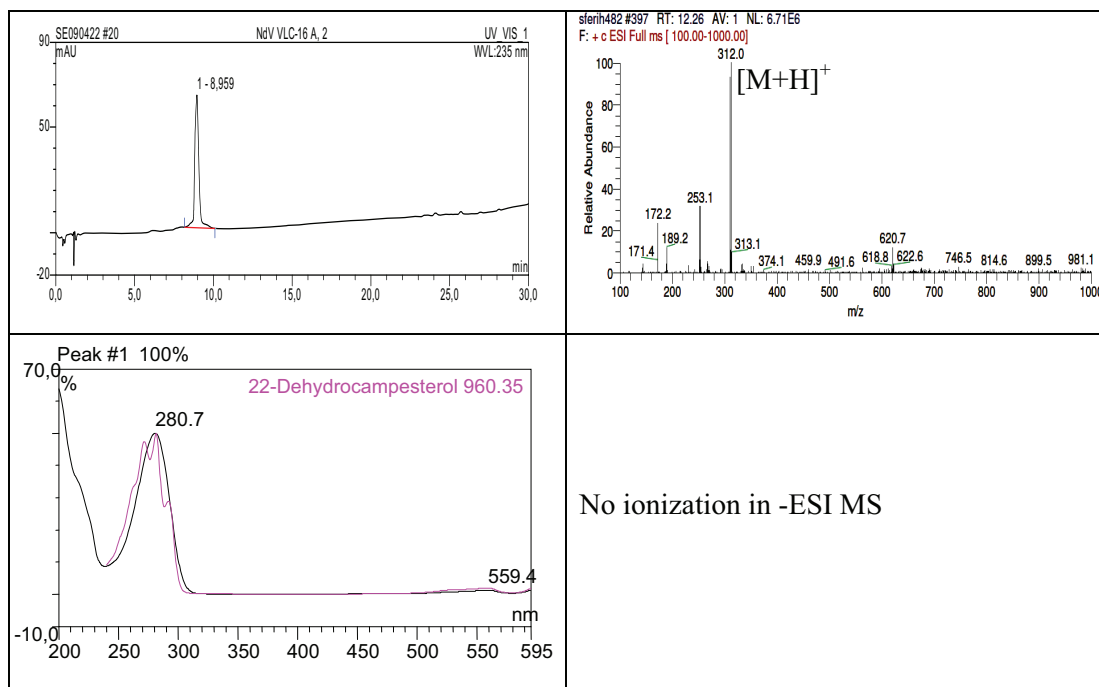
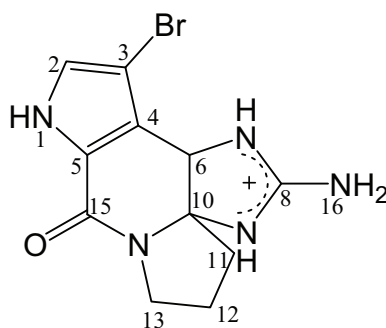
(-)-Dibromophakellin H ⁺ Cl ⁻	
Sample code	NdV VLC-16,A1
Biological source	<i>Stylissa massa</i>
Sample amount	5.0 mg
Physical description	White amorphous solid
Molecular formula	C ₁₁ H ₁₁ ⁷⁹ Br ₂ N ₅ O
Molecular weight	389 g/mol
Optical rotation [α] _D ²⁰	-46.0°C (c 0.08, CH ₃ OH)
Retention time (HPLC)	11.46 min (half-time gradient)



Results

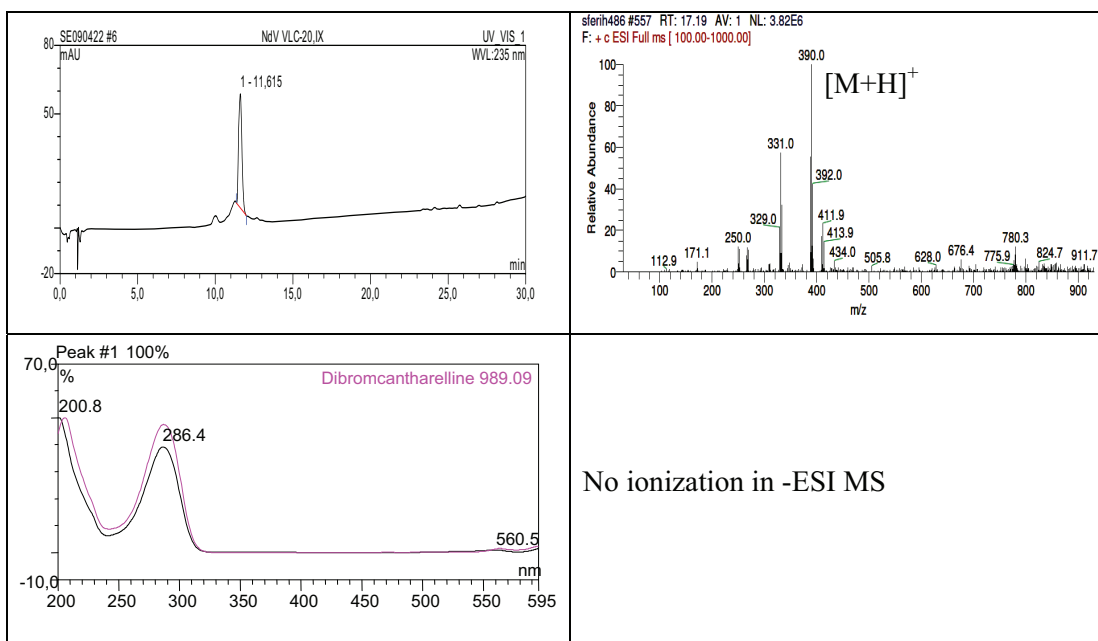
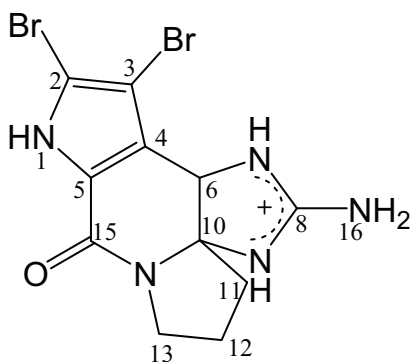
3.2.15. (-)-Monobromoisophakellin (28, known compound)

(-)-Monobromoisophakellin	
Sample code	NdV VLC-16,A2
Biological source	<i>Stylissa massa</i>
Sample amount	4.0 mg
Physical description	White amorphous solid
Molecular formula	C ₁₁ H ₁₂ ⁷⁹ BrN ₅ O
Molecular weight	310 g/mol
Optical rotation [α] _D ²⁰	-22.0°C (c 0.06, CH ₃ OH)
Retention time (HPLC)	8.96 min (half-time gradient)



3.2.16. (-)-Dibromocantharelline (32, known compound)

(-)-Dibromocantharelline	
Synonym(s)	(-)-Dibromoisophakellin
Sample code	NdV VLC-20,IX
Biological source	<i>Stylissa massa</i>
Sample amount	2.0 mg
Physical description	Yellowish amorphous solid
Molecular formula	C ₁₁ H ₁₁ ⁷⁹ Br ₂ N ₅ O
Molecular weight	389 g/mol
Optical rotation [α] _D ²⁰	-12.0°C (c 0.06, CH ₃ OH)
Retention time (HPLC)	11.62 min (half-time gradient)



Results

Compound (**27**) was isolated as a white amorphous solid. It showed pseudomolecular ion peaks at m/z 388, 390, and 392 $[M+H]^+$, (1:2:1) in its EI mass spectrum revealing that **27** is a dibrominated compound. The structure of **27** was further confirmed by interpretation of $^1H-^1H$ COSY, and HMBC spectra (Fig. 3.17). The $^1H-^1H$ COSY spectrum (Fig. 3.17) revealed two extended spin systems. The first spin system existed between H-6 [δ_H 6.30 (br s)], and NH-7 [δ_H 9.85 (br s)], and the second one was between H-11_A [δ_H 2.40 (m)], H-11_B [δ_H 2.28 (m)], =CH₂-12 [δ_H 2.05 (m)], H-13_A [δ_H 3.66 (m)], and H-13_B [δ_H 3.47 (m)]. Moreover, the HMBC spectrum (Fig. 3.17) revealed clear correlations from H-3 [δ_H 7.02 (s)] to C-2 (δ_C 106.0), and C-5 (δ_C 124.8) to which H-6 [δ_H 6.3 (br s)] showed a correlation in addition to C-10 (δ_C 82.2), and C-15 (δ_C 156.3). The optical rotation of **27** gave a value of $[\alpha]_D^{20}$ -46.0° (c 0.08, CH₃OH). According to the aforementioned data (Table 3.14) and by comparison to the reported literature (Sharma and Magdoff-Fairchild, 1977), **27** was evidenced to be (-)-dibromophakellin H^+Cl^- that was first isolated from the marine sponge *Phakellia flabellata*.

Compound (**28**) was isolated as a white amorphous solid. It showed pseudomolecular ion peaks at m/z 310, and 312 $[M+H]^+$, (1:1) in its EI mass spectrum revealing that **28** is a monobrominated compound. The structure of **28** was further confirmed by interpretation of $^1H-^1H$ COSY spectra. The $^1H-^1H$ COSY spectrum (Fig. 3.17) revealed one extended spin system between =CH₂-11 [δ_H 2.22 (m)], =CH₂-12 [δ_H 2.04 (m)], H-13_A [δ_H 3.57 (m)], and H-13_B [δ_H 3.47 (m)] in addition to the clear correlations between NH-pyrrole [δ_H 12.45 (br s)], and H-2 [δ_H 7.23 (d, 2.9 Hz)]; NH-7 [δ_H 8.58 (br s)], to both NH-9 [δ_H 9.52 (br s)], and H-6 [δ_H 5.22 (br s)]. The optical rotation of **28** gave a value of $[\alpha]_D^{20}$ -22.0° (c 0.06, CH₃OH). Based on the previously mentioned data (Table 3.14) and by comparison to the reported literature (Assmann and Köck, 2002), **28** was proven to be (-)-monobromoisophakellin that was first isolated from an unspecified Caribbean sponge of the genus *Agelas*.

Compound (**32**) was isolated as a white amorphous solid. It showed pseudomolecular ion peaks at m/z 388, 390, and 392 $[M+H]^+$, (1:2:1) in its EI mass spectrum revealing that **32** is a dibrominated compound. Compound (**32**) differed from **28** by more 79 amu. This difference was explained by the existence of one more bromine substituent in **32** than in **28**. This also was accompanied by disappearance of one proton resonance at [δ_H 7.23 (d, 2.9 Hz)] that was assigned to H-2 in **28**. The structure of **32** was further confirmed by interpretation of $^1H-^1H$ COSY spectra. The $^1H-^1H$ COSY spectrum revealed one extended spin system between =CH₂-11 [δ_H 2.21 (m)], =CH₂-12 [δ_H 2.01 (m)], H-13_A [δ_H

3.58 (m)], and H-13_B [δ_{H} 3.47 (m)]. The optical rotation of **32** gave a value of $[\alpha]_{\text{D}}^{20} -12.0^{\circ}$ (c 0.06, CH₃OH). According to the previously mentioned data (Table 3.14) and by comparing to the reported literature (De Nanteuil *et al.*, 1985), **32** was proven to be (-)-dibromoisophakellin that was given the trivial name (-)-dibromocantharelline which was firstly reported from the marine sponge *Pseudaxinyssa cantharella*.

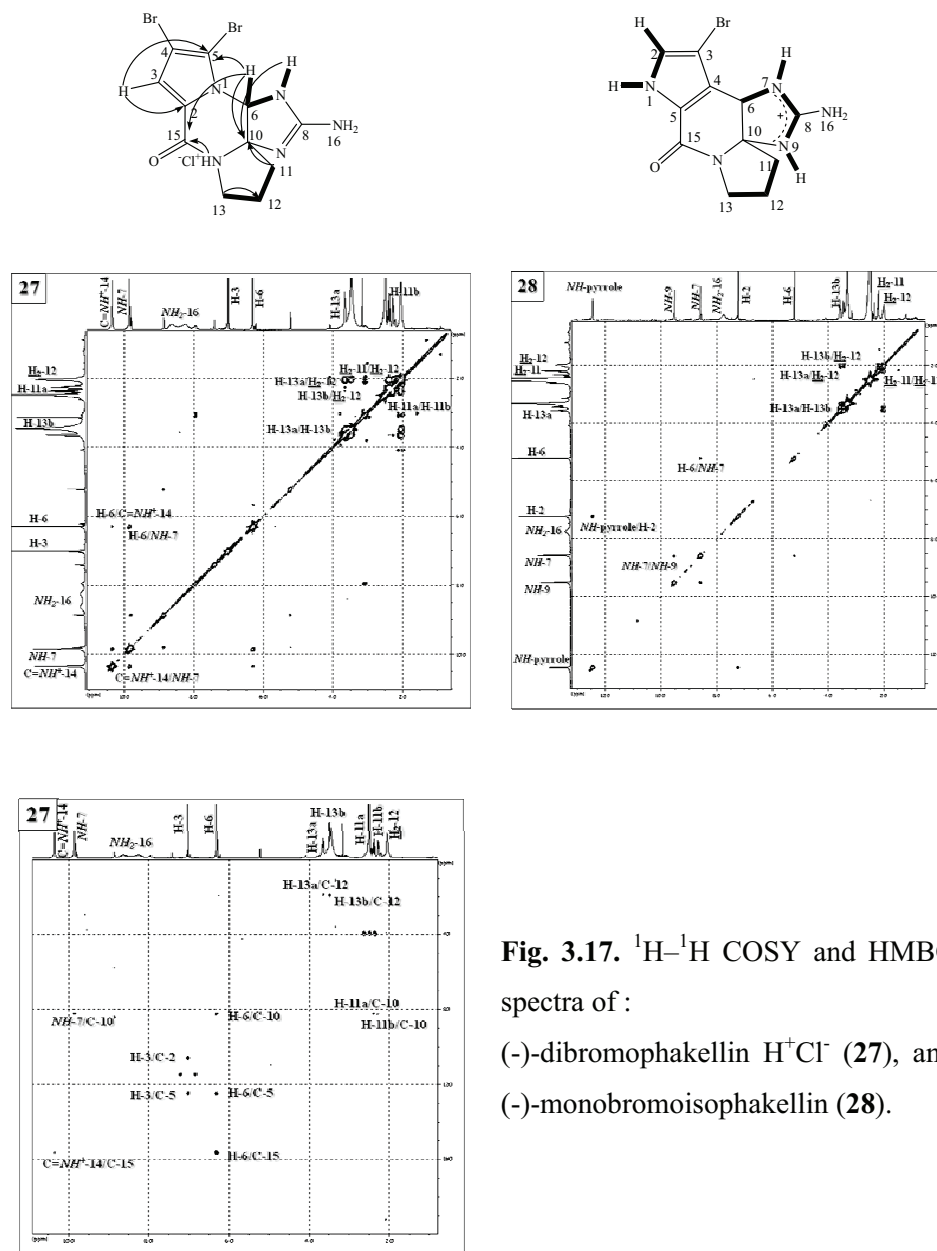


Fig. 3.17. ¹H-¹H COSY and HMBC spectra of :
(-)-dibromophakellin H⁺Cl⁻ (**27**), and
(-)-monobromoisophakellin (**28**).

Results

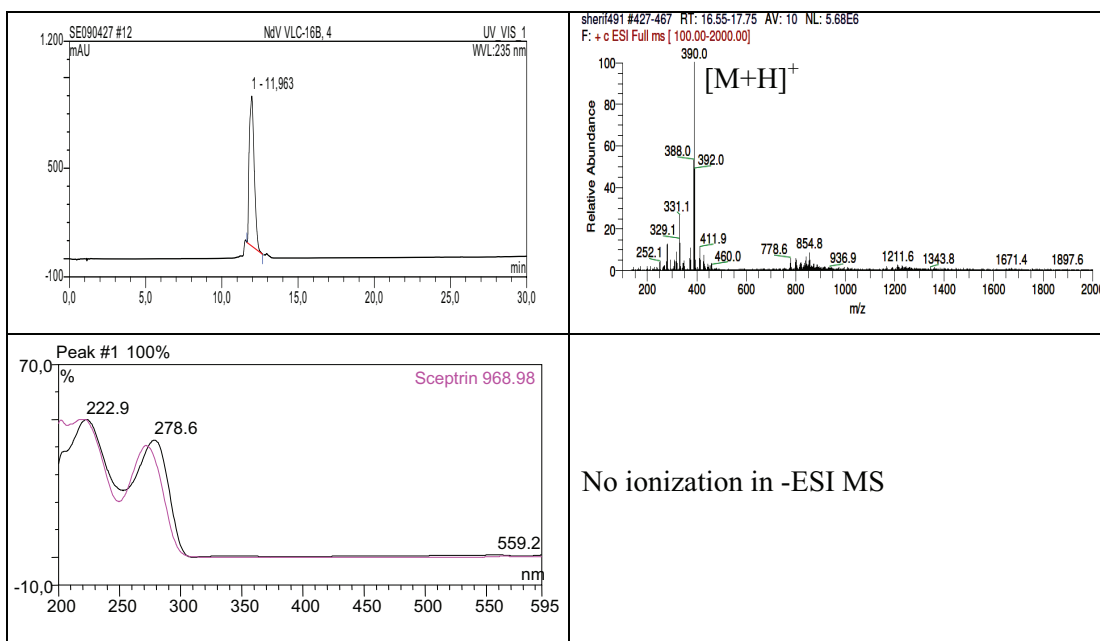
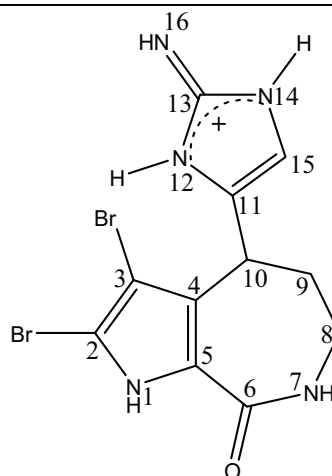
Table 3.14. NMR data of compounds (**26**, **28**, and **32**), measured in DMSO-*d*₆.

#	27		28	32
	δ_{H}	δ_{C}^*	δ_{H}	δ_{H}
1			12.45 (1H, br s, <i>NH</i> -pyrrole)	13.35 (1H, br s, <i>NH</i> -pyrrole)
2		106.0	7.23 (1H, <i>d</i> , 2.9 Hz)	
3	7.02 (1H, <i>s</i>)	114.7		
4				
5		124.8		
6	6.30 (1H, br <i>s</i>)		5.22 (1H, br <i>s</i>)	5.22 (1H, br <i>s</i>)
7	9.85 (1H, br <i>s</i> , <i>NH</i>)		8.58 (1H, br <i>s</i> , <i>NH</i>)	8.68 (1H, br <i>s</i> , <i>NH</i>)
8				
9			9.52 (1H, br <i>s</i> , <i>NH</i>)	9.54 (1H, br <i>s</i> , <i>NH</i>)
10		82.2		
11	A: 2.40 (1H, <i>m</i>) B: 2.28 (1H, <i>m</i>)		2.22 (2H, <i>m</i>)	2.21 (2H, <i>m</i>)
12	2.05 (2H, <i>m</i>)	19.0	2.04 (2H, <i>m</i>)	2.01 (2H, <i>m</i>)
13	A: 3.66 (1H, <i>m</i>) B: 3.47 (1H, <i>m</i>)		A: 3.57 (1H, <i>m</i>) B: 3.47 (1H, <i>m</i>)	A: 3.58 (1H, <i>m</i>) B: 3.47 (1H, <i>m</i>)
14	10.34 (1H, br <i>s</i> , C= <i>NH</i> ⁺)			
15		156.3		
16	8.63 (1H, br <i>s</i> , <i>NH</i> ₂ -16) 8.25 (1H, br <i>s</i> , <i>NH</i> ₂ -16)		7.75 (2H, br <i>s</i> , <i>NH</i> ₂ -16)	7.78 (2H, br <i>s</i> , <i>NH</i> ₂ -16)

*¹³C NMR values obtained from HMBC spectrum.

3.2.17. (-)-Hymenine (29, known compound)

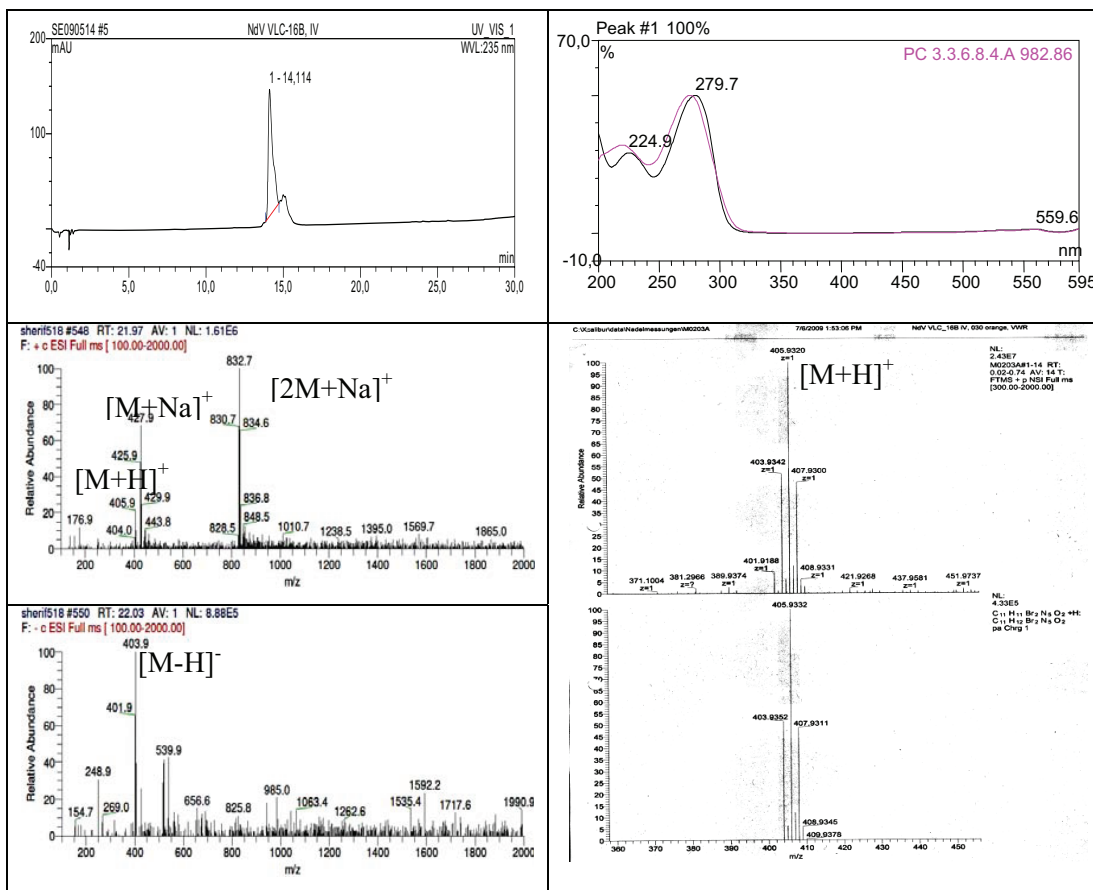
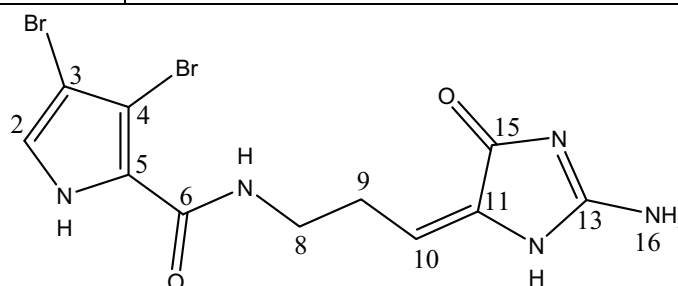
(-)-Hymenine	
Synonym(s)	(-)-9,10-Dihydrostevensine
Sample code	NdV VLC-16,B4
Biological source	<i>Stylissa massa</i>
Sample amount	7.0 mg
Physical description	White amorphous solid
Molecular formula	C ₁₁ H ₁₂ ⁷⁹ Br ₂ N ₅ O
Molecular weight	389 g/mol
Optical rotation [α]_D²⁰	-40.0°C (c 0.06, CH ₃ OH)
Retention time (HPLC)	11.96 min (half-time gradient)



Results

3.2.18. Dispacamide E (30, new natural product)

Dispacamide E	
Synonym(s)	
Sample code	NdV VLC-16B,IV
Biological source	<i>Stylissa massa</i>
Sample amount	4.0 mg
Physical description	White amorphous solid
Molecular formula	C ₁₁ H ₁₁ ⁷⁹ Br ₂ N ₅ O ₂
Molecular weight	405 g/mol
Retention time (HPLC)	14.11 min (half-time gradient)



Compound (**29**) was isolated as a yellow amorphous solid. It showed pseudomolecular ion peaks at m/z 388, 390, and 392 $[M+H]^+$, (1:2:1) in its EI mass spectrum revealing that **29** has two bromine substituents. The structure of **29** was further confirmed by interpretation of $^1H-^1H$ COSY and HMBC spectra. The $^1H-^1H$ COSY spectrum (Fig. 3.18) revealed one extended spin system between $NH-7$ [δ_H 7.95 (*t*, 5.1 Hz)], $=CH_2-8$ [δ_H 3.47 (*m*)], $=CH_2-9$ [δ_H 2.50 (*m*)], and H-10 [δ_H 5.96 (*t*, 7.6 Hz)]. The HMBC spectrum (Fig. 3.18) of **29** revealed clear correlations from NH -pyrrole [δ_H 12.62 (*br s*)] to C-3 (δ_C 100.5), and C-4 (δ_C 123.3); from H-15 [δ_H 6.22 (*s*)] to C-11 (δ_C 128.8), and C-13 (δ_C 146.8); and from H-10 to C-9 (δ_C 31.76). The optical rotation of **29** gave a value of $[\alpha]_D^{20}$ -40.0° (*c* 0.06, CH₃OH). Based on the preceding data (Table 3.15) and by comparing to the reported literature (Kobayashi *et al.*, 1986; Xu *et al.*, 1997), **29** was deduced to be (-)-hymenine that was firstly reported from an unspecified Okinawan marine sponge of the genus *Hymeniacidon*.

Compound (**30**) was isolated as a faint yellow amorphous solid. It showed two pseudomolecular ion clusters at m/z 404, 406, and 408 $[M+H]^+$; and at m/z 426, 428, and 430 $[M+Na]^+$, each at a 1:2:1 ratio in its ESI mass spectrum indicating that it was a dibrominated compound. The ^{13}C NMR spectrum showed 11 signals representing two methylene groups in addition to nine sp^2 carbons including two methine group and seven fully substituted carbons. The molecular formula of **30** was suggested to be C₁₁H₁₁⁷⁹Br₂N₅O₂ that was confirmed by HRESIMS (m/z 405.9320 $[M+H]^+$ calcd for C₁₁H₁₂⁷⁹Br₂N₅O₂, Δ +1.0 ppm). The structure of **30** was further confirmed by interpretation of $^1H-^1H$ COSY, and HMBC spectra. The $^1H-^1H$ COSY spectrum (Fig. 3.18) showed a cross peak between NH -pyrrole [δ_H 12.69, (*br s*)] and the aromatic proton H-2 [δ_H 6.90 (*d*, 1.3 Hz); δ_C 112.6] in addition to an extended spin system among $NH-7$ [δ_H 8.28 (*t*, 6.0 Hz)], $=CH_2-8$ [δ_H 3.47 (*m*); δ_C 37.4], $=CH_2-9$ [δ_H 2.50 (*m*); δ_C 27.3], and H-10 [δ_H 5.96 (*t*, 7.6 Hz); δ_C 116.8]. The HMBC spectrum (Fig. 3.18) further supported the proposed structure and revealed correlations between H-2 to C-4 (δ_C 104.7), and C-5 (δ_C 128.0); H-10 to C-8 (δ_C 37.4), C-11 (δ_C 129.6), and C-15 (δ_C 163.6); $=CH_2-8$ to C-9 (δ_C 27.3), C-10 (δ_C 116.8), and C-6 (δ_C 158.9). According to the aforementioned data (Table 3.15) and by comparison to the other reported dispacamides in literature (Cafieri *et al.*, 1996; Cafieri *et al.*, 1997). Therefore, **30** was confirmed to be N-((*9E*)-3-(2-amino-4-oxo-1*H*-imidazol-5(4*H*)-ylidene)propyl)-3,4-dibromo-1*H*-pyrrole-2-carboxamide that was given the trivial name, dispacamide E.

Results

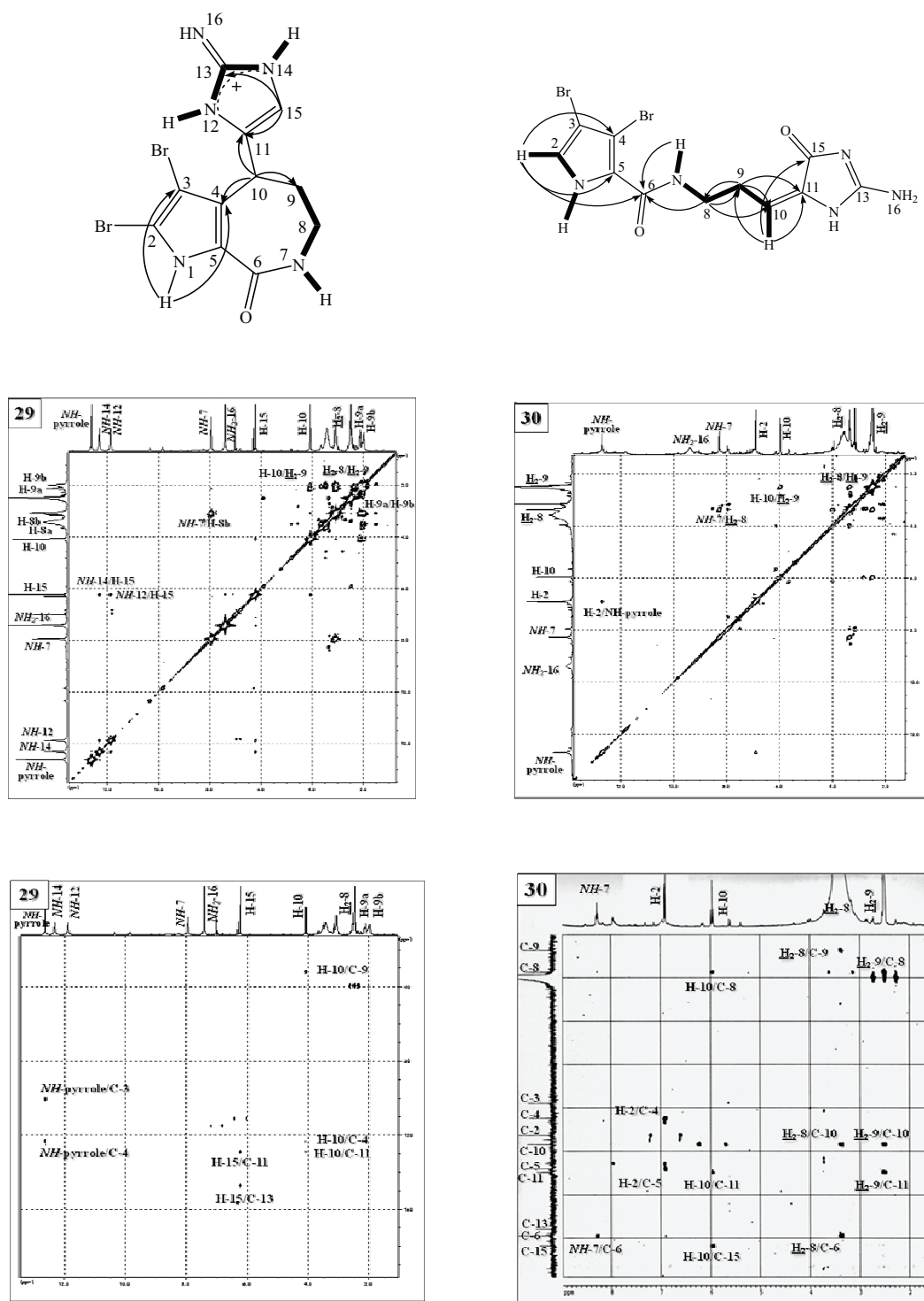


Fig. 3.18. ^1H - ^1H COSY and HMBC spectra of (-)-hymenine (29), and dispacamide E (30).

Table 3.15. NMR data of compounds (**29** and **30**), measured in DMSO-*d*₆.

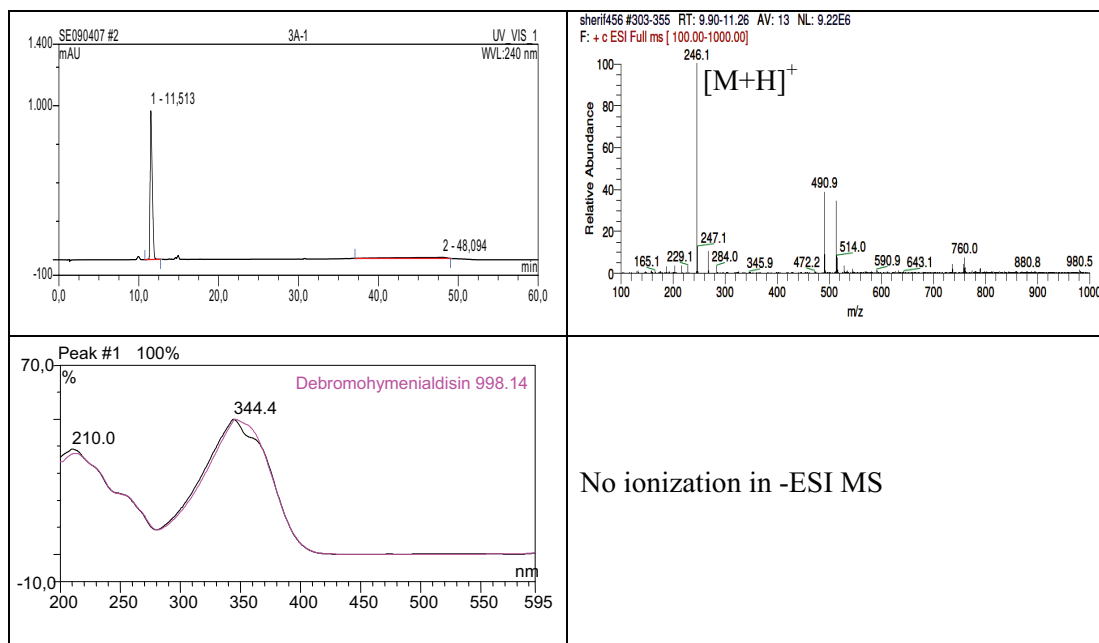
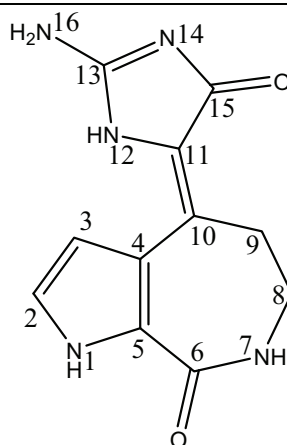
#	29		30	
	δ_{H}	δ_{C}^*	δ_{H}	δ_{C}
1	12.62 (1H, br <i>s</i> , <i>NH</i> -pyrrole)		12.69 (1H, br <i>s</i> , <i>NH</i> -pyrrole)	
2			6.90 (1H, <i>d</i> , 1.3 Hz)	112.6
3		100.5		97.8
4		123.3		104.7
5				128.0
6				158.9
7	7.95 (1H, <i>t</i> , 5.1 Hz, <i>NH</i>)		8.28 (1H, <i>t</i> , 6.0 Hz, <i>NH</i>)	
8	3.10 (2H, <i>m</i>)		3.47 (2H, <i>m</i>)	37.4
9	A: 2.15 (1H, <i>m</i>) B: 1.98 (1H, <i>m</i>)	31.76	2.50 (2H, <i>m</i>)	27.3
10	4.10 (1H, <i>t</i> , 4.1 Hz)		5.96 (1H, <i>t</i> , 7.6 Hz)	116.8
11		128.8		129.6
12	11.88 (1H, br <i>s</i> , <i>NH</i> -14)			
13		146.8		156.0
14	12.31 (1H, br <i>s</i> , <i>NH</i> -14)			
15	6.22 (1H, <i>s</i> , H-15)	111.1		163.6
16	7.41 (2H, <i>s</i> , <i>NH</i> ₂ -16)		9.38 (2H, <i>s</i> , <i>NH</i> ₂ -16)	

*¹³C NMR values obtained from HMBC spectrum.

Results

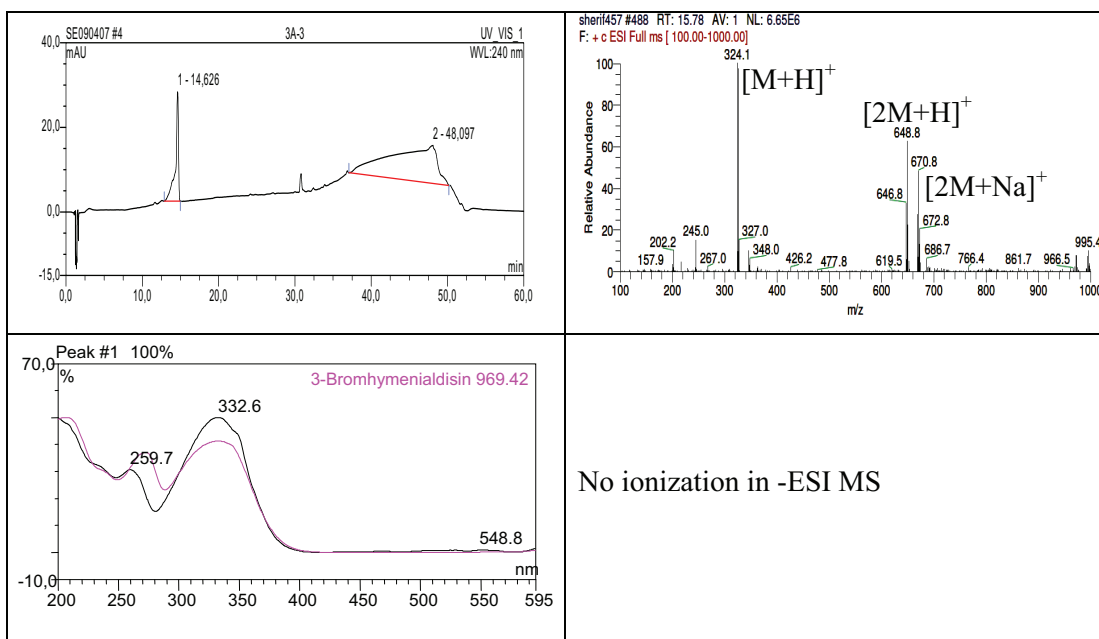
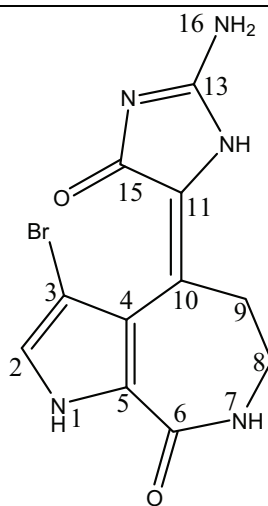
3.2.19. (10Z)-Debromohymenialdisine (33, known compound)

(10Z)-Debromohymenialdisine	
Synonym(s)	(10Z)-Debromohymenialdisine
Sample code	3A-1
Biological source	<i>Stylissa massa</i>
Sample amount	24.0 mg
Physical description	Pale yellow needle crystals
Molecular formula	C ₁₁ H ₁₁ N ₅ O ₂
Molecular weight	245 g/mol
Retention time (HPLC)	11.51 min (standard gradient)



3.2.20. Spongiacidin B (34, known compound)

Spongiacidin B	
Synonym(s)	(1 <i>E</i>)-3-Bromo-2-debromohymenialdisine
Sample code	3A-3
Biological source	<i>Stylissa massa</i>
Sample amount	4.0 mg
Physical description	Pale yellow powder
Molecular formula	C ₁₁ H ₁₀ ⁷⁹ BrN ₅ O ₂
Molecular weight	324 g/mol
Retention time (HPLC)	14.63 min (standard gradient)



Results

Compound (**33**) was isolated as a faint yellow powder. It showed pseudomolecular ion peak at m/z 246 $[M+H]^+$ in its ESI mass spectrum. The ^{13}C NMR and DEPT spectra of **33** showed 11 carbon resonances defined into two methylene groups in addition to nine sp^2 carbons including two methine groups and seven fully substituted carbons. The structure of **33** was further confirmed by interpretation of ^1H — ^1H COSY, and HMBC spectra. The ^1H — ^1H COSY spectrum (Fig. 3.19) revealed two extended spin systems. The first one existed among *NH*-pyrrole [δ_{H} 12.14, (br *s*)] and the two aromatic protons H-2 [δ_{H} 7.13 (*t*, 2.6 Hz); δ_{C} 122.7], and H-3 [δ_{H} 6.52 (*t*, 2.6 Hz); δ_{C} 109.6] in addition to an extended spin system over *NH*-7 [δ_{H} 8.06 (*t*, 4.5 Hz)], = CH_2 -8 [δ_{H} 3.30 (*m*); δ_{C} 39.6], and = CH_2 -9 [δ_{H} 3.30 (*m*); δ_{C} 31.6]. The HMBC spectrum (Fig. 3.19) further confirmed the structure and revealed correlations from both H-2 and H-3 to C-4 (δ_{C} 120.3), C-5 (δ_{C} 126.7), and C-11 (δ_{C} 120.5); and from both = CH_2 -8 and = CH_2 -9 to C-10 (δ_{C} 130.0). According to the formerly reported notion by Williams and Faulkner in 1996, compound (**33**) revealed similarly two sets of signals in the NMR spectra of DMSO solutions which were attributed to tautomerism of debromohymenialdisine between *Z* and *E* form. Based on the preceding data (Table 3.16) and by comparison to the reported literature, **33** was confirmed to be (10*Z*)-debromohymenialdisine which was first isolated from the marine sponge *Phakellia flabellata* (Sharma *et al.*, 1980) and also reported from *Axinella verrucosa* and *Acanthella aurantiaca* (Cimino *et al.*, 1982).

Compound (**34**) was isolated as a yellow powder. It showed pseudomolecular ion peaks at m/z 324, and 326 $[M+H]^+$ in a 1:1 ratio in its ESI mass spectrum which indicating that **34** is a monobrominated compound. The structure of **33** was further confirmed by interpretation of ^1H — ^1H COSY spectrum. The ^1H — ^1H COSY spectrum (Fig. 3.19) revealed a clear cross peak between *NH*-pyrrole [δ_{H} 12.55, (br *s*)] and the aromatic proton H-2 [δ_{H} 7.28 (*d*, 3.2 Hz)] in addition to another spin system extending over *NH*-7 [δ_{H} 8.00 (*t*, 4.7 Hz)], = CH_2 -8 [δ_{H} 3.24 (*m*)], and = CH_2 -9 [δ_{H} 3.24 (*m*)]. According to the aforementioned data (Table 3.16) and by comparison to the reported literature (Inaba *et al.*, 1998), **34** was confirmed to be (10*E*)-3-bromo-2-debromohymenialdisine, trivially named as spongiacidin B, which was first isolated from an unspecified Okinawan marine sponge of the genus *Hymeniacidon*.

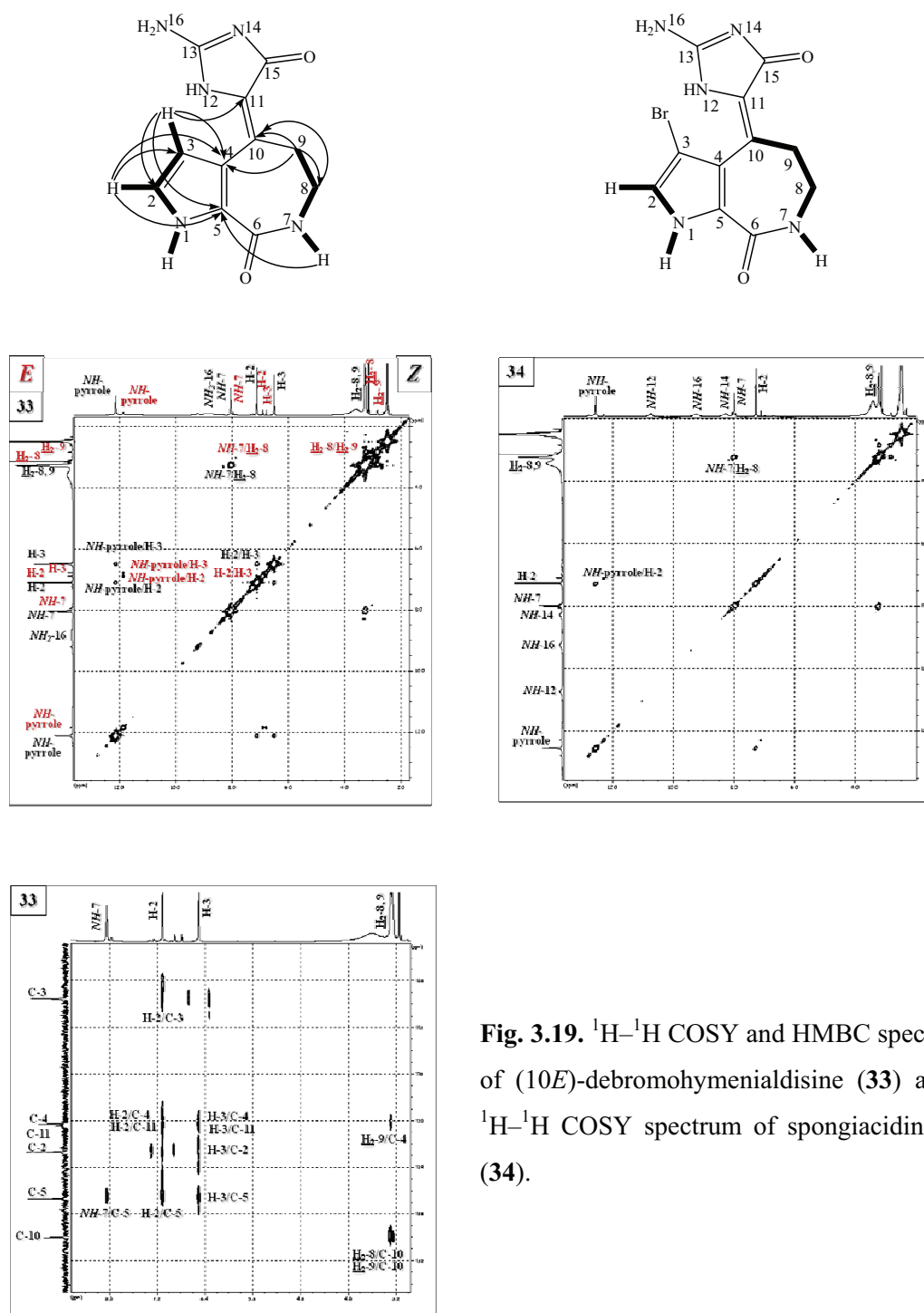
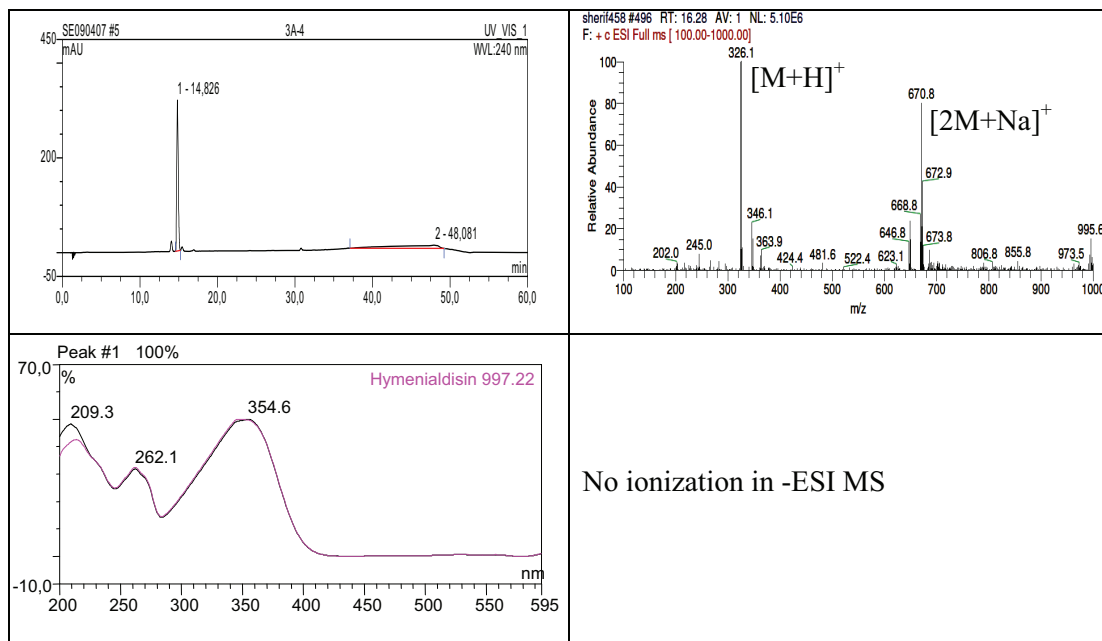
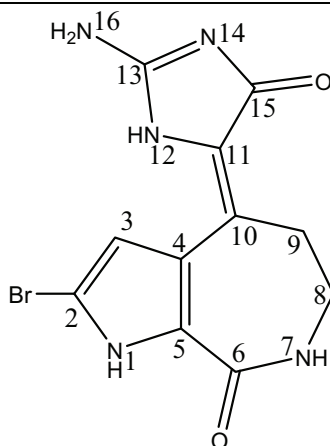


Fig. 3.19. ^1H - ^1H COSY and HMBC spectra of (10E)-debromohymenialdisine (33) and ^1H - ^1H COSY spectrum of spongiacidin B (34).

Results

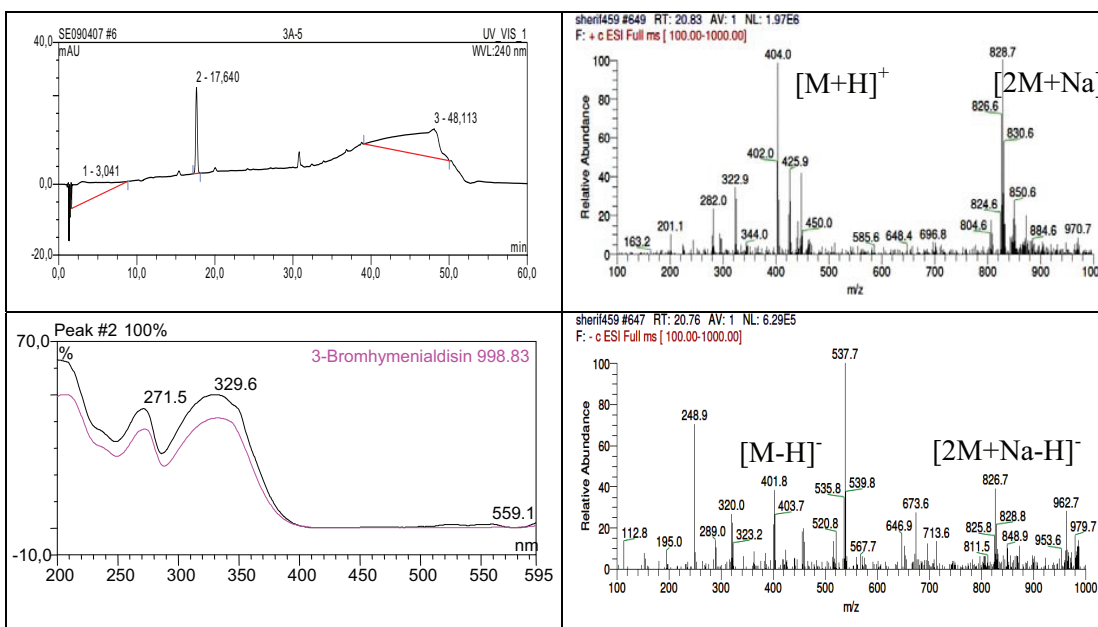
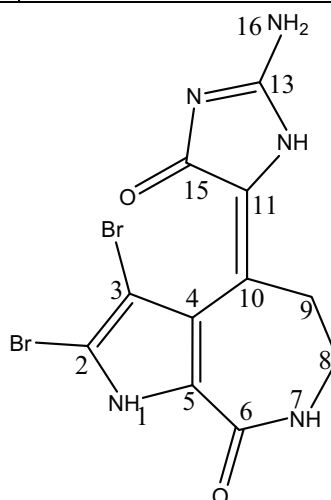
3.2.21. (10Z)-Hymenialdisine (35, known compound)

(10Z)-Hymenialdisine	
Synonym(s)	4-(2-Amino-4-oxo-2-imidazolidin-5-ylidene)-2-bromo-4,5,6,7-tetrahydropyrrolo[2,3-c]azepin-8-one
Sample code	3A-4
Biological source	<i>Stylissa massa</i>
Sample amount	5.0 mg
Physical description	Pale yellow powder
Molecular formula	C ₁₁ H ₁₀ ⁷⁹ BrN ₅ O ₂
Molecular weight	324 g/mol
Retention time (HPLC)	14.83 min (standard gradient)



3.2.22. (10Z)-3-Bromohymenialdisine (36, known compound)

(10Z)-3-Bromohymenialdisine	
Synonym(s)	(10Z)-3-Bromohymenialdisine
Sample code	3A-5
Biological source	<i>Stylissa massa</i>
Sample amount	1.0 mg
Physical description	Pale yellow powder
Molecular formula	C ₁₁ H ₉ ⁷⁹ Br ₂ N ₅ O ₂
Molecular weight	403 g/mol
Retention time (HPLC)	17.64 min (standard gradient)



Results

Compound (**35**) was isolated as a yellow powder. It showed pseudomolecular ion peaks at m/z 324, and 326 $[M+H]^+$ in a 1:1 ratio in its ESI mass spectrum which indicating that **35** is a monobrominated compound. The molecular mass was similar to that of **34** and 79 amu more than that of **33**. Based on the close resemblance of UV spectrum of **35** and **33**, the former was suggested to be a monobrominated derivative of **33**. The structure of **35** was further confirmed by interpretation of $^1H-^1H$ COSY spectrum. The $^1H-^1H$ COSY spectrum revealed a clear spin system extending over $NH-7$ [δ_H 7.95 (*t*, 4.8 Hz)], $=CH_2-8$ [δ_H 3.20 (*m*)], and $=CH_2-9$ [δ_H 3.32 (*m*)]. According to these data (Table 3.17) and by comparison to the reported literature (Williams and Faulkner, 1996), **35** was confirmed to be (10*Z*)-hymenialdisine which was first isolated from *Axinella verrucosa* and *Acanthella aurantiaca* (Cimino *et al.*, 1982).

Compound (**36**) was isolated as a yellow powder. It showed two pseudomolecular ion clusters at m/z 402, 404, and 406 $[M+H]^+$, and at m/z 424, 426, and 428 each in a 1:2:1 ratio in its ESI mass spectrum which indicating that **36** is a dibrominated compound. The molecular mass was 79 amu more than that of **34**. Based on the close resemblance of UV spectrum of **36** and **34**, the former was suggested to be a brominated derivative of **34**. The structure of **36** was further confirmed by interpretation of $^1H-^1H$ COSY spectrum. The $^1H-^1H$ COSY spectrum revealed a clear spin system extending over $NH-7$ [δ_H 8.03 (*t*, 4.6 Hz)], $=CH_2-8$ [δ_H 3.24 (*m*)], and $=CH_2-9$ [δ_H 3.24 (*m*)]. According to these data (Table 3.17) and by comparison to the reported literature (Supriyono *et al.*, 1995), **36** was confirmed to be (10*Z*)-3-bromohymenialdisine which was first isolated from the tropical marine sponge *Axinella carteri*.

Table 3.16. NMR data of compounds (**33** and **34**), measured in DMSO-*d*₆.

#	33		34
	δ_{H}	δ_{C}	δ_{H}
1	12.14 (1H, br <i>s</i> , <i>NH</i>)		12.55 (1H, br <i>s</i> , <i>NH</i>)
2	7.13 (1H, <i>t</i> , 2.6 Hz)	122.7, CH	7.28 (1H, <i>d</i> , 3.2 Hz)
3	6.52 (1H, <i>t</i> , 2.6 Hz)	109.6, CH	
4		120.3, C	
5		126.7, C	
6		163.0, C	
7	8.06 (1H, <i>t</i> , 4.5 Hz, <i>NH</i>)		8.00 (1H, <i>t</i> , 4.7 Hz, <i>NH</i>)
8	3.30 (2H, <i>m</i>)	39.6, CH ₂	3.24 (2H, <i>m</i>)
9	3.30 (2H, <i>m</i>)	31.6, CH ₂	3.24 (2H, <i>m</i>)
10		130.0, C	
11		120.5, C	
12			10.73 (1H, br <i>s</i> , <i>NH</i>)
13		154.6, C	
14			8.27 (1H, br <i>s</i> , <i>NH</i>)
15		163.9, C	
16	8.70 (2H, br <i>s</i> , <i>NH</i> ₂)		9.26 (1H, br <i>s</i> , <i>NH</i>)

Table 3.17. NMR data of compounds (**35** and **36**), measured in DMSO-*d*₆.

#	35	36
	δ_{H}	δ_{H}
1	12.39 (1H, br <i>s</i> , <i>NH</i>)	13.34 (1H, br <i>s</i> , <i>NH</i>)
2		
3	7.20 (1H, br <i>s</i>)	
4		
5		
6		
7	7.95 (1H, <i>t</i> , 4.8 Hz, <i>NH</i>)	8.03 (1H, <i>t</i> , 4.6 Hz, <i>NH</i>)
8	3.20 (2H, <i>m</i>)	3.24 (2H, <i>m</i>)
9	3.32 (2H, <i>m</i>)	3.24 (2H, <i>m</i>)
10		
11		
12	10.78 (1H, br <i>s</i> , <i>NH</i>)	10.59 (1H, br <i>s</i> , <i>NH</i>)
13		
14		8.20 (1H, br <i>s</i> , <i>NH</i>)
15		
16		9.0 (1H, br <i>s</i> , <i>NH</i>)

Results

3.2.23. Biological activity of bromopyrrole alkaloids isolated from Indonesian marine sponge *Stylissa massa*

Isolated bromopyrrole alkaloids from the methanolic extract of *Stylissa massa* were subjected to cytotoxicity (MTT) assay against mouse lymphoma (L5178Y) cells whose results (Table 3.18) interestingly revealed that some of the tested compounds proved significantly cytotoxic with IC₅₀ values ranging between 6.33 and 28.28 μM compared to kahalalide F as standard (IC₅₀ = 4.30 μM).

Table 3.18. Cytotoxicity (MTT) assay of compounds isolated from *Stylissa massa*.

Sample tested	L5178Y growth in % (@ 10 $\mu\text{g}/\text{mL}$)	EC ₅₀	
		($\mu\text{g}/\text{mL}$)	(μM)
Ethyl 3,4-dibromo-1 <i>H</i> -pyrrole-2-carboxylate (15)	27.2		
4-Bromopyrrole-3-carboxamide (16)	100.0		
3,4-Dibromopyrrole-2-carboxamide (17)	75.8		
(-)-Longamide B methyl ester (18)	70.0		
(-)-Longamide B ethyl ester, Hanishin (19)	14.1	9.3	24.47
Aldisine (20)	100.0		
2,3-Dibromoaldisine (21)	98.8		
2-Bromoaldisine (22)	100.0		
3-Bromoaldisine (23)	100.0		
(-)-Mukanadin C (24)	100.0		
(-)-Longamide (25)	100.0		
Latonduine A (26)	18.6	10.0	26.81
(-)-Dibromophakellin H ⁺ Cl ⁻ (27)	1.0	11.0	28.28
(-)-Monobromoisophakellin (28)	73.7		
(-)-Hymenine (29)	16.0		
Dispacamide E (30)	77.2		
(-)-Longamide B (31)	100.0		
(-)-Dibromocantharelline (=Dibromoisophakellin) (32)	35.3		
(10 <i>Z</i>)-Debromohymenialdisine (33)	0.0	1.55	6.33
Spongiacidin B (34)	0.0	2.40	7.41
(10 <i>Z</i>)-Hymenialdisine (35)	0.0	2.70	8.33
(10 <i>Z</i>)-3-Bromohymenialdisine (36)	0.0	3.90	9.68
Kahalalide F (positive control)		6.30	4.30

In antimicrobial activity, only ethyl 3,4-dibromo-1*H*-pyrrole-2-carboxylate (**15**) showed antifungal activity against *Aspergillus faecalis* and *A. fumigatus* with the same MIC value of 62.5 $\mu\text{g}/\text{mL}$. However, 4-bromo-1*H*-pyrrole-3-carboxamide (**16**) and aldisine (**20**) demonstrated antiviral activity against human rhino viruses (HRV2, HRV8, and HRV39) and respiratory syncytial virus A (RSVA) with IC₅₀ values of 6.25, 0.78, 0.78, 0.78 $\mu\text{g}/\text{mL}$, respectively for **16** and 3.13, 1.56, 1.56, 0.78 $\mu\text{g}/\text{mL}$, respectively for **20**.

Furthermore, protein kinase inhibitory activity of the isolated bromopyrrole metabolites against six protein kinases namely, dual-specificity tyrosine-(Y)-phosphorylation regulated kinase 1A (DYRK1A), cyclin-dependent kinase (CDK5), glycogen synthase kinase-3 (GSK-3), CDC-like kinase 1 (CLK-1), casein kinase 1 (CK1), and *Plasmodium falciparum* glycogen synthase kinase-3 (*Pf*GSK-3).

Table 3.19. Protein kinase inhibitory activity of compounds isolated from *Stylissa massa*.

Sample tested	IC ₅₀ (μM)					
	DYRK1A	CDK5	GSK-3	CLK-1	CK-1	<i>Pf</i> GSK-3
4-Bromo-1 <i>H</i> -pyrrole-3-carboxamide (16)	12.7	>53	>53	10.6	48	>53
3,4-Dibromo-1 <i>H</i> -pyrrole-2-carboxamide (17)	14.9	>37.3	>37.3	7.5	18.7	>37.3
(-)-Longamide B ethyl ester, hanishin (19)	>26.3	>26.3	>26.3	1.7	7.9	>26.3
Aldisine (20)	50.6	>61	>61	13.4	25.6	>61
2,3-Dibromoaldisine (21)	11.2	>31	31	2.0	3.7	>31
2-Bromoaldisine (22)	>41.2	>41.2	>41.2	2.3	1.6	>41.2
3-Bromoaldisine (23)	10.3	27.6	21	1.6	1.3	15.6
(-)-Mukanadin C (24)	0.6	2.4	2.4	0.5	0.6	1.3
(-)-Longamide (25)	7.1	13.2	7.4	1.9	1.6	16.8
Latonduine A (26)	6.2	24	18.8	3.2	6.2	18.8
(-)-Dibromophakellin H ⁺ Cl ⁻ (27)	3.6	3.9	3.1	2.8	6.4	5.4
(-)-Hymenine (29)	0.2	0.4	0.3	0.2	0.4	0.4
Dispacamide E (30)	6.2	16	2.1	10.4	4.9	18.8
(-)-Longamide B (31)	15.6	>28.4	>28.4	6.5	2.1	25.6
(-)-Dibromocantharelline (32)	0.3	0.6	0.8	0.3	0.3	0.6
(10 <i>Z</i>)-Debromohymenialdisine (33)	0.02	0.09	0.13	0.01	0.05	0.16
Spongiacidin B (34)	0.04	0.09	0.04	0.03	0.06	0.04
(10 <i>Z</i>)-Hymenialdisine (35)	0.01	0.26	0.29	0.01	0.13	0.2
(10 <i>Z</i>)-3-Bromohymenialdisine (36)	0.07	0.07	0.04	0.04	0.27	0.07

The results of protein kinase inhibitory activity assay (Table 3.19) revealed a correspondence with the respective cytotoxicity (MTT) assay results (Table 3.18). For example, compounds (**33–36**), that showed IC₅₀ values between 6.33 and 9.68 μM in MTT assay, proved significant inhibitory activity against tested protein kinases with IC₅₀ values in the submicromolar range (Table 3.19). This conclusively suggested that protein kinase inhibition might be a plausible mechanism through which these compounds exerted their antiproliferative activity.

Results

3.3. Secondary metabolites isolated from *Jaspis splendens*

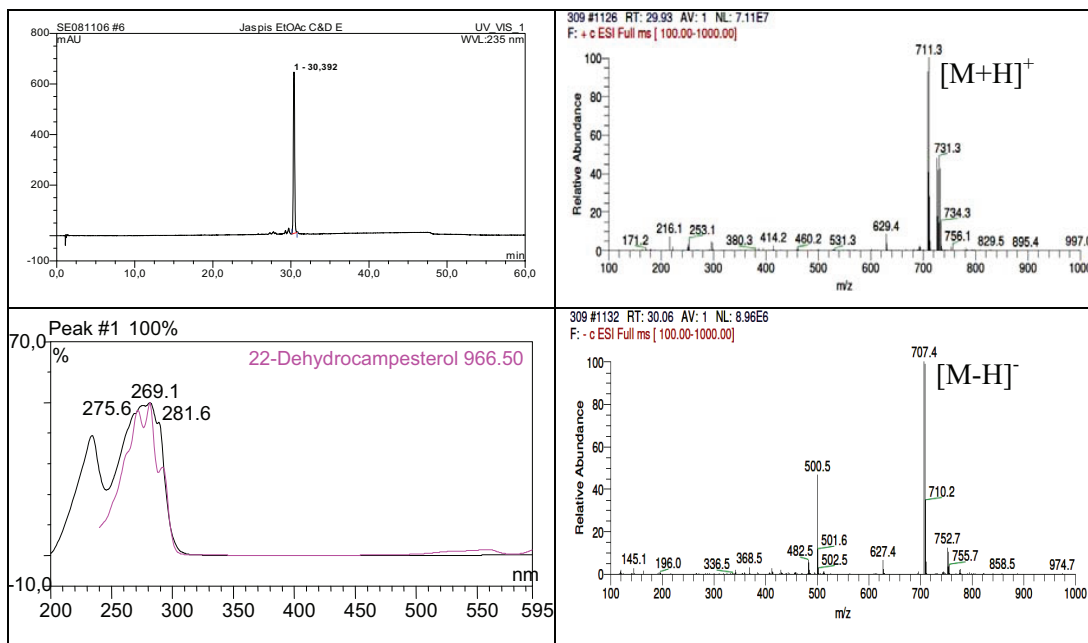
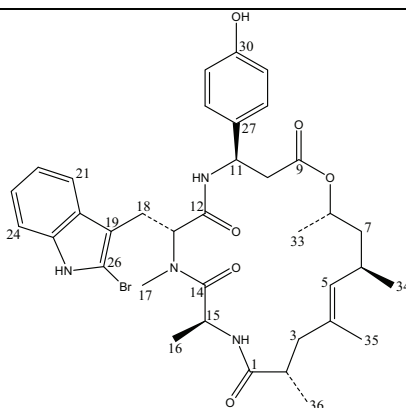
Jaspamide (jasplakinolide, **37**), a cyclodepsipeptide isolated from marine sponges of the genus *Jaspis*, is known for its pronounced biological activities which include antifungal (Scott *et al.*, 1988), insecticidal (Zabriskie *et al.*, 1986; Crews *et al.*, 1986), and cytotoxic activity against 36 human solid tumor cell cultures (Inman and Crews, 1989). The biological properties and structural features of jaspamide stimulated numerous efforts aiming at a total synthesis and structural modification (Tannert *et al.*, 2009). As a part of our ongoing studies on bioactive natural products from marine sponges we investigated a specimen of *Jaspis splendens* collected at Kalimantan (Indonesia).

The crude methanolic extract exhibited considerable *in vitro* cytotoxic activity against mouse lymphoma (L5178Y) cells. Eight compounds were isolated through a bioactivity-guided isolation scheme from the ethyl acetate soluble fraction of the total methanolic extract of *Jaspis splendens*. In addition to the known compounds, 6 β -hydroxy-24-methylcholesta-4,22-dien-3-one (**40**), 6 β -hydroxy-24-methylcholesta-4-en-3-one (**41**), 6 β -hydroxy-24-ethylcholesta-4-en-3-one (**42**), maculosin-1 (*cyclo*-L-Pro-L-Tyr) (**43**), sangivamycin (**44**), two new jaspamide derivatives (**38** and **39**), were isolated together with the parent compound jaspamide (**37**). The structures of isolated compounds were unambiguously elucidated based on 1D and 2D NMR spectral data, mass spectrometry, and comparison with the reported literature.

All isolated compounds exhibited cytotoxicity against mouse lymphoma (L5178Y) cells using MTT assay when they were qualitatively tested at a concentration of 10 $\mu\text{g/mL}$. New jaspamide derivatives (**38** and **39**), together with jaspamide (**37**), maculosin-1 (**43**), and sangivamycin (**44**) exhibited the highest cytotoxicity with IC_{50} values ranging from <0.1 to 0.28 $\mu\text{g/mL}$, compared to kahalalide F [IC_{50} = 6.3 $\mu\text{g/mL}$ (4.3 μM)].

3.3.1. Jaspamide (37, known compound)

Jaspamide	
Synonym(s)	Jasplakinolide
Sample code	Jaspis EtOAc C&D E
Biological source	<i>Jaspis splendens</i>
Sample amount	105.0 mg
Physical description	Pale yellow amorphous solid
Molecular formula	C ₃₆ H ₄₅ ⁷⁹ BrN ₄ O ₆
Molecular weight	710 g/mol
Optical rotation $[\alpha]_D^{20}$	-128.0°C (c 0.02, CHCl ₃)
Retention time (HPLC)	30.39 min (standard gradient)



Results

Compound (**37**) was obtained as a white amorphous solid. Being a monobrominated compound was supported by ESI mass spectrum which exhibited pseudomolecular ion peaks at m/z 709, and 711 $[M+H]^+$; and at m/z 731, and 733 $[M+Na]^+$, each in a ratio of 1:1. The molecular formula of **37** was revealed to be $C_{36}H_{46}^{79}BrN_4O_6$ by HRESIMS (m/z 711.2571 $[M+H]^+$, Δ +1.0 ppm), and the characteristic UV absorption spectrum [λ_{max} 225, 280 nm] was indicative of the parent cyclodepsipeptide, jaspamaide. Structural elucidation of **37** was based on results of 1D and 2D NMR spectral analyses including 1H -NMR, 1H — 1H COSY and HMBC spectra (Table 3.20), (Fig. 3.20). The close resemblance of 1H , and ^{13}C resonances between jaspamide (**37**) and the reported values (Zabriskie *et al.*, 1986; Crews *et al.*, 1986) implied that the chiral centers of alanine, 2-bromoabrine (*N*-methyltryptophan), β -tyrosine, and of the polypropionate fragment had the same relative configurations. From these data (Table 3.20), compound **37** was deduced to be the parent cyclodepsipeptide, jaspamide.

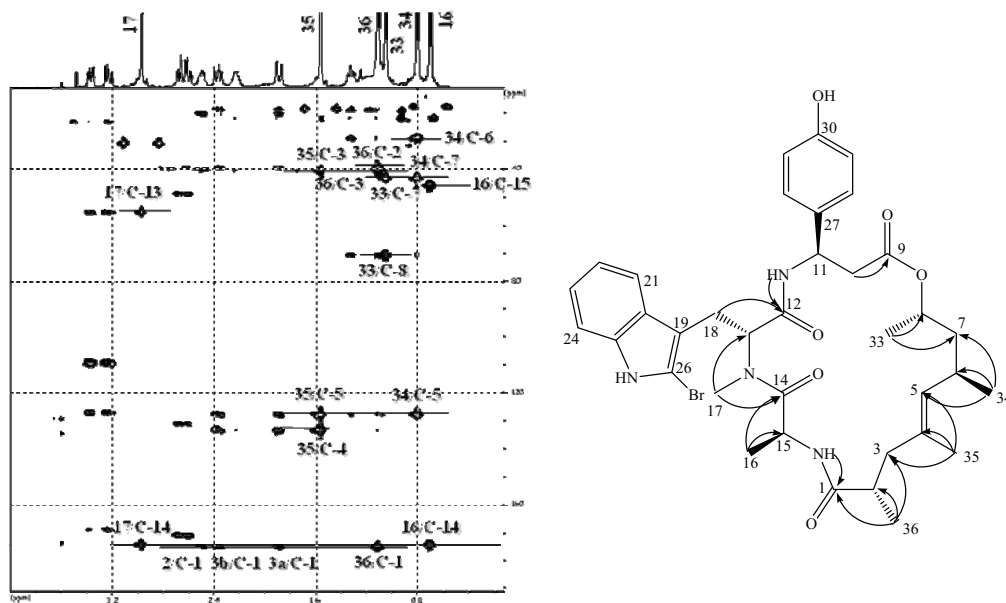
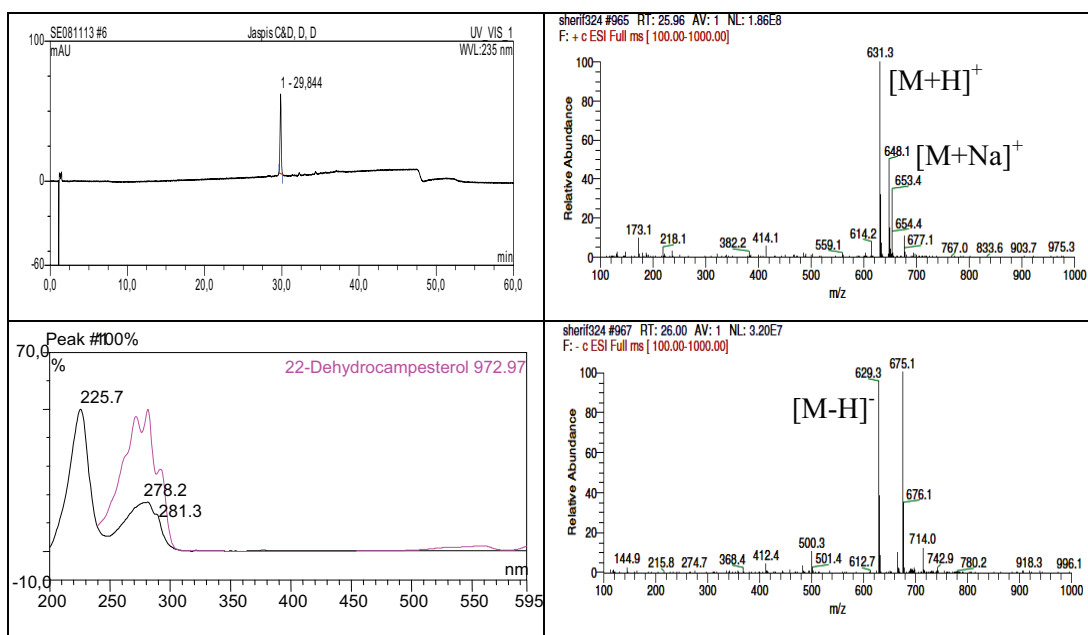
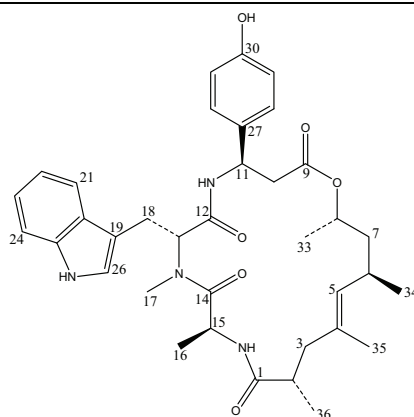


Fig. 3.20. Key HMBC correlations of jaspamide (**37**).

3.3.2. Jaspamide Q (38, new natural product)

Jaspamide Q	
Synonym(s)	26-Debromoaspamide
Sample code	Jaspis EtOAc C&D D,D
Biological source	<i>Jaspis splendens</i>
Sample amount	0.7 mg
Physical description	White amorphous solid
Molecular formula	C ₃₆ H ₄₆ N ₄ O ₆
Molecular weight	631 g/mol
Optical rotation $[\alpha]_D^{20}$	-62.0°C (c 0.01, CHCl ₃)
Retention time (HPLC)	29.84 min (standard gradient)



Results

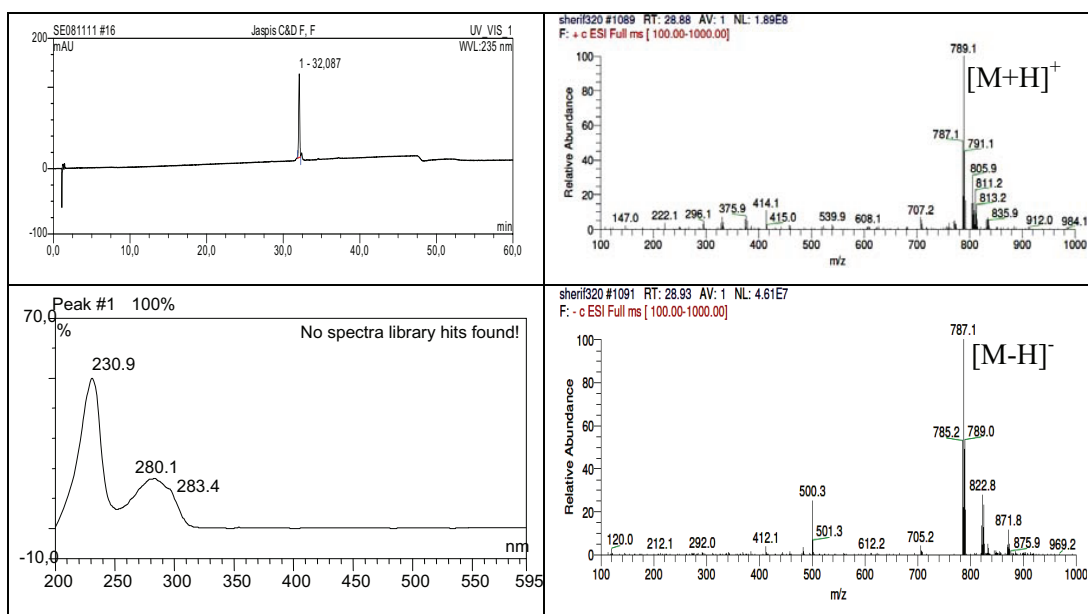
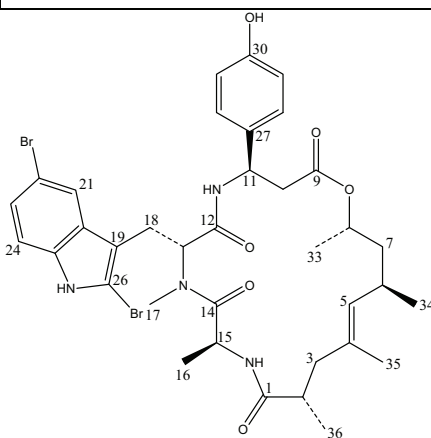
Compound (**38**) was obtained as a white amorphous solid, and the ESIMS spectrum showed a pseudomolecular ion peaks at m/z 631.3 $[M+H]^+$, and at m/z 653.4 $[M+Na]^+$, which was 79 amu smaller than that of jaspamide (**37**), the parent compound. This difference was assigned to the absence of the bromine atom at C-26 in jaspamide (**37**). The molecular formula of **38** was deduced to be $C_{36}H_{46}N_4O_6$, based on HRFTMS (m/z 631.3491 $[M+H]^+$, Δ +1.0 ppm), therefore **38** was identified as the debromo analogue of **37**. 1H NMR spectral data (Table 3.20) revealed that the resonances of **38** were superimposable with those of **37** with only one additional proton resonance at $[\delta_H$ 6.87 (br s)] that was ascribed to H-26. The complete structure of **38** was unambiguously elucidated and assigned on the basis of 1H - 1H COSY, TOCSY, ROESY, and HMBC spectra.

In particular, the similarity of 1H , and ^{13}C resonances between **38** and jaspamide **37** evidenced that the chiral centers of alanine, abrine (*N*-methyltryptophan), β -tyrosine, and of the polypropionate fragment had the same relative configurations in both molecules. Therefore, the stereochemistry depicted for **38** was tentatively assigned by analogy with the parent compound together with ROESY spectrum (Fig. 3.21) that revealed a clear correlation between Me-16 and Me-34; and Me-33 and Me-36. However, an apparent deshielding of Me-16 was noted in **38** [δ_H 1.04 (3H, *d*, 6.6 Hz)] compared to **37** [δ_H 0.70 (3H, *d*, 6.7 Hz)] resembling that between jaspamide M [δ_H 1.17 (3H, *d*, 6.8 Hz)] (Gala *et al.*, 2009) and jaspamide H [δ_H 0.72 (3H, *d*, 6.7 Hz)] (Gala *et al.*, 2008). These differences in chemical shifts for the latter congeners were proven to be caused by D-Ala or L-Ala residues, respectively. Analysis of the absolute configurations of the amino acids of **38** could not be performed due to the small amount of compound isolated (0.7 mg).

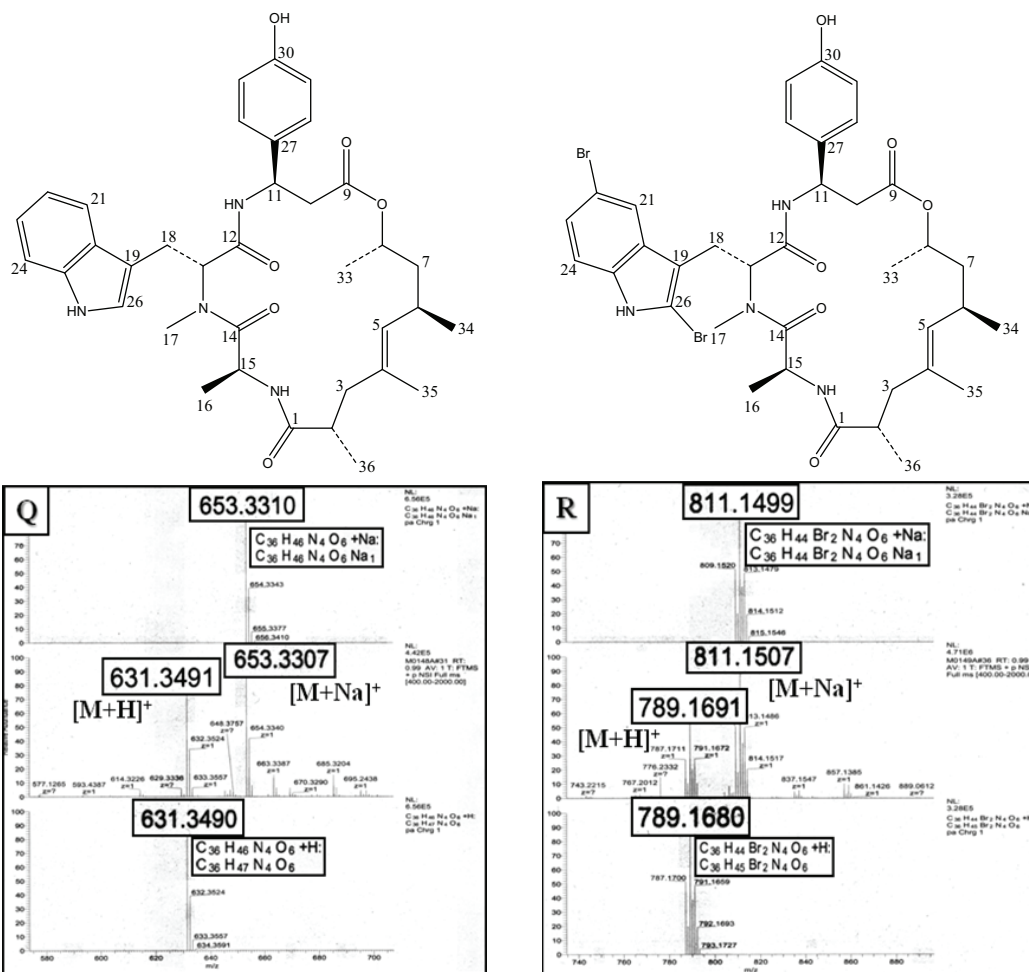
A partial ^{13}C assignment of **38** was achieved through HMBC spectrum (Fig. 3.21) which revealed clear correlations at δ_c 174.5, δ_c 40.4, δ_c 40.9, δ_c 133.6, δ_c 128.2, δ_c 29.5, δ_c 43.6, δ_c 70.4, δ_c 56.4, δ_c 173.6, and δ_c 46.0 ppm that were ascribed to C-1 to C-8, and C-13 to C-15, respectively. Moreover, HMBC spectra evidenced and confirmed the amino acid sequence in **38** through cross-peaks between *NH*-Tyr and C-12, Me-17 and C-14, and between *NH*-Ala and C-1. From the aforementioned data, compound (**38**) was deduced to be a debromo analogue of jaspamide, which was given the trivial name jaspamide Q.

3.3.3. Jaspamide R (39, new natural product)

Jaspamide R	
Synonym(s)	22-Bromoaspamide
Sample code	Jaspis EtOAc C&D F,F
Biological source	<i>Jaspis splendens</i>
Sample amount	0.5 mg
Physical description	White amorphous solid
Molecular formula	C ₃₆ H ₄₄ ⁷⁹ Br ₂ N ₄ O ₆
Molecular weight	789 g/mol
Optical rotation $[\alpha]_D^{20}$	-100.0°C (<i>c</i> 0.01, CHCl ₃)
Retention time (HPLC)	32.09 min (standard gradient)



Results



Compound (**39**) was isolated as a white amorphous solid. Its ESI mass spectrum exhibited pseudomolecular ion peaks at m/z 787.1, 789.1, and 791.1 $[M+H]^+$, in a ratio of 1:2:1, supporting the existence of two bromine atoms in the compound. The molecular formula of **39** was determined to be $C_{36}H_{44}Br_2N_4O_6$ by HRFTMS (m/z 789.1691 $[M+H]^+$, Δ +1.0 ppm) which exceeds that of jaspamide (**37**) by 79 amu revealing that **39** is a dibromo analogue of jaspamide Q (**38**).

This difference was explained by the 1H NMR spectral data (Table 3.20) which revealed close similarity between **39** and jaspamide (**37**) except for the proton resonances corresponding to the indole moiety of the 2-bromoabrine unit. Compound (**39**) showed three proton resonances at $[\delta_H$ 7.41 (br s)], $[\delta_H$ 7.20 (d, 8.2 Hz)], and $[\delta_H$ 7.42 (d, 8.2 Hz)] that were assigned to H-21, H-23, and H-24, respectively. Whereas for jaspamide (**37**), four resonances, at $[\delta_H$ 7.23 (d, 8.0 Hz)], $[\delta_H$ 7.10 (t, 8.0 Hz)], $[\delta_H$ 7.12 (t, 8.0 Hz)], and $[\delta_H$ 7.54 (d, 8.0 Hz)], ascribed for H-21 to H-24, were observed. Based on this finding, the additional bromine atom of **39** was assumed to be located at C-22. This hypothesis was

further confirmed by 2D NMR spectral analyses including ^1H - ^1H COSY, TOCSY, and NOESY spectra (Fig. 3.21) that revealed a clear NOE correlation between proton resonance at $[\delta_{\text{H}} 7.41 (\text{br } s)]$, and *NH*-Tyr at $[\delta_{\text{H}} 7.53 (d, 8.6 \text{ Hz})]$ proving the attachment of the second bromine atom to be at C-22. Moreover, the close resemblance in ^1H resonances between **39**, and jaspamide (**37**) supports the notion that the chiral centers of alanine, 2,5-dibromoabrine, β -tyrosine, and the polypropionate fragment have the same relative configurations in both molecules. Again, due to the lack of material isolated of **39** (0.5 mg), analysis of the absolute configurations of the amino acids, e.g. by Marfey's method, could not be performed. From the preceding data, compound (**39**) was concluded to be a dibromo analogue of **38** which was named as jaspamide R (**39**).

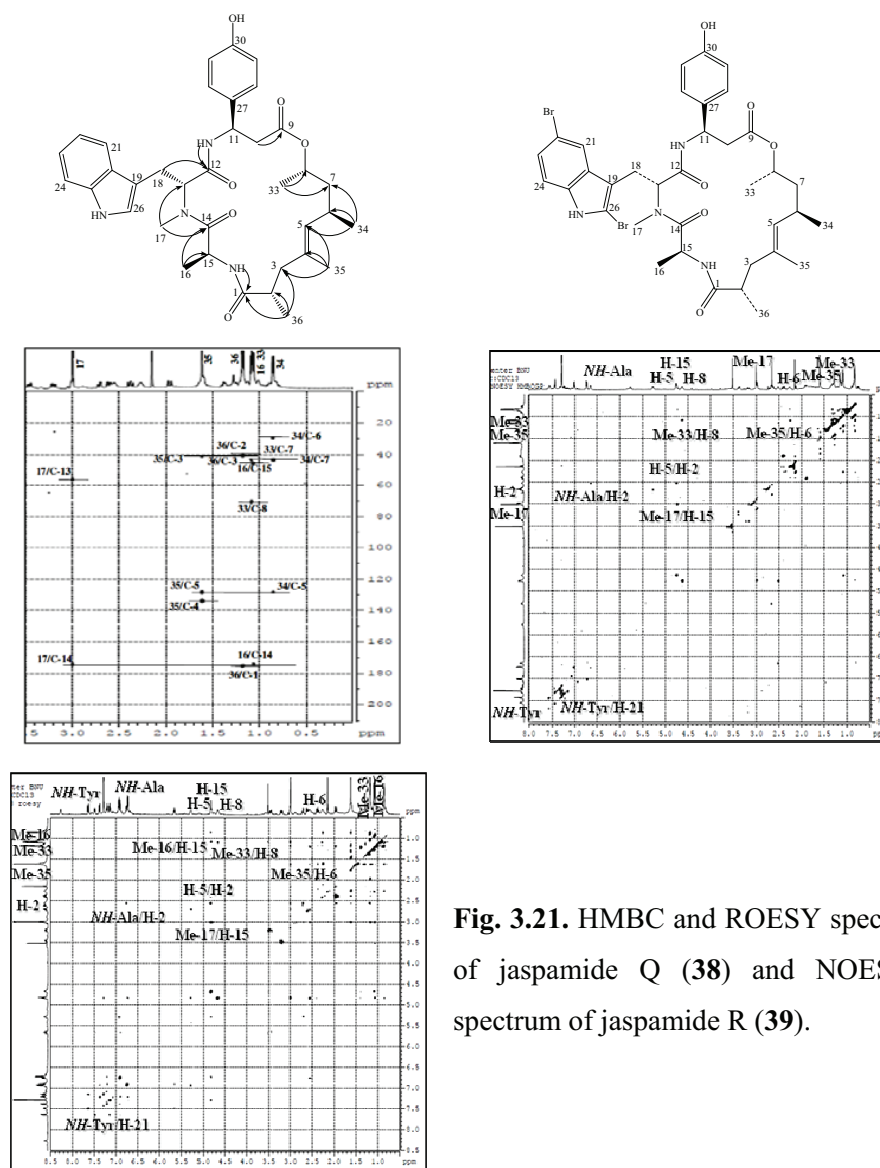


Fig. 3.21. HMBC and ROESY spectra of jaspamide Q (**38**) and NOESY spectrum of jaspamide R (**39**).

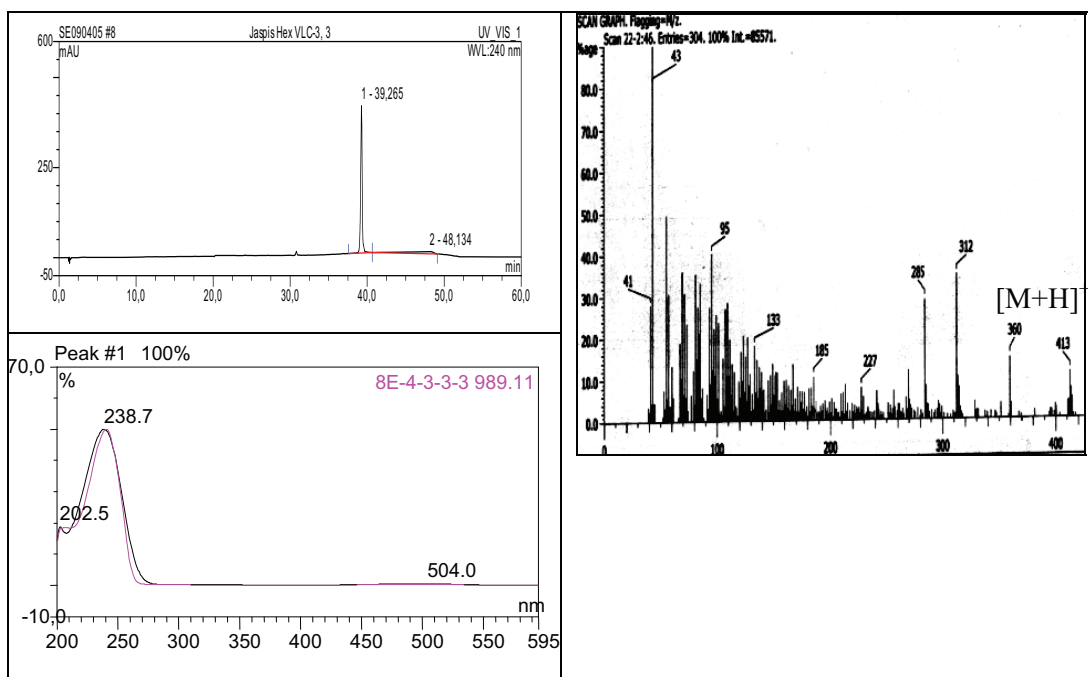
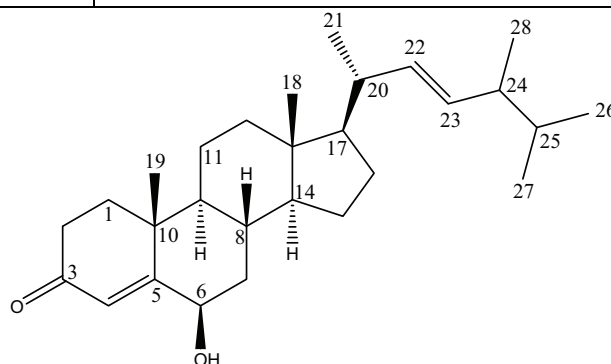
Results

Table 3.20. NMR data of jaspamide (**37**), jaspamide Q (**38**) and R (**39**).

#	37	38	39
	δ_{H} mult. (J Hz)	δ_{H} mult. (J Hz)	δ_{H} mult. (J Hz)
2	2.50 (<i>m</i>)	2.51 (<i>m</i>)	2.49 (<i>m</i>)
3	A) 2.37 (<i>dd</i> , 11.5, 15.8 Hz)	A) 2.37 (<i>dd</i> , 11.5, 15.8 Hz)	A) 2.37 (<i>dd</i> , 11.5, 15.8 Hz)
	B) 1.89 (<i>d</i> , 15.8 Hz)	B) 1.90 (<i>d</i> , 15.8 Hz)	B) 1.90 (<i>d</i> , 15.8 Hz)
5	4.75 (<i>d</i> , 7.9 Hz)	4.79 (<i>d</i> , 6.7 Hz)	4.74 (<i>d</i> , 6.7 Hz)
6	2.23 (<i>m</i>)	2.23 (<i>m</i>)	2.23 (<i>m</i>)
7	A) 1.32 (<i>m</i>), B) 1.10 (<i>m</i>)	A) 1.32 (<i>m</i>), B) 1.10 (<i>m</i>)	A) 1.32 (<i>m</i>), B) 1.10 (<i>m</i>)
8	4.62 (<i>m</i>)	4.64 (<i>m</i>)	4.60 (<i>m</i>)
10	A) 2.67 (<i>dd</i> , 4.7, 15.0 Hz)	A) 2.67 (<i>dd</i> , 4.7, 15.0 Hz)	A) 2.67 (<i>dd</i> , 4.7, 15.0 Hz)
	B) 2.61 (<i>dd</i> , 5.7, 14.8 Hz)	B) 2.61 (<i>dd</i> , 5.7, 14.8 Hz)	B) 2.61 (<i>dd</i> , 5.7, 14.8 Hz)
11	5.26 (<i>dd</i> , 5.3, 8.6 Hz)	5.25 (<i>dd</i> , 5.3, 8.6 Hz)	5.25 (<i>dd</i> , 5.3, 8.6 Hz)
13	5.83 (<i>dd</i> , 6.3, 10.0 Hz)	5.63 (<i>dd</i> , 6.3, 10.0 Hz)	5.73 (<i>dd</i> , 6.3, 10.0 Hz)
15	4.73 (<i>m</i>)	4.77 (<i>m</i>)	4.72 (<i>m</i>)
16	0.70 (3H, <i>d</i> , 6.7 Hz)	0.83 (3H, <i>d</i> , 6.5 Hz)	0.81 (3H, <i>d</i> , 6.7 Hz)
17	2.97 (3H, <i>s</i>)	2.97 (3H, <i>s</i>)	2.98 (3H, <i>s</i>)
18	A) 3.38 (<i>dd</i> , 6.3, 15.5 Hz)	A) 3.43 (<i>dd</i> , 6.3, 15.5 Hz)	A) 3.33 (<i>dd</i> , 6.3, 15.5 Hz)
	B) 3.23 (<i>dd</i> , 10.4, 15.2 Hz)	B) 3.17 (<i>dd</i> , 10.4, 15.2 Hz)	B) 3.18 (<i>dd</i> , 10.4, 15.2 Hz)
21	7.23 (<i>d</i> , 8.1 Hz)	7.61 (<i>d</i> , 7.9 Hz)	7.41 (<i>br s</i>)
22	7.12 (<i>td</i> , 1.3, 7.7 Hz)	7.11 (<i>d</i> , 7.7 Hz)	
23	7.10 (<i>td</i> , 1.3, 7.7 Hz)	7.18 (<i>d</i> , 7.7 Hz)	7.20 (<i>d</i> , 8.4 Hz)
24	7.54 (<i>br d</i> , 7.8 Hz)	7.35 (<i>d</i> , 8.0 Hz)	7.42 (<i>d</i> , 8.4 Hz)
26		6.87 (<i>br s</i>)	
28	6.93 (<i>d</i> , 8.5 Hz)	6.90 (<i>d</i> , 8.3 Hz)	6.98 (<i>d</i> , 8.4 Hz)
29	6.66 (<i>d</i> , 8.5 Hz)	6.69 (<i>d</i> , 8.3 Hz)	6.71 (<i>d</i> , 8.4 Hz)
31	6.66 (<i>d</i> , 8.5 Hz)	6.69 (<i>d</i> , 8.3 Hz)	6.71 (<i>d</i> , 8.4 Hz)
32	6.93 (<i>d</i> , 8.5 Hz)	6.90 (<i>d</i> , 8.3 Hz)	6.98 (<i>d</i> , 8.4 Hz)
33	1.05 (3H, <i>d</i> , 6.3 Hz)	1.06 (3H, <i>d</i> , 6.3 Hz)	1.05 (3H, <i>d</i> , 6.1 Hz)
34	0.80 (3H, <i>d</i> , 6.3 Hz)	1.04 (3H, <i>d</i> , 6.6 Hz)	0.81 (3H, <i>d</i> , 6.7 Hz)
35	1.56 (3H, <i>s</i>)	1.59 (3H, <i>s</i>)	1.57 (3H, <i>s</i>)
36	1.12 (3H, <i>d</i> , 7.0 Hz)	1.15 (3H, <i>d</i> , 6.8 Hz)	1.13 (3H, <i>d</i> , 6.8 Hz)
NH-Tyr	7.63 (<i>d</i> , 8.6 Hz)	7.46 (<i>d</i> , 8.6 Hz)	7.53 (<i>d</i> , 8.6 Hz)
NH-Trp	8.80 (<i>br s</i>)	8.24 (<i>br s</i>)	8.42 (<i>br s</i>)
NH-Ala	6.65 (<i>br s</i>)	6.73 (<i>d</i> , 6.4 Hz)	6.65 (<i>d</i> , 6.5 Hz)

3.3.4. 6 β -hydroxy-24-methylcholesta-4,22-dien-3-one (40, known compound)

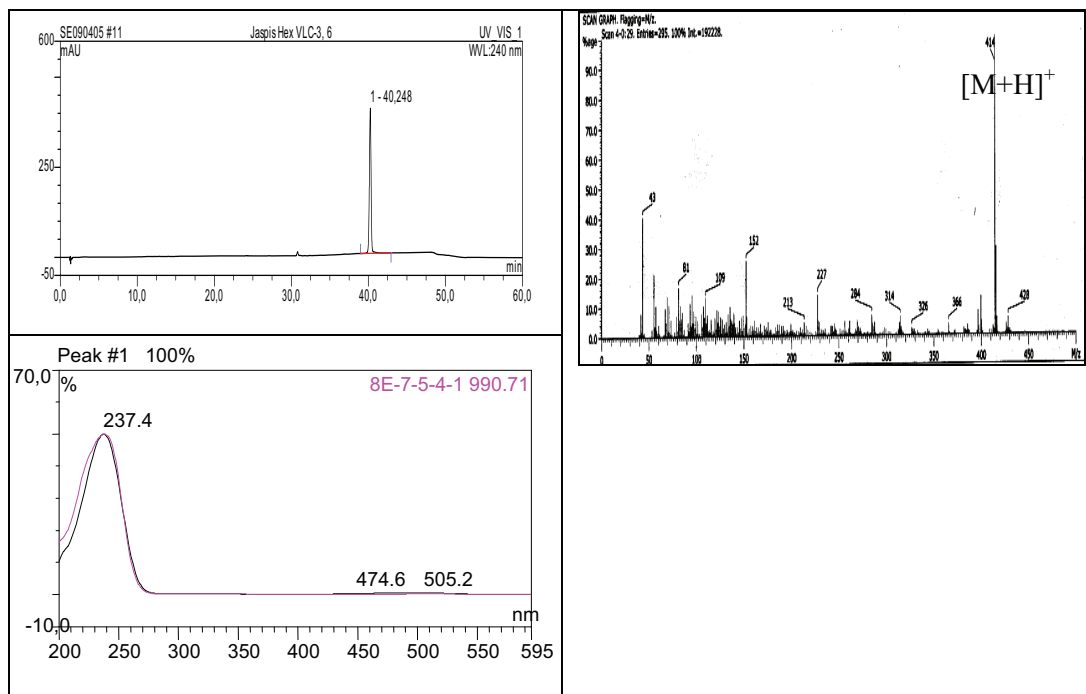
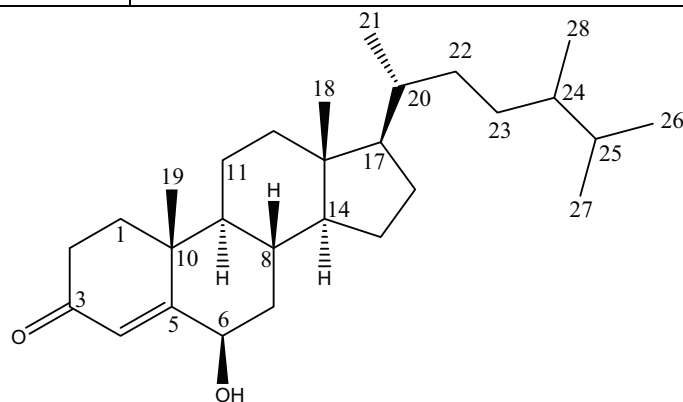
6 β -hydroxy-24-methylcholesta-4,22-dien-3-one	
Synonym(s)	6 β -hydroxy-24-methylcholesta-4,22-dien-3-one
Sample code	Jaspis Hex VLC-3,3
Biological source	<i>Jaspis splendens</i>
Sample amount	3.0 mg
Physical description	White needle crystals
Molecular formula	C ₂₈ H ₄₄ O ₂
Molecular weight	412 g/mol
Optical rotation [α] _D ²⁰	-56.0°C (c 0.08, CHCl ₃)
Retention time (HPLC)	39.27 min (standard gradient)



Results

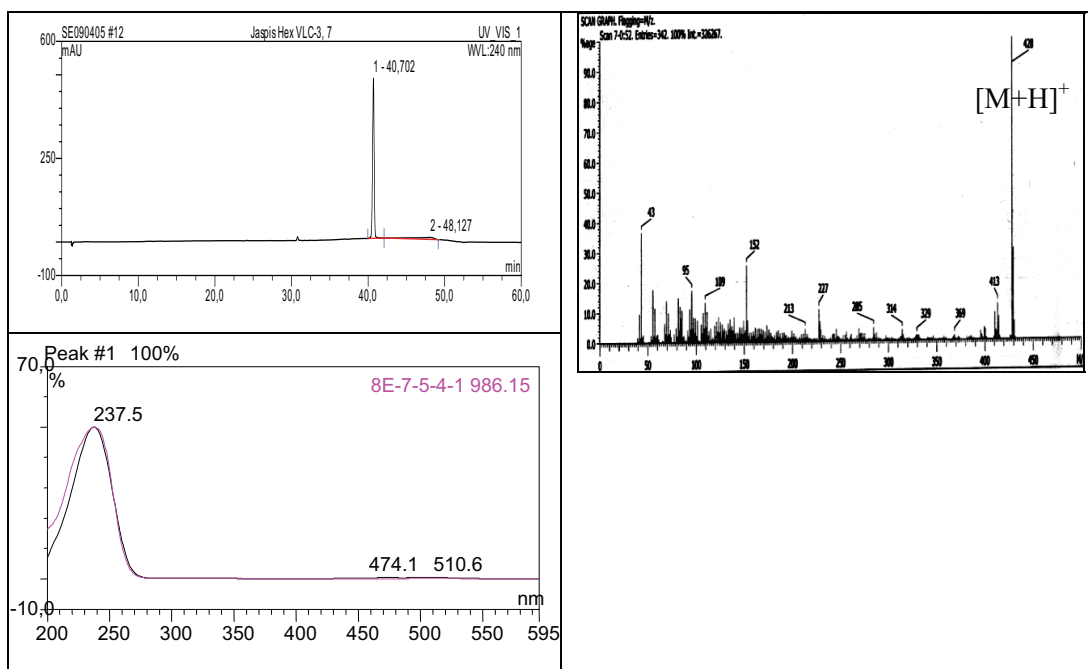
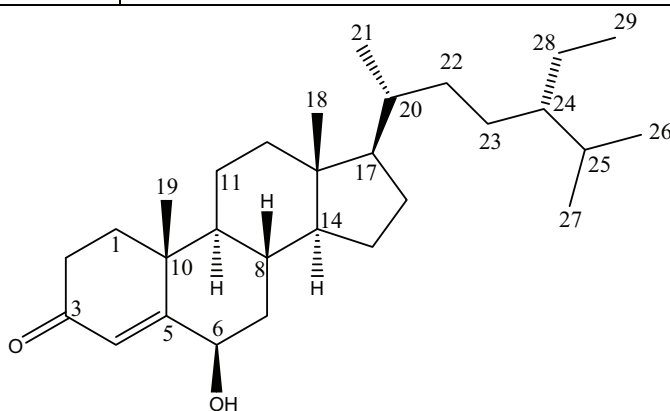
3.3.5. 6 β -hydroxy-24-methylcholesta-4-en-3-one (41, known compound)

6 β -hydroxy-24-methylcholesta-4-en-3-one	
Synonym(s)	6 β -hydroxy-24-methylcholesta-4-en-3-one
Sample code	Jaspis Hex VLC-3,6
Biological source	<i>Jaspis splendens</i>
Sample amount	3.0 mg
Physical description	White needle crystals
Molecular formula	C ₂₈ H ₄₆ O ₂
Molecular weight	414 g/mol
Optical rotation $[\alpha]_D^{20}$	-52.0°C (c 0.08, CHCl ₃)
Retention time (HPLC)	40.25 min (standard gradient)



3.3.6. 6 β -hydroxy-24-ethylcholesta-4-en-3-one (42, known compound)

6 β -hydroxy-24-ethylcholesta-4-en-3-one	
Synonym(s)	6 β -hydroxy-24-ethylcholesta-4-en-3-one
Sample code	Jaspis Hex VLC-3,7
Biological source	<i>Jaspis splendens</i>
Sample amount	3.0 mg
Physical description	White needle crystals
Molecular formula	C ₂₉ H ₄₈ O ₂
Molecular weight	428 g/mol
Optical rotation $[\alpha]_D^{20}$	-65.0°C (c 0.08, CHCl ₃)
Retention time (HPLC)	40.70 min (standard gradient)



Results

Compounds (**40–42**) were isolated as white solid crystals. Their EI mass spectrum exhibited pseudomolecular ion peaks at m/z 412 $[M]^+$, m/z 414 $[M]^+$ and m/z 428 $[M]^+$, respectively. They revealed λ_{\max} at 238.7, 237.4 and 237.5 nm in UV absorption, respectively. Both notions highlighted being structurally related in addition to being isolated from the same hexane soluble fraction of the methanolic extract of *J. splendens*. Structural elucidation of compounds (**40–42**) was done based on 1D and 2D NMR spectral analyses data (Table 3.21) including ^1H , ^{13}C NMR, HMBC and HMQC and compared to reported literature (Kontiza *et al.*, 2006; Georges *et al.*, 2006).

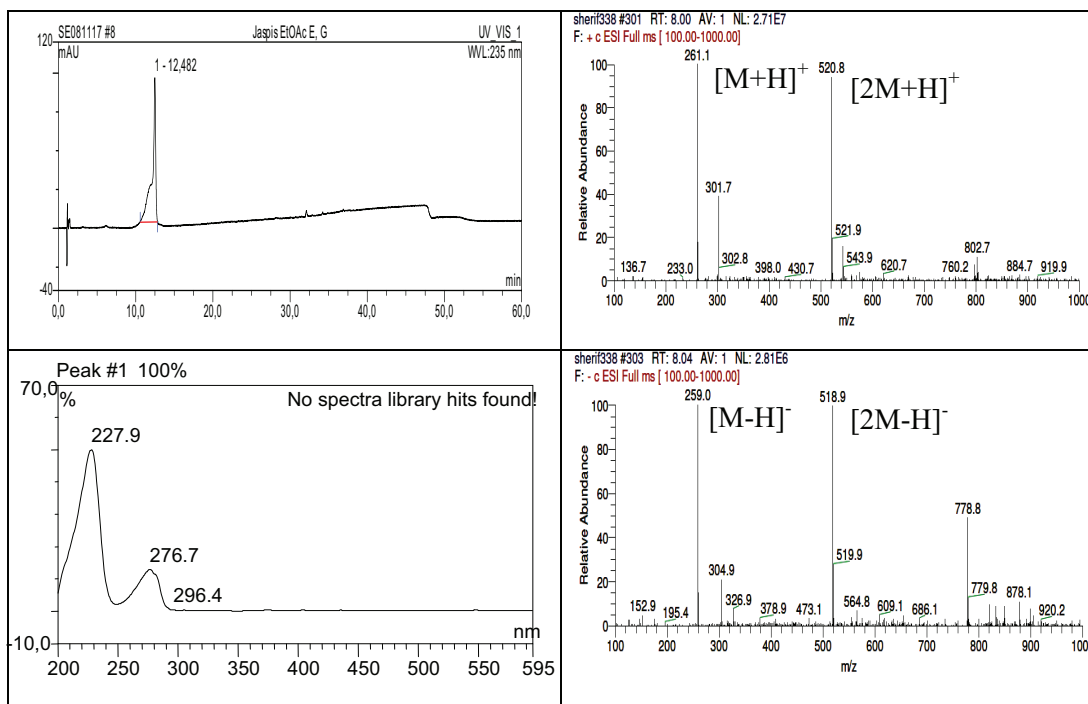
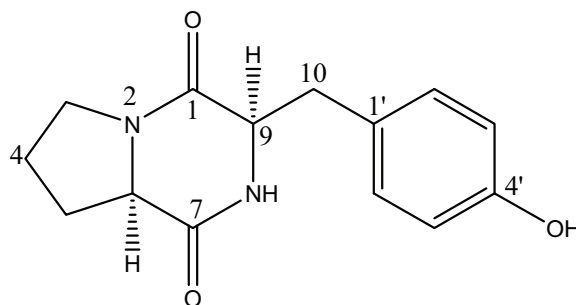
Table 3.21. NMR data of compounds (**40–42**), measured in CDCl_3 , 500 MHz.

#	40		41		42	
	δ_{H} (J Hz)	δ_{C}	δ_{H} mult. (J Hz)	δ_{C} mult.	δ_{H} mult. (J Hz)	δ_{C} mult.
1a	1.70 (<i>m</i>)	35.5	1.77 (<i>m</i>)	37.2, CH ₂	1.82 (<i>m</i>)	37.2, CH ₂
1b	2.01 (<i>m</i>)		2.02 (<i>m</i>)		2.03 (<i>m</i>)	
2a	2.53 (<i>m</i>)	34.0	2.53 (<i>m</i>)	34.3, CH ₂	2.53 (<i>m</i>)	34.3, CH ₂
2b	2.37 (<i>m</i>)		2.36 (<i>m</i>)		2.37 (<i>m</i>)	
3		n.d.		200.0, C		200.4, C
4	5.82 (<i>s</i>)	126.5	5.82 (<i>s</i>)	126.4, CH	5.82 (<i>s</i>)	126.4, CH
5		168.0		169.0, C		168.4, C
6	4.35 (<i>t</i> , 2.5 Hz)	73.3	4.35 (<i>t</i> , 2.8 Hz)	74.4, CH	4.35 (<i>t</i> , 2.5 Hz)	73.4, CH
7	1.98 (<i>m</i>)	38.5	1.99 (<i>m</i>)	39.1, CH ₂	2.00 (<i>m</i>)	39.4, CH ₂
	1.24 (<i>m</i>)		1.22 (<i>m</i>)		1.21 (<i>m</i>)	
8	1.55 (<i>m</i>)	30.0	1.54 (<i>m</i>)	30.6, CH	1.53 (<i>m</i>)	29.8, CH
9	0.90 (<i>m</i>)	53.3	0.90 (<i>m</i>)	53.7, CH	0.90 (<i>m</i>)	53.7, CH
10		38.0		39.0, C		39.2, C
11	1.10–1.60 (<i>m</i>)	21.1	1.10–1.60 (<i>m</i>)	21.0, CH ₂	1.10–1.60 (<i>m</i>)	21.0, CH ₂
12	1.97 (<i>m</i>)	39.5	1.99 (<i>m</i>)	39.6, CH ₂	2.00 (<i>m</i>)	39.7, CH ₂
	1.21 (<i>m</i>)		1.20 (<i>m</i>)		1.21 (<i>m</i>)	
13		42.5		42.6, C		42.6, C
14	1.10–1.60 (<i>m</i>)	54.0	1.10–1.60 (<i>m</i>)	56.0, CH	1.10–1.60 (<i>m</i>)	56.1, CH
15	1.10–1.60 (<i>m</i>)	24.8	1.10–1.60 (<i>m</i>)	24.2, CH ₂	1.10–1.60 (<i>m</i>)	24.2, CH ₂
16	1.60–2.00 (<i>m</i>)	29.5	1.60–2.00 (<i>m</i>)	28.2, CH ₂	1.60–2.00 (<i>m</i>)	28.2, CH ₂
17	1.00 (<i>m</i>)	n.d.	1.00 (<i>m</i>)	55.9, CH	1.12 (<i>m</i>)	55.9, CH
18	0.75 (<i>s</i>)	12.4	0.74 (<i>s</i>)	12.1, CH ₃	0.74 (<i>s</i>)	12.1, CH ₃
19	1.38 (<i>s</i>)	19.6	1.37 (<i>s</i>)	20.2, CH ₃	1.38 (<i>s</i>)	19.0, CH ₃
20	2.04 (<i>m</i>)	39.5	1.36 (<i>m</i>)	35.9, CH	1.34 (<i>m</i>)	35.6, CH
21	1.00 (<i>d</i> , 6.6 Hz)	21.1, CH ₃	0.91 (<i>d</i> , 6.6 Hz)	19.6, CH ₃	0.92 (<i>d</i> , 6.6 Hz)	19.6, CH ₃
22	5.20 (<i>dd</i> , 7.0, 15.0 Hz)	n.d.	1.10–1.60 (<i>m</i>)	34.3, CH ₂	1.10–1.60 (<i>m</i>)	34.3, CH ₂
23	5.14 (<i>dd</i> , 7.0, 15.0 Hz)	n.d.	1.10–1.60 (<i>m</i>)	31.0, CH ₂	1.10–1.60 (<i>m</i>)	24.2, CH ₂
24	1.50 (<i>m</i>)	53.0	1.20 (<i>m</i>)	40.6, CH	0.94 (<i>m</i>)	42.6, CH
25	1.65 (<i>m</i>)	31.9	1.68 (<i>m</i>)	32.8, CH	1.62 (<i>m</i>)	29.8, CH
26	0.83 (<i>d</i> , 7.0 Hz)	19.6	0.77 (<i>d</i> , 7.0 Hz)	20.5, CH ₃	0.81 (<i>d</i> , 7.0 Hz)	20.9, CH ₃
27	0.84 (<i>d</i> , 7.0 Hz)	19.0	0.78 (<i>d</i> , 7.0 Hz)	19.6, CH ₃	0.82 (<i>d</i> , 7.0 Hz)	19.6, CH ₃
28	0.91 (<i>d</i> , 7.0 Hz)	20.5	0.86 (<i>d</i> , 7.0 Hz)	15.4, CH ₃	1.10–1.60 (<i>m</i>)	21.0, CH ₂
29					0.87 (<i>t</i> , 7.0 Hz)	12.4, CH ₃

n.d. not determined.

3.3.7. Maculosin-1, *cyclo*-(L-Pro-L-Tyr) (43, known compound)

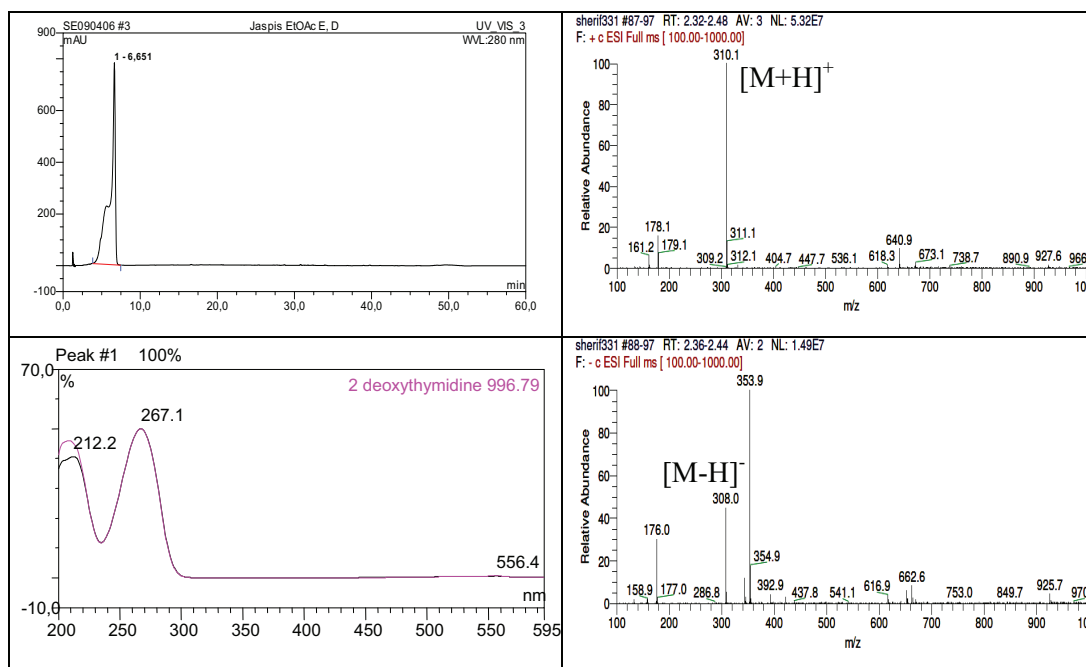
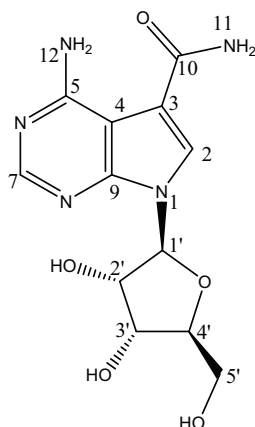
Maculosin-1, <i>cyclo</i> -(L-Pro-L-Tyr)	
Synonym(s)	<i>cyclo</i> -(L-Pro-L-Tyr)
Sample code	Jaspis EtOAc E,G
Biological source	<i>Jaspis splendens</i>
Sample amount	0.8 mg
Physical description	White amorphous solid
Molecular formula	C ₁₄ H ₁₆ N ₂ O ₃
Molecular weight	260 g/mol
Optical rotation $[\alpha]_D^{20}$	+88.0°C (<i>c</i> 0.02, Ethanol)
Retention time (HPLC)	12.48 min (standard gradient)



Results

3.3.8. Sangivamycin (44, known compound)

Sangivamycin	
Synonym(s)	Sangivamycic acid; amide
Sample code	Jaspis EtOAc J-L,F
Biological source	<i>Jaspis splendens</i>
Sample amount	1.0 mg
Physical description	White amorphous solid
Molecular formula	C ₁₂ H ₁₅ N ₅ O ₅
Molecular weight	309 g/mol
Optical rotation $[\alpha]_D^{20}$	-28.0°C (c 0.02, CH ₃ OH)
Retention time (HPLC)	6.65 min (standard gradient)



Compound (**43**) was obtained as a white amorphous solid. Its ESI mass spectrum exhibited pseudomolecular ion peaks at m/z 261.1 $[M+H]^+$ and m/z 259.0 $[M-H]^-$. It showed λ_{\max} at 228 and 276.7 nm in UV absorption. Structural elucidation of compound (**43**) was done based on 1D and 2D NMR spectral analyses data (Table 3.22) including 1H , ^{13}C NMR, HMBC, HMQC and NOESY spectra (Fig. 3.22) together with comparison to reported literature (Rudi *et al.*, 1994). From these data, compound (**43**) was concluded to be maculosin-1, *cyclo*-(L-Pro-L-Tyr).

Compound (**44**) was isolated as a white amorphous solid. Its ESI mass spectrum revealed pseudomolecular ion peaks at m/z 310 $[M+H]^+$ and m/z 308 $[M-H]^-$. Structural elucidation was performed by means of 1D and 2D NMR spectroscopy particularly 1H , ^{13}C NMR, HMBC and ROESY spectra (Table 3.22) (Fig. 3.23) in addition to comparison with reported literature (Zabriskie and Ireland, 1989).

Both compounds (**43**) and (**44**) were firstly reported as secondary metabolites from *Jaspis digonoxea* and *J. Johnstoni*, respectively. Later, they were obtained from microorganisms associated with the sponge. Hence, they were proven to be in fact a microbial secondary metabolites, produced by symbiont microorganisms associated with the marine sponge of the genus *Jaspis* (Jayatilake *et al.*, 1996; Fdhila *et al.*, 2003).

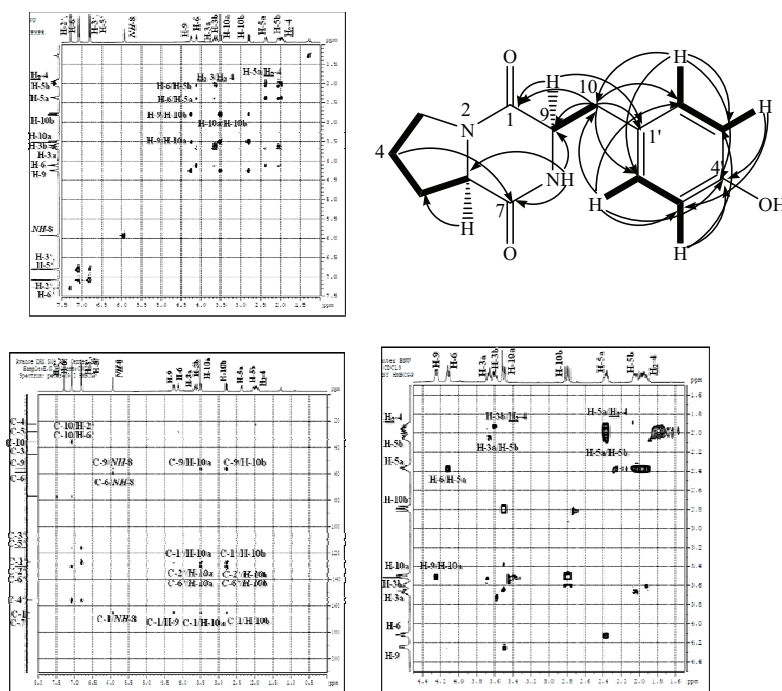


Fig. 3.22. 1H - 1H COSY, HMBC and NOESY spectra of maculosin-1 (**43**).

Results

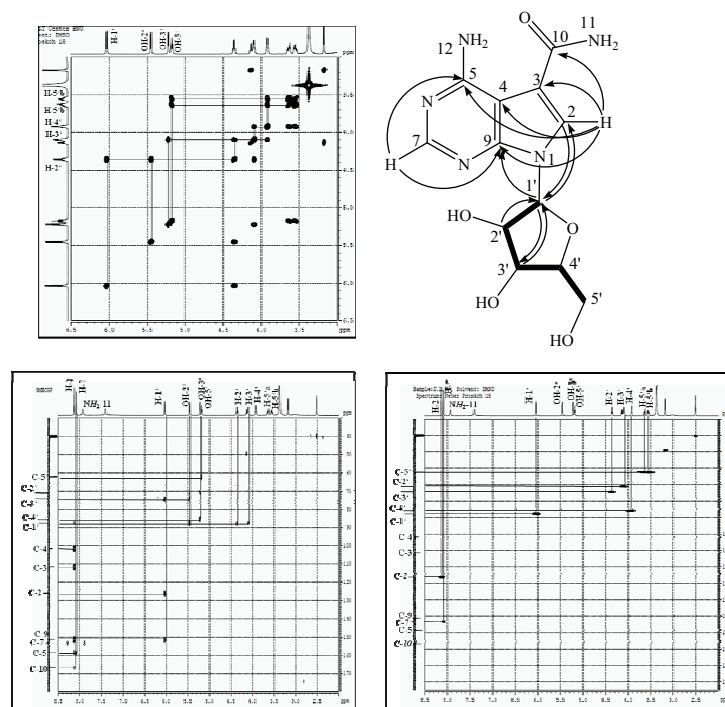


Fig. 3.23. ^1H - ^1H COSY, HMBC and HMQC spectra of sangivamycin (**44**).

Table 3.22. NMR data of compounds (**43** and **44**), measured in CDCl_3 , 500 MHz.

#	43		#	44	
	δ_{H} mult. (J Hz)	δ_{C} mult.		δ_{H} mult. (J Hz)	δ_{C} mult.
1		165.16, C	2	8.11 (1H, <i>s</i>)	125.6, CH
3	H-3a: 3.59 (1H, <i>m</i>) H-3b: 3.57 (1H, <i>m</i>)	45.44, CH_2	3		111.0, C
4	1.93 (2H, <i>m</i>)	22.47, CH_2	4		101.1, C
5	H-5a: 2.32 (1H, <i>m</i>) H-5b: 2.01 (1H, <i>m</i>)	28.33, CH_2	5		158.1, C
6	4.09 (1H, <i>t</i> , 9.0 Hz)	59.13, CH	7	8.06 (1H, <i>s</i>)	152.8, CH
7		169.70, C	9		150.8, C
8	5.91 (1H, <i>br s</i> , <i>NH</i>)		10		166.3, C
9	4.22 (1H, <i>dd</i> , 3.3, 11.9 Hz)	56.25, CH	1'	6.01 (1H, <i>d</i> , 6.0 Hz)	87.2, CH
10	H-10a: 3.47 (1H, <i>dd</i> , 3.9, 14.6 Hz) H-10b: 2.77 (1H, <i>dd</i> , 10.1, 14.5 Hz)	35.92, CH_2	2'	4.34 (1H, <i>q</i> , 5.8 Hz)	70.5, CH
1'		127.02, C	3'	4.08 (1H, <i>q</i> , 5.0 Hz)	73.8, CH
2'	7.05 (1H, <i>d</i> , 8.4 Hz)	130.31, CH	4'	3.90 (1H, <i>q</i> , 4.0 Hz)	85.3, CH
3'	6.78 (1H, <i>d</i> , 8.4 Hz)	116.15, CH	5'	3.60 (1H, <i>m</i>) 3.53 (1H, <i>m</i>)	61.9, CH_2
4'		155.54, C	NH_2 -11	7.91 and 7.40 (1H, <i>br s</i>)	
5'	6.78 (1H, <i>d</i> , 8.4 Hz)	116.15, CH	OH-2'	5.43 (1H, <i>d</i> , 6.3 Hz)	
6'	7.05 (1H, <i>d</i> , 8.4 Hz)	130.31, CH	OH-3'	5.20 (1H, <i>d</i> , 5.0 Hz)	
			OH-5'	5.15 (1H, <i>d</i> , 5.8 Hz)	

3.3.9. Biological activity of compounds isolated from *Jaspis splendens* collected in Kalimantan (Indonesia)

To the best of our knowledge, fifteen jaspamide congeners (B–P) were hitherto isolated from the genus *Jaspis* and all of them show antiproliferative activity with IC₅₀ values ranging from 0.01 to 33 μ M against human breast adenocarcinoma (MCF-7), and colon carcinoma (H-29) cell lines (Gala *et al.*, 2009).

Since jaspamide Q (**38**) and R (**39**) together with the parent jaspamide (**37**) differ in the bromination pattern of the abrine (*N*-methyltryptophan) moiety. Since these modifications were claimed as essential for the observed biological activity (Kahn *et al.*, 1991), compounds (**38** and **39**) together with other compounds isolated from *J. splendens* collected in Kalimantan (Indonesia) were subjected to a cytotoxicity (MTT) assay against mouse lymphoma (L5178Y) cell lines. They exhibited potent activities with IC₅₀ values between <0.1 and 10 μ g/mL (Table 3.23), compared to kahalalide F (IC₅₀ = 6.3 μ g/mL, 4.3 μ M) which was used as a positive control.

Table 3.23. Cytotoxicity assay of *J. splendens* extract, fractions and isolated compounds.

Sample tested	(L5178Y) growth in % (@ 10 μ g/mL)	IC ₅₀	
		(μ g/mL)	(μ M)
<i>J. splendens</i> methanolic Extract	0.0		
Hexane Soluble Fraction	0.6		
Ethyl Acetate Soluble Fraction	0.0		
Jaspamide (37)	0.0	<0.1	<0.14
Jaspamide Q (38)	0.3	<0.1	<0.16
Jaspamide R (39)	0.0	<0.1	<0.13
6 β -hydroxy-24-methylcholesta-4,22-dien-3-one (40)	34.5	10	24.3
6 β -hydroxy-24-methylcholesta-4-en-3-one (41)	14.4	9.3	22.5
6 β -hydroxy-24-ethylcholesta-4-en-3-one (42)	0.4	2.9	6.8
Maculosin-1 (43)	0.0	0.28	1.1
Sangivamycin (44)	0.0	<0.1	<0.34
Kahalalide F (positive control)		6.3	4.3

Results

3.4. Secondary metabolites isolated from *Thalassia testudinum*

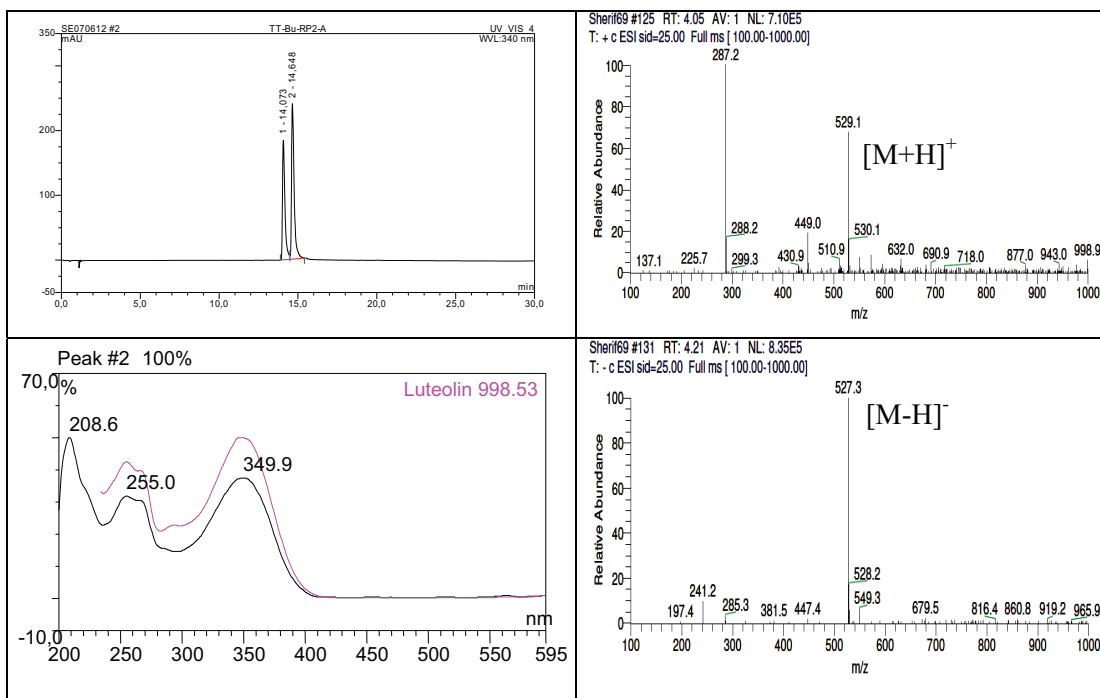
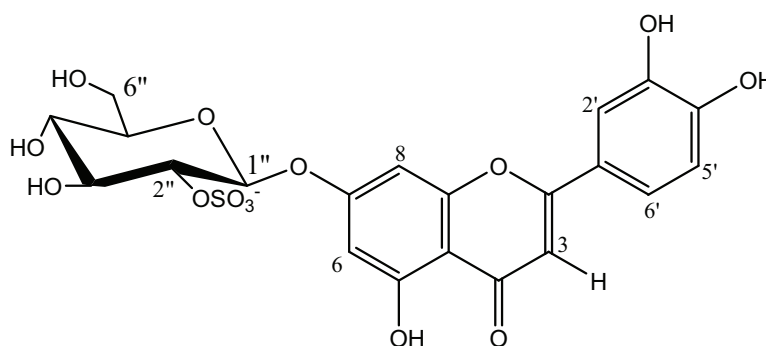
The seagrass *Thalassia testudinum* (turtle grass, family Hydrocharitaceae) is an important component of nearshore marine ecosystems, providing nursery grounds for commercially relevant fish and invertebrate species. Seagrasses are rich resources of secondary metabolites, particularly phenolic compounds (McMillan *et al.*, 1980) that include sulfated flavonoids, a group of conjugated metabolites for which the sulfate component is believed to represent a marine adaptation (Harborne *et al.*, 1976).

In this part, a detailed chemical investigation of the methanolic extract of *T. testudinum*, collected by snorkeling at 2 m depth off Muk Island, Trang Province, Thailand in July, 2007, was performed and led to the isolation of two sulfated flavonoid glycosides, thalassiolin A (**45**) and thalassiolin C (**46**), both were previously reported from the same species.

Interestingly, luteolin-3'-*O*-glucuronide (**47**) was also isolated and to the best of our knowledge, it is the first report for this compound from marine habitat, however it was reported from Sage (*Salvia officinalis*), a popular herb from the mint family (Labiatae) which has been the subject of several studies as a resource of some potent antioxidants (Lu and Foo, 2000). Additionally, all the isolated flavonoids glycosides were tested for radical scavenging (DPPH) activity using quercetin and kaempferol as standards, and the results would be reported.

3.4.1. Thalassiolin A (45, known compound)

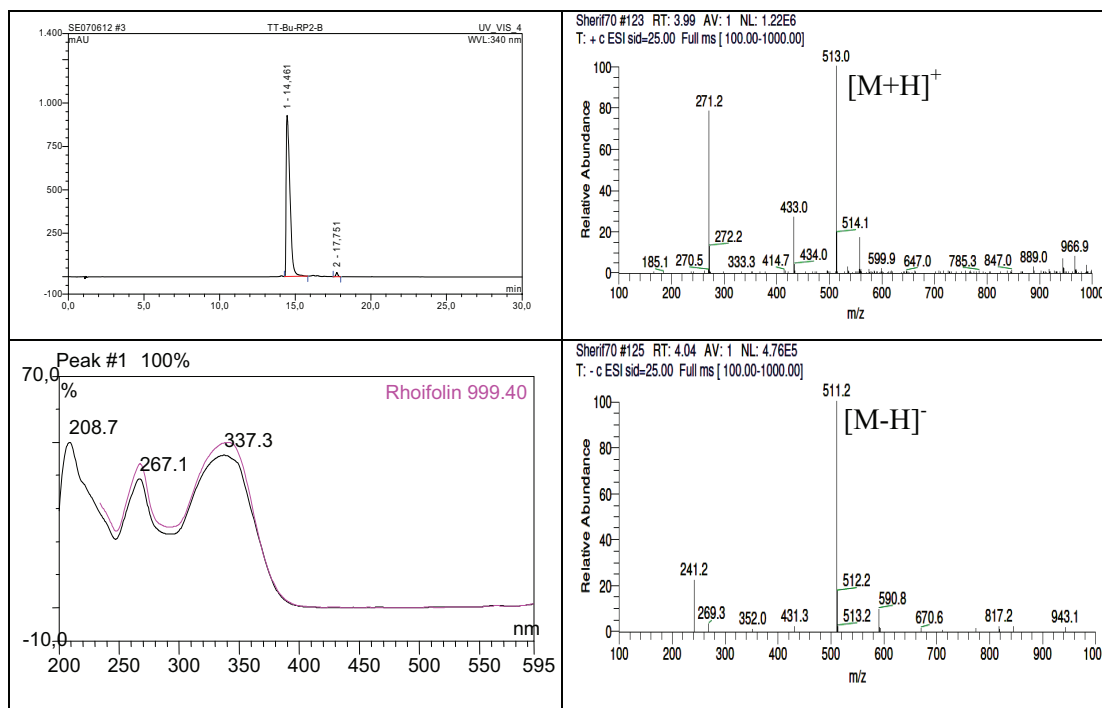
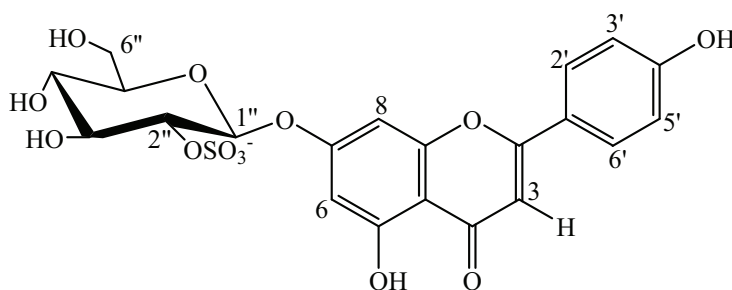
Thalassiolin A	
Synonym(s)	2''-Sulfoglucoluteolin
Sample code	TT-Bu-RP2-A
Biological source	<i>Thalassia testudinum</i>
Sample amount	1.0 mg
Physical description	Pale yellow amorphous solid
Molecular formula	C ₂₁ H ₁₉ O ₁₄ S ⁻
Molecular weight	528 g/mol
Retention time (HPLC)	14.07 min (half-time gradient)



Results

3.4.2. Thalassiolin C (46, known compound)

Thalassiolin C	
Synonym(s)	2''-Sulfoglucoapigenin
Sample code	TT-Bu-RP2-B
Biological source	<i>Thalassia testudinum</i>
Sample amount	2.0 mg
Physical description	Pale yellow amorphous solid
Molecular formula	C ₂₁ H ₁₉ O ₁₃ S ⁻
Molecular weight	512 g/mol
Retention time (HPLC)	14.46 min (half-time gradient)



Compounds (**45** and **46**) were obtained as pale yellow powder. They revealed, in their ESI mass spectra, pseudomolecular ion peaks at m/z 529 $[M+H]^+$ and at m/z 513 $[M+H]^+$, respectively. The observed difference of 16 amu in molecular weight was expected to be due to the presence of an additional oxygen atom in **45** more than **46**.

Based on comparison of NMR spectral data of compounds (**45** and **46**) (Table 3.24) to the reported literature (Jensen *et al.*, 1998; Rowley *et al.*, 2002), they were identified as thalassiolin A (luteolin 7- β -D-glucopyranosyl-2''-sulfate) and C (apigenin 7- β -D-glucopyranosyl-2''-sulfate), respectively.

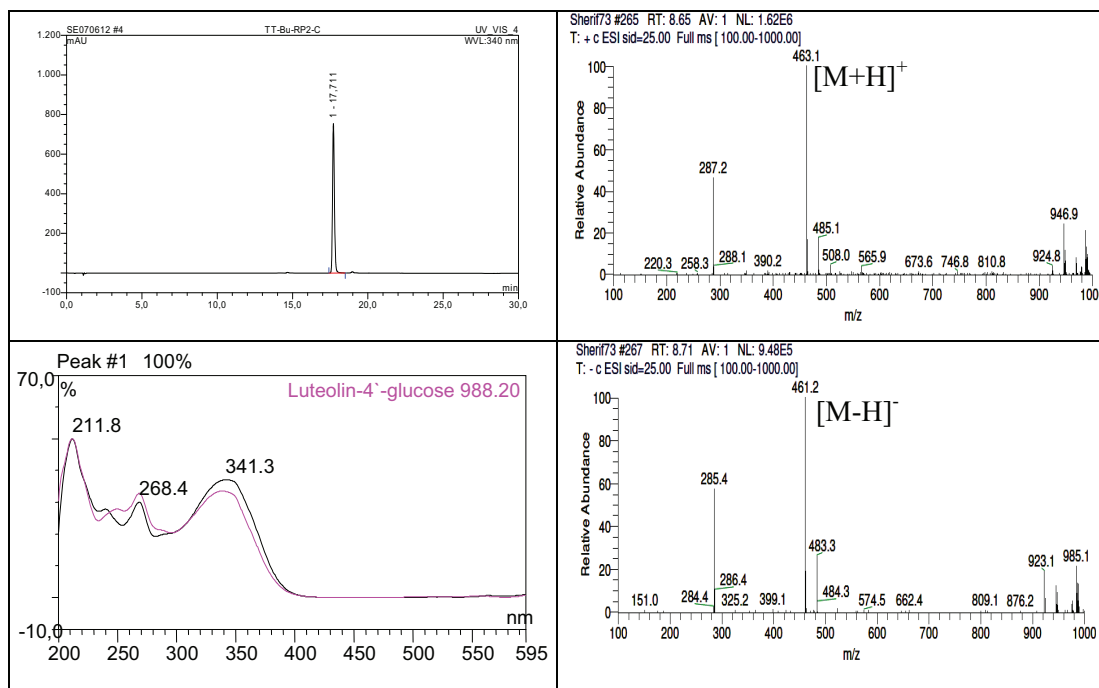
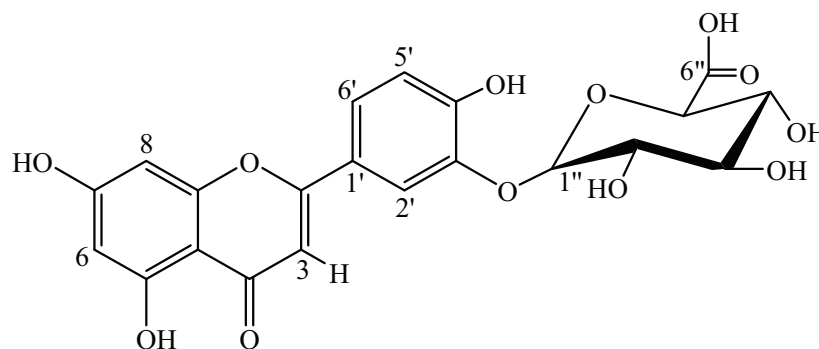
Table 3.24. ^1H NMR data of compounds (**45** and **46**), measured in DMSO- d_6 , 500 MHz.

#	45	46
	δ_{H} mult. (J Hz)	δ_{H} mult. (J Hz)
3	6.75 (1H, <i>s</i>)	6.85 (1H, <i>s</i>)
6	6.37 (1H, <i>d</i> , 1.9 Hz)	6.39 (1H, <i>d</i> , 1.6 Hz)
8	6.87 (1H, <i>s</i>)	6.89 (1H, <i>s</i>)
2'	7.56 (1H, <i>s</i>)	8.00 (1H, <i>d</i> , 8.5 Hz)
3'		6.90 (1H, <i>d</i> , 8.5 Hz)
5'	6.90 (1H, <i>d</i> , 8.2 Hz)	6.90 (1H, <i>d</i> , 8.5 Hz)
6'	7.47 (1H, <i>dd</i> , 8.2, 2.2 Hz)	8.00 (1H, <i>d</i> , 8.5 Hz)
1''	5.00 (1H, <i>d</i> , 7.3 Hz)	5.00 (1H, <i>d</i> , 7.3 Hz)
2''	4.10 (1H, <i>d</i> , 10.7 Hz)	4.10 (1H, <i>d</i> , 11.0 Hz)
3''	3.60 (1H, <i>dd</i> , 8.5, 7.3 Hz)	3.60 (1H, <i>dd</i> , 8.5, 6.6 Hz)
4''	3.10 (1H, <i>m</i>)	3.10 (1H, <i>m</i>)
5''	3.40–3.50 (1H, <i>m</i>)	3.40–3.50 (1H, <i>m</i>)
6''	3.73 (1H, <i>m</i>) 3.40–3.50 (1H, <i>m</i>)	3.70 (1H, <i>dd</i> , 11.0, 6.9, 6.6 Hz) 3.40–3.50 (1H, <i>m</i>)
5-OH	12.92 (1H, <i>br s</i>)	12.95 (1H, <i>br s</i>)
3'-OH	9.28 (1H, <i>br s</i>)	
4'-OH	9.86 (1H, <i>br s</i>)	10.4 (1H, <i>br s</i>)

Results

3.4.3. Luteolin-3'-*O*-glucuronide (47, known compound)

Luteolin-3'- <i>O</i> -glucuronide	
Synonym(s)	Luteolin-3'- <i>O</i> -glucuronide
Sample code	TT-Bu-RP2-C
Biological source	<i>Thalassia testudinum</i>
Sample amount	10.0 mg
Physical description	Pale yellow amorphous solid
Molecular formula	C ₂₁ H ₁₈ O ₁₂
Molecular weight	462 g/mol
Retention time (HPLC)	17.71 min (half-time gradient)



Compound (**47**) was isolated as pale yellow powder. It revealed, in its ESI mass spectra, pseudomolecular ion peaks at m/z 463 $[M+H]^+$ and at m/z 461 $[M-H]^-$. Structural elucidation of **47** was concluded based on 1D and 2D NMR spectral analyses including 1H , ^{13}C NMR, COSY and HMBC spectra (Fig. 3.24).

Based on comparison of NMR spectral data of compound (**47**) (Table 3.25) to the reported literature (Lu and Foo, 2000), it was identified as luteolin-3'-*O*-glucuronide that was firstly reported from *Salvia officinalis* and in this study it was the first report from *Thalassia testudinum*.

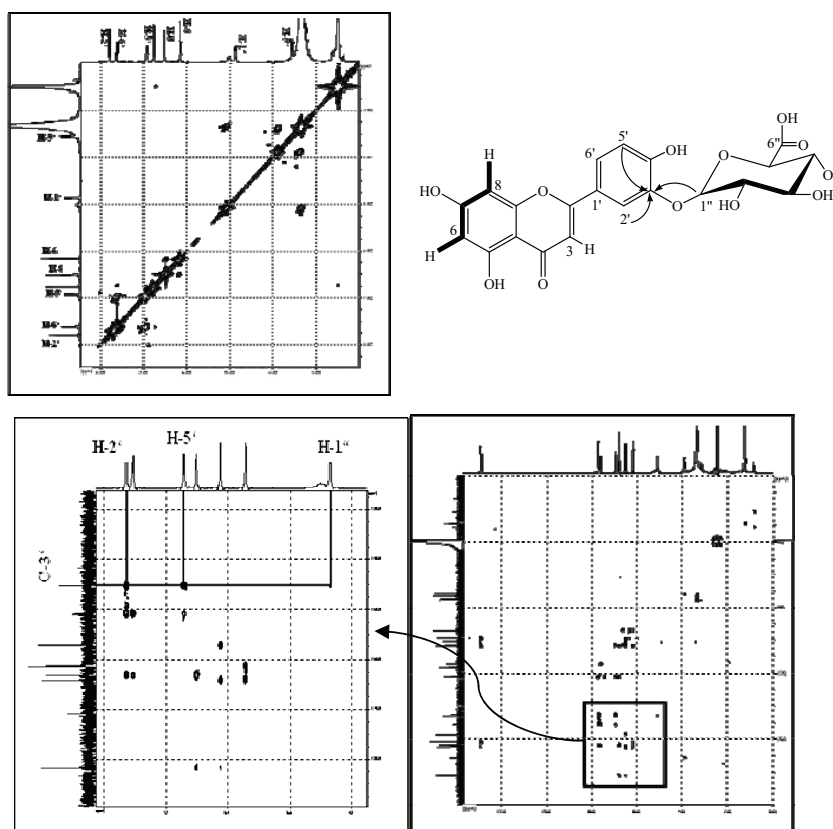


Fig. 3.24. 1H - 1H COSY and HMBC spectra of Luteolin-3'-*O*-glucuronide (**47**).

Results

Table 3.25. NMR data of luteolin-3'-*O*-glucuronide (**47**), measured in DMSO-*d*₆.

47					
#	δ_{H} mult. (J Hz)	δ_{C} mult.	#	δ_{H} mult. (J Hz)	δ_{C} mult.
2		164.3, C	4'		151.0, C
3	6.76, (1H, <i>s</i>)	103.2, CH	5'	6.90, (1H, <i>d</i> , 8.5 Hz)	116.6, CH
4		181.7, C	6'	7.60, (1H, <i>dd</i> , 8.5, 2.0 Hz)	121.9, CH
5		161.4, C	1''	4.86, (1H, <i>d</i> , 6.5 Hz)	101.2, CH
6	6.16, (1H, <i>d</i> , 1.6 Hz)	98.9, CH	2''	3.17–3.45 (1H, <i>m</i>)	73.0, CH
7		163.3, C	3''		75.6, CH
8	6.50, (1H, <i>d</i> , 1.6 Hz)	94.1, CH	4''		71.7, CH
9		157.3, C	5''	3.55, (1H, <i>d</i> , 9.1 Hz)	74.9, CH
10		103.6, C	6''		170.9, C
1'		121.5, C			
2'	7.80, (1H, <i>d</i> , 2.0 Hz)	114.4, CH			
3'		145.3, C			

3.4.4. Biological activity of compounds isolated from *Thalassia testudinum*

Compounds (45–47) isolated from *T. testudinum* were identified as flavonoid glycosides namely, thalassiolin A, thalassiolin C, and luteolin-3'-*O*-glucuronide, respectively. Thalassiolin A (45) was reported in literature as an *in vitro* inhibitor of HIV cDNA integrase ($IC_{50} = 0.4 \mu\text{M}$) and antiviral against HIV with IC_{50} value of $30 \mu\text{M}$ (Rowely *et al.*, 2002) compared to thalassiolin C (46) that exhibited moderate to low activity. However, none of them exhibited cellular toxicity against human colon cancer HCT-116 cells at concentration up to $75 \mu\text{M}$ (Rowely *et al.*, 2002).

Based on these reports, compounds (45–47) were subjected to cytotoxicity (MTT) assay against mouse lymphoma (L5178Y) cells, protein kinase inhibitory activity against 24 different enzymes, only thalassiolin A (45) revealed inhibitory activities (Table 3.26) against some protein kinases which proved interesting for further investigation.

In addition compounds (45–47) were tested for their radical scavenging activities using antioxidant (DPPH) assay using quercetin and kaempferol as standards. Outcomes of this assay revealed that thalassiolin A (45) and luteolin-3'-*O*-glucuronide (47) possess radical scavenging activity with IC_{50} values of $48 \mu\text{M}$ for both compared to quercetin ($IC_{50} = 6.0 \mu\text{M}$) and kaempferol ($IC_{50} = 23 \mu\text{M}$).

Table 3.26. Protein kinase inhibitory activity of thalassiolin A (45).

IC ₅₀ (μg/mL)												
AKT1	ARK5	Aurora-A	Aurora-B	AXL	B-RAF-VE	CDK2/CycA	CDK4/CycD1	CK2-alpha1	COT	COT	EGF-R	
>10	>10	2.1	1.5	>10	>10	>10	>10	>10	>10	4.3	>10	
IC ₅₀ (μg/mL)												
EPHB4	ERBB2	FAK	IGF1-R	INS-R	MET	PDGFR-beta	PLK1	PRK1	SAK	SRC	VEGF-R2	
>10	>10	>10	>10	>10	9.0	0.63	>10	>10	3.9	>10	9.1	

Results

3.5. Secondary metabolites isolated from *Comanthus* sp.

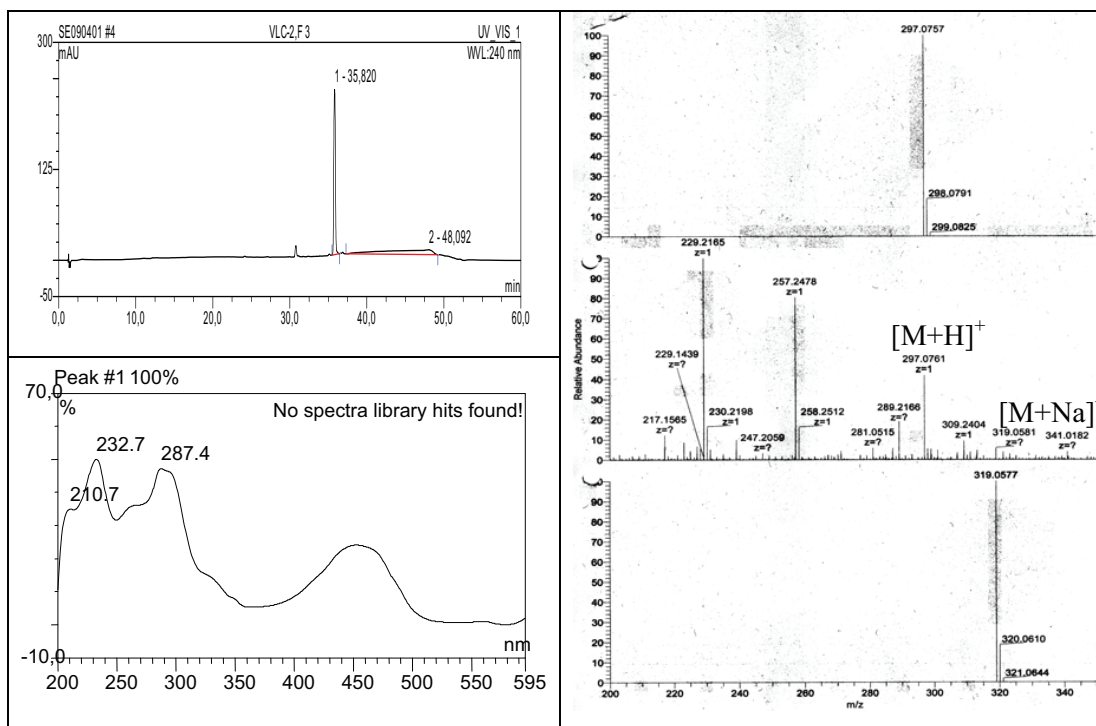
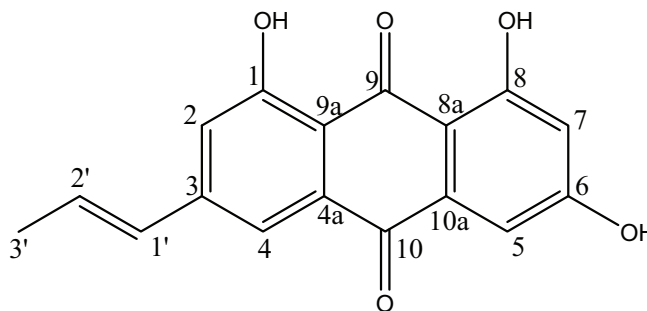
“Of all the animals in the sea there are none that exceeds in beauty of colouration the shallow water crinoids. Flowerlike in form and almost flowerlike in the fixity of their habit, they are also flowerlike in the variety and distribution of their pigments.” This comment was written by Clark, A.H. in 1921 in his “Monograph of the Existing Echinoderms” (Sutherland and Wells, 1967). The echinoderms constitute a class of the phylum Echinodermata whose animals’ pigments have attracted the interests for chemical studies, particularly in the early stage of the development of marine natural product chemistry. As a result, a number of polyketide pigments, naphthoquinones, anthraquinones, and naphthopyrones, have been isolated from various species of echinoderms (Sakuma *et al.*, 1987). Naphthoquinones have been obtained from four of the five classes of the phylum, while the occurrence of anthraquinones and naphthopyrones has so far been confined to a single class, the echinoderms (sea lilies) (Kent *et al.*, 1970; Smith and Sutherland, 1971; Francesconi, 1980). Some of these echinoderm pigments have been reported to play an ecological role, for example as feed deterrent (Rideout *et al.*, 1979). Echinoderms, in contrast to the familiar starfishes and sea urchins, are perhaps the little known and have been described from a restricted geographical area, the Indo-Pacific including the coast of Thailand (Barnes, 1987).

Bioactivity-guided fractionation strategy of *Comanthus* sp. extract was performed leading to the isolation of sixteen compounds; five of them were anthraquinones (**48–52**), five were naphthopyrones (**53–57**), one nucleoside, 2'-deoxythymidine (**58**), and five were steroidal secondary metabolites (**59–63**). Herein, we would comprehensively report isolation, structural elucidation based on the analysis of spectroscopic and spectrometric data in addition to comparison with the related literature, absolute stereochemistry of **50** and **52** would be reported here for the first time using Mosher reaction which revealed that both of them are (*S*)-(-) isomers.

All the isolated compounds were subjected qualitatively and quantitatively to radical scavenging (DPPH) assay, cytotoxic (MTT) assay against L5178Y mouse lymphoma cell line, protein kinase *in vitro* inhibitory activity assay against 24 different protein kinases, antimicrobial, antifungal and antiviral activities.

3.5.1. 1'-Deoxyrhodoptilometrene (48, new natural product)

1'-Deoxyrhodoptilometrene	
Synonym(s)	1,6,8-Trihydroxy-3- <i>trans</i> -(prop-1-enyl)anthraquinone
Sample code	VLC-2,F 3
Biological source	<i>Comanthus</i> sp.
Sample amount	8.0 mg
Physical description	Brick red powder
Molecular formula	C ₁₇ H ₁₂ O ₅
Molecular weight	296 g/mol
Retention time (HPLC)	35.82 min (standard gradient)



Results

Compound (**48**) was isolated as a red powder. Its ESIMS spectrum gave a molecular ion peak at 295.3 [M-H]⁻. ¹³C NMR (Table 3.27) revealed the presence of seventeen carbon atoms, and together with DEPT experiment they were found to be one methyl, six methine, and ten quaternary carbons. This suggested the probable existence of five oxygen atoms to give a molecular formula C₁₇H₁₂O₅ which was confirmed by HRFTMS (ion peak at *m/z* 297.0761 [M+H]⁺, Δ +1.0 ppm from calcd for C₁₇H₁₃O₅, and *m/z* 319.0581 [M+Na]⁺, Δ +1.0 ppm from calcd for C₁₇H₁₂O₅Na). ¹H NMR (Table 3.27) exhibited the presence of four doublet aromatic protons at [δ_H 6.50 (*d*, 2.20 Hz)], [δ_H 7.07 (*d*, 2.20 Hz)], [δ_H 7.28 (*d*, 1.25 Hz)], and [δ_H 7.64 (*d*, 1.25 Hz)] which were assigned to be H-7, H-5, H-2, and H-4, respectively. This assignment was evidenced by ¹H—¹H COSY (Fig. 3.25) that revealed clear correlations between H-5/H-7; and H-2/H-4. Moreover, H-2 and H-4 were correlated together with the two olefinic protons at [δ_H 6.52 (*dd*, 14.00, 1.00 Hz)], and [δ_H 6.65 (*m*)] which were ascribed to be H-1' and H-2', respectively. The latter olefinic proton, H-2', revealed a clear correlation to methyl group at [δ_H 1.90 (*dd*, 6.70, 1.00 Hz)]. Based on the coupling constant (*J* value) of H-1', the 1-propenyl side chain confirmed to have a *trans* configuration.

According to the previous data, and to the reported literature, compound (**48**) was proposed to be 1,6,8-trihydroxy-3-*trans*-(prop-1-enyl) anthraquinone which was obtained only as a synthetic product in 1976 by Banville and Brassard. Further confirmation of the proposed structure was provided by HMBC spectrum (Fig. 3.25) spectrum that exhibited correlations between the following: C-10 to H-4, and H-5; C-9a to H-2, and H-4; C-8a to H-5, and H-7; and C-1' to H-2, H-4, and H-3'. These findings unambiguously established the chemical structure of **48** to be 1,6,8-trihydroxy-3-*trans*-(prop-1-enyl) anthraquinone which was given the trivial name 1'-deoxyrhodoptilometrene.

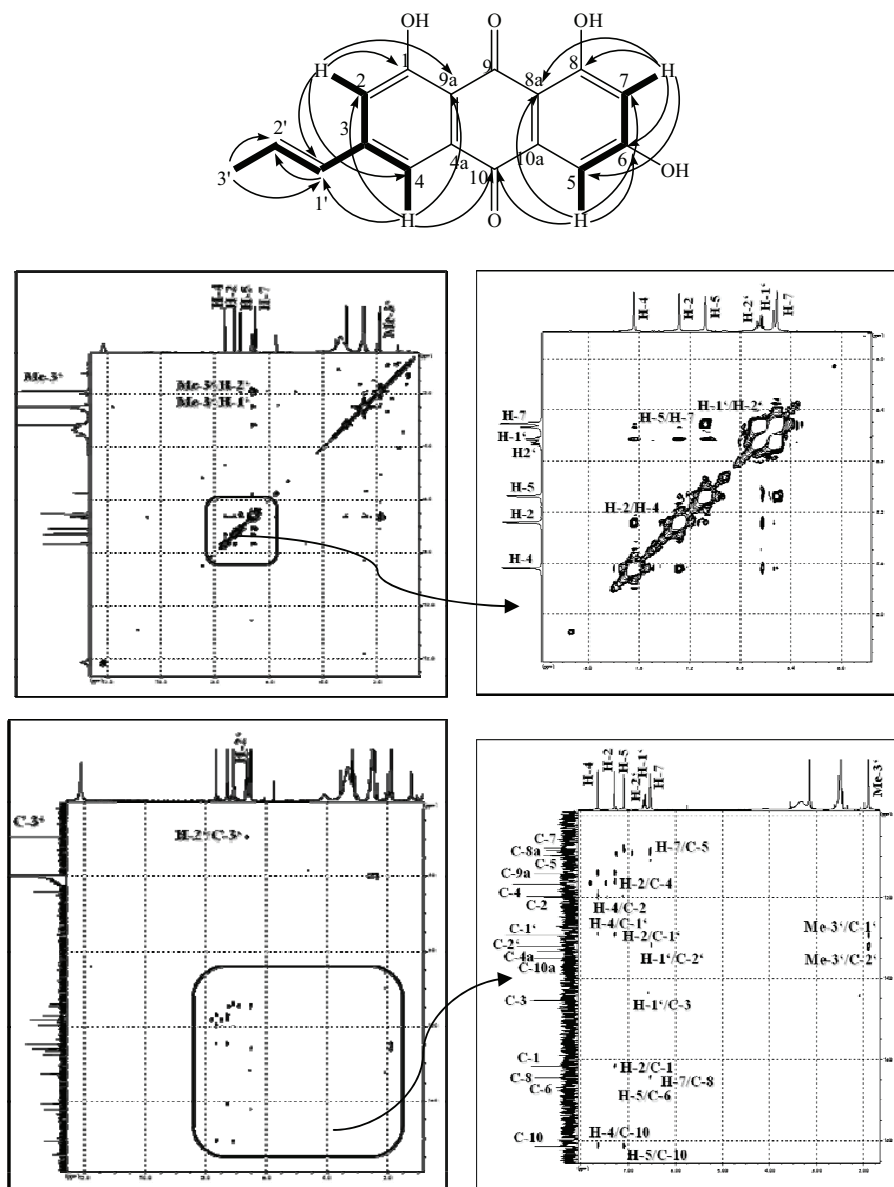
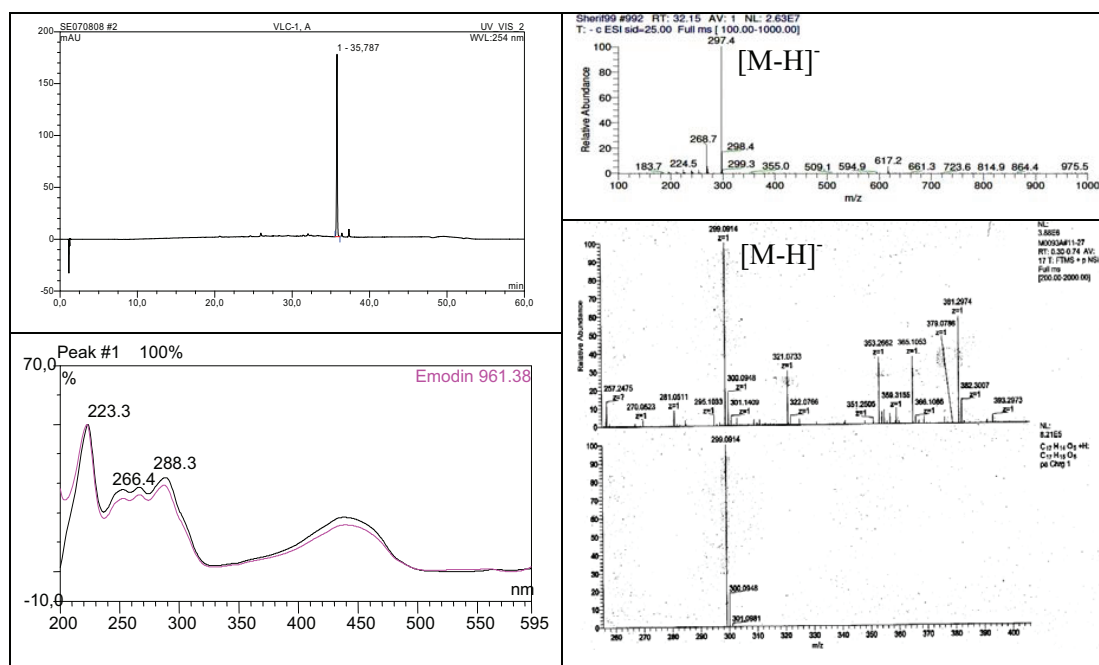
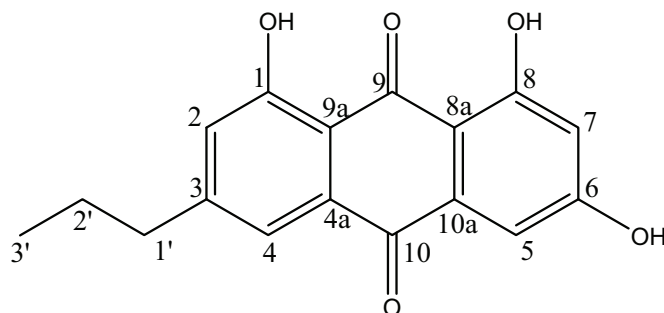


Fig. 3.25. ^1H - ^1H COSY and HMBC spectra of 1'-deoxyrhodoptilometrene (48).

Results

3.5.2. 1'-Deoxyrhodoptilometrin (49, known compound)

1'-Deoxyrhodoptilometrin	
Synonym(s)	1,6,8-trihydroxy-3-propyl-9,10-anthraquinone
Sample code	VLC-1,A
Biological source	<i>Comanthus</i> sp.
Sample amount	10.0 mg
Physical description	Red powder
Molecular formula	C ₁₇ H ₁₄ O ₅
Molecular weight	298 g/mol
Retention time (HPLC)	35.79 min (standard gradient)



Compound (**49**) was obtained as a red powder. ^{13}C NMR and DEPT (Table 3.27) revealed the presence of seventeen carbon atoms divided into one methyl, two methylene, four methine, and ten quaternary carbons. In ESIMS spectrum, it showed a molecular ion peak at 297.4 $[\text{M}-\text{H}]^-$ indicating the probable existence of five oxygen atoms, and suggesting a molecular formula of $\text{C}_{17}\text{H}_{14}\text{O}_5$. This suggestion was confirmed by HRESIMS (ion peak at m/z 299.0914 $[\text{M}+\text{H}]^+$, Δ +1.0 ppm from calc for $\text{C}_{17}\text{H}_{15}\text{O}_5$). Based on the reported literature, **48** was identified as 1,6,8-trihydroxy-3-propyl-9,10-anthraquinone which was first isolated in 1967 by Powell and Sutherland and no ^{13}C NMR data have been reported. ^1H NMR (Table 3.27) showed the presence of four aromatic protons at $[\delta_{\text{H}} 6.45$ (*d*, 2.20 Hz)], $[\delta_{\text{H}} 7.09$ (*d*, 2.20 Hz)], $[\delta_{\text{H}} 7.50$ (*d*, 1.25 Hz)], and $[\delta_{\text{H}} 7.02$ (*d*, 1.25 Hz)]. The first two were proven to be correlated by $^1\text{H}-^1\text{H}$ COSY (Fig. 3.26). The other two protons were correlated together with two methylene groups at $[\delta_{\text{H}} 2.64$ (2H, *t*, 7.85 Hz)] and $[\delta_{\text{H}} 1.68$ (2H, *m*)] and one methyl group at $[\delta_{\text{H}} 0.98$ (3H, *t*, 7.25 Hz)] forming an extended spin system.

Analysis of HMBC spectrum of **49** (Fig. 3.26) revealed the presence of long range couplings between the following: C-9 to H-2, H-4, H-5, and H-7; C-10 to H-4, and H-5; and C-3 to H-2, H-4, and 2H-1'. These couplings established the chemical structure of **49** to be 1,6,8-trihydroxy-3-propyl-9,10-anthraquinone which was given the trivial name 1'-deoxyrhodoptilometrin.

Results

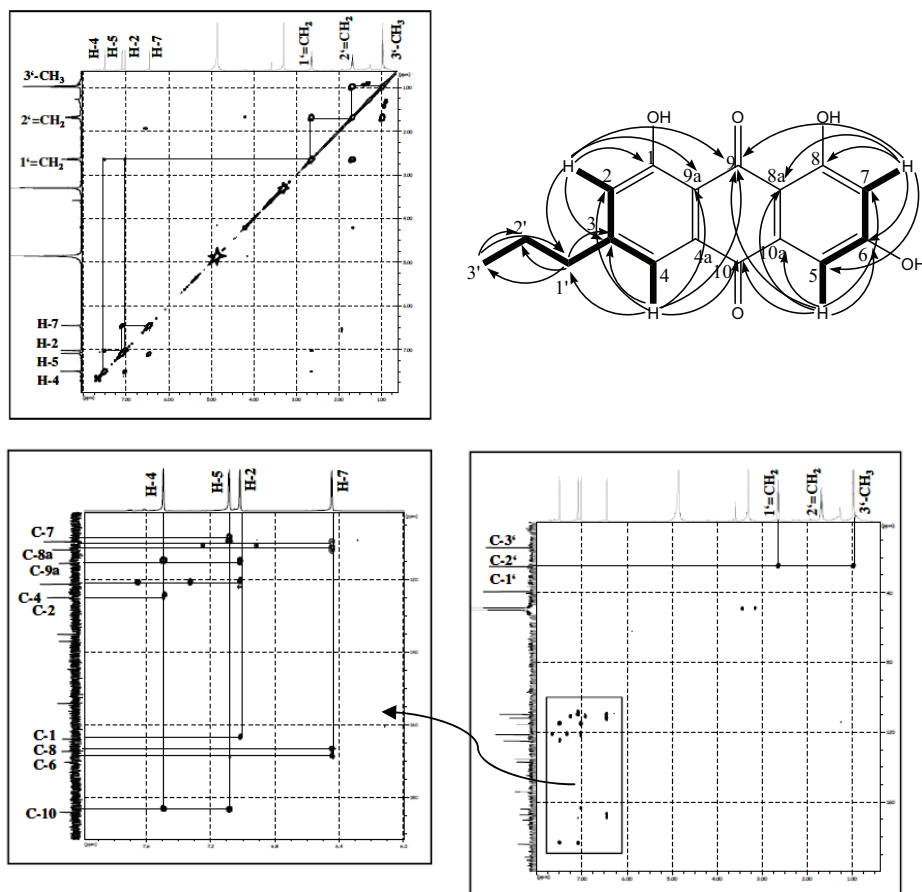


Fig. 3.26. ¹H-¹H COSY and HMBC spectra of 1'-deoxyrhodoptilometrin (49).

Table 3.27. NMR data of compounds (48 and 49).

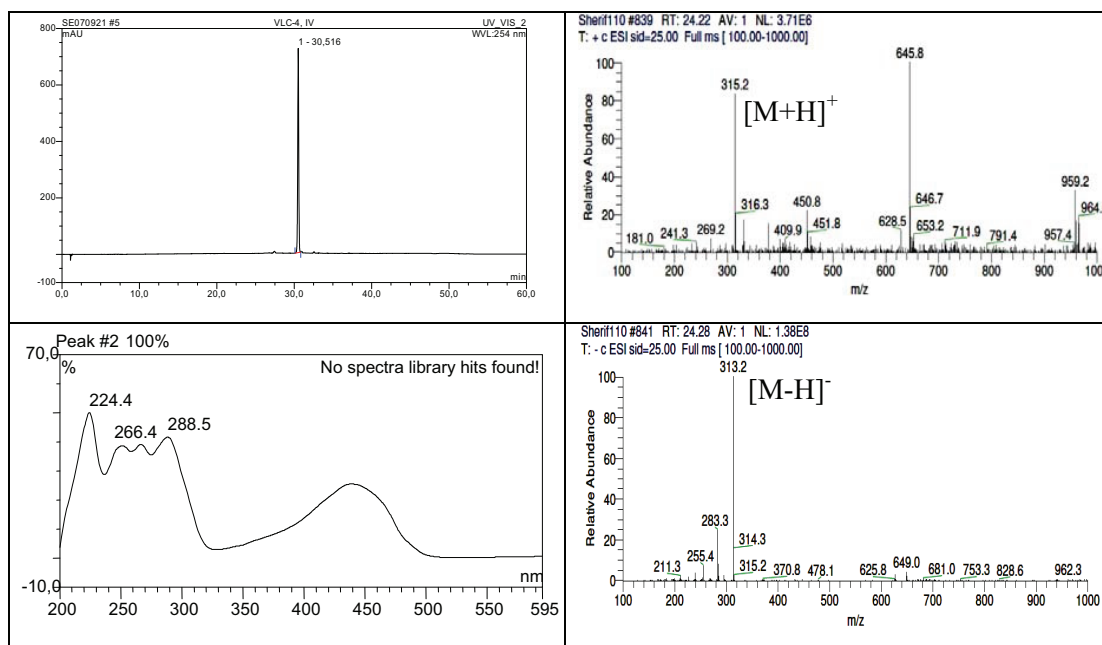
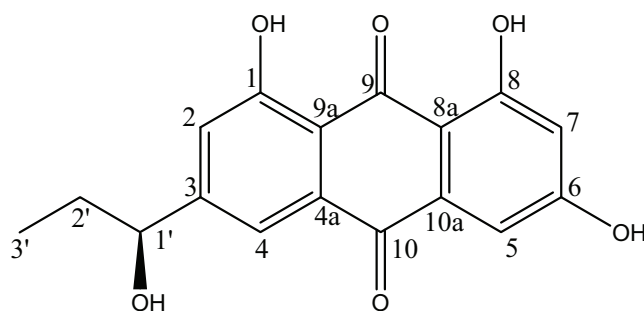
#	48 ^{a)}		49 ^{b)}	
	$\delta_{\text{H}}^{\text{c)}$ mult. (J Hz)	$\delta_{\text{C}}^{\text{d)}$ mult.	$\delta_{\text{H}}^{\text{c)}$ mult. (J Hz)	$\delta_{\text{C}}^{\text{d)}$ mult.
1		161.7, C		163.5, C
2	7.28 (1H, <i>d</i> , 1.25 Hz)	119.9, CH	7.02 (1H, <i>d</i> , 1.25 Hz)	124.6, CH
3		145.4, C		153.7, C
4	7.64 (1H, <i>d</i> , 1.25 Hz)	116.7, CH	7.50 (1H, <i>d</i> , 1.25 Hz)	120.9, CH
4a		133.4, C		134.7, C
5	7.07 (1H, <i>d</i> , 2.20 Hz)	109.7, CH	7.09 (1H, <i>d</i> , 2.20 Hz)	111.5, CH
6		166.7, C		169.8, C
7	6.50 (1H, <i>d</i> , 2.20 Hz)	107.9, CH	6.45 (1H, <i>d</i> , 2.20 Hz)	109.3, CH
8		164.6, C		166.8, C
8a		108.4, C		109.6, C
9		188.6, C		191.0, C
9a		114.2, C		115.2, C
10		181.6, C		183.6, C
10a		135.0, C		136.7, C
1'	6.52 (1H, <i>dd</i> , 14.00, 1.00 Hz)	129.4, CH	2.64 (2H, <i>t</i> , 7.85 Hz)	39.1, CH ₂
2'	6.65 (1H, <i>m</i>)	132.2, CH	1.68 (2H, <i>m</i>)	24.8, CH ₂
3'	1.90 (3H, <i>dd</i> , 6.70, 1.00 Hz)	18.6, CH ₃	0.98 (3H, <i>t</i> , 7.25 Hz)	14.0, CH ₃
1-OH	12.00 (1H, <i>br s</i>)		12.00 (1H, <i>s</i>)	
6-OH	12.00 (1H, <i>br s</i>)		12.04 (1H, <i>s</i>)	
8-OH	11.33 (1H, <i>br s</i>)		11.36 (1H, <i>br s</i>)	

^{a)}Measured in DMSO-*d*₆, ^{b)}Measured in MeOH-*d*₄, ^{c)}Measured at 500 MHz, ^{d)} at 125 MHz.

Results

3.5.3. (S)-(-) Rhodoptilmetrin (50, known compound)

(S)-(-) Rhodoptilmetrin	
Synonym(s)	1,6,8-trihydroxy-3-((S)-1'-hydroxypropyl)anthracene-9,10-dione
Sample code	VLC-4, IV
Biological source	<i>Comanthus</i> sp.
Sample amount	21.0 mg
Physical description	Red crystals
Molecular formula	C ₁₇ H ₁₄ O ₆
Molecular weight	314 g/mol
Optical rotation $[\alpha]_D^{20}$	-8.2°C (c 0.2, CH ₃ OH)
Retention time (HPLC)	30.52 min (standard gradient)



Compound (**50**) was obtained as a red powder. The UV absorption spectrum proved to be closely similar to that of **49** [λ_{max} 224, 266, 288, and 440 nm] which implied a similar chromophore in common. ESIMS of **50** exhibited a pseudomolecular ion peak at 315 $[\text{M}+\text{H}]^+$, and 313 $[\text{M}-\text{H}]^-$ revealing an additional 16 amu compared to 1'-dexoyrhodoptilometrin (**49**). This difference was expected to be due to an introduced oxygen atom, and explained by the differences in ^1H NMR and DEPT (Table 3.28) revealed the presence of seventeen carbon atoms divided into one methyl, one methylene, five methine, and ten quaternary carbons. ^1H NMR (Table 3.28) showed the presence of four aromatic protons at $[\delta_{\text{H}} 6.22 (d, 2.20 \text{ Hz})]$, $[\delta_{\text{H}} 6.79 (d, 2.20 \text{ Hz})]$, $[\delta_{\text{H}} 7.44 (d, 1.25 \text{ Hz})]$, and $[\delta_{\text{H}} 7.05 (d, 1.25 \text{ Hz})]$. The first two were proven to be correlated by ^1H — ^1H COSY spectrum (Fig. 3.27). The other two protons were correlated together with one methine at $[\delta_{\text{H}} 4.53 (t, 7.60 \text{ Hz})]$, one methylene $[\delta_{\text{H}} 1.74 (2\text{H}, m)]$ and one methyl groups at $[\delta_{\text{H}} 0.98 (3\text{H}, t, 7.50 \text{ Hz})]$ forming an extended spin system.

Analysis of HMBC spectrum of **50** (Fig. 3.27) revealed the presence of long range couplings between the following: C-9 to H-2, H-4, H-5, and H-7; C-10 to H-4, and H-5; and C-3 to H-2, H-4, and H-1'. Accordingly these couplings established the chemical structure of **50** to be 1,6,8-trihydroxy-3-(1'-hydroxypropyl)-9,10-anthraquinone which was given the trivial name rhodoptilometrin (Powell and Sutherland, 1967; Bartolini *et al.*, 1973; Lee and Kim, 1995).

Results

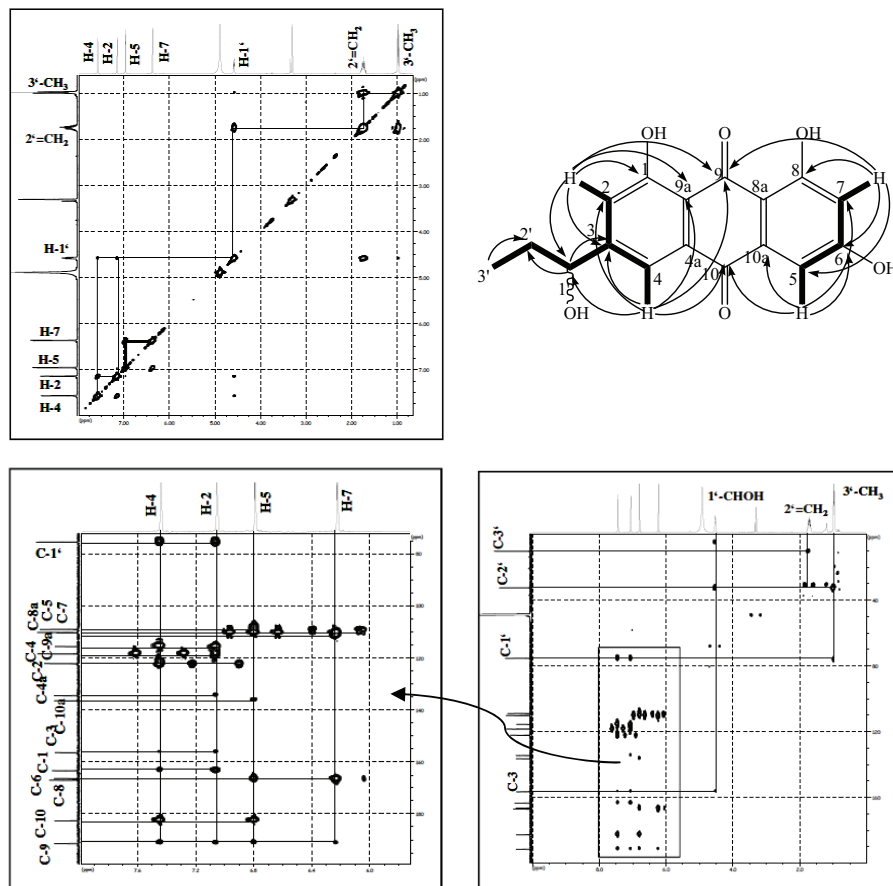
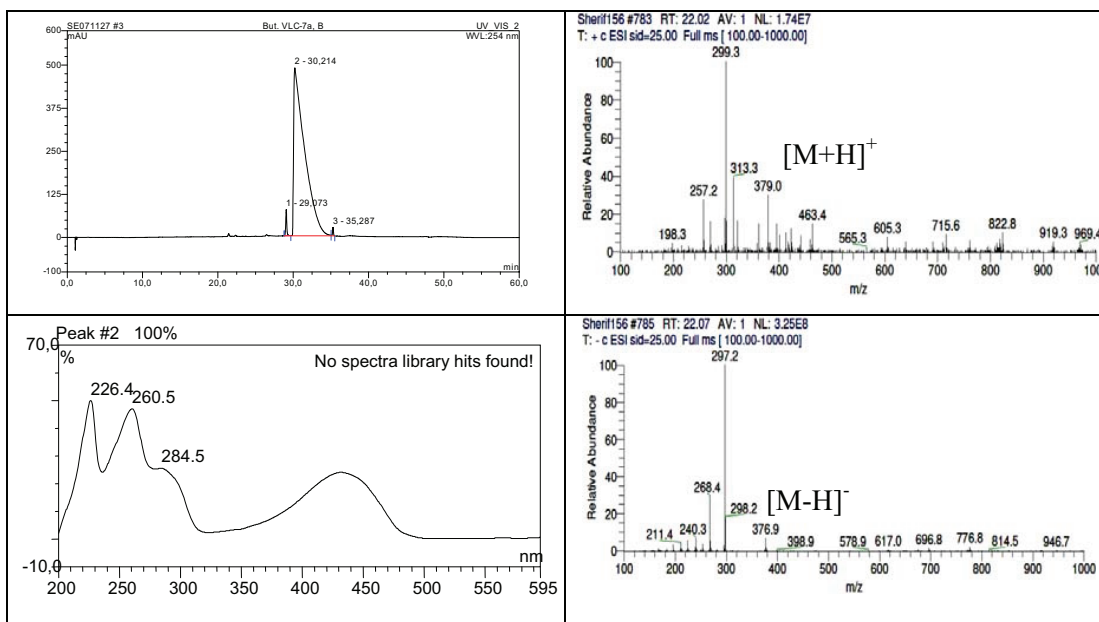
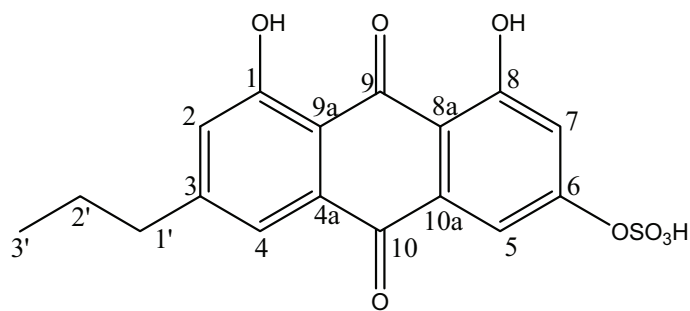


Fig. 3.27. ¹H-¹H COSY and HMBC spectra of (S)-(-)-rhodoptilometrins (50).

3.5.4. 1'- Deoxyrhodoptilometrins-6-O-sulfate (51, known compound)

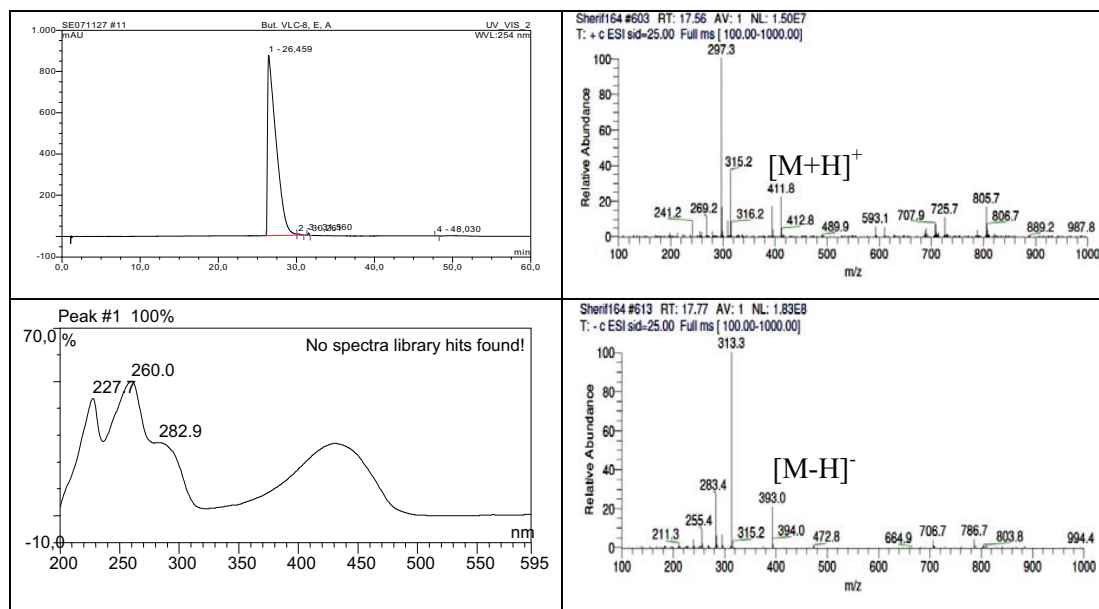
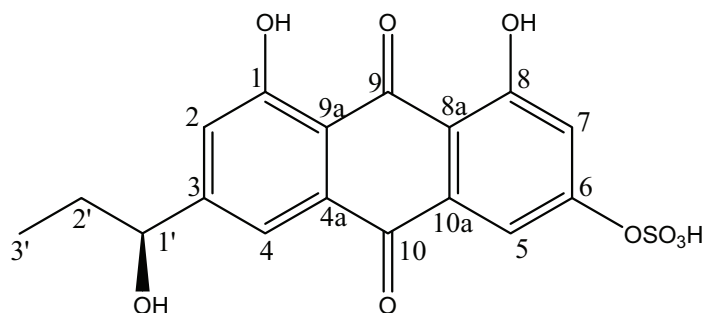
1'- Deoxyrhodoptilometrins-6-O-sulfate	
Synonym(s)	1,6,8-trihydroxy-3-propyl-9,10-anthraquinone-6-O-sulfate
Sample code	But. VLC-7a, B
Biological source	<i>Comanthus</i> sp.
Sample amount	4.0 mg
Physical description	Red powder
Molecular formula	C ₁₇ H ₁₄ O ₈ S
Molecular weight	378 g/mol
Retention time (HPLC)	30.21 min (standard gradient)



Results

3.5.5. Rhodoptilometrin-6-*O*-sulfate (52, known compound)

Rhodoptilometrin-6- <i>O</i> -sulfate	
Synonym(s)	1,6,8-trihydroxy-3-((<i>S</i>)-1'-hydroxypropyl)anthracene-9,10-dione-6- <i>O</i> -sulfate
Sample code	But. VLC-8,E,A
Biological source	<i>Comanthus</i> sp.
Sample amount	5.0 mg
Physical description	Red powder
Molecular formula	C ₁₇ H ₁₄ O ₉ S
Molecular weight	394 g/mol
Optical rotation [α] _D ²⁰	-13.8°C (<i>c</i> 0.2, CH ₃ OH)
Retention time (HPLC)	30.21 min (standard gradient)



Compound (**51**) was obtained as a greenish red powder. The UV absorption spectrum resembled that of **49** [λ_{\max} 224, 260, 285, and 440 nm] which implied a similar chromophore in common. ESIMS of **51** exhibited a pseudomolecular ion peak at 379 $[M+H]^+$, and 377 $[M-H]^-$ revealing an additional 80 amu compared to 1'-deoxyrhodoptilometrin (**49**). This difference was expected to be due to an additional sulfate ($-\text{SO}_3^-$) moiety in **51** than in **49**. The downfield shift in ^1H NMR (Table 3.28) [δ_{H} , DMSO- d_6 , **51**: C₅-H: 7.61 (*d*, 3.50 Hz), C₇-H: 7.20 (*d*, 3.5 Hz), *cf* **49**: C₅-H: 7.09 (*d*, 2.20 Hz), C₇-H: 6.45 (*d*, 2.20 Hz)] was consistent with the attachment of sulfate moiety at C-6 position.

Analysis of HMBC spectrum of **51** revealed the presence of long range couplings between the following: C-9 to H-2, H-4, H-5, and H-7; C-10 to H-4, and H-5; and C-3 to H-2, H-4, and H-1'. Based on these couplings, the chemical structure of **50** established to be 1,6,8-trihydroxy-3-propyl-9,10-anthraquinone-6-*O*-sulfate which was given the trivial name 1'-deoxyrhodoptilometrin-6-*O*-sulfate (Powell and Sutherland, 1967; Bartolini *et al.*, 1973; Lee and Kim, 1995).

Compound (**52**) was obtained as a red powder. The UV absorption spectrum resembled that of **50** [λ_{\max} 227, 260, 283, and 440 nm] which implied a similar chromophore in common. ESIMS of **52** exhibited a pseudomolecular ion peak at 395 $[M+H]^+$, and 393 $[M-H]^-$ revealing an additional 80 amu compared to rhodoptilometrin (**50**). This difference was expected to be due to an additional sulfate ($-\text{SO}_3^-$) moiety in **52** than in **50**. The downfield shift in ^1H NMR (Table 3.28) [δ_{H} , DMSO- d_6 , **52**: C₅-H: 7.66 (*br s*), C₇-H: 7.21 (*br s*), *cf* **50**: C₅-H: 6.79 (*d*, 2.20 Hz), C₇-H: 6.22 (*d*, 2.20 Hz)] was consistent with the attachment of sulfate moiety at C-6 position.

Analysis of HMBC spectrum of **52** revealed the presence of long range couplings between the following: C-9 to H-2, H-4, H-5, and H-7; C-10 to H-4, and H-5; and C-3 to H-2, H-4, and H-1'. Accordingly these findings confirmed the chemical structure of **52** to be 1,6,8-trihydroxy-3-(1'-hydroxypropyl)-9,10-anthraquinone-6-*O*-sulfate which was given the trivial name rhodoptilometrin-6-*O*-sulfate (Powell and Sutherland, 1967; Bartolini *et al.*, 1973; Lee and Kim, 1995).

Results

Table 3.28. NMR data of compounds (**50–52**).

#	50^{a)}		51^{b)}		52^{b)}	
	$\delta_{\text{H}}^{\text{c)}$ mult. (J Hz)	$\delta_{\text{C}}^{\text{d)}$ mult.	$\delta_{\text{H}}^{\text{c)}$ mult. (J Hz)	$\delta_{\text{C}}^{\text{d)}$ mult.	$\delta_{\text{H}}^{\text{c)}$ mult. (J Hz)	$\delta_{\text{C}}^{\text{d)}$ mult.
1		163.7, C		164.1, C		164.1, C
2	7.05 (1H, <i>d</i> , 1.3 Hz)	122.4, CH	7.07 (1H, <i>s</i>)	124.9, CH	7.28 (1H, <i>s</i>)	122.6, CH
3		156.1, C		154.6, C		158.2, C
4	7.44 (1H, <i>d</i> , 1.3 Hz)	116.6, CH	7.60 (1H, <i>s</i>)	121.2, CH	7.77 (1H, <i>s</i>)	116.2, CH
4a		135.3, C		134.7, C		135.2, C
5	6.79 (1H, <i>d</i> , 2.2 Hz)	113.6, CH	7.61 (1H, <i>d</i> , 2.5 Hz)	113.1, CH	7.66 (1H, <i>br d</i>)	113.7, CH
6		160.2, C		161.1, C		161.6, C
7	6.22 (1H, <i>d</i> , 2.2 Hz)	109.7, CH	7.20 (1H, <i>d</i> , 2.5 Hz)	115.2, CH	7.21 (1H, <i>br s</i>)	115.2, CH
8		167.5, C		165.9, C		165.8, C
8a		113.9, C		113.8, C		113.9, C
9		192.0, C		192.3, C		193.0, C
9a		118.4, C		115.1, C		119.0, C
10		184.3, C		182.8, C		182.9, C
10a		136.9, C		136.4, C		136.7, C
1'	4.53 (1H, <i>t</i> , 7.0 Hz)	75.5, CH	2.68 (2H, <i>t</i> , 7.5 Hz)	39.2, CH ₂	4.58 (1H, <i>t</i> , 6.5 Hz)	75.7, CH
2'	1.74 (2H, <i>m</i>)	32.6, CH ₂	1.64 (2H, <i>m</i>)	32.6, CH ₂	1.76 (2H, <i>m</i>)	32.9, CH ₂
3'	0.98 (3H, <i>t</i> , 7.5 Hz)	10.3, CH ₃	0.90 (3H, <i>t</i> , 7.5 Hz)	13.9, CH ₃	0.96 (3H, <i>t</i> , 7.5 Hz)	10.5, CH ₃

^{a)}Measured in MeOH-*d*₄, ^{b)}Measured in DMSO-*d*₆, ^{c)}Measured at 500 MHz, ^{d)} at 125 MHz.

Absolute and relative configurations of the optically active anthraquinone derivatives, compounds (**50**) and (**52**), were determined by performing Mosher reaction and measuring optical rotation, respectively. The optical rotations $[\alpha]_D^{20}$ measured for compounds (**3**) and (**5**), which have similarly single chiral center at C-1', gave values of -8.0° (c 0.2, MeOH) and -14.0° (c 0.2, MeOH), respectively which were related to those reported in literature (Lee and Kim, 1995). These results established that both **50** and **52** are (-) isomer.

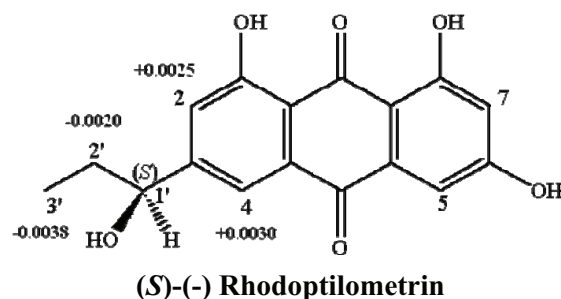


Table 3.29. Chemical shift differences between the (*S*)-MTPA and (*R*)-MTPA esters of **50**.

position	Chemical shift (δ_H , in C_5D_5N , 500 MHz)			Δ $\Delta(S) - \delta(R)$
	Rhodptilometrin (50)	(<i>S</i>)-MTPA ester	(<i>R</i>)-MTPA ester	
2	8.2081	8.0350	8.0325	+0.0025
4	7.6890	7.4156	7.4126	+0.0030
2'	1.8914	1.8790	1.8810	-0.0020
3'	1.0744	1.0567	1.0605	-0.0038

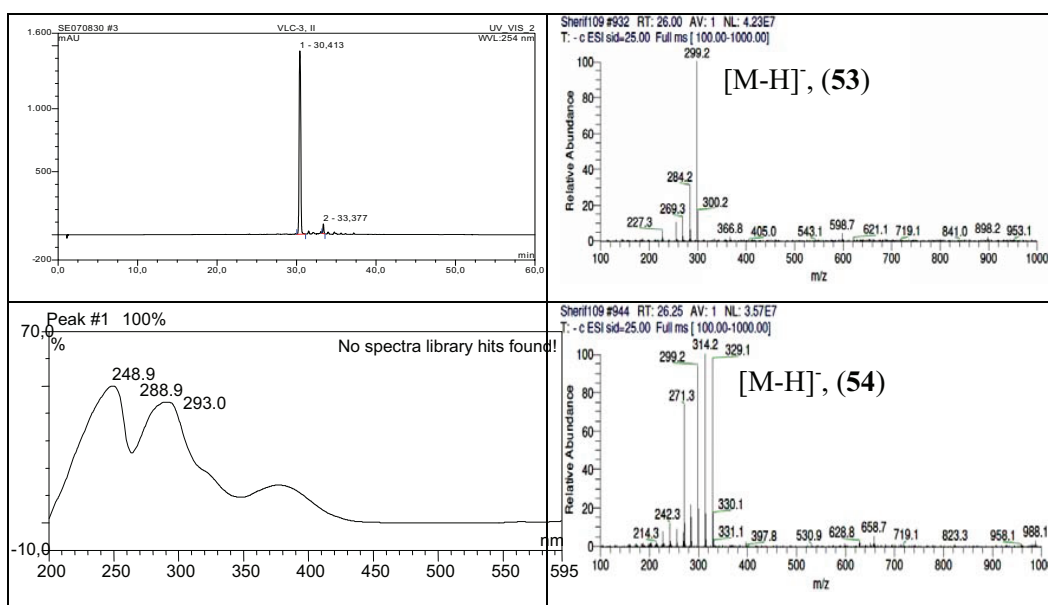
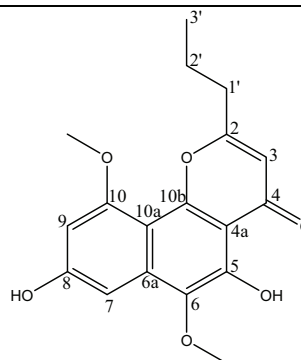
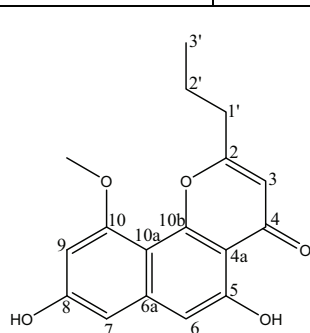
Absolute configuration of **50** was determined following Mosher reaction procedure (Dale and Mosher, 1973; Su *et al.*, 2002) and the results (Table 3.29) proved the assignment of the chiral center at C-1' in **50** to be *S* configuration and consequently **52** was considered to be the same isomer based on being (-) isomer as well. So, both compounds (**50**) and (**52**) were concluded to be (*S*)-(-) isomers of rhodoptilometrin and rhodoptilometrin-6-*O*-sulfate, respectively.

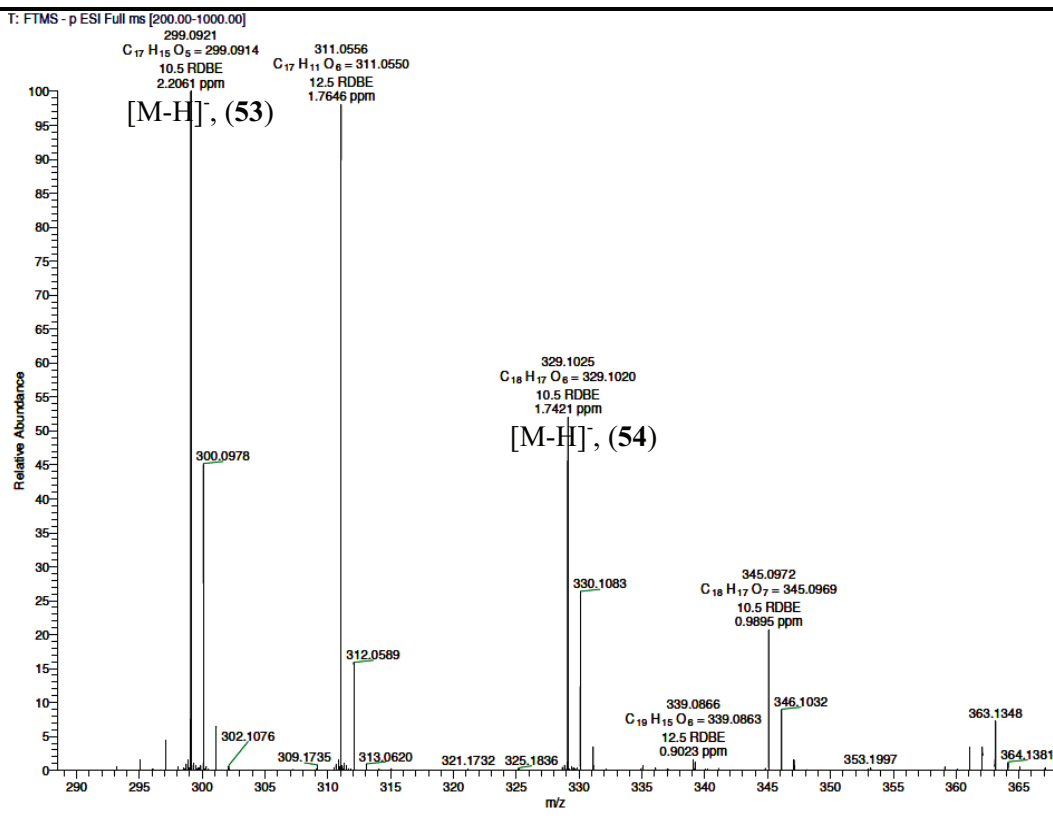
Results

3.5.6. Comaparvin (53, known compound)

3.5.7. 6-Methoxycomaparvin (54, known compound)

Comaparvin (55) / 6-Methoxycomaparvin (56), (3:2)	
Synonym(s)	5,8-dihydroxy-10-methoxy-2-propyl-benzo[<i>h</i>]chromen-4-one 5,8-dihydroxy-6,10-dimethoxy-2-propyl-benzo[<i>h</i>]chromen-4-one
Sample code	VLC-3,II
Biological source	<i>Comanthus</i> sp.
Sample amount	30.0 mg
Physical description	Greenish yellow powder
Molecular formula	Comaparvin: C ₁₇ H ₁₆ O ₅ 6-Methoxy Comaparvin: C ₁₈ H ₁₈ O ₆
Molecular weight	Comaparvin: 300 g/mol, 6-Methoxycomaparvin: 330 g/mol
Retention time (HPLC)	30.41 min (standard gradient)





Compound (**53**) was obtained as yellow powder and its ^{13}C NMR spectral data (Table 3.30) revealed resonances for seventeen carbons and together with DEPT indicated the presence of two methyl, two methylene, four methine, and nine quaternary carbon atoms. In ESI mass spectrum, it showed a molecular ion peak at m/z 299.2 $[M-H]^-$ that suggested the probable existence of further five oxygen atoms, leading to a molecular formula of $C_{17}H_{16}O_5$. This deduction was confirmed by HRESIMS (ion peak at m/z 299.0921 $[M-H]^-$, Δ +2.2 ppm from calc for $C_{17}H_{15}O_5$). The taxonomic information and the molecular formula pointed toward **53** being naphthopyrone comaparvin, which was first isolated by Smith and Sutherland in 1971, and for which no ^{13}C NMR data have been recorded. 1H NMR (Table 3.30) revealed the presence of three aromatic protons at $[\delta_H$ 6.75 (1H, *s*)], $[\delta_H$ 6.59 (1H, *d*, 1.85 Hz)], and $[\delta_H$ 6.44 (1H, *d*, 1.85 Hz)], in addition to one proton at $[\delta_H$ 6.41 (1H, *s*)], that were ascribed to be H-6, H-7, H-9, and H-3, respectively. Also, 1H NMR showed two proton resonances at $[\delta_H$ 12.84 (1H, *s*)], and $[\delta_H$ 10.26 (1H, *s*)] which correspond to $-OH$ protons at C-5, and C-8, respectively. The assignment of H-7 and H-9 was confirmed by $^1H-^1H$ COSY spectrum that revealed a clear correlation between them. The ascription of H-3 was proven by $^1H-^1H$ COSY which displayed a correlation to methylene group at $[\delta_H$ 2.71 (2H, *t*, 7.25 Hz)], then the spin system extends over methylene

Results

group at [δ_{H} 1.80 (2H, *m*)] and methyl group at [δ_{H} 0.96 (3H, *t*, 7.25 Hz)], forming altogether the *n*-propyl side chain at C-2. ^1H NMR exhibited one more methyl resonance at [δ_{H} 3.91 (3H, *s*)] which was an oxygen-substituted singlet and correlated to ^{13}C resonance at δ_{C} 55.9 ppm, and both were assigned for methoxy group at C-10. The structural elucidation of **53** was further confirmed by HMBC spectrum which exhibited long range couplings between: C-10 to H-9, and C-10-OCH₃; C-2 to H-3, and H₂-1'; C-4 to H-3; and C-10a to H-6, H-7, and H-9. The angular orientation of **53** was confirmed by ROESY spectrum that revealed an obvious correlation between methoxy group 10-OCH₃ at δ_{H} 3.91 with the terminal methyl and two methylene groups of the *n*-propyl side chain.

Based on these data (Table 3.30) and by comparison with reported literature (Smith and Sutherland, 1971; Sakurai *et al.*, 2002), compound (**53**) was deduced to be 5,8-dihydroxy-10-methoxy-2-propyl-benzo[*h*]chromen-4-one known as comaparvin.

The ^{13}C NMR data of compound (**54**) (Table 3.30), which was obtained as a reddish yellow powder, displayed eighteen carbon resonances distributed into three methyl, two methylene, three methine, and nine quaternary carbons. The LRESIMS data (m/z 329.2 [M-H]⁺) supposed the presence of six oxygen atoms and molecular formula was established to be C₁₈H₁₈O₆ based on the results from HRESIMS (m/z 329.1025 [M-H]⁺, Δ +1.7 ppm) which was more than **53** by 30 amu. Dereplication based on the taxonomic information and the molecular formula supported **54** to be naphthopyrone 6-methoxycomaparvin, that was first isolated by Smith and Sutherland. ^1H NMR spectral data of **54** (Table 3.30) explained this difference in mass spectrum by revealing the disappearance of one aromatic proton resonance and the emergence of one methyl resonance which was oxygen-substituted singlet at [δ_{H} 3.83 (3H, *s*)]. The presence of this methoxy group was confirmed by ^{13}C NMR (Table 3.30) which displayed one additional carbon resonance at δ_{C} 59.4 ppm. Apart from that ^1H NMR of **54** exhibited the presence of two aromatic protons at [δ_{H} 6.89 (1H, *d*, 2.20 Hz)], [δ_{H} 6.50 (1H, *d*, 2.20 Hz)], and one more proton at [δ_{H} 6.40 (1H, *s*)], which were oriented as H-7, H-9, and H-3, respectively. Moreover, ^1H NMR showed two methylene groups at [δ_{H} 2.72 (2H, *t*, 7.25 Hz)], [δ_{H} 1.81 (2H, *m*)], and two methyl groups at [δ_{H} 3.92 (3H, *s*)], and [δ_{H} 0.97 (3H, *t*, 7.25 Hz)]. Like in Comaparvin (**53**), ^1H NMR of **54** exhibited two resonances at [δ_{H} 13.06 (1H, *s*)], and [δ_{H} 10.36 (1H, *s*)], that were assigned for -OH groups at C-5 and C-8, respectively. ^1H - ^1H COSY confirmed the correlation between H-7 and H-9. Also, it established the correlation between H-3 and methylene group at C-1' and hence the *n*-propyl side chain at C-2. HMBC spectrum of **54** revealed some key long range couplings between: C-10 to H-9, and C-10-OCH₃; C-6 to H-7, and C-6-OCH₃; and as in

comparvin (**53**), it showed couplings between C-4 to H-3; C-2 to H-3, and H₂-1'; C-10a to H-7, and H-9. ROESY spectrum supported the proposed angular structure of compound (**54**), by exhibiting correlations between methoxy group 10-OCH₃ at δ_H 3.92 with the terminal methyl and two methylene groups of the *n*-propyl side chain at C-2. From these data and by comparison with the available literature (Smith and Sutherland, 1971; Sakurai *et al.*, 2002; Folmer *et al.*, 2008), compound (**54**) was found to be 5,8-dihydroxy-6,10-dimethoxy-2-propyl-benzo[*h*]chromen-4-one which was called 6-methoxycomparvin.

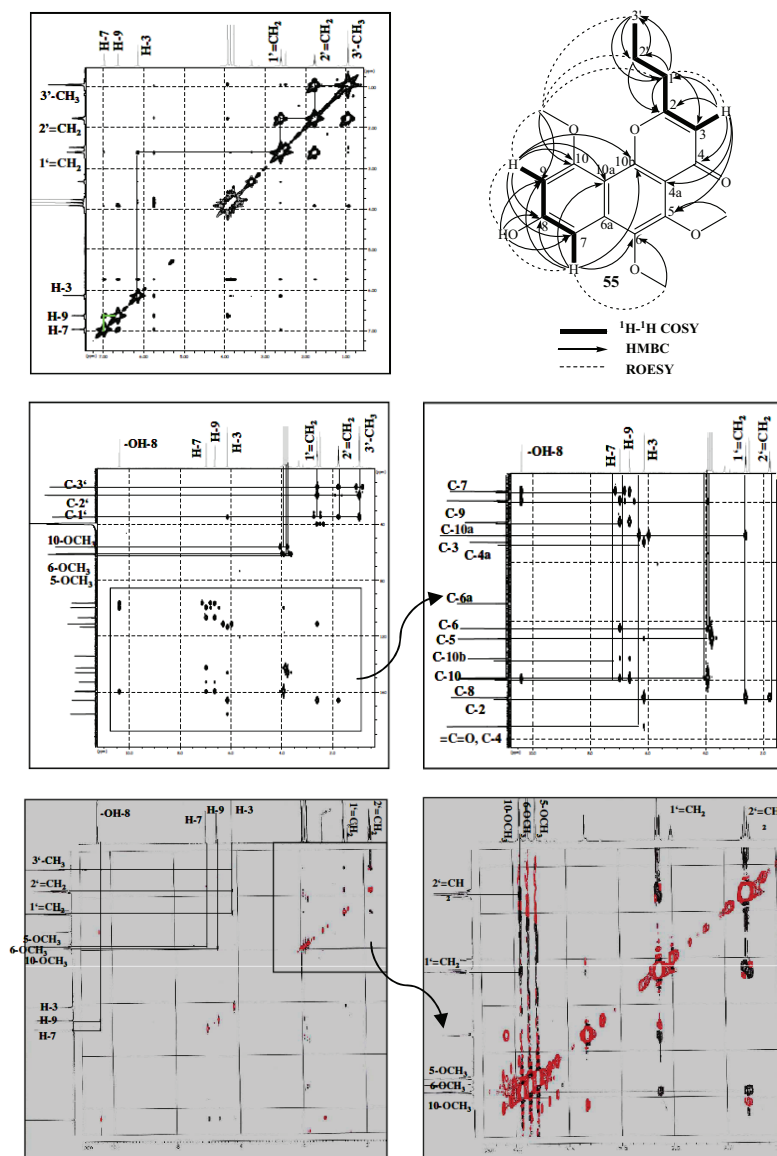
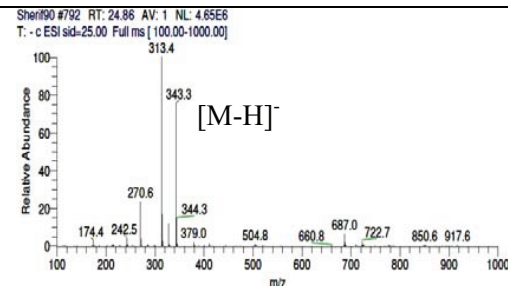
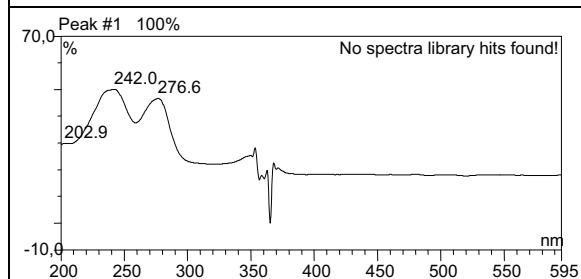
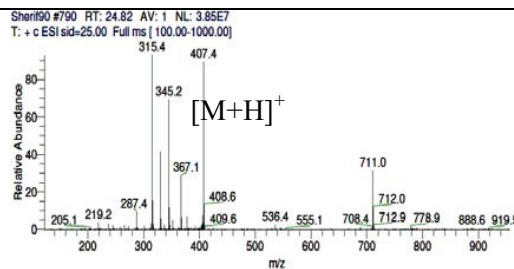
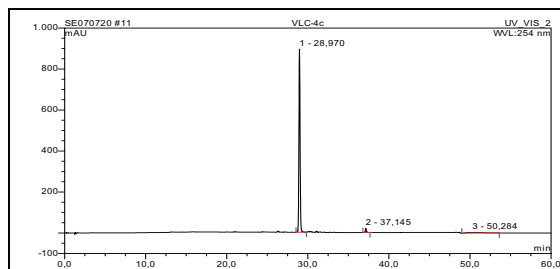
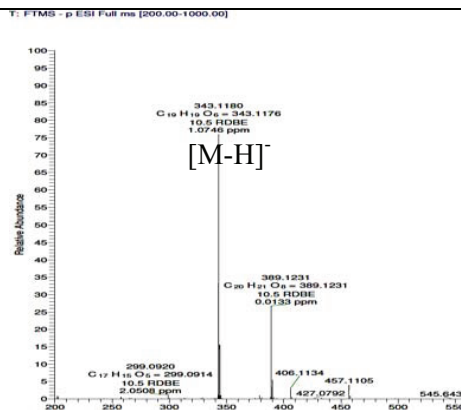
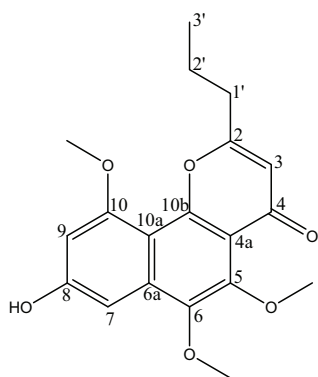


Fig. 3.28. ¹H-¹H COSY, HMBC, and ROESY spectra of **55**.

Results

3.5.8. 6-Methoxycomaparvin-5-methyl ether (55, known compound)

6-Methoxycomaparvin-5-methyl ether	
Synonym(s)	8-hydroxy-5,6,10-trimethoxy-2-propyl-benzo[<i>h</i>]chromen-4-one
Sample code	VLC-4,C
Biological source	<i>Comanthus</i> sp.
Sample amount	26.0 mg
Physical description	Pale yellow rods
Molecular formula	C ₁₉ H ₂₀ O ₆
Molecular weight	344 g/mol
Retention time (HPLC)	28.97 min (standard gradient)



Compound (**55**) was dereplicated and in LRESIMS, it displayed a molecular ion peak at m/z 343.2 [M-H]⁻, which has 14 amu more than 6-methoxycomaparvin (**54**). The molecular formula of was confirmed to be C₁₉H₂₀O₆ by HRESIMS (m/z 343.1180 [M-H]⁻, Δ +1.1 ppm) and **55** was deduced to be 6-methoxycomaparvin 5-methyl ether that was first isolated by Smith and Sutherland in 1971. The NMR spectral data of **55** (Table 3.30) were also similar to those of **54**. The main differences in the spectra of the two compounds were the presence of ¹H and ¹³C resonances in compound (**55**) at [δ_H 3.77 (3H, *s*)], and at δ_C 61.6 ppm, respectively, and the disappearance of proton resonance at [δ_H 13.06 (1H, *s*)] that was corresponding to -OH group at C-5 in 6-methoxycomaparvin (**54**). These differences were consistent with the presence of a methoxy group at C-5 in **55** instead of hydroxyl group in **54**, which explained the 14 amu difference between them. ¹H—¹H COSY spectrum (Fig. 3.28) revealed a correlation between two aromatic protons at [δ_H 6.63 (1H, *d*, 2.20 Hz)], and [δ_H 6.97 (1H, *d*, 2.20 Hz)] which were ascribed to be H-9, and H-7, respectively. In addition it has established the correlation between H-3 at [δ_H 6.14 (1H, *s*)] to C-1' methylene group at [δ_H 2.61 (2H, *t*, 7.25 Hz)] and continuing over the *n*-propyl side chain forming an extended spin system. Further confirmation for the chemical structure of **55** was provided by HMBC and ROESY spectra (Fig. 3.28).

According to these previous data and comparing to the corresponding literature (Smith and Sutherland, 1971; Sakurai *et al.*, 2002; Folmer *et al.*, 2008), the identity of compound (**55**) was deduced to be 8-hydroxy-5,6,10-trimethoxy-2-propylbenzo [*h*]chromen-4-one which was named as 6-methoxycomaparvin-5-methyl ether.

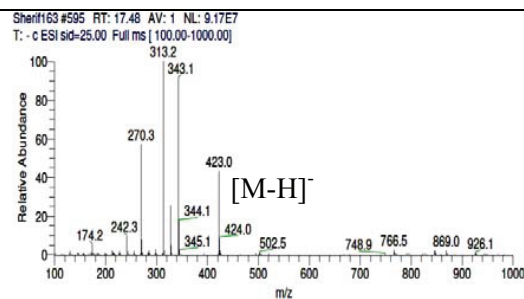
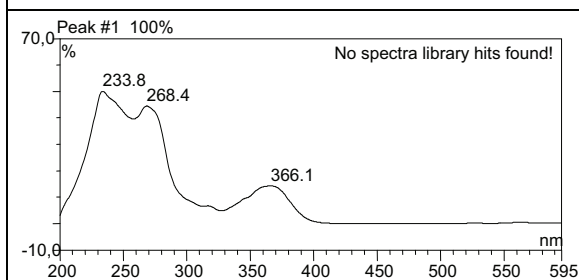
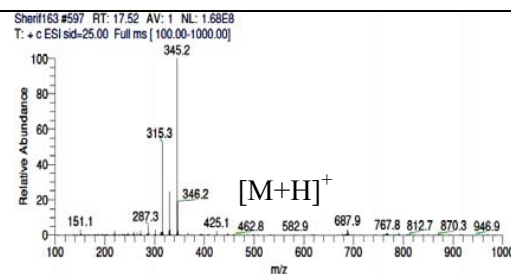
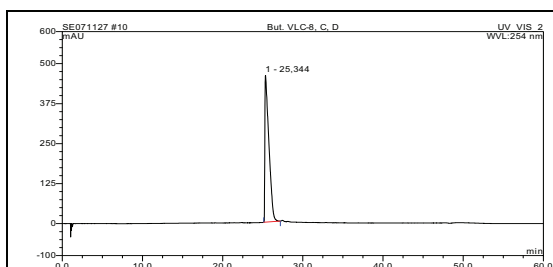
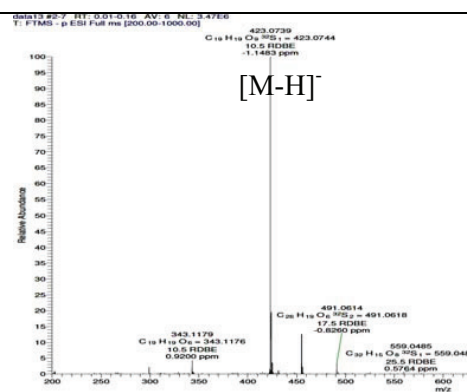
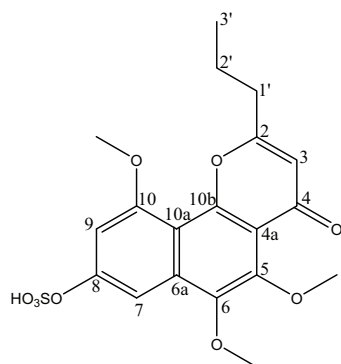
Results

Table 3.30. NMR data of compounds (53–55), measured in DMSO-*d*₆, 500 MHz.

#	53		54		55	
	δ_{H} mult. (J Hz)	δ_{C} mult.	δ_{H} mult. (J Hz)	δ_{C} mult.	δ_{H} mult. (J Hz)	δ_{C} mult.
2		170.1,C		170.1,C		165.9, C
3	6.41 (1H, <i>s</i>)	109.3,CH	6.40 (1H, <i>s</i>)	108.7,CH	6.14 (1H, <i>s</i>)	111.2,CH
4		182.4,C		182.1,C		175.7,C
4a		107.7,C		107.5,C		113.5,C
5		155.5,C		145.8,C		146.0,C
6	6.75 (1H, <i>s</i>)	97.5,CH		133.5,C		142.6,C
6a		140.7,C		135.4,C		134.2,C
7	6.59 (1H, <i>d</i> , 2.20 Hz)	101.1,CH	6.90 (1H, <i>d</i> , 2.20 Hz)	95.3,CH	6.97 (1H, <i>d</i> , 2.20 Hz)	96.3,CH
8		159.9,C		160.2,C		159.7,C
9	6.44 (1H, <i>d</i> , 2.20 Hz)	97.2,CH	6.50 (1H, <i>d</i> , 2.20 Hz)	97.5,CH	6.63 (1H, <i>d</i> , 2.20 Hz)	99.5,CH
10		159.0,C		159.4,C		159.2,C
10a		104.1,C		103.1,C		106.7,C
10b		151.5,C		151.5,C		152.8,C
1'	2.72 (2H, <i>t</i> , 7.25 Hz)	35.2,CH ₂	2.72 (2H, <i>t</i> , 7.25 Hz)	35.2,CH ₂	2.60 (2H, <i>t</i> , 7.25 Hz)	34.7,CH ₂
2'	1.79 (2H, <i>m</i>)	19.1,CH ₂	1.82 (2H, <i>m</i>)	19.1,CH ₂	1.77 (2H, <i>m</i>)	19.1,CH ₂
3'	0.95 (3H, <i>t</i> , 7.25 Hz)	13.3,CH ₃	0.97 (3H, <i>t</i> , 7.25 Hz)	13.3,CH ₃	0.94 (3H, <i>t</i> , 7.25 Hz)	13.3,CH ₃
5-OCH ₃					3.77 (3H, <i>s</i>)	61.4,CH ₃
6-OCH ₃			3.83 (1H, <i>s</i>)	59.4,CH ₃	3.85 (3H, <i>s</i>)	60.9,CH ₃
10-OCH ₃	3.90 (3H, <i>s</i>)	55.8,CH ₃	3.92 (3H, <i>s</i>)	55.9,CH ₃	3.92 (3H, <i>s</i>)	56.1,CH ₃
5-OH	12.84 (1H, <i>s</i>)		13.06 (1H, <i>s</i>)			
6-OH						
8-OH	10.26 (1H, <i>s</i>)		10.36 (1H, <i>s</i>)		10.38 (1H, <i>s</i>)	

3.5.9. 6-Methoxycomaparvin-5-methyl ether-8-O-sulfate (56, known compound)

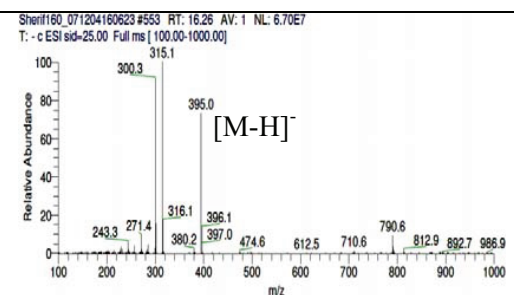
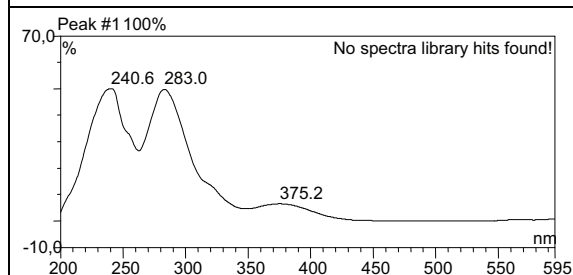
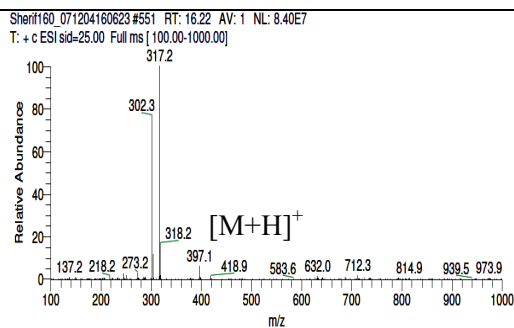
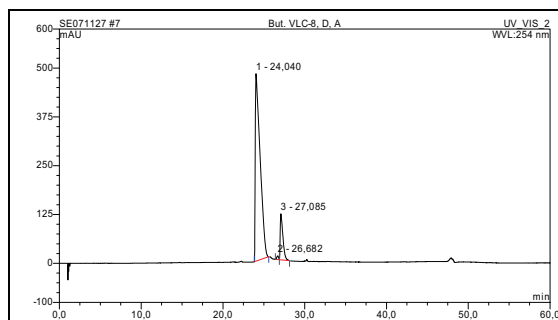
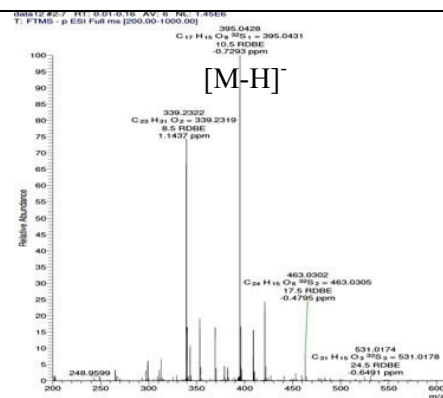
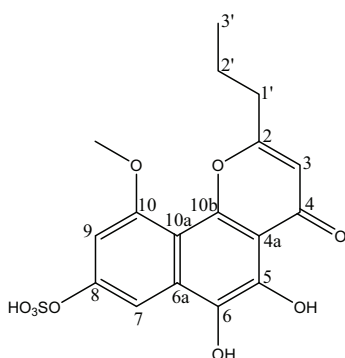
6-Methoxycomaparvin-5-methyl ether-8-O-sulfate	
Synonym(s)	5,6,10-trimethoxy-2-propyl-benzo[<i>h</i>]chromen-4-one-8-O-sulfate
Sample code	But. VLC-8,C,D
Biological source	<i>Comanthus</i> sp.
Sample amount	2.0 mg
Physical description	Greenish yellow powder
Molecular formula	C ₁₉ H ₂₀ O ₉ S
Molecular weight	424 g/mol
Retention time (HPLC)	25.34 min (standard gradient)



Results

3.5.10. 6-Hydroxycomaparvin-8-O-sulfate (57, known compound)

6-Hydroxycomaparvin-8-O-sulfate	
Synonym(s)	5,6-dihydroxy-10-methoxy-2-propyl-benzo[h]chromen-4-one-8-O-sulfate
Sample code	But. VLC-8,D,A
Biological source	<i>Comanthus</i> sp.
Sample amount	2.0 mg
Physical description	Pale yellow powder
Molecular formula	C ₁₇ H ₁₆ O ₉ S
Molecular weight	396 g/mol
Retention time (HPLC)	24.04 min (standard gradient)



The ESI mass spectrum of compound (**56**) showed a molecular ion peak at m/z 423.0 [M-H]⁻. Its molecular formula was deduced to be C₁₉H₂₀O₉³²S₁ by HRESIMS (m/z 423.0739 [M-H]⁻, Δ -1.1 ppm), which differs from **55** by more 80 amu. Based on the literature, compound (**56**) was identified to be 6-methoxycomaparvin 5-methyl ether-8-*O*-sulfate, which was first reported by Smith and Sutherland but without giving NMR spectral data. ¹H NMR spectral data of **56** and **55** were similar. The main difference between them was the absence of proton resonance at [δ_{H} 10.38 (1H, *s*)] corresponding to -OH group at C-8 in 6-methoxycomaparvin-5-methylether (**55**). Based on analysis of HRESIMS data of **56** and **55**, it was concluded that the former contained sulfate (-SO₃⁻) moiety at C-8 which is not present in **55** and compensated for the 80 amu difference between them. The downfield shift in ¹H NMR [δ_{H} , DMSO-*d*₆, **56**: C₇-H: 7.54 (*d*, 2.00 Hz), C₉-H: 6.96 (*d*, 2.00 Hz), *cf* **55**: C₇-H: 6.97 (*d*, 2.20 Hz), C₉-H: 6.63 (*d*, 2.20 Hz)] was consistent with the attachment of sulfate moiety at C-8 position. The elucidated structure of **56** was further supported by the results of 2D NMR spectra including ¹H—¹H COSY and ROESY spectra. From the previous data (Table 3.31) and by comparison with the related literature (Smith and Sutherland, 1971; Sakurai *et al.*, 2002), compound (**56**) was concluded to be 5,6,10-trimethoxy-2-propyl-benzo[*h*]chromen-4-one-8-sulfate which was named as 6-methoxycomaparvin-5-methylether-8-*O*-sulfate.

The molecular formula of compound (**57**) was confirmed to be C₁₇H₁₆O₉³²S₁ by HRESIMS (m/z 395.0428 [M-H]⁻, Δ -0.7 ppm), which differs from 6-methoxycomaparvin (**54**) by 66 amu. The NMR spectral data of **57** (Table 3.31) were comparable to those of **54**. The major differences between them were that compound (**57**) showed only two methyl resonances in ¹H NMR, of which one was an oxygen-substituted singlet at δ_{H} 3.94 and the other was the terminal methyl group of *n*-propyl side chain at [δ_{H} 0.98 (3H, *t*, 7.85 Hz)], and devoided of the resonance for the second methoxy group at C-6 in 6-methoxycomaparvin (**54**). Also, ¹H NMR spectrum of **57** showed only two proton resonances at [δ_{H} 13.01 (1H, *s*)], and at [δ_{H} 10.31 (1H, *s*)] which were assigned to be belonging to -OH groups at C-5 and C-6, respectively. Judging from the data of HRESIMS of **57** and **54**, it was deduced that the former contained a sulfate (-SO₃⁻) moiety as substituent instead of methyl group in **54**, which explained the 66 amu difference between them. Similar to **56**, the attachment of sulfate moiety at C-8 was evidenced by the downfield shift in ¹H NMR [δ_{H} , DMSO-*d*₆, **57**: C₇-H: 7.23 (*d*, 2.20 Hz), C₉-H: 7.21 (*d*, 2.20 Hz), *cf* **54**: C₇-H: 6.89 (*d*, 2.20 Hz), C₉-H: 6.50 (*d*, 2.20 Hz)]. ROESY spectrum and comparison with the respective literature (Smith and Sutherland, 1971; Sakurai *et al.*,

Results

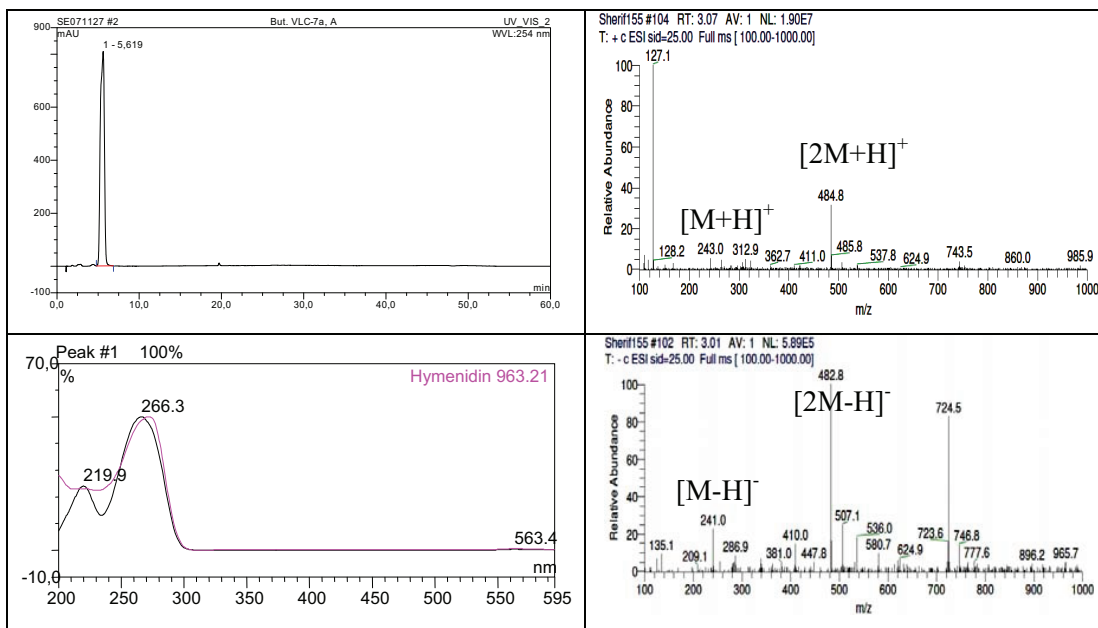
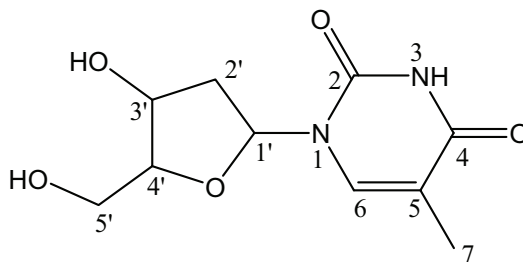
2002) provided further evidences supporting that the elucidated structure for compound (57) to be 5,6-dihydroxy-10-methoxy-2-propyl-benzo[*h*]chromen-4-one-8-*O*-sulfate that was given the trivial name 6-hydroxycomaparvin-8-*O*-sulfate.

Table 3.31. ¹H NMR data of compounds (56 and 57), measured in DMSO-*d*₆, 500 MHz.

proton	56	57
	δ_{H} mult. (JHz)	δ_{H} mult. (JHz)
3-H	6.19 (1H, <i>s</i>)	6.40 (1H, <i>s</i>)
6-H		
7-H	7.54 (1H, <i>d</i> , 2.00 Hz)	7.15 (1H, <i>d</i> , 2.00 Hz)
9-H	6.96 (1H, <i>d</i> , 2.00 Hz)	7.02 (1H, <i>d</i> , 2.00 Hz)
1'	2.66 (2H, <i>t</i> , 7.25 Hz)	2.74 (2H, <i>t</i> , 7.25 Hz)
2'	1.80 (2H, <i>m</i>)	1.83 (2H, <i>m</i>)
3'	0.97 (3H, <i>t</i> , 7.25 Hz)	0.92 (3H, <i>t</i> , 7.25 Hz)
5-OCH ₃	3.79 (3H, <i>s</i>)	3.79 (3H, <i>s</i>)
6-OCH ₃	3.86 (3H, <i>s</i>)	3.86 (3H, <i>s</i>)
10-OCH ₃	3.94 (3H, <i>s</i>)	3.94 (3H, <i>s</i>)
5-OH		13.00 (1H, <i>s</i>)
6-OH		10.30 (1H, <i>s</i>)
8-OH		

3.5.11. 2'-Deoxythymidine (58, known compound)

2'-Deoxythymidine	
Synonym(s)	Thymine 2-deoxyriboside
Sample code	But. VLC-7a,A
Biological source	<i>Comanthus</i> sp.
Sample amount	3.0 mg
Physical description	White amorphous solid
Molecular formula	C ₁₀ H ₁₄ N ₂ O ₅
Molecular weight	242 g/mol
Retention time (HPLC)	5.62 min (standard gradient)



Results

Compound (**58**) was obtained as a white amorphous solid from BuOH soluble fraction. In its ESIMS, it showed a pseudomolecular ion peak at m/z 243 $[M+H]^+$, and at m/z 484.8 $[2M+H]^+$. The NMR spectral data of **58** (Table 3.32) together with the molecular weight suggested a nucleosidic nature. The structure was unambiguously elucidated and confirmed based on 1D and 2D NMR spectra including, ^1H NMR, ^{13}C NMR, ^1H - ^1H COSY and HMBC (Fig. 3.29). Based on this finding together with comparison of reported literature (Allore *et al.*, 1983; Lidgern *et al.*, 1988), **58** was found to be 2'-deoxythymidine nucleoside.

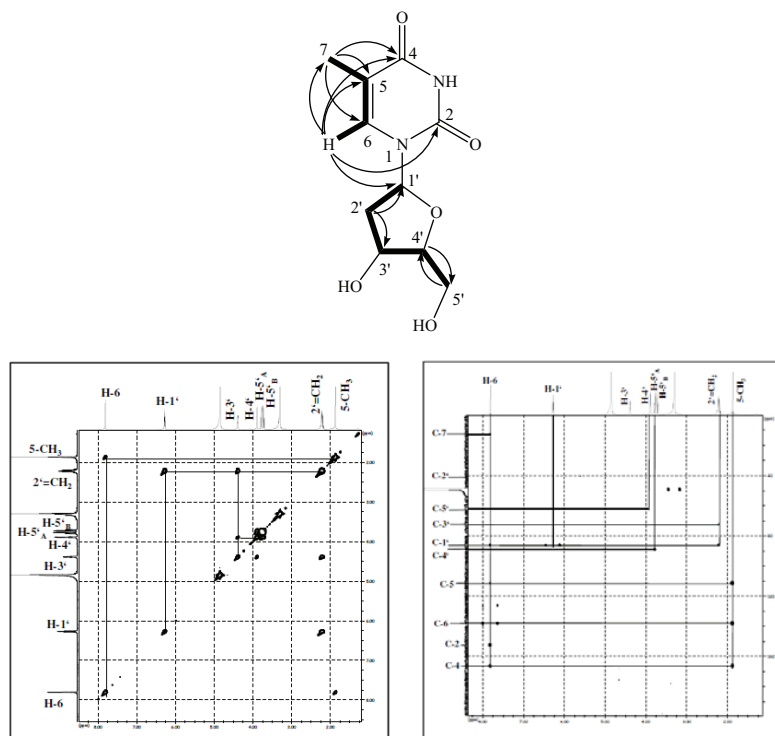


Fig. 3.29. ^1H - ^1H COSY and HMBC spectra of 2'-deoxythymidine (**58**).

Table 3.32. NMR data of 2'-deoxythymidine (**58**), measured in MeOD- d_4 , 500 MHz.

58					
#	δ_{H} mult. (JHz)	δ_{C} mult.	#	δ_{H} mult. (JHz)	δ_{C} mult.
2		152.4, C	1'	6.27 (1H, <i>t</i> , $J= 6.90$ Hz)	86.2, CH
3*	11.26 (1H, br <i>s</i>)		2'	2.24 (2H, <i>m</i>)	41.2, CH ₂
4		166.4, C	3'	4.38 (1H, <i>m</i> , $J= 3.50$ Hz)	72.2, CH
5		111.5, C	4'	3.90 (1H, <i>q</i> , $J= 3.50$ Hz)	88.8, CH
6	7.80 (1H, <i>d</i> , $J= 1.10$ Hz)	138.2, CH	5'	3.78 (1H, <i>dd</i> , $J= 11.95, 3.15$ Hz)	62.8, CH ₂
				3.71 (1H, <i>dd</i> , $J= 11.95, 3.75$ Hz)	
7	1.87 (3H, <i>d</i> , $J= 1.10$ Hz)	12.4, CH ₃	3'-OH*	5.21 (1H, br <i>d</i> , $J= 3.80$ Hz)	
			5'-OH*	5.00 (1H, br <i>s</i>)	

3.5.12. Biological activity of anthraquinones and naphthopyrones isolated from the marine Echinoderm *Comanthus* sp.

All the isolated anthraquinones, naphthopyrones, and emodin as well were subjected to preliminary cytotoxicity (MTT) assay against L5178Y mouse lymphoma cells at a dose of 10 $\mu\text{g/mL}$. IC_{50} values were determined quantitatively for the potentially active candidates (Table 3.33), using kahalalide F as positive control. Regarding anthraquinones, the results indicated that *n*-propyl side chain as in 1'-deoxyrhodoptilometrin (**49**) instead of methyl group in Emodin has escalated the cytotoxic activity of the former. This revealed its importance which could be more evidenced by the abundant declined activity in case of **48** and **50** that had 1'-propenyl and 1'-hydroxypropyl side chains, respectively. In case of naphthopyrones, it was concluded that 6-methoxycomaparvin-5-methylether (**55**) together with the mixture of comaparvin (**53**) and 6-methoxycomaparvin (**54**) exhibited significant cytotoxicity with IC_{50} of 4.6 and 5.2 $\mu\text{g/mL}$, respectively. Furthermore, the sulfate derivatives had reduced activity compared to their corresponding unsulfated derivatives, probably caused by the increased polarity of these compounds which will affect the cellular uptake.

Table 3.33. Cytotoxicity (MTT) assay of extract, fractions, and isolated compounds from the Echinoderm *Comanthus* sp.

Sample tested	L5178Y growth in % (@ 10 $\mu\text{g/mL}$)	IC_{50}	
		($\mu\text{g/mL}$)	(μM)
<i>Comanthus</i> methanolic extract	99.8		
<i>n</i> -Hexane Soluble Fraction	86.5		
Ethyl Acetate Soluble Fraction	0.1		
<i>n</i> -Butanol soluble Fraction	97.3		
1'-Deoxyrhodoptilometrene (48)	89.7	>10	
1'-Deoxyrhodoptilometrin (49)	0.2	2.3	7.7
(<i>S</i>)-(-)-Rhodoptilometrin (50)	64.1	>10	
1'-Deoxyrhodoptilometrin-6- <i>O</i> -sulfate (51)	75.5	>10	
(<i>S</i>)-(-)-Rhodoptilometrin-6- <i>O</i> -sulfate (52)	59.6	>10	
Comaparvin (53) and 6-Methoxycomaparvin (54), (3:2)	4.3	5.2	
6-Methoxycomaparvin-5-methyl ether (55)	6.1	4.6	13.4
6-Methoxycomaparvin-5-methyl ether-8- <i>O</i> -sulfate (56)	57.2	>10	
6-Hydroxycomaparvin-8- <i>O</i> -sulfate (57)	24.4	7.5	18.9
2'-Deoxythymidine (58)	71.3	> 10	
Emodin	77.0	> 10	
Kahalalide F (positive control)		6.3	4.3

Results

Interestingly, testing all compounds at a dose of 1 $\mu\text{g}/\text{mL}$ in biochemical protein kinase activity assays revealed a similar pattern of activity to that found in the MTT assay for L5178Y cells (Table 3.34) (Fig. 3.30). Six of the tested compounds inhibited the activity of at least one of the 24 kinases that were investigated by at least 40%. For each of these compounds IC_{50} values against all 24 protein kinases were determined. Compounds inhibited cellular growth in the MTT assay proved to be active as kinase inhibitors.

Table 3.34. IC_{50} values of Selected Compounds against 24 Different Protein Kinases^a

Cpd	AKT1	ARK5	Aurora-A	Aurora-B	AXL	B-RAF-VE	CDK2/CycA	CDK4/CycD1	CK2-alpha1	COT	EGF-R	EPHB4
49	9.8	n.a.	0.90	0.54	4.2	2.9	8.0	5.2	n.a.	6.2	1.2	2.8
51	n.a.	n.a.	3.9	2.8	9.9	n.a.	n.a.	n.a.	n.a.	n.a.	3.4	8.6
50	n.a.	n.a.	1.3	1.3	n.a.	n.a.	9.5	n.a.	8.2	n.a.	3.9	n.a.
52	n.a.	n.a.	4.0	1.6	n.a.	n.a.	n.a.	n.a.	n.a.	n.a.	n.a.	n.a.
53/54, (3:2)	n.a.	n.a.	2.2	3.7	3.5	1.1	n.a.	1.2	3.3	8.0	2.1	4.1
Cpd	ERBB2	FAK	IGF1-R	INS-R	MET	PDGFR-beta	PLK1	PRK1	SAK	SRC	VEGF-R2	COT
49	2.0	5.5	1.5	5.5	n.a.	2.8	n.a.	8.1	1.7	1.1	0.56	n.a.
51	8.5	n.a.	3.7	n.a.	n.a.	4.0	n.a.	n.a.	n.a.	2.1	1.0	n.a.
50	3.8	7.0	9.8	n.a.	n.a.	n.a.	n.a.	n.a.	3.2	n.a.	5.9	n.a.
52	n.a.	n.a.	n.a.	n.a.	8.3	n.a.	n.a.	n.a.	n.a.	n.a.	n.a.	n.a.
53/54, (3:2)	5.7	2.1	3.5	5.5	7.3	2.3	n.a.	6.7	2.6	2.2	1.9	n.a.

^aInhibitory potentials of compounds at various concentrations were determined in biochemical protein kinase activity assays. Listed are IC_{50} values in $\mu\text{g}/\text{mL}$. n.a.: not active, i.e., $\text{IC}_{50} > 10 \mu\text{g}/\text{mL}$.

Among the tested compounds, both **49** and the mixture of **53** and **54** inhibited a broad panel of kinases with IC_{50} values ranging from 0.54 to 9.8 $\mu\text{g}/\text{mL}$. The parallel pattern of activity in the cellular assay and in the biochemical protein kinase assays observed for compounds (**49**), (**50**), and their respective 6-*O*-sulfate derivatives (**51**) and (**52**) suggests that the inhibition of protein kinases may be one of the major mechanisms contributing to the cytotoxic activity of these compounds. On the contrary, 6-methoxycomparvin-5-methyl ether (**55**) lacked such pattern in both assays. Although, it showed a potent cytotoxic activity in the MTT assay with IC_{50} value of 4.6 $\mu\text{g}/\text{mL}$ (13.4 μM). It didn't

inhibit any of the 24 protein kinases by $\geq 40\%$. This discrepancy may perhaps be either because of the poor solubility of **55** in water, incorporated in protein kinase assays, leading to its precipitation or the cytotoxic activity of **55** proceeds through different pathways other than inhibition of the tested protein kinases.

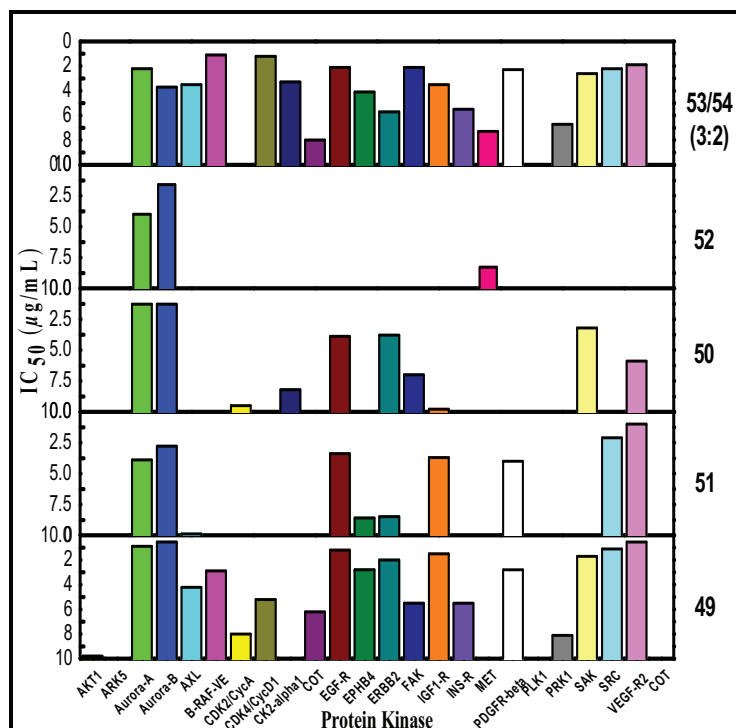


Fig. 3.30. *In vitro* protein kinase inhibitory activity assay against 24 different enzymes.

In the radical scavenging (DPPH) assay on TLC, active compounds appear as yellow spots against a purple background. Then, for active ones, a spectrophotometric assay was carried out as described in 2007 by Tsevegsuren *et al.* in order to evaluate the radical scavenging activity by measuring the percentage of reduction of a 100 μM DPPH solution. Only naphthopyrone derivatives displayed radical scavenging activity, and their results revealed that the mixture of comaparvin (**53**) and 6-methoxycomaparvin (**54**) together with 6-hydroxycomaparvin-8-*O*-sulfate (**57**), and 6-methoxycomaparvin-5-methylether (**55**) exhibited moderate to low antioxidant activities with IC_{50} values of 83.4, 124.6, and 130.7 μM , respectively compared to quercetin ($\text{IC}_{50} = 6.1 \mu\text{M}$).

In addition (*S*)-(-)-rhodoptilometrin (**50**) proved to be active against Gram positive bacteria with MIC values of 7.81 $\mu\text{g/mL}$ (24.9 μM) against multiresistant *Staphylococcus aureus* (MRSA). Whereas, 1'-deoxyrhodoptilometrene (**48**) and 1'-deoxyrhodoptilometrin (**49**) showed antiviral activity against human rhinoviruses (HRV2), (HRV8), and (HRV39); and respiratory syncytial virus A (RSVA) with MIC values of 5.3, 10.6, 10.6, and 10.6 μM for **48**, respectively; and 5.2, 5.2, 5.2, and 1.3 μM for **49**, respectively.

Discussion

4. Discussion

4.1. Methods for natural products tracing

Natural products research needs to be continuously improved with regards to the efficiency of the selection, screening, dereplication, isolation and structure elucidation processes so as to keep being competitive with purely synthetic based discovery methods (Butler, 2004). The marine ecosystems proved appealing for the scientific interests from chemists and biologists because of the immeasurable diversity in chemical and biological aspects. Hence, the extracts were selected based on the chemical profiling and applying a bioactivity-guided strategy.

Due to their chemically diverse structures, natural products profiling retained being a challenging task and therefore a single analytical method does not exist (Wolfender *et al.*, 2005). However, advanced analytical and hyphenated spectroscopic techniques coupled to HPLC offered an intelligent means to provide a useful idea about the natural products in fields of chemical structures and/or substituent moieties as well.

Of these advanced techniques, HPLC/UV-photodiode array detection (LC/UV-DAD) which allowed an online record of the UV spectra of the compounds together with a library of UV spectra in a rather straightforward manner which in turn is extremely valuable for dereplication of compounds previously isolated. In addition some related secondary metabolites shared the basic chemical chromophore and hence the same UV absorption maxima, they were not the same in fact. These differences were noticeable through different retention times attributing the existence of a non-chromophoric moiety(ies). This was further confirmed by a difference in their molecular weights that were determined by HPLC/ESI-MS, another technique coupling LC to a mass spectrometric unit using electron spray ionization (ESI) mode.

Many examples in the present study elicited the applicability of these hyphenated techniques such as related bromopyrrole alkaloids which revealed differences in the bromination pattern or the side chain substituent. Another example, the sulfated derivatives that proved a different retention times from their respective non-sulfated ones that were explained by a more 80 amu (i.e. SO_3^- moiety) in the molecular weights of the sulfated derivatives as represented by the sulfated anthraquinones and naphthopyrones isolated from the echinoderm *Comanthus* sp. in this study.

4.2. Bromopyrroles: a typical class of marine alkaloids

Bromopyrrole alkaloids constitute a family of exclusively marine alkaloids and represent a fascinating example of the large variety of secondary metabolites elaborated by marine sponges. The first member of this group to be isolated was oroidin (Fig. 4.1), initially from the sponge *Agelas oroides* in 1971 (Forenza *et al.*, 1971). Oroidin is considered as the key metabolite of this family of alkaloids, since many of them possessing a pyrrole-imidazole structure can be conceived as derivatives of the C₁₁N₅ skeleton of oroidin. These can vary with regard to (a) oxidation, reduction, or hydration of the 2-amino-4(5)-vinylimidazole unit, (b) dimerization, and (c) cyclization. The pyrrole-2-carboxamide moiety can be non-, mono-, or dibrominated in 2-, 3-, and/or 4-position.

Since the mid-1970s, more than 150 derivatives, with a vast array of structures and interesting biological activities, have been isolated from more than 20 different sponges of various genera, essentially belonging to the Agelasidae, Axinellidae, and Halichondridae families. It is currently believed that these alkaloids are taxon-specific of at least the Agelasida order and can be used as chemical markers of these phylogenetically related sponges (Braeckman *et al.*, 1992).

The antipredatory role of these alkaloids can be ecologically considered as the most important biological function as noticed by the Caribbean reef sponge of the genus *Agelas* (Wilson *et al.*, 1999). Bromopyrrole alkaloids are important not only for their ecological role and for chemotaxonomic considerations, but also for the number of interesting pharmacological activities they have been shown to possess. Among them, the cytotoxicity of agelastatin and the immunosuppressive activity of palau'amine are remarkable. This is probably why they proved appealing to the organic chemists for total syntheses of bromopyrrole alkaloids since 2000 for the purpose of further biological evaluation. However, current interest in this group of marine natural products has been concerned not only with preparative synthesis and biological activity but also with their biogenetic chemical reactions.

In the group of bromopyrrole alkaloids, all compounds can be considered closely related; they seem to share a common biogenetic pathway even if a plausible biosynthetic mechanism leading to these marine alkaloids is still unproven. The first, and maybe the only to the best of our knowledge, biosynthetic study performed in cell cultures of the sponge *Teichaxinella morchella* using [¹⁴C]-labeled amino acids (Fig. 4.1) revealed that histidine and proline / ornithine are precursors of stevensine (Andrade *et al.*, 1999).

In the light of these studies, it has been proposed that both proline and ornithine can be converted to pyrrole-2-carboxylic acid prior to halogenations; subsequently amide

Discussion

formation by reaction with 3-amino-1-(2-aminoimidazolyl)-prop-1-ene, derived from histidine, generates oroidin, followed by cyclization to stevensine (Fig. 4.1).

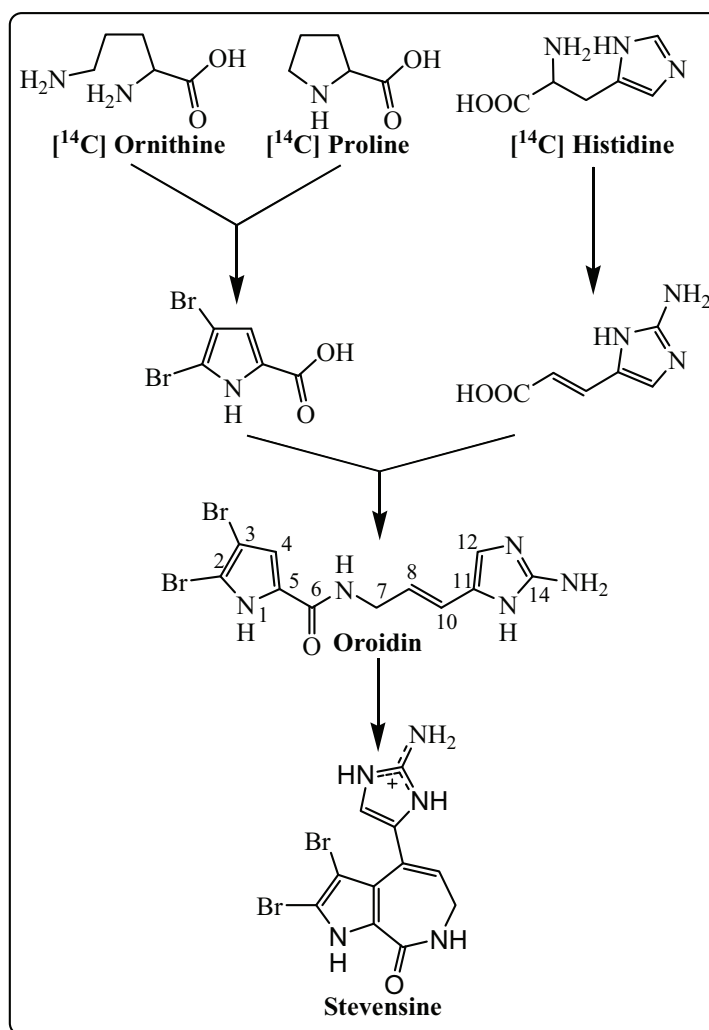


Fig. 4.1. The biogenetic origin of stevensine from the sponge *Teichaxinella morchella*.

Recently, a new biomimetic spontaneous conversion of proline to 2-aminoimidazolone derivatives using a self-catalyzed intramolecular transamination reaction together with peroxide dismutation as key steps pointing to dispacamide A (Fig. 4.2) as the forerunner of oroidin. Additionally 2,3-dibromo-1*H*-pyrrole-2-carboxylic acid and (*Z*)-3-(2-amino-1*H*-imidazol-5-yl)acrylic acid (Fig. 4.1) were considered as probable hydrolysis products of oroidin (Travert and Al-Mourabit, 2004).

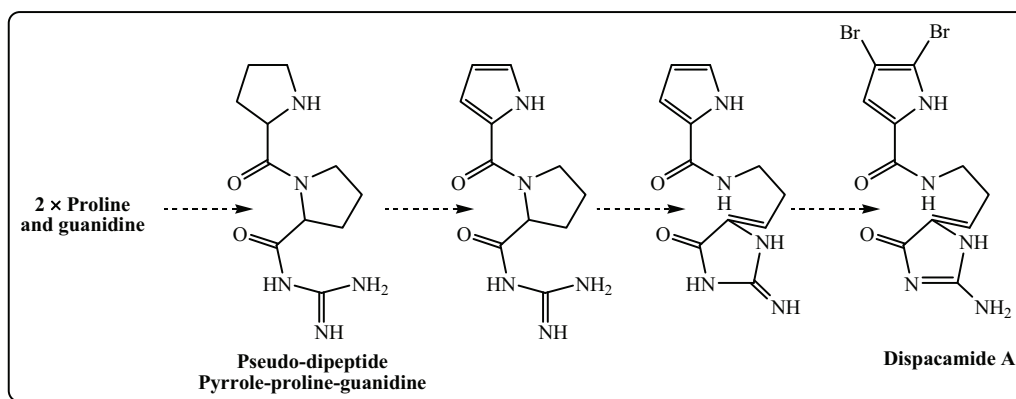


Fig. 4.2. Postulated formation of pyrrole and 2-aminoimidazolinone moieties.

According to their chemical architecture, bromopyrrole alkaloids divided into:

- Oroidin-like linear monomer**, whose structures contain the skeleton of oroidin without any further C–C or C–N bond formation. This group was represented by mukanadin D (**9**) and displacamide E (**30**) isolated from the Indonesian marine sponges *Acanthostylotella* sp. and *Stylissa massa* in this study, respectively.
- Polycyclic oroidin-derivatives**, whose structures can be rationalized by one the many intramolecular cyclizations of oroidin or oroidin-like linear monomers (Fig. 4.3).

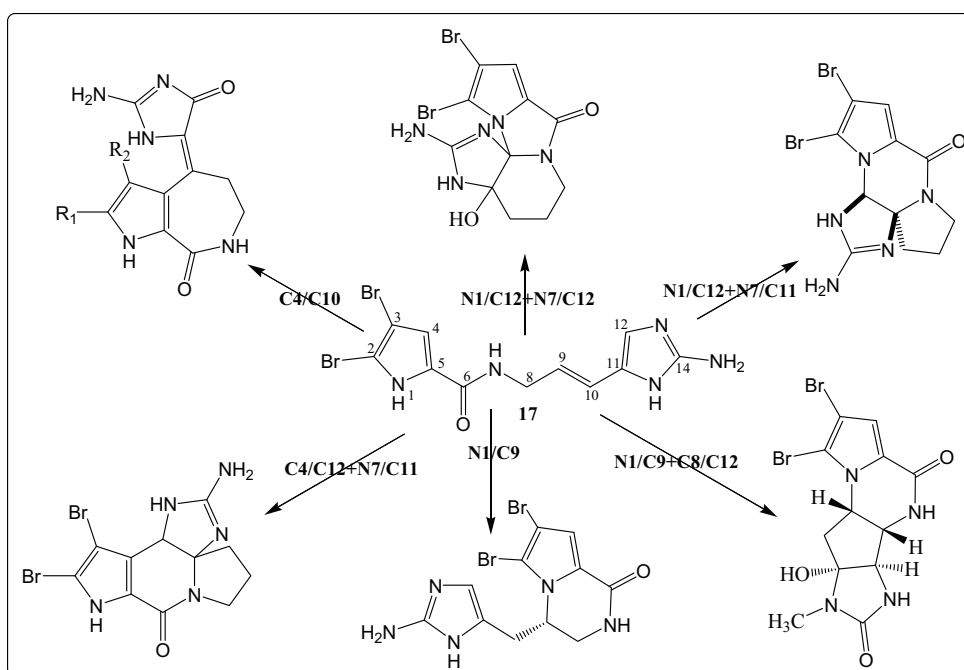


Fig. 4.3. An overview of the five cyclization modes of polycyclic oroidin-derivatives.

Discussion

The cyclization modes can be hence divided into:

- i) **C4/C10 derivatives:** represented by (-)-hymenine (**29**), (10*Z*)-hymenialdisine analogues (**33–36**) in addition to other related derivatives latonduine A (**26**) and aldisines (**20–23**) which were all isolated from the methanolic extract of *Stylissa massa* in this study.
- ii) **N1/C12+N7/C11 derivatives:** represented by (-)-dibromophakellin H⁺Cl⁻ (**27**) that was obtained from the marine sponge *S. massa* as well.
- iii) **C4/C12+N7/C11 derivatives:** represented by monobrominated (**28**) and dibrominated (**32**) isophakellins which were both reported from *Stylissa massa* in this study.
- iv) **N1/C12+N7/C12 derivatives:** represented by a single member, dibromoagelaspongine (Fig. 4.3), isolated from an *Agelas* sp. collected along Tanzanian coasts (Fedoreyev *et al.*, 1989). This molecule is closely related to dibromophakellin (**27**), but in this case the nitrogen atoms N1 and N7 line the same carbon of the imidazole ring, namely C12, and consequently the pyrrole condensed ring is five-membered and not six-membered.
- v) **N1/C9 derivatives:** cyclooroidin (Fig. 4.3) was isolated from the Mediterranean sponge *Agelas oroides* (Fattorusso and Tagliatalata-Scafati, 2000) as a prototype of this class. Cyclooroidin could be envisaged as the precursor of the non-imidazole bromopyrrole alkaloids such as longamide (**12** and **25**), its debromo derivative mukanadin C (**24**), longamide B (**11** and **31**), longamide B methyl ester (**10** and **18**) and longamide B ethyl ester known as hanishin (**19**) which have been obtained in this study from both Indonesian marine sponges *Acanthostylotella* sp. and *Stylissa massa*.
- vi) **N1/C9+C8/C12 derivatives:** only agelastatins A–D represent this class of bromopyrrole alkaloids which have been isolated from *Agelas dendromorpha* (D'Ambrosio *et al.*, 1993) and *Cymbastela* sp. (Hong *et al.*, 1998). Agelastatins are potent nanomolar antiproliferative agents against several cancer cell lines (D'Ambrosio *et al.*, 1996). Moreover, agelastatin A inhibited glycogen synthase kinase-3β (GSK-3β), an activity that could be useful for the treatment of serious diseases including Alzheimer's disease, cancer, and type 2 diabetes (Meijer *et al.*, 2000). Therefore, it proved appealing for the intensive synthetic efforts.

- (c) **Simple or cyclized oroidin-like dimers:** such as sceptrin which was first reported from the Caribbean marine sponge *Agelas sceptrum* in 1981 and after which it was trivially named (Walker and Faulkner, 1981). Sceptrin was considered as the parent of this group and structurally it was found to be a symmetrical dimer of 2-debromooroidin. Sceptrin displayed a broad spectrum of bioactivities such as antimicrobial against a vast array of bacterial and fungal microorganisms and as antiviral as well (Walker and Faulkner, 1981; Keifer *et al.*, 1991).
- (d) **Other bromopyrrole alkaloids:** which could not be classified under the previous groups, basically because they lack the pyrrole-imidazole moieties. This class represents either plausible precursors or hydrolysis products of the bromopyrrole alkaloids and in this study it was represented by many examples including acanthamides A–D (1–4) and compounds (5–7, 13 and 14) which were all isolated from *Acanthostylotella* sp. in addition to compounds (15–17) that were obtained from the marine sponge *Stylissa massa*.

4.3. Biological activity of bromopyrrole alkaloids

Bromopyrrole alkaloids represent a group of secondary metabolites belonging particularly to marine organisms mainly sponges. In addition to their important role as chemical defense against predators or deterrents, they have exhibited an immense diversity of biological activities such as cytotoxicity, antimicrobial against a broad spectrum of microorganisms and viruses as well and as protein kinase inhibitors which are the nowadays targets for treatment of a vast array of ailments including cancer, type 2 diabetes, malaria and neurodegenerative disorders such as Alzheimer's disease.

In this study, more than 30 bromopyrrole alkaloids have been isolated from two Indonesian marine sponges *Acanthostylotella* sp. and *Stylissa massa*. As reported above, they were distributed over different classes based on the chemical structures and hence the biogenetic cyclization. They were all tested for their antiproliferative activity against mouse lymphoma (L5178Y) cells using cytotoxicity (MTT) assay, antibacterial, antifungal, antiviral and protein kinase inhibitory activity.

Of those isolated from *Acanthostylotella* sp., only mukanadin D (9) showed moderate activity with an IC_{50} of 21.67 $\mu\text{mol/L}$. While in the *in vitro* antimicrobial and antiviral activity assays, methyl 3,4-dibromo-1*H*-pyrrole-2-carboxylate (5) revealed antibacterial activity with MIC values of 62.5 $\mu\text{g/mL}$ against both multi-resistant *Staphylococcus aureus* (MRSA), and *Enterococcus faecalis*. In addition it showed antifungal activity with

Discussion

MIC values of 62.5, and 125 $\mu\text{g/mL}$ against *Aspergillus faecalis*, and *Aspergillus fumigatus*, respectively. Whereas with the same MIC value of 62.5 $\mu\text{g/mL}$, ethyl 3,4-dibromo-1*H*-pyrrole-2-carboxylate (**15**), obtained from *Stylissa massa*, showed antifungal activity against *Aspergillus faecalis* and *A. fumigatus*. Moreover, 4-bromo-1*H*-pyrrole-3-carboxamide (**16**) and aldisine (**20**) exhibited antiviral activity against human rhino viruses (HRV2, HRV8, and HRV39) and respiratory syncytial virus A (RSVA) with IC_{50} values of 6.25, 0.78, 0.78, 0.78 $\mu\text{g/mL}$, respectively for **16** and 3.13, 1.56, 1.56, 0.78 $\mu\text{g/mL}$, respectively for **20**.

On the other hand, in cytotoxicity (MTT) assay of the bromopyrrole alkaloids isolated from *Stylissa massa*, some of them interestingly proved potent cytotoxicity with (IC_{50} = 6.33–28.28 μM) compared to kahalalide F as standard (IC_{50} = 4.30 μM). Those active candidates were (-)-longamide B ethyl ester, hanishin (**19**), latonduine A (**26**), (-)-dibromophakellin H^+Cl^- (**27**) and hymenialdisine analogues (**33–36**).

Interestingly, the results of protein kinase inhibitory activity assay (Table 3.19) revealed a correspondence with the respective cytotoxicity (MTT) assay results (Table 3.18). For example, compounds (**33–36**), that showed IC_{50} values between 1.50 and 4.0 $\mu\text{g/mL}$ in the MTT assay, proved significant inhibitory activity against tested protein kinases with IC_{50} values in the nanogram range ($<0.1 \mu\text{g/mL}$). This conclusively suggested that protein kinase inhibition might be a plausible mechanism through which these compounds exerted their antiproliferative activity. Although, (-)-hymenine (**29**), (-)-dibromocantharelline (= dibromoisophakellin) (**32**) and (-)-mukanadin C (**24**) proved to be potential inhibitors against the tested protein kinases (IC_{50} = 0.092–0.55 $\mu\text{g/mL}$), none of them revealed a respective cytotoxicity in the MTT assay. This may be attributed to their selective activity against other cell lines and/or being active in other discipline of bioactivity other than antiproliferative activity. Additionally, 3-bromoaldisine (**23**) proved the best activity profile compared to other aldisines (**20–22**), however they all shared a sort of selective inhibitory activities against CLK-1 and CK-1 protein kinases with IC_{50} values between 0.3 and 4.2 $\mu\text{g/mL}$ (Table 3.19) which seemed to be corresponded to the presence and the position of bromine substituent.

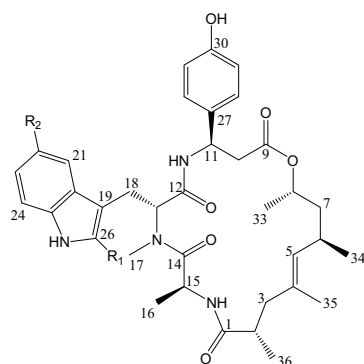
4.4. Jaspamides: a unique group of cyclodepsipeptides

Sponges of the genus *Jaspis* (Jaspidae) have been a rich source of biologically active, structurally novel natural products. After the discovery of the cyclodepsipeptide jaspamide (jasplakinolide, **37**) in the sponge *Jaspis* cf. *johnstoni* in 1986 by each of Ireland and Crews, which is known for its pronounced biological activities including antifungal (Scott *et al.*, 1988), anthelmintic, insecticidal (Zabriskie *et al.*, 1986; Crews *et al.*, 1986) and cytotoxic activity (Inman and Crews, 1989), sponges of the genus *Jaspis* have received considerable attention, and since then the chemistry of *Jaspis* sponges has been the subject of more than 90 publications. A wide variety of constituents has been isolated from this genus including several jaspamide derivatives from *Jaspis splendens* (Zampella *et al.*, 1999; Gala *et al.*, 2007; 2008; 2009), isomalabaricane triterpenes from *Jaspis stellifera* (Ravi *et al.*, 1981; Tsuda *et al.*, 1991; Kobayashi *et al.*, 1996), cytotoxic macrolides from the Okinawan sponge *Jaspis* sp. (Kobayashi *et al.*, 1993), bengazoles (Rodriguez *et al.*, 1993; Searle *et al.*, 1996) that stand out as unique bis-oxazoles containing a carbohydrate-like polyol side chain, antiparasitic, antimicrobial, and cytotoxic amino acid derivatives known as bengamides (D'Auria *et al.*, 1997, Groweiss *et al.*, 1999, Thale *et al.*, 2001), cytotoxic bromotyrosine derivatives (Park *et al.*, 2003, Shinde *et al.*, 2008), and a series of dihydroxystyrene sulphate derivatives (Ohta *et al.*, 1994; Tsukamoto *et al.*, 1994; Chang *et al.*, 2008).

During the course of this study and as a part of our ongoing research on bioactive natural products from marine sponges, we investigated a specimen of *Jaspis splendens* collected at Kalimantan (Indonesia) whose crude methanolic extract completely inhibited the cellular growth of mouse lymphoma (L5178Y) cells in the *in vitro* cytotoxicity (MTT) assay. Bioactivity-guided isolation scheme of the total methanolic extract was applied and it yielded eight compounds including three ketosteroids, 6 β -hydroxy-24-methylcholesta-4,22-dien-3-one (**40**), 6 β -hydroxy-24-methylcholesta-4-en-3-one (**41**), 6 β -hydroxy-24-ethylcholesta-4-en-3-one (**42**), a diketopiperazine derivative maculosin-1 (*cyclo*-L-Pro-L-Tyr) (**43**), a nucleoside derivative sangivamycin (**44**), two new jaspamides Q (**38**) and R (**39**), were isolated together with the parent compound jaspamide (**37**).

All the isolated compound were reported from the marine sponge of the genus *Jaspis* except **43** and **44** that were both firstly purified as secondary metabolites from *Jaspis digonoxea* and *J. Johnstoni*, respectively but later, they were obtained from microorganisms associated with the sponge. Hence, they were proven to be in fact microbial secondary metabolites, produced by symbiont microorganisms associated with the marine sponge of the genus *Jaspis* (Jayatilake *et al.*, 1996; Fdhila *et al.*, 2003).

Discussion

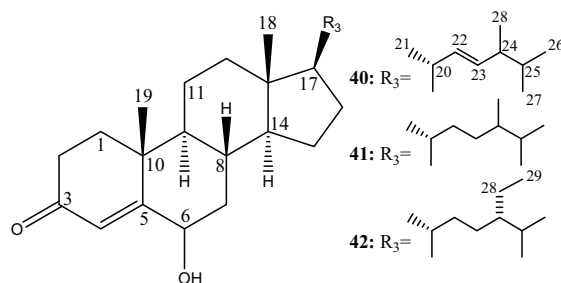


R₁= Br, R₂= H: Jaspamide (**37**)

R₁, R₂= H: Jaspamide Q (**38**)

R₁, R₂= Br: Jaspamide R (**39**)

Based on the reported literature that all of the formerly isolated fifteen jaspamide derivatives (B–L) showed antiproliferative activity against human breast (MCF-7) and colon carcinoma (H-29) cell lines with IC₅₀ values ranging from 0.01 to 33 μ M (Gala *et al.*, 2009). Since jaspamide Q (**38**) and R (**39**) together with the parent jaspamide (**37**) differ in the bromination pattern of the abrine (*N*-methyltryptophan) moiety. Since these modifications were claimed as essential for the observed biological activity (Kahn *et al.*, 1991), compounds (**38** and **39**) together with other compounds isolated from *J. splendens* collected in Kalimantan (Indonesia) were subjected to the *in vitro* cytotoxicity (MTT) assay against mouse lymphoma (L5178Y) cell lines. They exhibited potent activities with IC₅₀ values between <0.1 and 10 μ g/mL (<0.13 and 24.3 μ M) (Table 3.23), compared to kahalalide F (IC₅₀ = 6.3 μ g/mL, 4.3 μ M) which was used as a positive control. Among the tested compounds, the three jaspamide derivatives (**37–39**) together with the nucleoside derivative sangivamycin (**44**) revealed the highest cytotoxicity with IC₅₀ values in the ng/mL range (<0.1 μ g/mL).



Whereas the isolated ketosteroids differed in the side chain attached to the pentacyclic structure. Interestingly, compounds (**40–42**) revealed cytotoxicity in an ascending manner with IC₅₀ values of 10, 9.3, and 2.9 μ g/mL, respectively. This may propose some SARs, for example the presence of an ethyl moiety at C24 of the side chain in **42** significantly escalated the cytotoxic activity compared to **41** and **40** where a methyl group is present instead. In addition, the existence of a double bond between C22 and C23 as in **40** seems to diminish the cytotoxicity than in **41** but this effect seems to be of a minor impact.

4.5. Thalassiolins: sulfated flavonoids from *Thalassia testudinum*

Flavonoids represent a class of natural products that combine both shikimate and acetate biosynthetic pathways to build up the main aglycone skeleton (Fig. 4.4). Many modifications have been noticed regarding both the hydroxylation and the glycosylation patterns over the whole flavonoid skeleton.

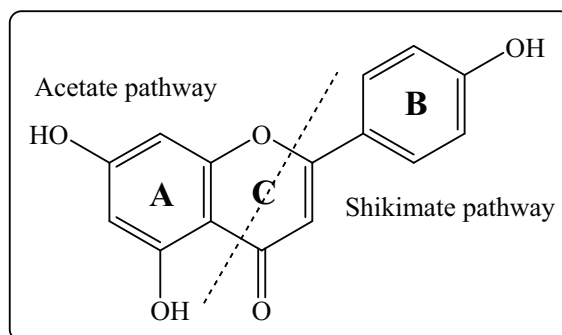


Fig. 4.4. Basic flavone aglycone skeleton and the involved biosynthetic pathways.

During the course of the present study, we have investigated the methanolic extract of a specimen of seagrass *Thalassia testudinum* collected off Muk Island, Trang Province, Thailand in 2007 that resulted in the isolation of two reported sulfated flavonoid glycosides from the same species, namely thalassiolin A (luteolin 7- β -D-glucopyranosyl-2''-sulfate) (**45**) and thalassiolin C (apigenin 7- β -D-glucopyranosyl-2''-sulfate) (**46**) in addition to luteolin-3'-O-glucuronide (**47**), previously isolated from *Salvia officinalis* (Labiatae) that was a subject of several studies as a resource of some potent antioxidants (Lu and Foo, 2000), and to the best of our knowledge it is the first report for **47** from marine environment.

Thalassiolin A (**45**) was reported in literature as an *in vitro* inhibitor of HIV cDNA integrase ($IC_{50} = 0.4 \mu\text{M}$) and antiviral against HIV with IC_{50} value of $30 \mu\text{M}$ (Rowely *et al.*, 2002) compared to thalassiolin C (**46**) that exhibited moderate to low activity. However, none of them exhibited cellular toxicity against human colon cancer HCT-116 cells at concentration up to $75 \mu\text{M}$ (Rowely *et al.*, 2002).

Based on the related reported literature, compounds (**45–47**) were tested for cytotoxic activity against mouse lymphoma (L5178Y) cells using the MTT assay, protein kinase *in vitro* inhibitory activity against 24 different enzymes and the radical scavenging activity using the DPPH assay.

However, none of the compounds (**45–47**) revealed potential cytotoxicity which was in accordance with the reported literature. Only thalassiolin A (**45**) exhibited moderate to

Discussion

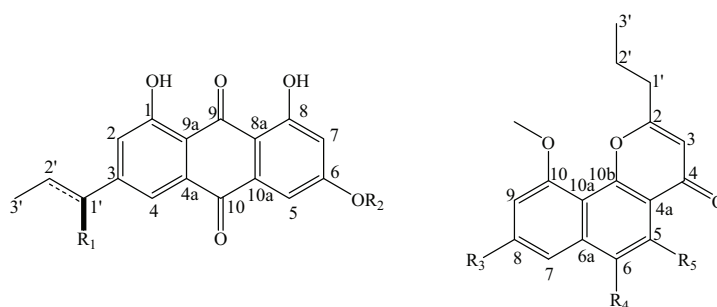
weak activity against some kinases such as PDGFR-beta (IC_{50} = 0.63 μ g/mL), Aurora-A (IC_{50} = 2.1 μ g/mL) and Aurora-B (IC_{50} = 1.5 μ g/mL) which were proven to play a role in prostate, pancreatic, and breast cancers, respectively.

Whereas in radical scavenging (DPPH) assay, results disclosed that thalassiolin A (**45**) and luteolin-3'-*O*-glucuronide (**47**) possess mild radical scavenging activity with IC_{50} values of 48 μ M for both compared to quercetin (IC_{50} = 6.0 μ M) and kaempferol (IC_{50} = 23 μ M).

4.6. Anthraquinones and naphthopyrones from *Comanthus* sp.

During the course of this study, we have investigated the methanolic extract of a Philippine specimen of the echinoderm *Comanthus* sp. collected off the northern shores of Mindoro Island along the so-called Manila Channel in 1994.

The detailed bioactivity-guided chemical analysis resulted in the isolation of five related anthraquinone derivatives (**48–52**) and the same number of naphthopyrone analogues (**53–57**).



	R ₁	R ₂	R ₃	R ₄	R ₅
48:	H, $\Delta^{1'(2')}$	H	53: OH	H	OH
49:	H, 1',2'-dihydro	H	54: OH	OCH ₃	OH
50:	OH	H	55: OH	OCH ₃	OCH ₃
51:	H	SO ₃ ⁻	56: SO ₃ ⁻	OCH ₃	OCH ₃
52:	OH	SO ₃ ⁻	57: SO ₃ ⁻	OH	OH

4.6.1. Biosynthesis of anthraquinones and naphthopyrones

Anthraquinones are biosynthesized by a linear head-to-tail combination of acetate and malonate moieties yielding an octaketide precursor, a process that is catalyzed by polyketide synthase enzyme followed by the loss of carboxylic acid carbon from the terminal unit at C-3, but the detailed sequence of condensation, dehydration and hydroxylation steps is not well known (Fig. 4.5) (Han *et al.*, 2002; Dewick, 2002).

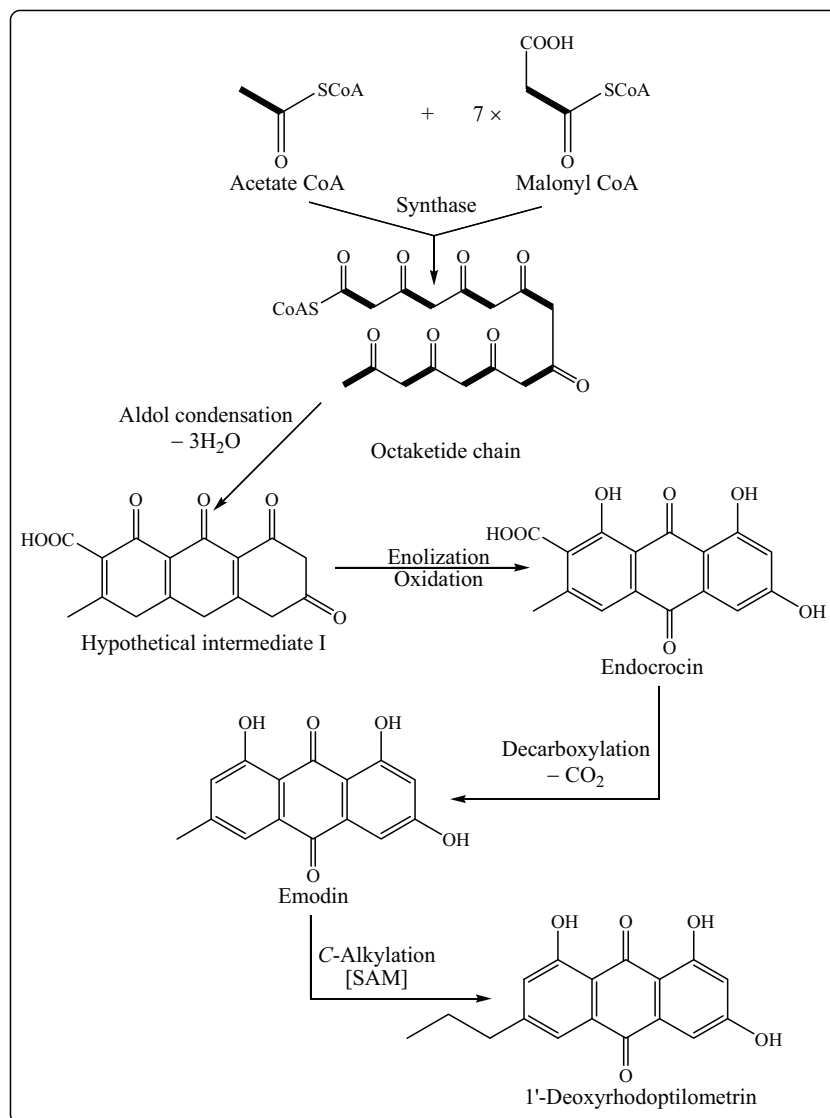


Fig. 4.5. Postulated biosynthetic pathway for anthraquinones (Han *et al.*, 2002).

The periphery of the carbon skeleton is constructed by folding the octaketide chain, and then the ring at the centre of the fold is formed first, followed in turn by the next two rings (Dewick, 2002). The validity of the octaketide pathway was confirmed by spectroscopic studies utilizing single and double labeled acetates (Stoessl *et al.*, 1983, Suemitsu *et al.*, 1989, Ohnishi *et al.*, 1992). In the end, modification of the basic structure resulted from either oxidation alone or together with dehydration to form different anthraquinone derivatives.

The biosynthetic pathway of naphthopyrone as postulated below (Fig. 4.6) was based on those reported for 2,5-dimethyl-7-hydroxychromone (Ayer and Racok, 1990) and for anthraquinones (Han *et al.*, 2002). 2,5-Dimethyl-7-hydroxychromone has been isolated

Discussion

from the roots of *Polygonum cuspidatum*, a plant used in Chinese and Japanese traditional medicines (Kimura *et al.*, 1983). As illustrated below, the postulated biosynthetic pathway for 2,5-dimethyl-7-hydroxychromone revealed that it probably originates from a hexaketide precursor not pentaketide as with other chromones (Ayer and Racok, 1990).

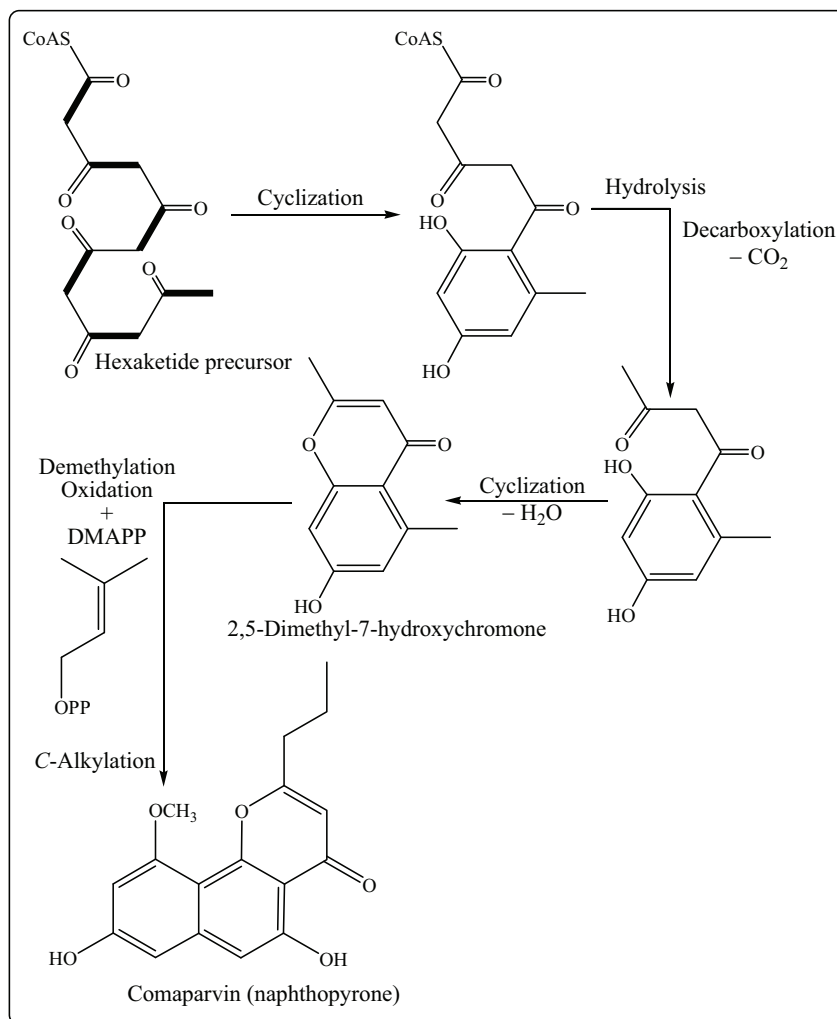


Fig. 4.6. Postulated biosynthetic pathway for naphthopyrones (Ayer and Racok, 1990).

Afterwards, the biosynthesis of naphthopyrone was postulated to be continued through incorporation of a C_5 unit through dimethylallyl pyrophosphate moiety (DMAPP) to build up the third aromatic ring in the naphthopyrone basic skeleton and hence the end step would be either oxidation or methylation to modify the substituent moieties between hydroxyl or methoxy groups affording the different isolated naphthopyrone derivatives.

4.6.2. Biological activity of anthraquinones and naphthopyrones

Nuclear factor κ B (NF- κ B) is an inducible transcription factor that plays a role in cancer development and inflammation (Karin, 2004). Formerly, the effects of 6-methoxycomaparvin (**54**) and 6-methoxycomaparvin-5-methyl ether (**55**) on TNF α -induced transcriptional activity of NF- κ B were examined. The results revealed that both of them completely inhibit TNF α -induced NF- κ B activation and NF- κ B-DNA binding at MIC of 300 μ M (Folmer *et al.*, 2008).

All the isolated anthraquinones, naphthopyrones, and emodin as well were subjected to preliminary cytotoxicity (MTT) assay against L5178Y mouse lymphoma cells at a dose of 10 μ g/mL. IC₅₀ values were determined quantitatively for the potentially active candidates (see Table 3.33), using kahalalide F as positive control. Regarding anthraquinones, the results indicated that *n*-propyl side chain as in 1'-deoxyrhodoptilometrin (**49**) instead of methyl group in emodin has elevated the cytotoxic activity of the former. This might implicate its importance which could be more evidenced by the abundant declined activity in case of **48** and **50** that had 1'-propenyl and 1'-hydroxypropyl side chains, respectively. In case of naphthopyrones, it was concluded that 6-methoxycomaparvin-5-methyl ether (**55**) together with the mixture of comaparvin (**53**) and 6-methoxycomaparvin (**54**) exhibited significant cytotoxicity with IC₅₀ of 4.6 and 5.2 μ g/mL, respectively. Furthermore, the sulfate derivatives had reduced activity compared to their corresponding unsulfated ones, probably caused by the increased polarity of these compounds which would affect the cellular uptake.

Interestingly, testing all compounds at a dose of 1 μ g/mL in biochemical protein kinase activity assays revealed a similar pattern of activity to that found in the MTT assay for L5178Y cells (see Table 3.34) (see Fig. 3.30), i.e. compounds inhibited cellular growth in the MTT assay proved to be active as kinase inhibitors.

Among the tested compounds, both **49** and the mixture of **53** and **54** inhibited a broad panel of kinases with IC₅₀ values ranging from 0.54 to 9.8 μ g/mL. The parallel pattern of activity in the cellular assay and in the biochemical protein kinase assays observed for compounds (**49**), (**50**), and their respective 6-*O*-sulfate derivatives (**51**) and (**52**) suggests that the inhibition of protein kinases may be one of the major mechanisms contributing to the cytotoxic activity of these compounds. On the contrary, 6-methoxycomaparvin-5-methyl ether (**55**) lacked such pattern in both assays. Although, it showed a potent cytotoxic activity in the MTT assay with IC₅₀ value of 4.6 μ g/mL. It didn't inhibit any of the 24 protein kinases by \geq 40%. This discrepancy may perhaps be either because of the poor solubility of **55** in water, incorporated in protein kinase assays, leading to its

Discussion

precipitation or the cytotoxic activity of **55** proceeds through different pathways other than inhibition of the tested protein kinases.

In the radical scavenging (DPPH) assay, a spectrophotometric assay was carried out as described in 2007 by Tsevegsuren *et al.* Only naphthopyrone derivatives displayed mild radical scavenging activity, and their results revealed that the mixture of comaparvin (**53**) and 6-methoxycomaparvin (**54**) together with 6-hydroxycomaparvin-8-*O*-sulfate (**57**), and 6-methoxycomaparvin-5-methyl ether (**55**) exhibited only moderate to weak antioxidant activities with IC₅₀ values of 83.4, 124.6, and 130.7 μ M, respectively compared to quercetin (IC₅₀ = 6.1 μ M).

In addition (*S*)-(-)-rhodoptilometrin (**50**) proved to be active against Gram positive bacteria with MIC values of 7.81 μ g/mL against multi-resistant *Staphylococcus aureus* (MRSA). Whereas, 1'-deoxyrhodoptilometrene (**48**) and 1'-deoxyrhodoptilometrin (**49**) showed antiviral activity against human rhinoviruses (HRV2), (HRV8), and (HRV39); and respiratory syncytial virus A (RSVA) with MIC values of 1.56, 3.13, 3.13, and 3.13 μ g/mL for **48**, respectively; and 1.56, 1.56, 1.56, and 0.39 μ g/mL for **49**, respectively. Therefore, compounds (**48–50**) are considered as interesting candidates for further biological investigations.

4.7. Sulfated secondary metabolites: occurrence and influence

Sulfur is found in the amino acids cysteine and methionine, often responsible for protein structure and enzymatic activity; in coenzymes, such as iron-sulfur centres, thiamine, lipoic acid, or coenzyme A; and in many secondary metabolites, e.g., glucosinolates, alliins, etc. Not surprisingly, therefore, sulfur is an essential micronutrient for all living organisms (Kopriva *et al.*, 2007).

Glucosinolates are a well-studied example of compounds involved in plant defense against biotic stress, particularly against herbivores and pathogens in Brassicales (Halkier and Gershenzon, 2006). They exert their defensive action through enzymatic reaction of myrosinase, producing toxic volatile isothiocyanates and nitrils. Finally, sulfation mediated by sulfotransferase (SOT) takes place as an essential end step.

Plants possess many other sulfated compounds, including sulfoflavonoids and sulfated oligosaccharides, play different roles in defense against plant stress (Varin *et al.*, 1997; Menrad *et al.*, 2004).

In mammals, sulfation is a major contributor to the homeostasis and regulation of numerous biologically potent endogenous chemicals, such as catecholamines, steroids, and iodothyronines, as well as contributing to the detoxification of xenobiotics (Coughtrie *et al.*,

1998). In bacterial, sulfation is essential for the signalling of rhizobial nod factors to the plant (Truchet *et al.*, 1991).

In this study, a sum of six secondary metabolites have been reported of which two were thalassiolins A (**45**) and C (**46**) that were isolated and reported from the same seagrass species *Thalassia testudinum*. The other four sulfated metabolites were two anthraquinones (**51** and **52**) and two naphthopyrones (**56** and **57**) that were obtained and reported from the same echinoderm genus *Comanthus*. The existence of sulfate moiety has imparted a partially higher polarity of these metabolites and therefore they were all purified from *n*-BuOH fraction of the total methanolic extract of the corresponding organism. This partially imparted higher polarity by sulfate moieties in anthraquinones and naphthopyrones has influenced the cellular uptake of these metabolites and resulted in diminished bioactivity compared to the respective metabolites lacking sulfate as shown above.

Summary

5. Summary

Marine sponges are the source of the greatest chemical diversity of natural products. From which one-third of all marine natural products have been isolated and hence considered as the most popular source of novel compounds. The marine sponges are considered not only as a very important source of new natural products but also as a source for bioactive compounds. These compounds are interesting candidates for new drugs, primarily in the fields of cancer, anti-inflammatory, anti-infective and analgesic.

Recently, two marine natural products have been introduced as new medicaments: Prialt[®] (also known as ziconotide) as a potent analgesic for severe chronic pain and Yondelis[®] (known also as trabectedin or ET-743) as antitumor agent for the treatment of advanced soft tissue sarcoma. Moreover, Aplidin[®] (plitidepsin), kahalalide F, and Zalypsis[®] (jorumycin derivative) are in clinical trial phases for treatment of solid tumors and haematological malignancies.

Many successful cases, as shown above, proved to have various pharmaceutical significances, which have been developed to preclinical or clinical trial phases for treatment of serious diseases such as Alzheimer's disease, type 2 diabetes, cancer and infectious diseases in addition to pain killing and anti-inflammatory activities.

Therefore, the aim of this study was directed toward the isolation and structural elucidation of marine natural products, either known or preferentially new ones, in appreciable amounts so as to enable testing various biological activities.

Secondary metabolites isolation and structural elucidation were performed by means of new sophisticated analytical techniques including mass spectrometry and nuclear magnetic resonance spectroscopy. Moreover, the absolute configuration of the selected optically active natural products were determined and reported based on the chiral derivatization using Mosher reaction. For the assessment of biological activity, a vast array of assays has been performed including cytotoxicity (MTT), antibacterial, antifungal, antiviral, protein kinase inhibitory and antioxidant (DPPH) activities.

Different types of marine organisms have been involved in this study including sponges, seagrasses and echinoderms that have been collected off various geographic locations namely Indonesia, Philippine, and Thailand.

1. *Acanthostylorella* sp.

Six new dibromopyrrole alkaloids have been isolated from the methanolic extract of the Indonesian marine sponge *Acanthostylorella* sp. (Indonesia). They include four new acanthamides (A–D) in addition to methyl 3,4-dibromo-1*H*-pyrrole-2-carboxylate and 3,5-

dibromo-1*H*-pyrrole-2-carboxylic acid. Furthermore, eight known dibromopyrrole alkaloids were obtained from the same extract. Among the isolated compounds, mukonadin D revealed moderate cytotoxicity against mouse lymphoma (L5178Y) cells. Whereas, methyl 3,4-dibromo-1*H*-pyrrole-2-carboxylate exhibited moderate antimicrobial and antiviral activities.

2. *Stylissa massa*

Twenty two bromopyrrole alkaloids have been purified and identified from the methanolic extract of the marine sponge *Stylissa massa* (Indonesia) among which two new natural dibromopyrrole alkaloids have been isolated namely, ethyl 3,4-dibromo-1*H*-pyrrole-2-carboxylate and dispacamide E. The isolated compounds revealed interesting bioactivity results in different bioassays including cytotoxicity (MTT) assay, antimicrobial, antifungal, antiviral and *in vitro* protein kinase inhibitory activity.

3. *Jaspis splendens*

Eight compounds were isolated through a bioactivity-guided isolation scheme from the ethyl acetate soluble fraction of the total methanolic extract of *Jaspis splendens* (Indonesia). In addition to three known ketosteroids, a diketopiperazine derivative *cyclo*-L-Pro-L-Tyr, and nucleoside derivative sangivamycin, two new jaspamide derivatives, were isolated together with the parent compound jaspamide.

All isolated compounds exhibited cytotoxicity against mouse lymphoma (L5178Y) cells in particular new jaspamide derivatives together with jaspamide, *cyclo*-L-Pro-L-Tyr and sangivamycin showed the highest cytotoxicity with IC₅₀ values ranging from <0.1 to 0.28 µg/mL, compared to kahalalide F (IC₅₀= 6.3 µg/mL).

4. *Thalassia testudinum*

A detailed chemical investigation of the methanolic extract of *T. testudinum* (Thailand) was carried out and led to the isolation of two sulfated flavonoid glycosides, thalassiolin A and thalassiolin C. Whilst luteolin-3'-*O*-glucuronide was also isolated and to the best of our knowledge, it is the first report for this compound from marine habitat, however it was reported from Sage (*Salvia officinalis*, family Labiatae) which has been the subject of several studies as a resource of some potent antioxidants. Finally, all the isolated flavonoids glycosides were tested for radical scavenging (DPPH) activity.

Summary

5. *Comanthus* sp.

Bioactivity-guided fractionation strategy of *Comanthus* sp. (Philippine) extract was performed leading to the isolation of sixteen compounds; five of them were anthraquinones including one new natural product, five were naphthopyrones, one nucleoside, 2'-deoxythymidine, and five were steroidal secondary metabolites. Herein, we would comprehensively report isolation, structural elucidation based on the analysis of spectroscopic and spectrometric data in addition to comparison with the related literature, absolute stereochemistry of two optically active anthraquinone derivatives, rhodoptilometrins and its 6-*O*-sulfate derivative has been reported here for the first time using Mosher reaction which revealed that both of them are (*S*)-(-) isomers.

All the isolated compounds were subjected qualitatively and quantitatively to radical scavenging (DPPH) assay, cytotoxic (MTT) assay against (L5178Y) mouse lymphoma cell line, protein kinase *in vitro* inhibitory activity assay against 24 different protein kinases, antimicrobial, antifungal and antiviral activities. Anthraquinones and naphthopyrones displayed interesting results that could be related in different assays.

6. References

- Allore B.D., Queen A., Blonski W.J., Hruska F.E. (1983). A kinetic and nuclear magnetic resonance study of methylated pyrimidine nucleosides. *Can. J. Chem.*, **61**, 2397–2402.
- Andrade P., Willoughby R., Pomponi S.A., Kerr R.G. (1999). Biosynthetic studies of the alkaloid, stevensine, in a cell culture of the marine sponge *Teichaxinella morchella*. *Tetrahedron Lett.*, **40**, 4775–4778.
- Ang K.K.H., Holmes M.J., Higa T., Hamann M.T., Kara U.A.K. (2000). *In vivo* antimalarial activity of the betacarboline alkaloid manzamine A. *Antimicrob. Agents Chemother.*, **44**, 1645–1649.
- Aoki S., Yoshioka Y., Miyamoto Y., Higuchi K., Setiawan A., Murakami N., Chen Z.S., Sumizawa T., Akiyama S., Kobayashi M. (1998). Agosterol A, a novel polyhydroxylated sterol acetate reversing multidrug resistance from a marine sponge of *Spongia* sp. *Tetrahedron Lett.*, **39**, 6303–6306.
- Assmann M., Köck M. (2002). Monobromoisophakellin, a new bromopyrrole alkaloids from the Caribbean sponge *Agelas* sp. *Z. Naturforsch.*, **57c**, 153–156.
- Ayer W.A., Racok J.S. (1990). The metabolites of *Talaromyces flavus*: Part 1. Metabolites of the organic extracts. *Can. J. Chem.*, **68**, 2085–2094.
- Banville J., Brassard P. (1976). Reactions of keten Acetals. Part VI. Total syntheses of the anthraquinones (±)-nalgiovensin, (±)-isorhodoptilometrin and (±)-rhodoptilometrin. *J. Chem. Soc. Perkin Trans 1*, 613–619.
- Barnes R. D., “Invertebrate Zoology,” 5th ed., Saunders College Publishing, Fort Worth, USA, 1987, pp. 826–834.
- Bartolini G.L., Erdman T.R., Scheuer P.J. (1973). Anthraquinone pigments from the crinoid *Comanthus bennetti*. *Tetrahedron*, **29**, 3699–3702.
- Bergmann W., Burke D.C. (1955). Contribution to the study of marine products. XXXIX the nucleosides of the sponges III. Spongothymidine and spongouridine. *J. Org. Chem.*, **20**, 1501–1507.
- Bergmann W., Feeney R.J. (1951). Contribution to the study of marine products. XXXII. The nucleotides of sponges I. *J. Org. Chem.*, **16**, 981–987.
- Bergmann W., Watkins J.C., Stempien M.F. (1957). Contribution to the study of marine products. XLV. Sponge nucleic acids. *J. Org. Chem.*, **22**, 1308–1313.
- Bhakuni D.S., Rawat, D.S. (2005). Bioactive Marine Natural Products: p. 26–77 (Springer-Anamaya, New York, New Delhi).

References

- Braeckman J.C., Daloze Q., Stoller C., Van Soest R.W. (1992). Chemotaxonomy of *Agelas* (Porifera: Demospongiae). *Biochem. Syst. Ecol.*, **20**, 417–430.
- Butler M.S. (2004). The role of natural product chemistry in drug discovery. *J. Nat. Prod.*, **67**, 2141–2153.
- Cafieri F., Carnuccio R., Fattorusso E., Tagliatela-Scafati O., Vallefucio T. (1997). Anti-histaminic activity of bromopyrrole alkaloids isolated from Caribbean *Agelas* sponges. *Bioorg. Med. Chem. Lett.*, **7**, 2283–2288.
- Cafieri F., Fattorusso E., Mangoni A., Tagliatela-Scafati O. (1995). Longamide and 3,7-dimethylisoguanine, two novel alkaloids from the marine sponge *Agelas longissima*. *Tetrahedron Lett.*, **36**, 7893–7896.
- Cafieri F., Fattorusso E., Mangoni A., Tagliatela-Scafati O. (1996). Dispacamides, anti-histamine alkaloids from Caribbean *Agelas* sponges. *Tetrahedron Lett.*, **37**, 3587–3590.
- Cafieri F., Fattorusso E., Tagliatela-Scafati O. (1998). Novel bromopyrrole alkaloids from the sponge *Agelas dispar*. *J. Nat. Prod.*, **61**, 122–125.
- Carmichael J., DeGraff W.G., Gazdar A.F., Minna J.D., Mitchell J.B. (1987). Evaluation of a tetrazolium-based semiautomated colorimetric assay: Assessment of radiosensitivity. *Cancer Res.*, **47**, 943–946.
- Chang Y.H., Shin D., Na Z., Lee H.-S., Kim D.-D., Oh K.-B., Shin J. (2008). Dihydroxystyrene metabolites from an association of the sponge *Poecillastra wondoensis* and *Jaspis* sp. *J. Nat. Prod.*, **71**, 779–783.
- Cimino G., De Rosa S., De Stefano S., Mazzarella L., Puliti R., Sodano G. (1982). Isolation and X-ray crystal structure of a novel bromo-compound from two marine sponges. *Tetrahedron Lett.*, **23**, 767–768.
- Cimino G., De Rosa S., De Stefano S., Mazzarella L., Puliti R., Sodano G. (1982). Isolation and X-ray crystal structure of a novel bromo compound from two marine sponges. *Tetrahedron Lett.*, **23**, 767–768.
- Claeson P., Bohlin L. (1997). Some aspects of bioassay methods in natural-product research aimed at drug lead discovery. *Trends. Biotech.*, **15**, 245–246.
- Coughtrie M.W.H., Sharp S., Maxwell K., Innes N.P. (1998). Biology and function of the reversible sulfation pathway catalyzed by human sulfotransferases and sulfatases. *Chem. Biol. Inter.*, **109**, 3–27.
- Crews P., Manes L.V., Boehler M. (1986). Jasplakinolide, a cyclodepsipeptide from the marine sponge, *Jaspis* sp. *Tetrahedron Lett.*, **27**, 2797–2800.

References

- Crompton D.W.T., Nesheim M.C. (2002). Nutritional impact of intestinal helminthiasis during the human life cycle. *Annu. Rev. Nutr.*, **22**, 35–59.
- D'Auria M.V., Paloma L.G., Minale L., Riccio R., Debitus C. (1992). Unique 3 β -methylsterols from the Pacific sponge *Jereicopsis graphidiophora*. *J. Nat. Prod.*, **55**, 311–320.
- D'Ambrosio M., Guerriero A., Debitus C., Ribes O., Pusset J., Leroy S., Pietra F. (1993). Agelastatin A, a new skeleton cytotoxic alkaloid of the oroidin family. Isolation from the Axinellid sponge *Agelas dendromorpha* of the Coral Sea. *J. Chem. Soc. Chem. Commun.*, **16**, 1305–1306.
- D'Ambrosio M., Guerriero A., Ripamonti M., Debitus C., Waikedre J., Pietra F. (1996). 65. The active centers of agelastatin A, a strongly cytotoxic alkaloid of the Coral Sea Axinellid sponge *Agelas dendromorpha*, as determined by comparative bioassays with semisynthetic derivatives. *Helv. Chim. Acta*, **79**, 727–735.
- D'Auria M.V., Giannini C., Minale L., Zampella A., Debitus C., Frostin M. (1997). Bengamides and related amino acid derivatives from the new Caledonian marine sponge *Jaspis carteri*. *J. Nat. Prod.*, **60**, 814–816.
- Dale J.A., Mosher H.S. (1973). Nuclear magnetic resonance enantiomer reagents. Configurational correlations via nuclear magnetic resonance chemical shifts of diastereomeric mandelate, *O*-methylmandelate and α -methoxy- α -trifluoromethylphenylacetate (MTPA) esters. *J. Amer. Chem. Soc.*, **95**, 512–519.
- Davidson S.K., Allen S.W., Lim G.E., Anderson C.M., Haygood M.G. (2001). Evidence for the biosynthesis of bryostatins by the bacterial symbiont "*Candidatus Endobugula sertula*" of the bryozoan *Bugula neritina*. *Appl. Environ. Microbiol.*, **67**, 4531–4537.
- De Nanteuil G., Ahond A., Guilhem J., Poupat C., Dau E.T.H., Potier P. (1985). "Invertebres marins du lagon neo-caledonien–V. Isolement et identification des metabolites d'une nouvelle espece de spongiaire, *Pseudaxinyssa cantharella*." *Tetrahedron*, **41**, 6019–6033.
- DeBusk L.M., Chen Y., Nishishita T., Chen J., Thomas J.W., Lin P.C. (2003). Tie2 receptor tyrosine kinase, a major mediator of tumor necrosis factor alpha-induced angiogenesis in rheumatoid arthritis. *Arthritis Rheum.*, **48**, 2461–2471.
- Dehm S., Senger M.A., Bonham K. (2001). SRC transcriptional activation in a subset of human colon cancer cell lines. *FEBS Letters*, **487**, 367–371.
- Dewick, P. M. (2002). *Medicinal natural products. A biosynthetic approach*. John Wiley & Sons Ltd, Baffins Lane, Chichester, England.

References

- Ebel R., Brenzinger M., Kunze A., Gross H.J., Proksch P. (1997). Wound activation of protoxins in marine sponge *Aplysina aerophoba*. *J. Chem. Ecol.*, **23**, 1451–1457.
- Fathi-Afshar R., Allen T.M. (1988). Biologically active metabolites from *Agelas mauritiana*. *Can. J. Chem.*, **66**, 45–50.
- Fattorusso E., Tagliatela-Scafati O. (2000) Two novel pyrrole-imidazole alkaloids from the Mediterranean sponge *Agelas oroides*. *Tetrahedron Lett.*, **41**, 9917–9922.
- Fdhila F., Vzquez V., Snchez J.L., Riguera R. (2003). dd-Diketopiperazines: antibiotics active against *Vibrio anguillarum* isolated from marine bacteria associated with cultures of *Pecten maximus*. *J. Nat. Prod.*, **66**, 1299–1301.
- Fedoreyev S.A., Ilyin S.G., Utkina N.K., Maximov O.B., Reshetnyak M.V., Antipin M.Y., Struchkov Y.T. (1989). The structure of dibromoagelospongin - a novel bromine-containing guanidine derivative from the marine sponge *Agelas* sp. *Tetrahedron*, **45**, 3487–3492.
- Folmer F., Harrison W.T.A., Tabudravu J.N., Jaspars M., Aalbersberg W., Feussner K., Wright A.D., Dicato M., Diederich M. (2008). NF- κ B inhibiting naphthopyrones from the Fijian echinoderm *Comanthus parvicirrus*. *J. Nat. Prod.*, **71**, 106–111.
- Forenza S., Minale L., Riccio R., Fattorusso E. (1971). New bromo-pyrrole derivatives from the sponge *Agelas oroides*. *J. Chem. Soc., Chem. Comm.*, 1129–1130.
- Francesconi K.A. (1980). Pigments of some echinoderms collected from Western Australian waters. *Aust. J. Chem.*, **33**, 2781–2784.
- Gala F., D'Auria M.V., De Marino S., Sepe V., Zollo F., Smith C.D., Copper J.E., Zampella A. (2008). Jaspamides H–L, new actin-targeting depsipeptides from the sponge *Jaspis splendens*. *Tetrahedron*, **64**, 7127–7130.
- Gala F., D'Auria M.V., De Marino S., Sepe V., Zollo F., Smith C.D., Keller S.N., Zampella A. (2009). Jaspamides M–P: new tryptophan modified jaspamide derivatives from the sponge *Jaspis splendens*. *Tetrahedron*, **65**, 51–56.
- Garces C.A., Kurenova E.V., Golubovska V.M., Cance W.G. (2006). Vascular endothelial growth factor receptor-3 and focal adhesion kinase bind and suppress apoptosis in breast cancer cells. *Cancer Res.*, **66**, 1446–1454.
- Garcia E.E., Benjamin L.E., Ian Fryer R. (1973). Reinvestigation into the structure of oroidin, a bromopyrrole derivatives from marine sponge. *J. Chem. Soc., Chem. Comm.*, 78–79.
- Georges P., Sylvestre M., Ruegger H., Bourgeois P. (2006). Ketosteroids and hydroxyketosteroids, minor metabolites of sugarcane wax. *Steroids*, **71**, 647–652.

References

- Groweiss A., Newcomer J.J., O'Keefe B.R., Blackman A., Boyd M.R. (1999). Cytotoxic metabolites from an Australian collection of the sponge *Jaspis* species. *J. Nat. Prod.*, **62**, 1691–1693.
- Gunasekera S.P., Cranick S., Longley R.E. (1989). Immunosuppressive compounds from a deep water marine sponge, *Agelas flabelliformis*. *J. Nat. Prod.*, **52**, 757–761.
- Halkier B.A., Gershenzon J. (2006). Biology and biochemistry of glucosinolates. *Ann. Rev. Plant Biol.*, **57**, 303–333.
- Han Y.S., van der Heijden R., Lefeber A.W.M., Erkelens C., Verpoorte R. (2002). Biosynthesis of anthraquinones in cell cultures of *Cinchona* 'Robusta' proceeds via the methylerythritol 4-phosphate pathway. *Phytochemistry*, **59**, 45–55.
- Handy S., Zhang Y. (2006). Regioselective couplings of dibromopyrrole esters. *Synthesis*, **2006**, 3883–3887.
- Harborne J.B., Williams C.A. (1976). Occurrence of sulfated flavones and caffeic acid esters in members of the fluviales. *Biochem. Syst. Ecol.*, **4**, 37–44.
- Hassan W., Elkhayat E., Edrada R., Ebel R., Proksch P. (2007). New bromopyrrole alkaloids from the marine sponges *Axinella damicornis* and *Stylissa flabelliformis*. *Nat. Prod. Commun.*, **2**, 1–6.
- Hofer M.D., Fecko A., Shen R., Setlur S.R., Pienta K.G., Tomlins S.A., Chinnaiya A.M., Rubin M.A. (2004). Expression of the platelet-derived growth factor receptor in prostate cancer and treatment implications with tyrosine kinase inhibitors. *Neoplasia*, **6**, 503–512.
- Hong T.W., Jimenez D.R., Molinski T.F. (1998). Agelastatins C and D, new pentacyclic bromopyrroles from the sponge *Cymbastela* sp., and potent anthropod toxicity of (–)-agelastatin A. *J. Nat. Prod.*, **61**, 158–161.
- Hu J., Peng J., Kazi A., Kelly M., Hamann M. (2005). Bromopyrrole alkaloids from the Jamaican sponge *Didiscus oxeata*. *J. Chem. Res.*, **7**, 427–428.
- Inaba K., Sato H., Tsuda M., Kobayashi J. (1998). Spongiacidins A–D, new bromopyrrole alkaloids from *Hymeniacidon* sponge. *J. Nat. Prod.*, **61**, 693–695.
- Inman W., Crews P. (1989). Novel marine sponge derived amino acids, 8. conformational analysis of jasplakinolide. *J. Am. Chem. Soc.*, **111**, 2822–2829.
- Iseki H., Ko T.C., Xue X.Y., Seapan A., Townsend C.M.Jr. (1998). A novel strategy for inhibiting growth of human pancreatic cancer cells by blocking cyclin dependent kinase activity. *J. Gastrointest. Surg.*, **2**, 36–43.

References

- Izeradjene K., Douglas L., Delaney A., Houghton J.A. (2004). Influence of casein kinase II in tumor necrosis factor-related apoptosis-inducing ligand-induced apoptosis in human rhabdomyosarcoma cells. *Clin. Cancer Res.*, **10**, 6650–6660.
- Jayatilake G.S., Thornton M.P., Leonard A.C., Grimwade J.E., Baker B.J. (1996). Metabolites from an Antarctic sponge-associated bacterium, *Pseudomonas aeruginosa*. *J. Nat. Prod.*, **59**, 293–296.
- Jensen P.R., Jenkins K.M., Porter D., Fenical W. (1998). Evidence that a new antibiotic flavone glycoside chemically defends the Seagrass *Thalassia testudinum* against zoosporic fungi. *Appl. Environ. Microbiol.*, **64**, 1490–1496.
- Kahn M., Nakanishi H., Su T., Lee J.H., Johnson M. (1991). Design and synthesis of nonpeptide mimetics of jaspamide. *Int. J. Pept. Protein Res.*, **38**, 324–334.
- Kalli K.R., Falowo O.I., Bale L.K., Zschunke M.A., Roche P.C., Conover C.A. (2002). Functional insulin receptors on human epithelial ovarian carcinoma cells: Implications for IGF-II mitogenic signaling. *Endocrinology*, **143**, 3259–3267.
- Karin M. (2006). Nuclear factor- κ B in cancer development and progression. *Nature*, **441**, 431–436.
- Keen N., Taylor S. (2004). Aurora-kinase inhibitors as anticancer agents. *Nature Rev. Cancers*, **4**, 927–936.
- Keifer P.A., Schwartz R.E., Koker M.E.S., Hughes R.G., Jr., Rittschof D., Rinehart K.L. (1991). Bioactive bromopyrrole metabolites from the Caribbean sponge *Agelas conifera*. *J. Org. Chem.*, **56**, 2965–2975.
- Kent R.A., Smith I.R., Sutherland M.D. (1970). Pigments of marine animals. X. Substituted naphthopyrones from the crinoid *Comantheria perplexa*. *Aust. J. Chem.*, **23**, 2325–2335.
- Kimura Y., Kozawa M., Baba K., Hata K. (1983). New constituents of roots of *Polygonum cuspidatum*. *Planta Med.*, **48**, 164–168.
- Kitagawa I., Kobayashi J., Kitanaka K., Kido M., Kyogoku Y. (1983). Marine natural products. XII. On the chemical constituents of the Okinawan marine sponge *Hymeniacidon aldis*. *Chem. Pharm. Bull.*, **3**, 2321–2328.
- Kitagawa I., Kobayashi M., Kitanaka K., Kido M., Kyogoku Y. (1983). Marine natural products. XII. On the chemical constituents of the Okinawan marine sponge *Hymeniacidon aldis*. *Chem. Pharm. Bull.*, **31**, 2321–2328.
- Kobayashi J., Murata O., Shigemori H., Sasaki T. (1993). Jaspisamides A–C, new cytotoxic macrolides from the Okinawan marine sponge *Jaspis* sp. *J. Nat. Prod.*, **56**, 787–791.

References

- Kobayashi J., Ohizumi Y., Nakamura H., Hirata Y., Wakamatsu K., Miyazawa T. (1986). Hymenine, a novel α -adrenoceptor blocking agent from the Okinawan marine sponge *Hymeniacidon* sp. *Experientia*, **42**, 1064–1065.
- Kobayashi J., Yuasa K., Kobayashi T., Sasaki T., Tsuda M. (1996). Jaspiferals A–G, new cytotoxic isomalabaricane-type nortriterpenes from Okinawan marine sponge *Jaspis stellifera*. *Tetrahedron*, **52**, 5745–5750.
- König G., Wright A., Linden A. (1998). Antiplasmodial and cytotoxic metabolites from the Maltese sponge *Agelas oroides*. *Planta Medica*, **64**, 443–447.
- König G.M., Wright A.D. (1996). Marine natural products research: current directions and future potential. *Planta Medica*, **62**, 193–211.
- Kontiza I., Abatis D., Malakate K., Vagias C., Roussis V. (2006). 3-Ketosteroids from the marine organisms *Dendrophyllia cornigera* and *Cymodocea nodosa*. *Steroids*, **71**, 177–181.
- Kopriva S., Wiedemann G., Reski R. (2007). Sulfate assimilation in basal land plants—what does genomic sequencing tell us? *Plant Biol.*, **9**, 556–564.
- Kusakai G., Suzuki A., Ogura T., Miyamoto S., Ochiai A., Kaminishi M., Esumi H. (2004). ARK5 expression in colorectal cancer and its implications for tumor progression. *Am. J. Pathol.*, **164**, 987–995.
- Lee J.W., Soung Y.H., Kim S.Y., Park W.S., Nam S.W., Kim S.H., Lee J.Y., Yoo N.J., Lee S.H. (2005). ERBB2 kinase domain mutation in a gastric cancer metastasis. *APMIS*, **113**, 683–687.
- Lee N.K., Kim Y.H. (1995). New cytotoxic anthraquinones from the crinoid *Ptilometra*: 1'-deoxyrhodoptilometrin-6-O-sulfate and rhodoptilometrin-6-O-sulfate. *Bull. Korean Chem. Soc.*, **16**, 1011–1013.
- Li C.-J., Schmitz F.J., Kelly-Borges M. (1998). A new lysine derivative and new 3-bromopyrrole carboxylic acid derivative from two marine sponges. *J. Nat. Prod.*, **61**, 387–389.
- Li D., Zhu J., Firozi P., Abbruzzese J.L., Evans D.B., Cleary K., Fries H., Sen S. (2003). Overexpression of oncogenic STK15/BTAK/Aurora A kinase in human pancreatic cancer. *Clin. Cancer Res.*, **9**, 991–997.
- Lidgren G., Bohlin L., Christophersen C. (1988). Studies of Swedish marine organisms, Part X. Biologically active compounds from the marine sponge *Geodia baretii*. *J. Nat. Prod.*, **51**, 1277–1280.
- Lindquist N., Hay M.E., Fenical W. (1992). Defense of ascidians and their conspicuous larvae, Adults versus Larval chemical defenses. *Ecol. Monogr.*, **62**, 547–568.

References

- Linington R.G., Williams D.E., Tahir A., van Soest R., Andersen R.J. (2003). Latonduines A and B, new alkaloids isolated from the marine sponge *Stylissa carteri*: structure elucidation, synthesis, and biogenetic implications. *Org. Lett.*, **5**, 2735–2738.
- Lu Y., Foo L.Y. (2000). Flavonoid and phenolic glycosides from *Salvia officinalis*. *Phytochemistry*, **55**, 263–267.
- Luca P.D., Rosa M.D., Minale L., Sodano G. (1972). Marine sterols with a new pattern of side chain alkylation from the sponge *Aplysina* (= *Verongia*) *aerophoba*. *J. Chem. Soc. Perkin Trans. I*, 2132–2135.
- Macmillan J.C., Hudson J.W., Bull S., Dennis J.W., Swallow C.J. (2001). Comparative expression of the mitotic regulators SAK and PLK in colorectal cancer. *Annals of Surgical Oncology*, **8**, 729–740.
- Mancini I., Guella G., Amade P., Roussakis C., Pietra F. (1997). Hanishin, a semiracemic, bioactive C₉ alkaloid of the Axinellid sponge *Acanthella carteri* from the Hanish Islands. A shunt metabolite? *Tetrahedron Letters*, **38**, 6271–6274.
- Martinez A., Castro A., Dorronsoro I., Alonso M. (2002). Glycogen synthase kinase (GSK-3) inhibitors as new promising drugs for diabetes, neurodegeneration, cancer and inflammation. *Med. Res. Rev.*, **22**, 373–384.
- Mattia C.A., Mazzarella L., Puliti R. (1982). 4-(2-Amino-4-oxo-2-imidazolin-5-ylidene)-2-bromo-4,5,6,7-tetrahydropyrrolo-[2,3-C] azepine -8-one Methanol solvate—a new bromo compound from the sponge *Acanthella aurantiaca*. *Acta Crystallogr., Sec B, Struct. Sci.*, **38**, 2513–2515.
- Mayer A.M.S., Glaser K.B., Cuevas C., Jacobs R.S., Kem W., Little R.D., McIntosh J.M., Newman D.J., Potts B.C., Shuster D.E. (2010). The odyssey of marine pharmaceuticals: a current pipeline perspective. *Trends Pharmacol. Sci.*, **31**, 255–265.
- McMillan C., Zapata O., Escobar L. (1980). Sulfated phenolic compounds in seagrasses. *Aquat. Bot.*, **8**, 267–278.
- Meijer L., Thunnissen A.M.W.H., White A.W., Garnier M., Nikolic M., Tsai L.H., Walter J., Cleverley K.E., Salinas P.C., Wu Y.Z., Biernat J., Mandelkow E.M., Kim S.H., Pettit G.R. (2000). Inhibition of cyclin-dependent kinases, GSK-3 beta and CK1 by hymenialdisine, a marine sponge constituent. *Chem. Biol.*, **7**, 51–63.
- Ménard R., Alban S., de Ruffray P., Jamois F., Franz G., Fritig B., Yvin J.C., Kauffmann S. (2004). β -1,3 Glucan sulfate, but not β -1,3 glucan, induces the salicylic acid signaling pathway in tobacco and *Arabidopsis*. *Plant Cell*, **16**, 3020–3032.

References

- Menezes D.E.L., Peng J., Garrett E.N., Louie S.G., Lee S.H., Wiesmann M., Tang Y., Shephard L., Goldbeck C., Oei Y., Ye H., Aukerman S.L., Heise C. (2005). CHIR-258: A potent inhibitor of FLT3 kinase in experimental tumor xenograft models of human acute myelogenous leukemia. *Clin. Cancer Res.*, **11**, 5281–5291.
- Miller F.A., Dixon G.J. Sloan B.J., Mclean I.W. (1968). Antimicrobial agents and chemotherapy. *Am. Soc. Microbiol.*, p. 136.
- Mishra S.K., Satpathy S.K., Mohanty S. (1999). Survey of malaria treatment and deaths. *Bull. World Health Organ.*, **77**, 1020.
- Molinski T.F., Dalisay D.S., Lievens S.L., Saludes J.P. (2009). Drug development from marine natural products. *Nature Rev. Drug Discovery*, **8**, 69–86.
- Nagai H., Murata M., Torigoe K., Satake M., Yasumoto T. (1992). Gambieric acids: new potent antifungal substances with unprecedented polyether structures from a marine dinoflagellate *Gambierdiscus toxicus*. *J. Org. Chem.*, **57**, 5448–5453.
- National Cancer Institute. (22 November 2005). Mutations in glioblastoma in multiforme predict responded to target therapies. *NCI Cancer Bulletin* (online), **2**(45).
- Neeman I., Fishelson L., Kashmann Y. (1975). Isolation of new toxin from the sponge *Lantrunculia magnifica* in the Gulf of Aquapa (Red Sea). *Mar. Biol.*, **30**, 293–296.
- Newman D.J., Cragg G.M. (2004). Advanced preclinical and clinical trials of natural products and related compounds from marine sources. *Curr. Med. Chem.*, **11**, 1693–1713.
- Newman D.J., Cragg G.M., Sander K.M. (2000). The influence of natural products upon drug discovery. *Nat. Prod. Rep.*, **17**, 215–234.
- Nikoulina S.E., Ciaraldi T.P., Mudaliar S., Mohideen P., Carter L., Henry R.R. (2000). Potential role of glycogen synthase kinase-3 in skeletal muscle insulin resistance of type 2 diabetes. *Diabetes*, **49**, 263–271.
- Ohnishi K., Tanabe H., Hayashi S., Suemitsu R. (1992). Biosynthesis of alterporriol A by *Alternaria porri*. *Biosci. Biotech. Biochem.*, **56**, 42–43.
- Ohta S., Kobayashi H., Ikegami S. (1994). Jaspisin, a novel styryl sulfate from the marine sponge, *Jaspis* species. *Biosci. Biotech. Biochem.*, **58**, 1752–1753.
- Ohtani I., Kusumi T., Kashman Y., Kakisawa H. (1991). High-field FT NMR application of Mosher's method. The absolute configurations of marine terpenoids. *J. Am. Chem. Soc.*, **113**, 4092–4096.
- Ouyang B., Knauf J.A., Smith E.P., Zhang L., Ramsey T., Yusuff N., Batt D., Fagin J.A. (2006). Inhibitors of Raf kinase activity block growth of thyroid cancer cells with RET/PTC or BRAF mutations *in vitro* and *in vivo*. *Clin. Cancer Res.*, **12**, 1785–1793.

References

- Park Y., Liu Y., Hong J., Lee C.-O., Cho H., Kim D.-K., Im K.S., Jung J.H. (2003). New bromotyrosine derivatives from an association of two sponges, *Jaspis wondoensis* and *Poecillastra wondoensis*. *J. Nat. Prod.*, **66**, 1495–1498.
- Patel J., Pelloux-Léon N., Minassian F., Vallée Y. (2005). Syntheses of S-enantiomers of hanishin, longamide B, and longamide B methyl ester from L-aspartic acid β -methyl ester: establishment of absolute stereochemistry. *J. Org. Chem.*, **70**, 9081–9084.
- Pawlik J.R. (1993). Marine invertebrate chemical defenses. *Chem. Rev.*, **93**, 1911–1922.
- Pettit G., Herald C., Leet J., Gupta R., Schaufelberger D., Bates R., Clewlow P., Doubek D., Manfredi K., Rützler K., Schmidt J., Tackett L., Ward F., Bruck M., Camou F. (1990). Antineoplastic agents. 168. Isolation and structure of axinohydantoin. *Can. J. Chem.*, **68**, 1621–1624.
- Pettit G.R., Cichacz Z.A., Gao F., Herald C.L., Boyed M.R., Schmidt J.M., Hooper J.N.A. (1993). Isolation and structure of spongistatin 1. *J. Org. Chem.*, **58**, 1302–1304.
- Pettit G.R., Herald C.L., Doubek D.L., Herald D.L. (1982). Isolation and structure of bryostatin 1. *J. Am. Chem. Soc.*, **104**, 6846–6848.
- Powell V.H., Sutherland M.D. (1967). Pigments of marine animals. VI. Anthraquinoid pigments of the crinoids *Ptilometra australis* Wilton and *Tropiometra afra* Hartlaub. *Aust. J. Chem.*, **20**, 541–553.
- Proksch P., Ebel R. (1998). Ecological significance of alkaloids from marine invertebrates alkaloids, biochemistry, ecology and medicinal application, Edited by Margaret F. Roberts and Michael Wink, Plenum Publishing, 379–394.
- Proksch P., Edrada R.A., Ebel, R. (2002). Drugs from the seas—current status and microbiological implications. *Appl. Microbiol. Biotechnol.*, **59**, 125–134.
- Qiao H., Hung W., Tremblay E., Wojcik J., Gui J., Ho J., Klassen J., Campling B., Elliot B. (2002). Constitutive activation of met kinase in non-small-cell lung carcinomas correlates with anchorage-independent cell survival. *J. Cell Biochem.*, **86**, 665–677.
- Ravi B.N., Wells R.J., Croft K.D. (1981). Malabaricane triterpenes from a Fijian collection of the sponge *Jaspis stellifera*. *J. Org. Chem.*, **46**, 1998–2001.
- Rideout J.A., Smith N.B., Sutherland M.D. (1979). Chemical defense of crinoids by polyketide sulfates. *Experientia*, **35**, 1273–1274.
- Rinehart K.L., Gloer J.B., Cook J.C., Mizsak S.A., Scahill T.A. (1981). Structures of the didemnins antiviral and cytotoxic depsipeptides from a Caribbean tunicate. *J. Am. Chem. Soc.*, **103**, 1857–1859.
- Rinehart K.L., Kobayashi J., Harbour G.C., Hughes R.G., Jr., Mizsak S.A., Scahill T.A. (1984). Eudistomins C, E, K, and L potent antiviral compounds containing a novel

References

- oxathiazepine ring from the Caribbean tunicate *Eudistoma olivaceum*. *J. Am. Chem. Soc.*, **106**, 1524–26.
- Rodriguez J., Nieto R.M., Crews P. (1993). New structures and bioactivity patterns of bengazole alkaloids from a choristid marine sponge. *J. Nat. Prod.*, **56**, 2034–2040.
- Rowley D.C., Hansen M.S.T., Rhodes D., Sottriffer C.A., Ni H., McCammon J.A., Bushman F.D., Fenical W. (2002). Thalassiolins A–C: new marine-derived inhibitors of HIV cDNA integrase. *Bioorg. Med. Chem.*, **10**, 3619–3625.
- Rubinstein I., Goad L.J. (1974). Occurrence of (24*S*)-24-methylcholesta-5,22-dien-3 β -ol in the diatom *Phaeodactylum tricornutum*. *Phytochemistry*, **13**, 485–487.
- Rudi A., Kashman Y., Benayahu Y., Schleyer M. (1994). Amino acid derivatives from the marine sponge *Jaspis digonoxea*. *J. Nat. Prod.*, **57**, 829–832.
- Sakuma Y., Tanaka J., Higa T. (1987). New naphthopyrone pigments from the crinoid *Comanthus parvicirrus*. *Aust. J. Chem.*, **40**, 1613–1616.
- Sakurai M., Kohno J., Yamamoto K., Okuda T., Nishio M., Kawano K., Ohnuki T. (2002). TMC-256A1 and C1, new inhibitors of IL-4 signal transduction produced by *Aspergillus niger* var *niger* TC 1629. *J. Antibiotics*, **55**, 685–692.
- Schmitz K.J., Grabellus F., Callies R., Otterbach F., Wohlschlaeger J., Levkau B., Kimmig R., Schmid K.W., Baba H.A. (2005). High expression of focal adhesion kinase (p125^{FAK}) in node-negative breast cancer is related to overexpression of HER-2/neu and activated Akt kinase but does not predict outcome. *Breast Cancer Res.*, **7**, R194–R203.
- Scott V.R., Boehme R., Matthews T.R. (1988). New class of antifungal agents: jasplakinolide, a cyclodepsipeptide from the marine sponge, *Jaspis* species. *Antimicrob. Agents Chemother.*, **32**, 1154–1157.
- Searle P.A., Richter R.K., Molinski T.F. (1996). Bengazoles C–G from the sponge *Jaspis* sp. synthesis of the side chain and determination of absolute configuration. *J. Org. Chem.*, **61**, 4073–4079.
- Sharma G., Magdoff-Fairchild B. (1977). Natural products of marine sponges. 7. The constitution of weakly basic guanidine compounds, dibromophakellin and monobromophakellin. *J. Org. Chem.*, **42**, 4118–4124.
- Sharma G.M., Buyer J.S., Pomerantz M.W. (1980). Characterization of a yellow compound isolated from the marine sponge *Phakellia flabellata*. *J. Chem. Soc. Chem. Commun.*, 435–436.
- Sharma V., Lansdell T.A., Jin G., Tepe J.J. (2004). Inhibition of cytokine production by hymenialdisine derivatives. *J. Med. Chem.*, **47**, 3700–3703.

References

- Sheikh Y.M., Djerassi C. (1974). Steroids from sponges. *Tetrahedron*, **30**, 4095–4103.
- Shinde P.B., Lee Y.M., Dang H.T., Hong J., Lee C.-O., Jung J.H. (2008). Cytotoxic bromotyrosine derivatives from a two-sponge association of *Jaspis* sp. and *Poecillastra* sp. *Bioorg. Med. Chem. Lett.*, **18**, 6414–6418.
- Smith I.R., Sutherland M.D. (1971). Pigments of marine animals. XI. Angular naphthopyrones from the crinoids *Comanthus parvicirrus timorensis*. *Aust. J. Chem.*, **24**, 1487–1499.
- Sourvinos G., Tsatsanis C., Spandidos D.A. (1999). Overexpression of the Tpl-2/Cot oncogene in human breast cancer. *Oncogene*, **18**, 4968–4973.
- Staal S.P. (1987). Molecular cloning of the akt oncogene and its human homologues AKT1 and AKT2: Amplification of AKT1 in a primary human gastric adenocarcinoma, *Proc. Natl. Acad. Sci. USA*, **84**, 5034–5037.
- Stoessl A., Unwin C.H., Stothers J.B. (1983). On the biosynthesis of some polyketide metabolites in *Alternaria solani*. ^{13}C and ^2H studies. *Can. J. Chem.*, **61**, 372–377.
- Su B.N., Park E.J., Mbwambo Z.H., Santarsiero B.D., Mesecar A.D., Fong H.H.S., Pezzuto J.M., Kinghorn A.D. (2002). New chemical constituents of *Euphorbia quinquecostata* and absolute configuration assignment by a convenient Mosher ester procedure carried out in NMR tubes. *J. Nat. Prod.*, **65**, 1278–1282.
- Suemitsu R., Ohnishi K., Yanagawase S., Yamamoto K., Yamada Y. (1989). Biosynthesis of macrosporin by *Alternaria porri*. *Phytochemistry*, **28**, 1621–1622.
- Supriyono A., Schwarz B., Wray V., Witte L., Müller W.E.G., van Soest R.W.M., Sumaryono W., Proksch P. (1995). Bioactive alkaloids from the tropical marine sponge *Axinella carteri*. *Z. Naturforsch. C, J. Biosci.*, **50c**, 669–674.
- Sutherland M.D., Wells J.W. (1967). Pigments of marine animals. IV. The anthraquinoid pigments of the crinoids, *Comatula pectinata* and *C. cratera* A.H. Clark. *Aust. J. Chem.*, **20**, 515–533.
- Tannert R., Hu T.-S., Arndt H.-D., Waldmann H. (2009). Solid-phase based total synthesis of jaspilakinolide by ring-closing metathesis. *Chem. Commun.*, **2009**, 1493–1495.
- Thale Z., Kinder F.R., Bair K.W., Bontempo J., Czuchta A.M., Versace R.W., Philips P.E., Sanders M.L., Wattanasin S., Crews P. (2001). Bengamides revisited: new structures and antitumor studies. *J. Org. Chem.*, **66**, 1733–1741.
- Travert N., Al-Mourabi A. (2004). A likely biogenetic gateway linking 2-aminoimidazolinone metabolites of sponges to proline: spontaneous oxidative conversion of the pyrrole-proline-guanidine pseudo-peptide to dispacamide A. *J. Am. Chem. Soc.*, **126**, 10252–10253.

References

- Truchet G., Roche P., Lerouge P., Vasse J., Camut S., de Billy F., Promé J.C., Dénarié J. (1991). Sulfated lipo-oligosaccharide signals of *Rhizobium meliloti* elicit root nodule organogenesis in alfalfa. *Nature*, **351**, 670–673.
- Tsevegsuren N., Edrada R.A., Lin W., Ebel R., Torre C., Ortlepp S., Wray V., Proksch P. (2007). Biologically active natural products from Mongolian medicinal plants *Scorzonera divaricata* and *Scorzonera pseudodivaricata*. *J. Nat. Prod.*, **70**, 962–967.
- Tsuda M., Ishibashi M., Agemi K., Sasaki T., Kobayashi J. (1991). Stelliferins A–F, new antineoplastic isomalabaricane triterpenes from the Okinawan marine sponge *Jaspis stellifera*. *Tetrahedron*, **47**, 2181–2194.
- Tsukamoto S., Kato H., Hirota H., Fusetani N. (1994). Narains: *N,N*-dimethylguanidinium styryl sulfates, metamorphosis inducers of ascidian larvae from a marine sponge *Jaspis* sp. *Tetrahedron Lett.*, **35**, 5873–5874.
- Uemoto H., Tsuda M., Kobayashi J. (1999). Mukanadin A–C, new bromopyrrole alkaloids from marine sponge *Agelas nakamurai*. *J. Nat. Prod.*, **62**, 1581–1583.
- Umeyama A., Ito S., Yuasa E., Arihara S., Yamada T. (1998). A new bromopyrrole alkaloid and the optical resolution of the racemate from the marine sponge *Homaxinella* sp. *J. Nat. Prod.*, **61**, 1433–1434.
- Varin L., Marsolais F., Richard M., Rouleau M. (1997). Biochemistry and molecular biology of plant sulfotransferases. *FASEB J.*, **11**, 517–525.
- Walker R.P., Faulkner D.J. (1981). Sceptrin, an antimicrobial agent from the sponge *Agelas sceptrum*. *J. Am. Chem. Soc.*, **103**, 6772–6773.
- Weichert W., Schmidt M., Gekeler V., Denkert C., Stephan C., Jung K., Loening S., Dietel M., Kristiansen G. (2004). Polo-like kinase 1 is overexpressed in prostate cancer and linked to higher tumor grades. *Prostate*, **60**, 240–245.
- Wender P.A., Hinkle K.W., Koehler M.F.T., Lippa, B. (1999). The rational design of potential chemotherapeutic agents: synthesis of bryostatin analogues. *Med. Res. Rev.*, **19**, 388–407.
- Whitehead R. (1999). Natural Product Chemistry. *Ann. Rep. Prog. Chem. Sec.*, **95B**, 183–205.
- Williams D.H., Faulkner D.J. (1996). Isomers and tautomers of hymenialdisine and debromohymenialdisine. *Nat. Prod. Lett.*, **9**, 57–64.
- Wilson D.M., Puyama M., Fenical W., Pawlik J.R. (1999). Chemical defense of the Caribbean reef sponge *Axinella corrugata* against predatory fishes. *J. Chem. Ecol.*, **25**, 2811–2823.

References

- Wolfender J.L., Queiroz E.F., Hostettmann K. (2005). Phytochemistry in the microgram domain – a LC-NMR perspective. *Magn. Reson. Chem.*, **43**, 697–709.
- Wright J.L.C., McInnes A.G., Shimizu S., Smith D.G., Walter J.A., Idler D., Khalil W. (1978). Identification of C-24 alkyl epimers of marine sterols by ¹³C nuclear magnetic resonance spectroscopy. *Can. J. Chem.*, **56**, 1898–1903.
- Xia G., Kumar S.R., Masood R., Zu S., Reddy R., Krasnaperov V., Quinn D.I., Henshal S.M., Sutherland R.L., Pinski J.K., Daneshmand S., Buscarini M., Stein J.P., Zong C., Broek D., Roy-Burman P., Gill P.S. (2005). EphB4 expression and biological significance in prostate. *Cancer Res.*, **65**, 4623–4632.
- Xu Y.-Z., Yakushijin K., Horne D.A. (1997). Synthesis of C₁₁N₅ marine sponge alkaloids: (±)-hymenine, stevensine, hymenialdisine, and debromohymenialdisine. *J. Org. Chem.*, **62**, 456–464.
- Yu Q., Sicinska E., Geng Y., Ahnstrom M., Zagozdou A., Kong Y., Gardner H., Kiyokawa H., Harris L.N., Stal O., Sicinski P. (2006). Requirement for CDK4 kinase function in breast cancer. *Cancer cell*, **9**, 23–32.
- Zabriskie T.E., Klocke J.A., Ireland C.M., Marcus A.H., Molinski T.F., Faulkner D.J., Xu C., Clardy J.C. (1986). Jaspamide, a modified peptide from a *Jaspis* sponge, with insecticidal and antifungal activity. *J. Am. Chem. Soc.*, **108**, 3123–3124.
- Zabriskie T.M., Ireland C.M. (1989). The isolation and structure of modified bioactive nucleosides from *Jaspis johnstoni*. *J. Nat. Prod.*, **52**, 1353–1356.
- Zhang X., Yee D. (2000). Tyrosine kinase signaling in breast cancer: Insulin-like growth factors and their receptors in breast cancer. *Breast Cancer Res.*, **2**, 170–175.

7. List of abbreviations

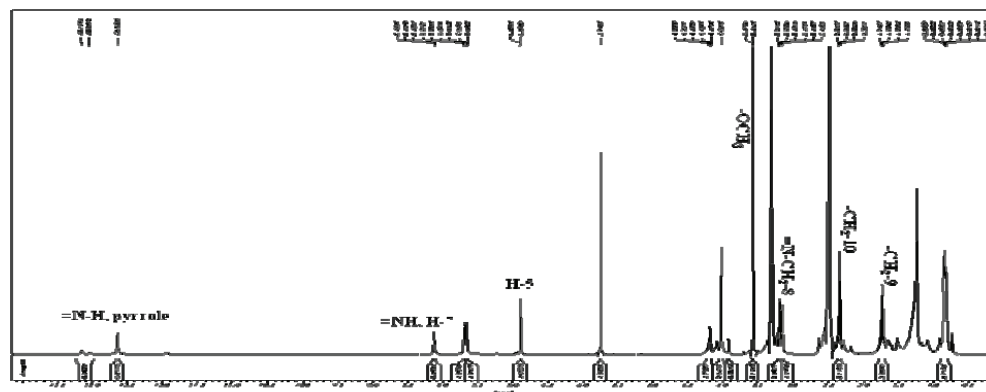
$[\alpha]_D^{20}$	Specific rotation at the sodium D-line
br	Broad signal
CDCl ₃	Deuterated chloroform
CHCl ₃	Chloroform
CI	Chemical ionization
COSY	Correlation spectroscopy
<i>d</i>	Doublet signal
DCM	Dichloromethane
<i>dd</i>	Doublet of doublet signal
DEPT	Distortionless enhancement by polarization transfer
DMSO	Dimethyl sulfoxide
DPPH	2,2-Diphenyl-1-picryl-hydrazyl
ED	Effective dose
EI	Electron impact ionization
ESI	Electron spray ionization
<i>et al.</i>	et altera (and others)
EtOAc	Ethyl acetate
eV	Electron Volt
FAB	Fast atom bombardment
g	Gram
HMBC	Heteronuclear multiple bond connectivity
HMQC	Heteronuclear multiple quantum coherence
H ₂ O	Water
HPLC	High performance liquid chromatography
hr	Hour
HR-MS	High resolution-mass spectrometry
Hz	Hertz
L	Liter
LC	Liquid chromatography
LC-MS	Liquid chromatography-mass spectrometry
<i>m</i>	Multiplet signal
MeOD	Deuterated methanol
MeOH	Methanol

Abbreviations

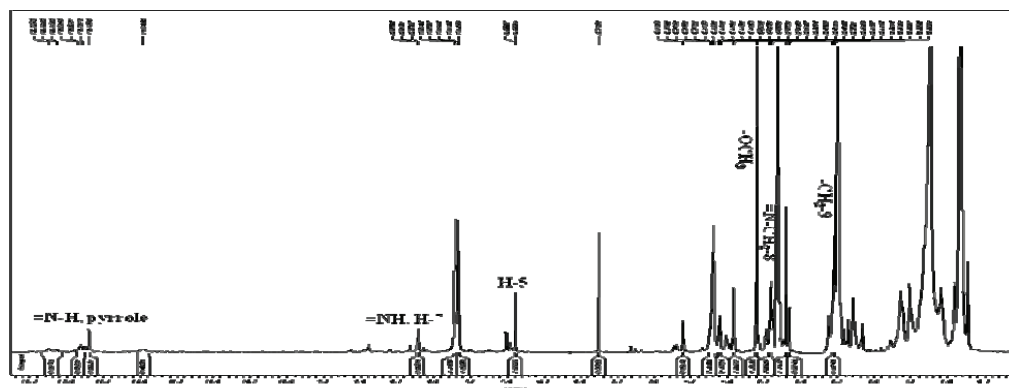
mg	Milligram
MHz	Mega Hertz
min	Minute
mL	Milliliter
MS	Mass spectrometry
MTT	Microculture tetrazolium assay
<i>m/z</i>	Mass per charge
μg	Microgram
μL	Microliter
μM	Micromolar
ng	Nanogram
NMR	Nuclear magnetic resonance
NOE	Nuclear Overhauser effect
NOESY	Nuclear Overhauser and exchange spectroscopy
<i>q</i>	Quartet signal
ROESY	Rotating frame Overhauser enhancement spectroscopy
RP 18	Reversed phase C 18
<i>s</i>	Singlet signal
<i>t</i>	Triplet signal
TFA	Trifluoroacetic acid
TLC	Thin layer chromatography
UV	Ultra-violet
VLC	Vacuum liquid chromatography
<i>n</i> -BuOH	<i>n</i> -Butanol

8. Attachments

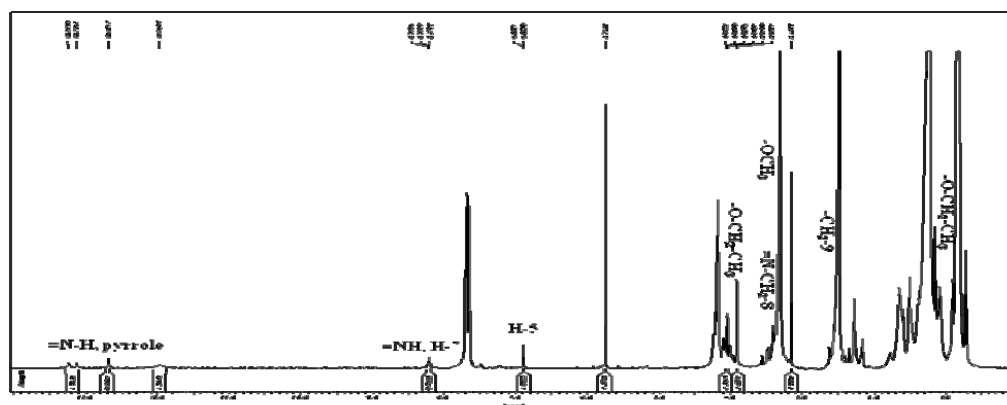
Attachment 1. ^1H NMR spectrum of acanthamide A (1).



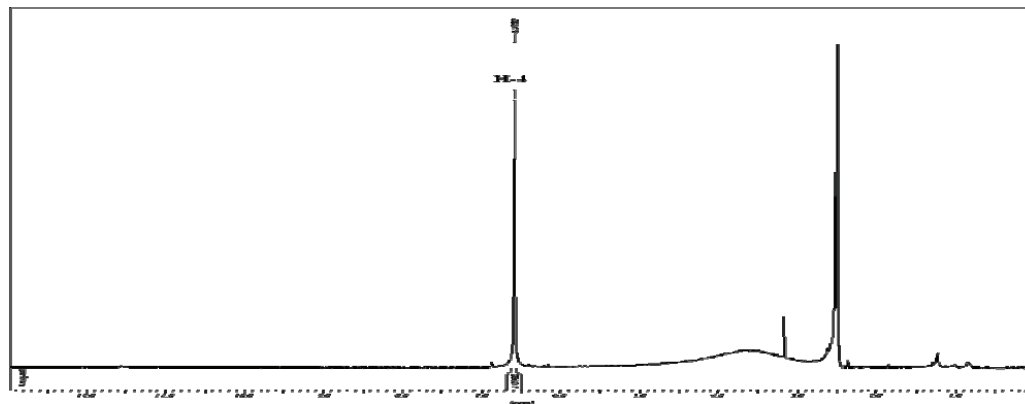
Attachment 2. ^1H NMR spectrum of acanthamide B (2).



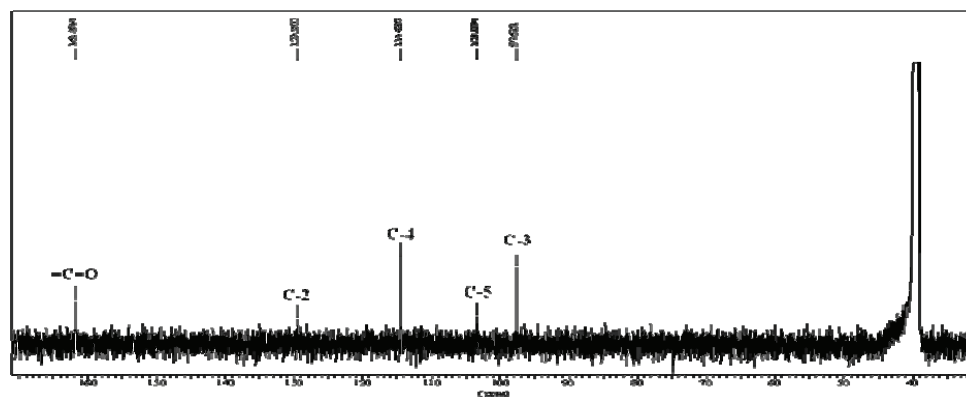
Attachment 3. ^1H NMR spectrum of acanthamide C (3).



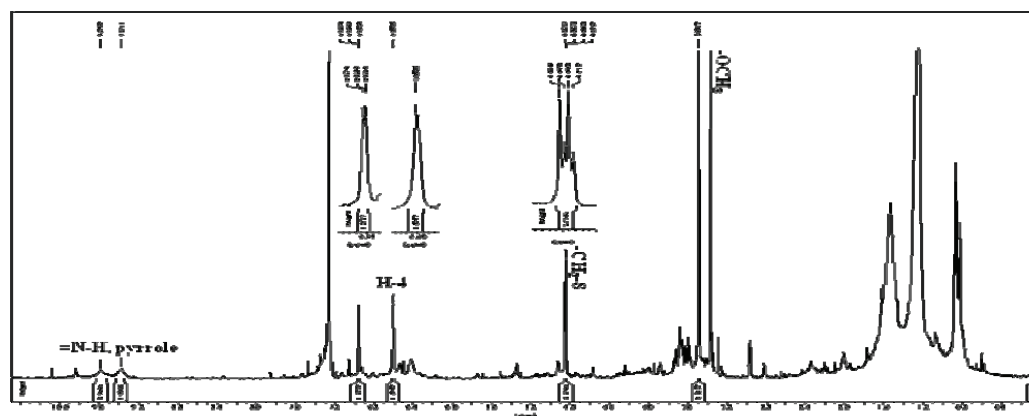
Attachment 7. ^1H NMR spectrum of 3,5-dibromo-1*H*-pyrrole-2-carboxylic acid (6).



Attachment 8. ^{13}C NMR spectrum of 3,5-dibromo-1*H*-pyrrole-2-carboxylic acid (6).

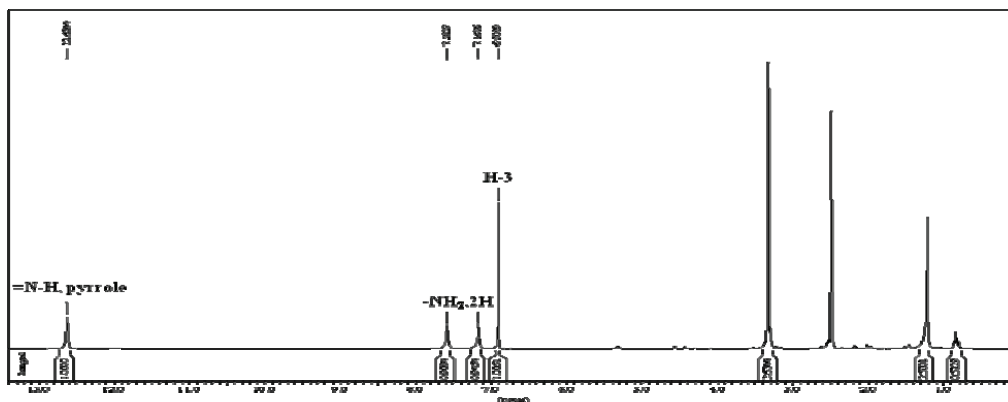


Attachment 9. ^1H NMR spectrum of 4,5-dibromo-*N*-(methoxymethyl)-1*H*-pyrrole-2-carboxamide (7).

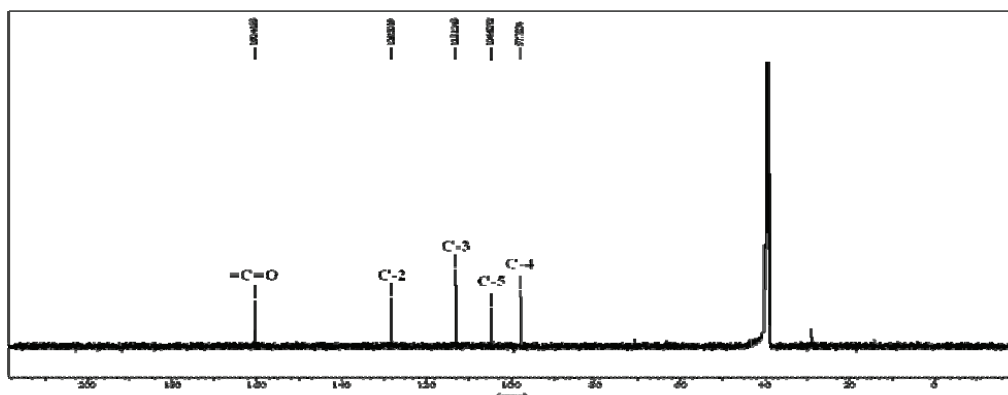


Attachments

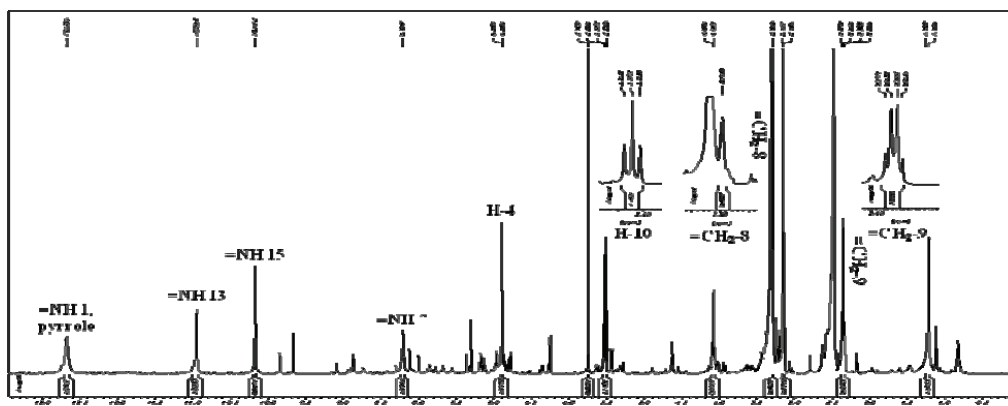
Attachment 10. ^1H NMR spectrum of 4,5-dibromo-1*H*-pyrrole-2-carboxamide (8).



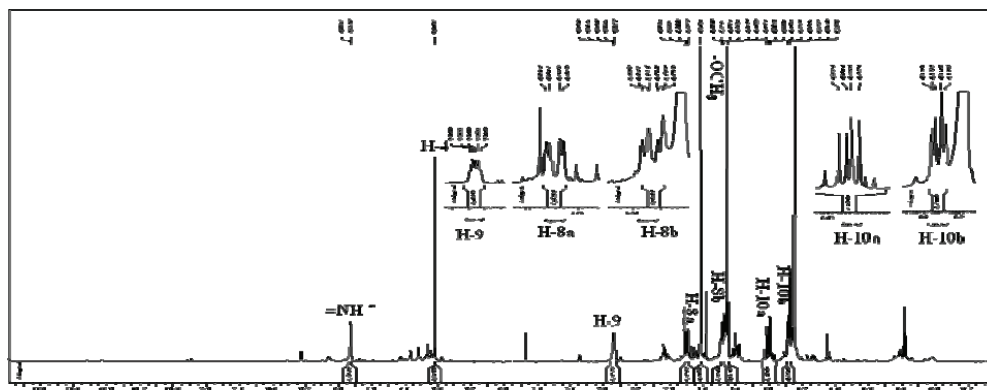
Attachment 11. ^{13}C NMR spectrum of 4,5-dibromo-1*H*-pyrrole-2-carboxamide (8).



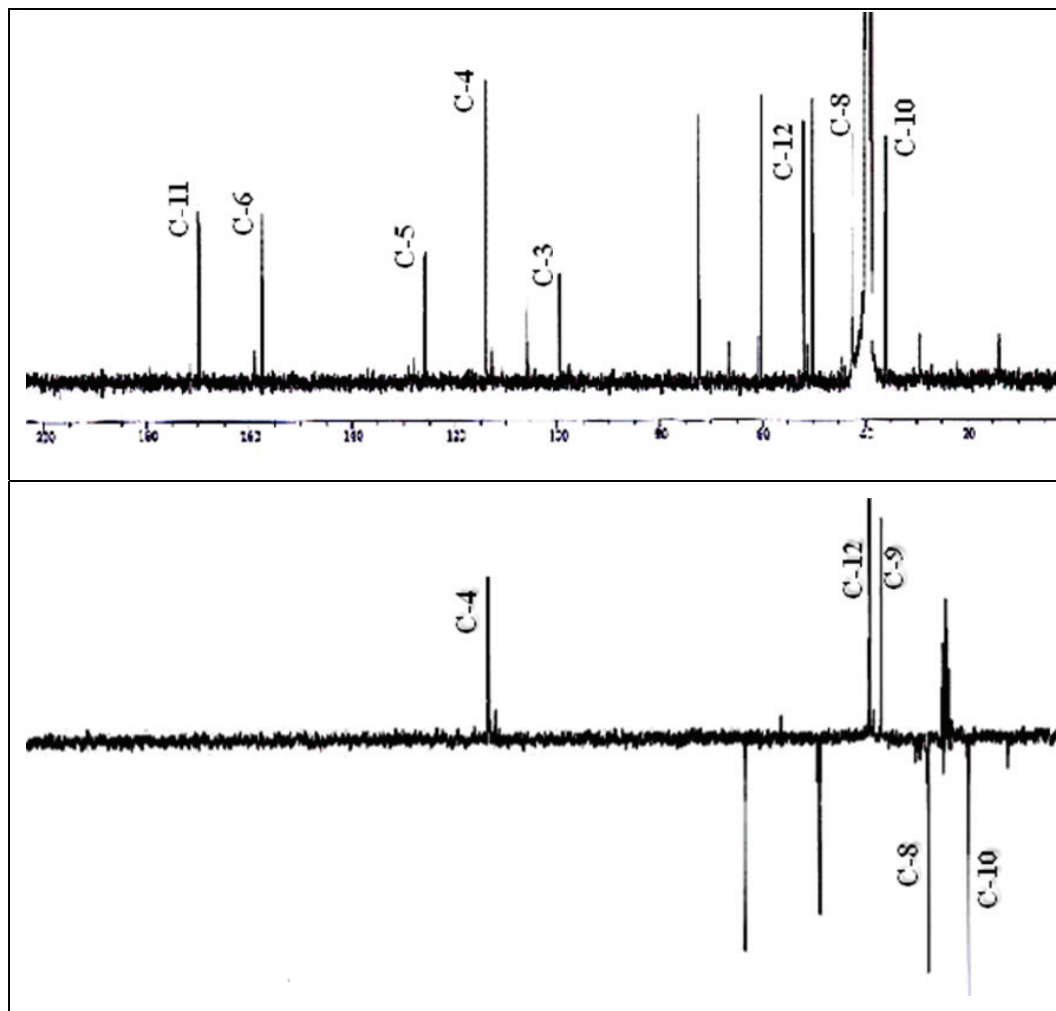
Attachment 12. ^1H NMR spectrum of mukanadin D (9).



Attachment 13. ^1H NMR spectrum of (\pm)-longamide B methyl ester (10).

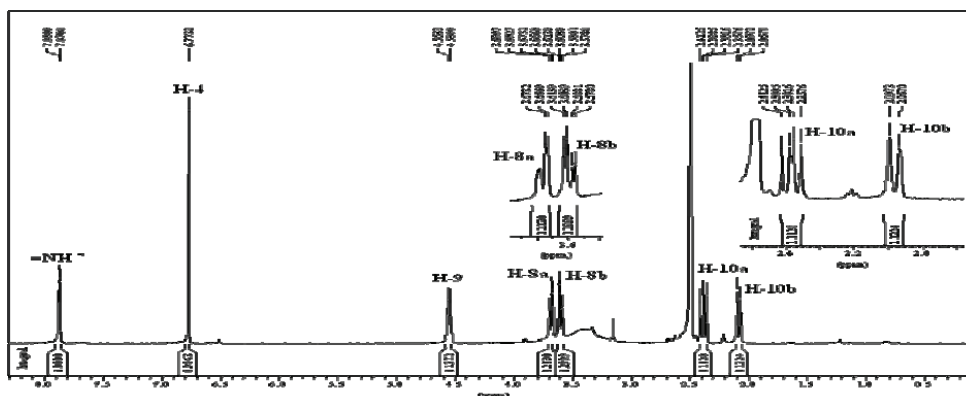


Attachment 14. ^{13}C NMR and DEPT spectra of (\pm)-longamide B methyl ester (10).

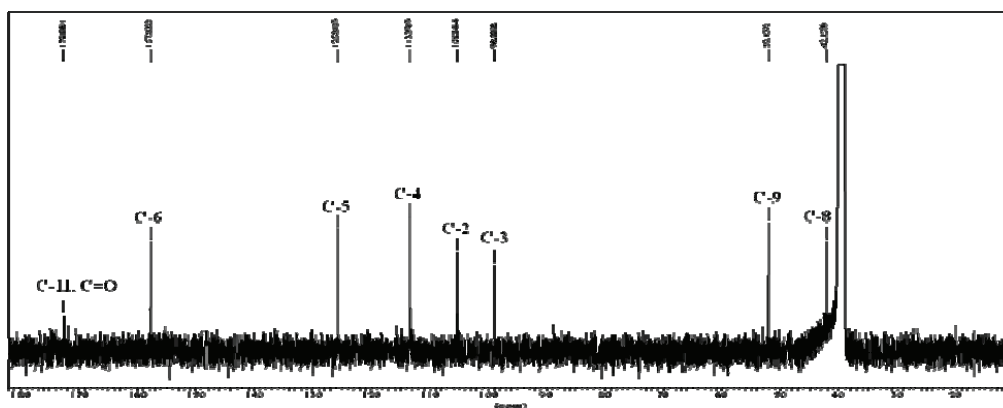


Attachments

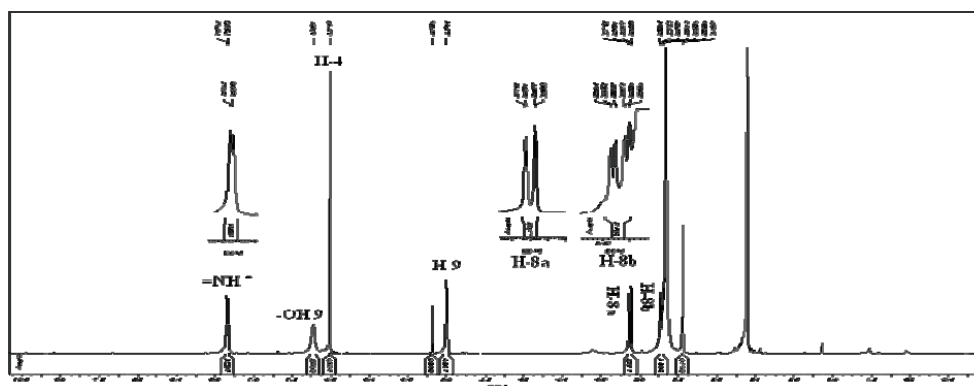
Attachment 15. ^1H NMR spectrum of (\pm)-longamide B (11).



Attachment 16. ^{13}C NMR spectrum of (\pm)-longamide B (11).

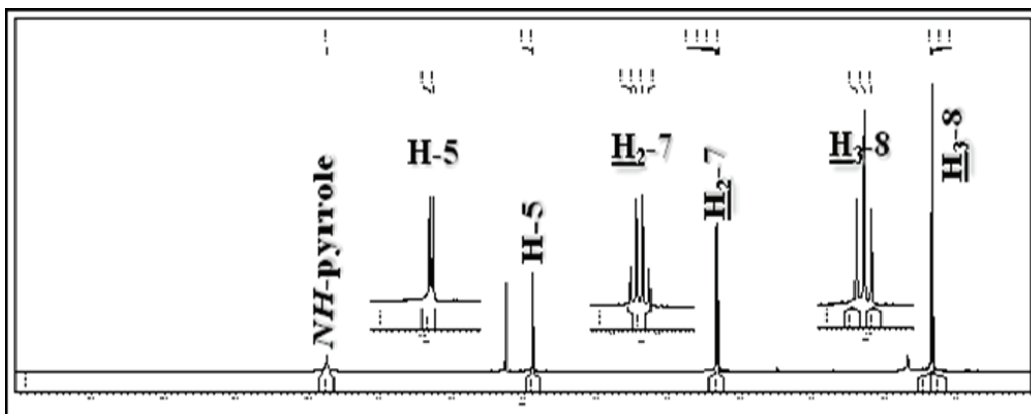


Attachment 17. ^1H NMR spectrum of (\pm)-longamide (12).

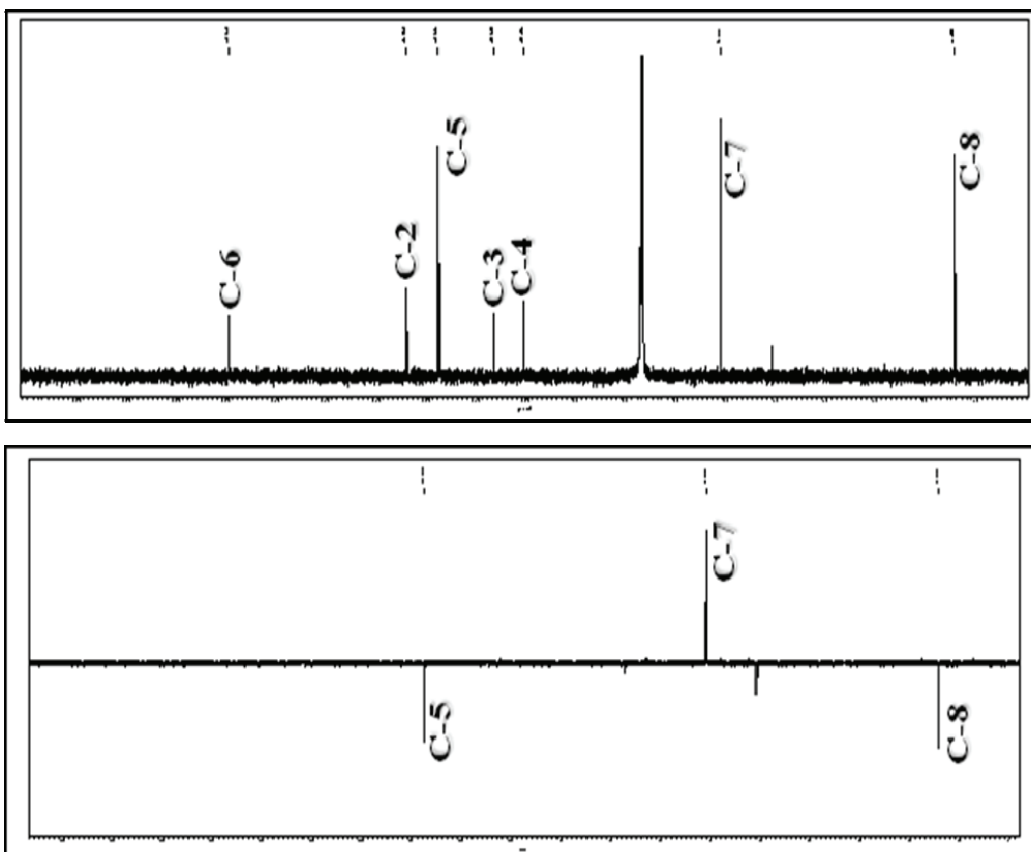


Attachments

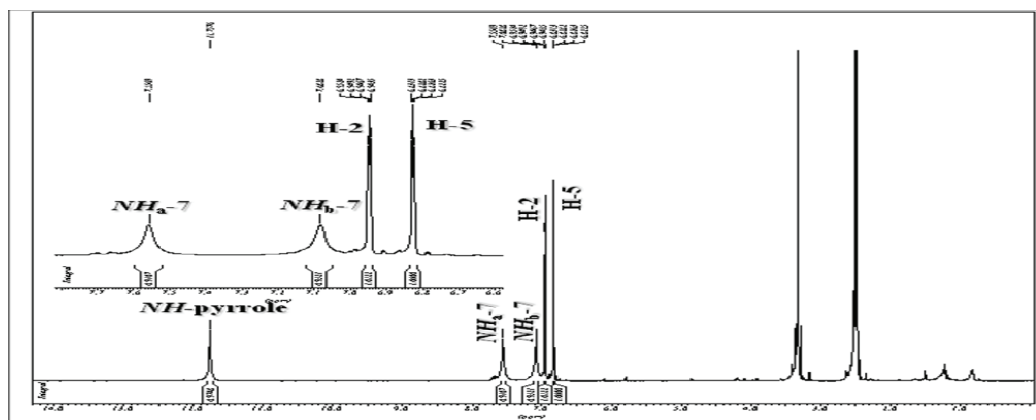
Attachment 21. ^1H NMR spectrum of ethyl 3,4-dibromo-1*H*-pyrrole-2-carboxylate (**15**).



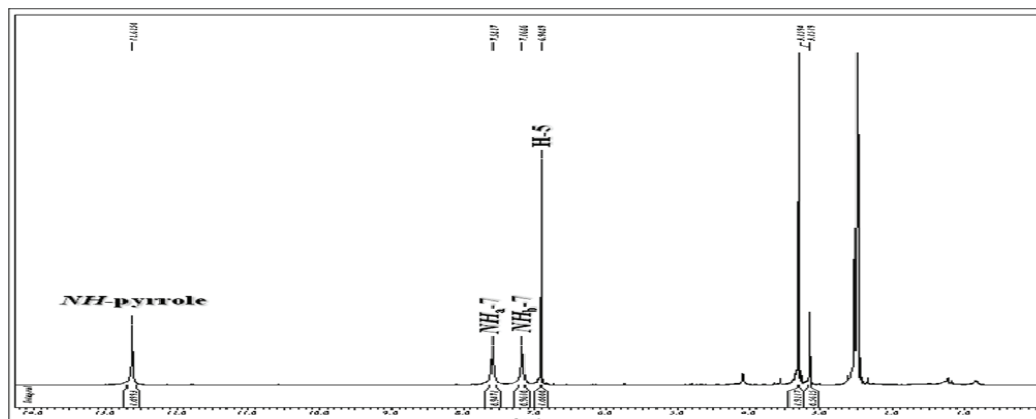
Attachment 22. ^{13}C NMR and DEPT of ethyl 3,4-dibromo-1*H*-pyrrole-2-carboxylate (**15**).



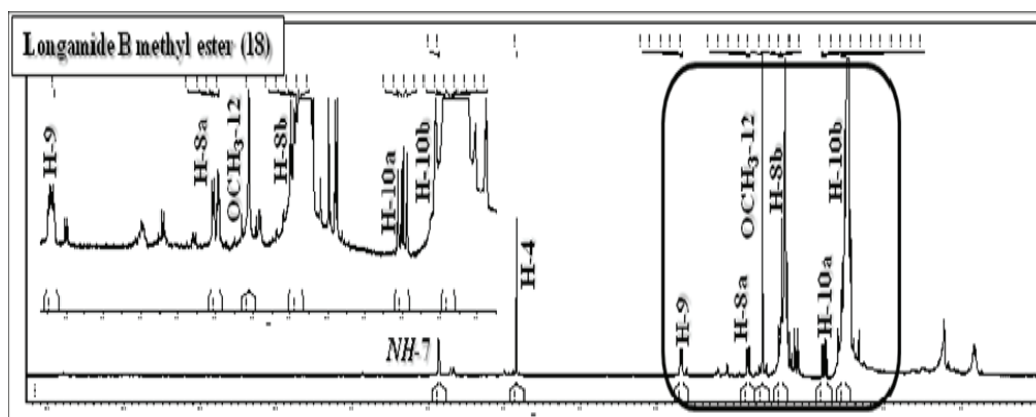
Attachment 23. ^1H NMR spectrum of 4-bromo-1*H*-pyrrole-3-carboxamide (16).



Attachment 24. ^1H NMR spectrum of 3,4-dibromo-1*H*-pyrrole-2-carboxamide (17).

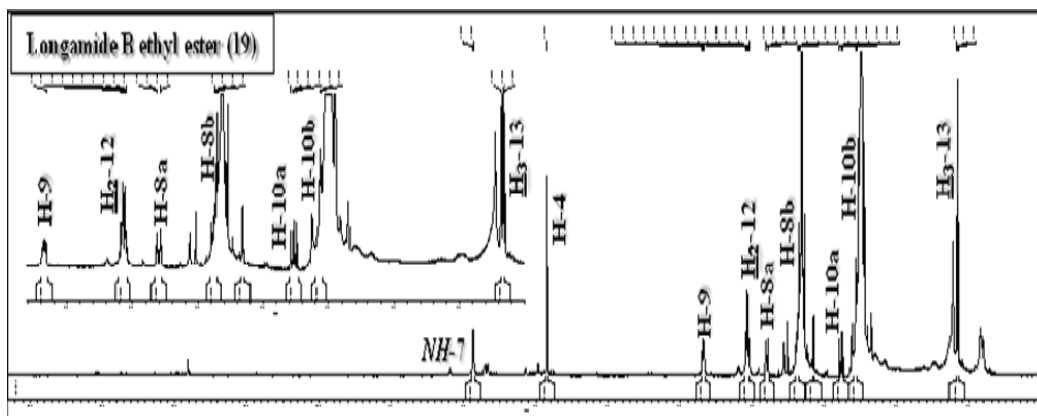


Attachment 25. ^1H NMR spectrum of (-)-longamide B methyl ester (18).

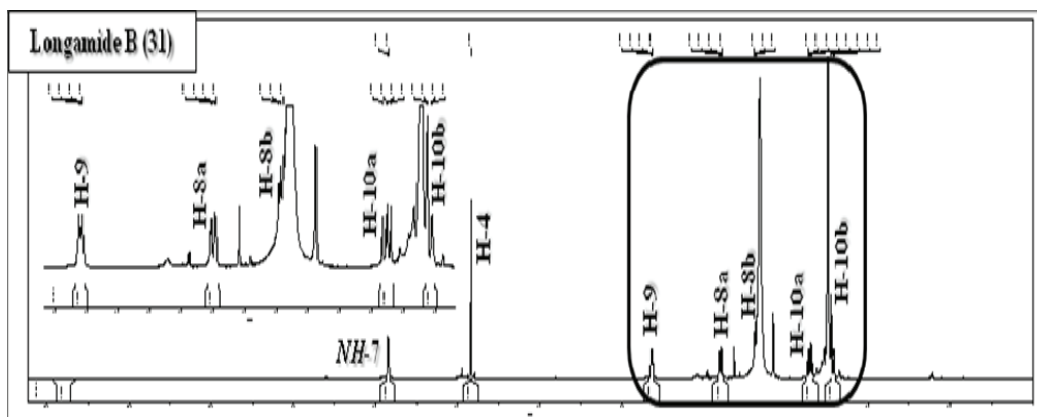


Attachments

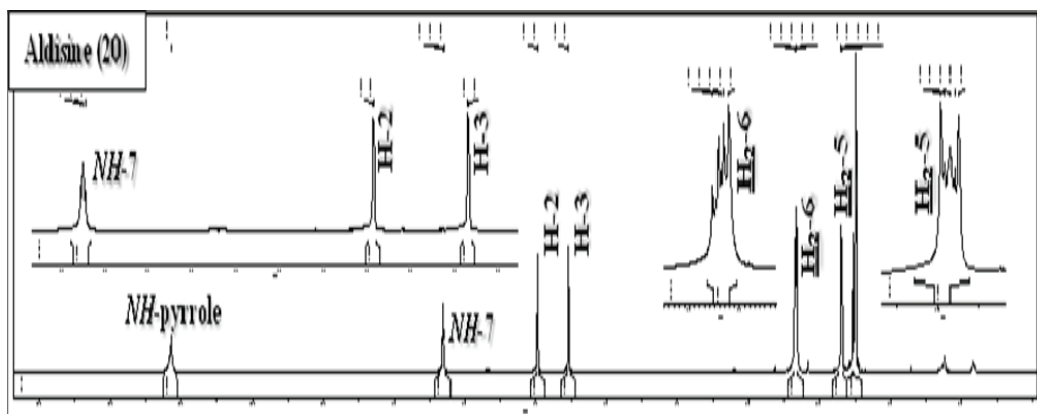
Attachment 26. ^1H NMR spectrum of (-)-longamide B ethyl ester, hanishin (**19**).



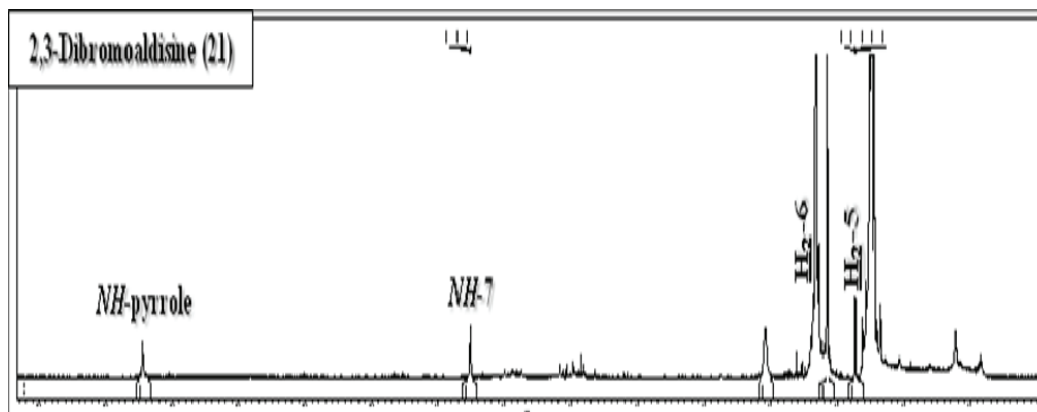
Attachment 27. ^1H NMR spectrum of (-)-longamide B (**31**).



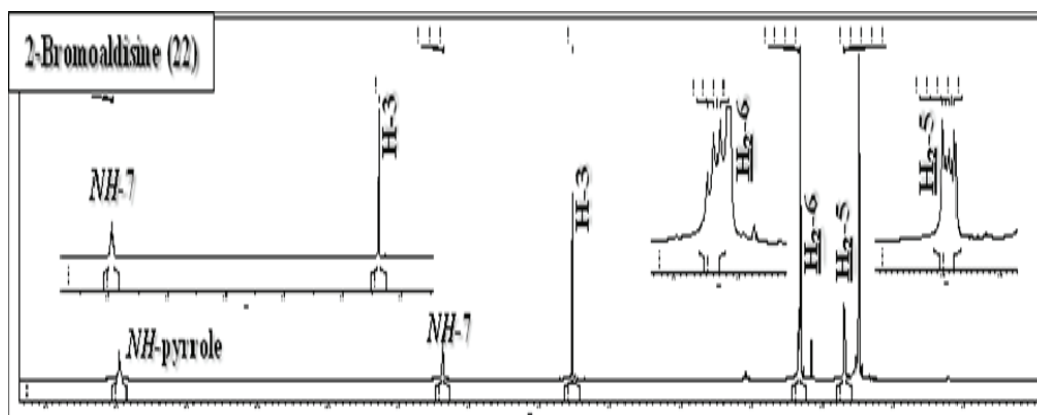
Attachment 28. ^1H NMR spectrum of aldisine (**20**).



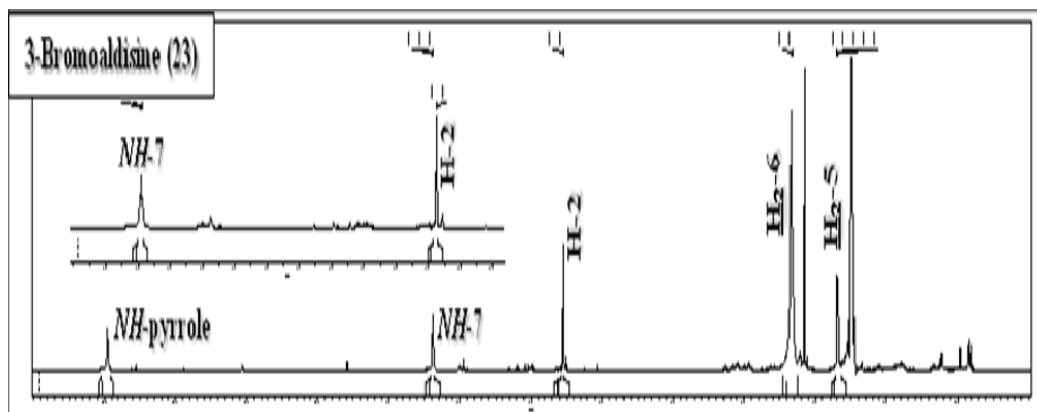
Attachment 29. ^1H NMR spectrum of 2,3-dibromoaldisine (21).



Attachment 30. ^1H NMR spectrum of 2-bromoaldisine (22).

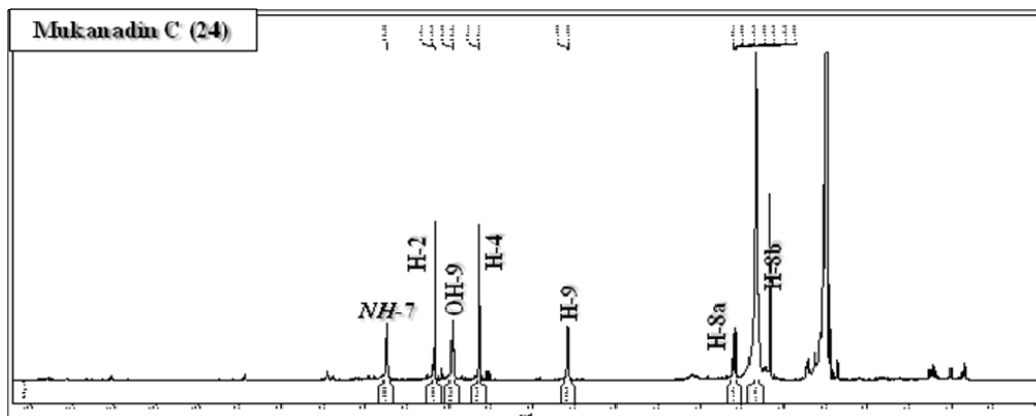


Attachment 31. ^1H NMR spectrum of 3-bromoaldisine (23).

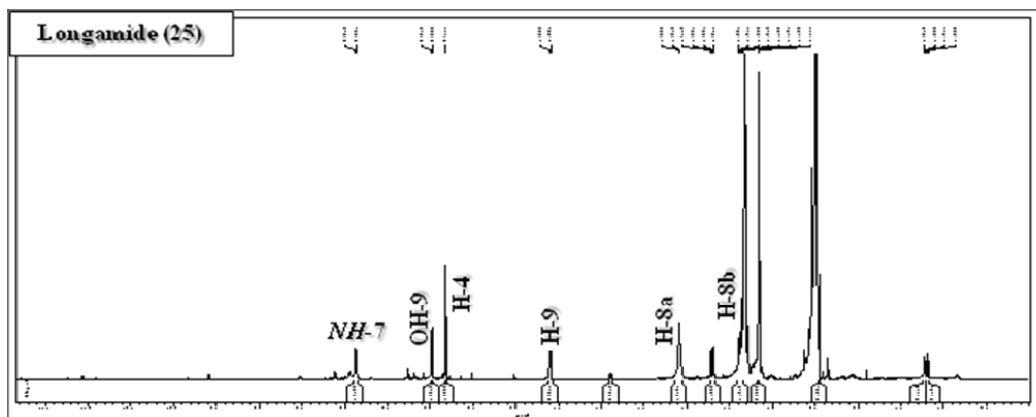


Attachments

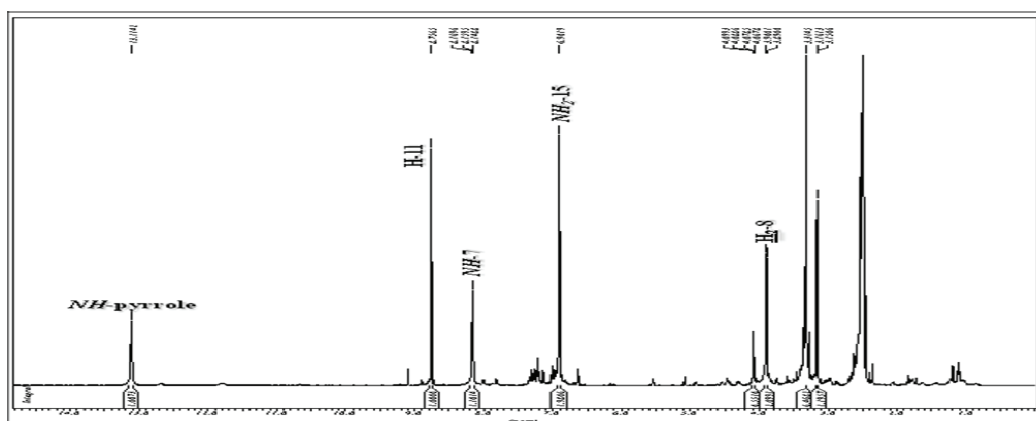
Attachment 32. ^1H NMR spectrum of (-)-mukanadin C (24).



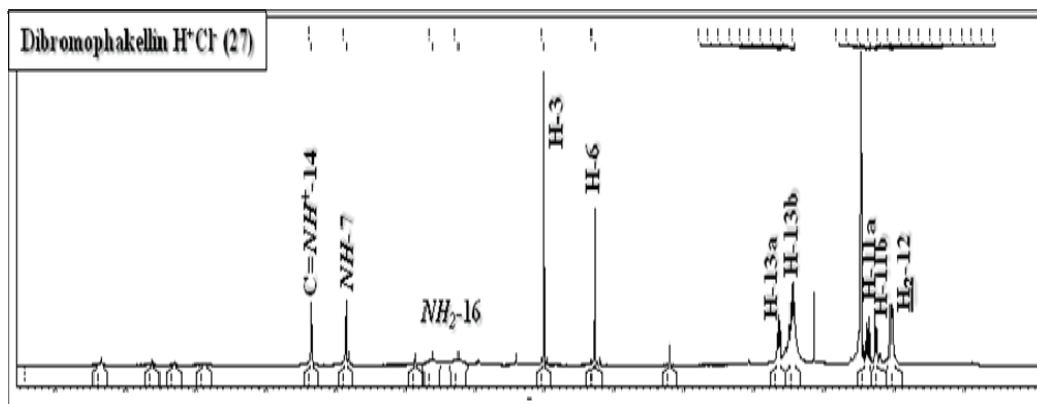
Attachment 33. ^1H NMR spectrum of (-)-longamide (25).



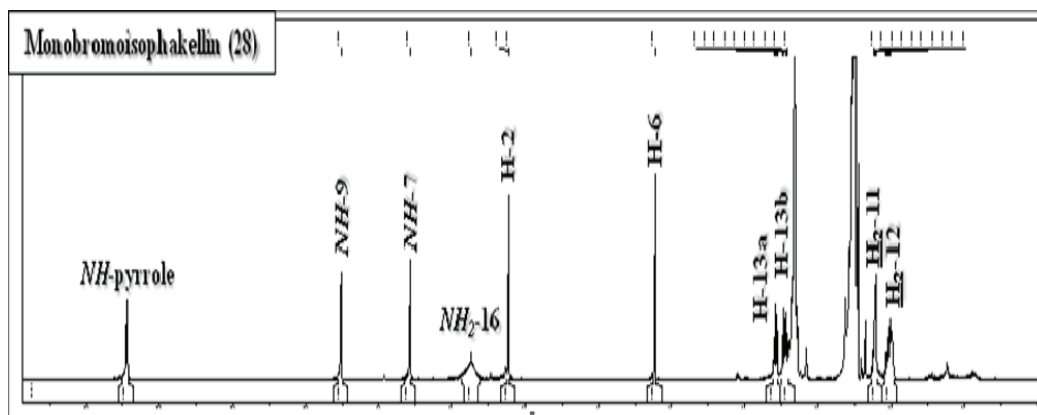
Attachment 34. ^1H NMR spectrum of latonduine A (26).



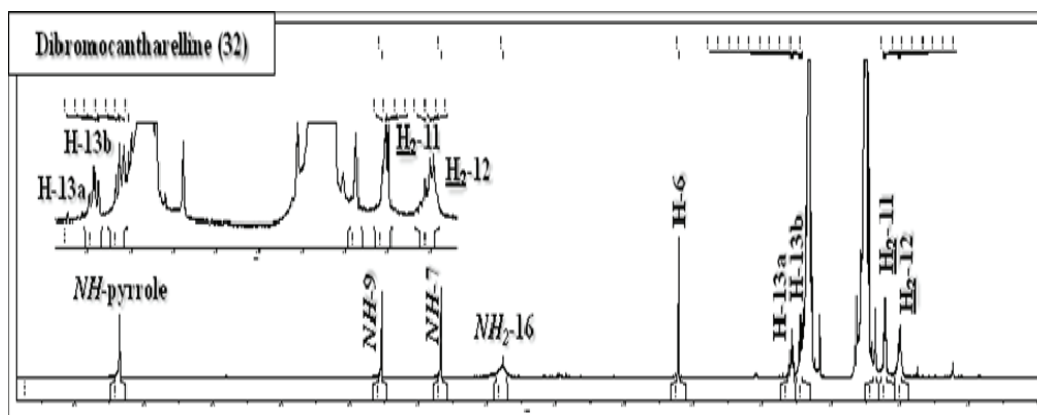
Attachment 35. ^1H NMR spectrum of (-)-dibromophakellin H^+Cl^- (27).



Attachment 36. ^1H NMR spectrum of (-)-monobromoisophakellin (28).

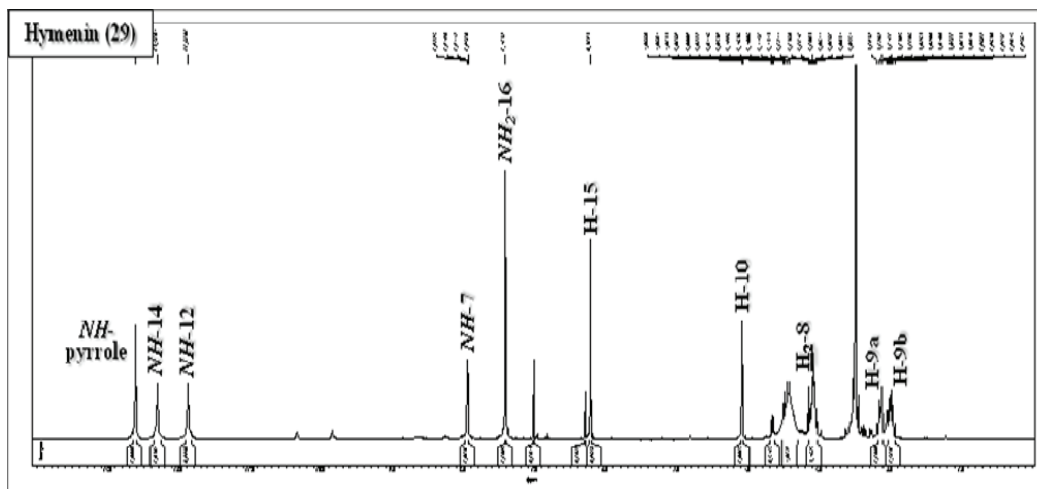


Attachment 37. ^1H NMR spectrum of (-)-dibromocantharelline (32).

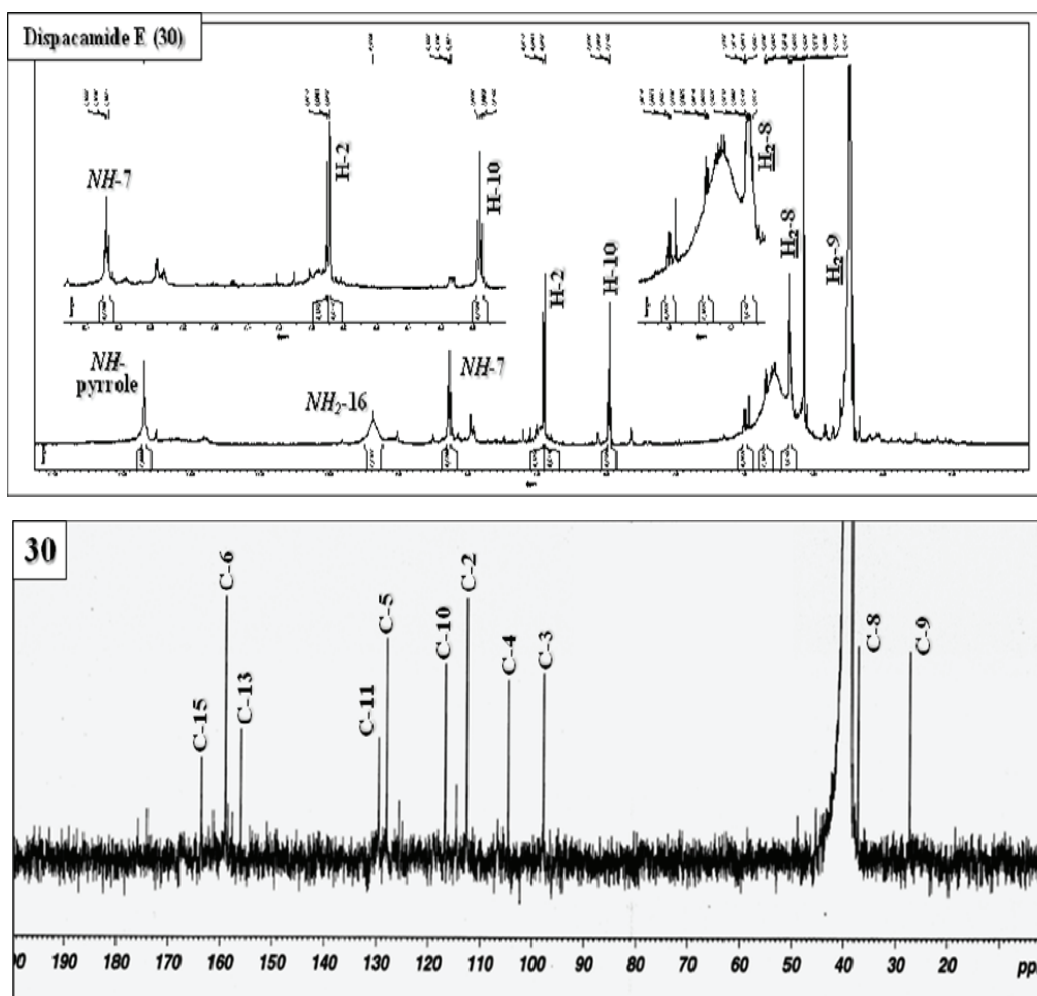


Attachments

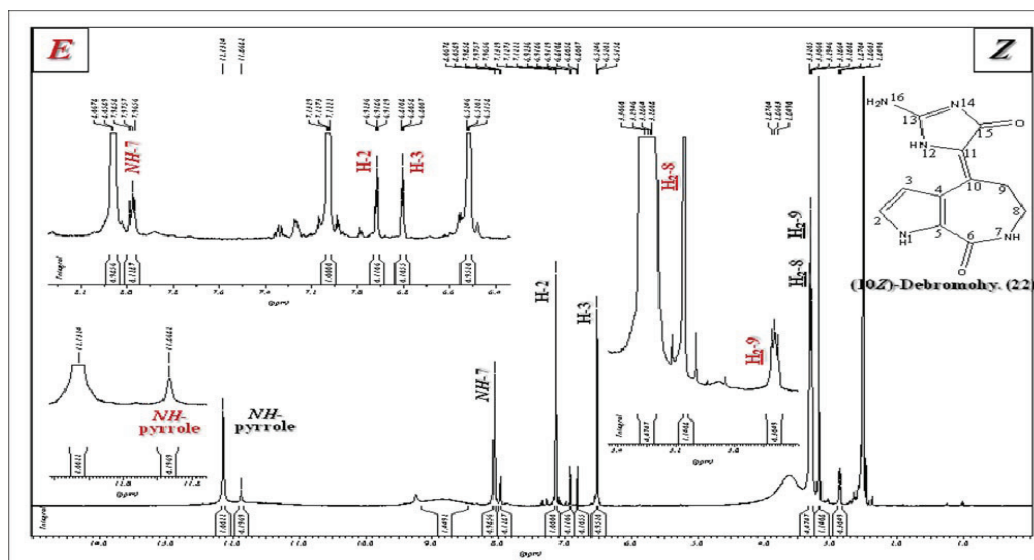
Attachment 38. ^1H NMR spectrum of (-)-hymenine (29).



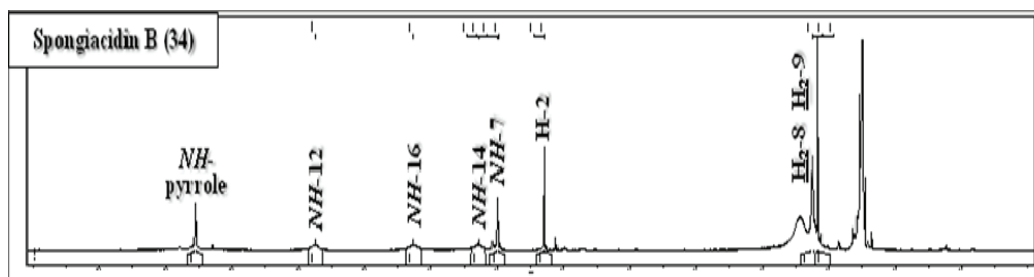
Attachment 39. ^1H NMR and ^{13}C NMR spectra of dispacamide E (30).



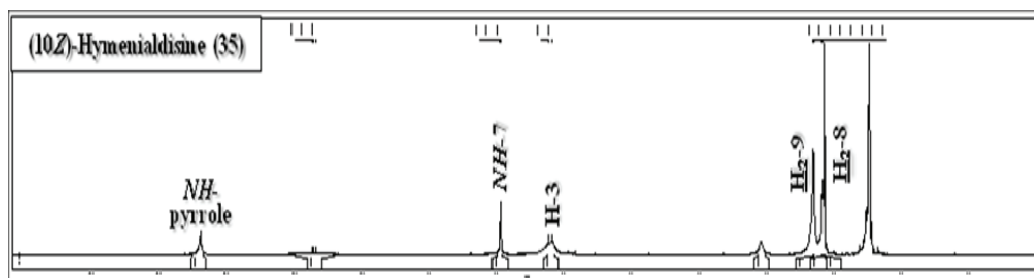
Attachment 40. ^1H NMR spectrum of (10*Z*)-debromohymenialdisine (33).



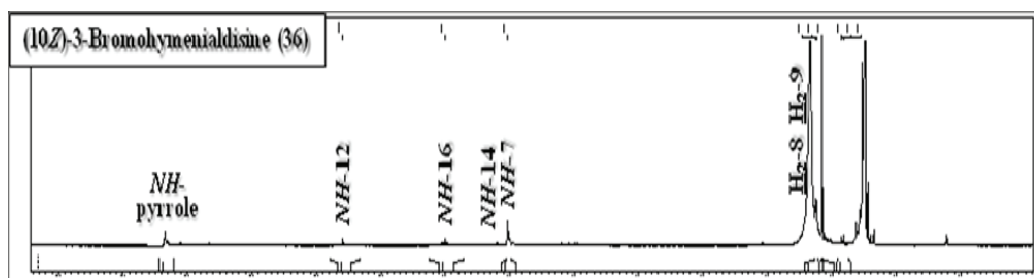
Attachment 41. ^1H NMR spectrum of spongiacidin B (34).



Attachment 42. ^1H NMR spectrum of (10*Z*)-hymenialdisine (35).

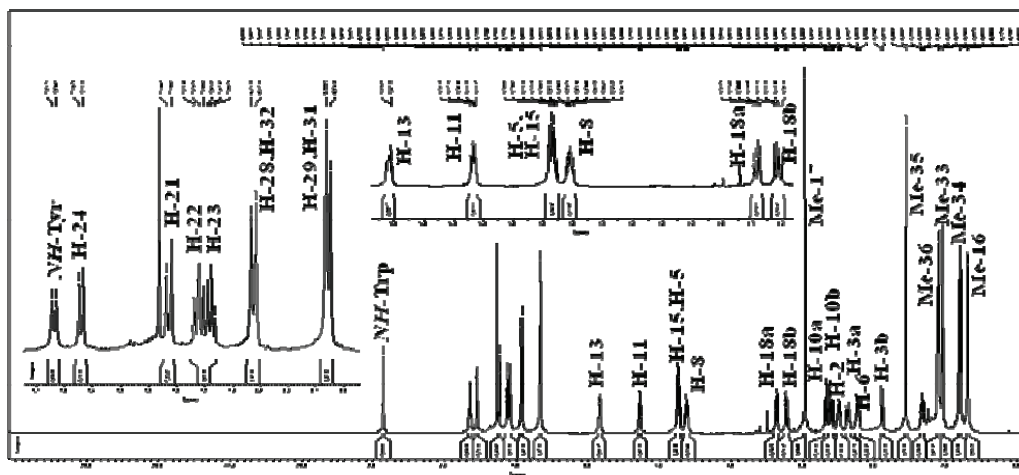


Attachment 43. ^1H NMR spectrum of (10*Z*)-3-bromohymenialdisine (36).

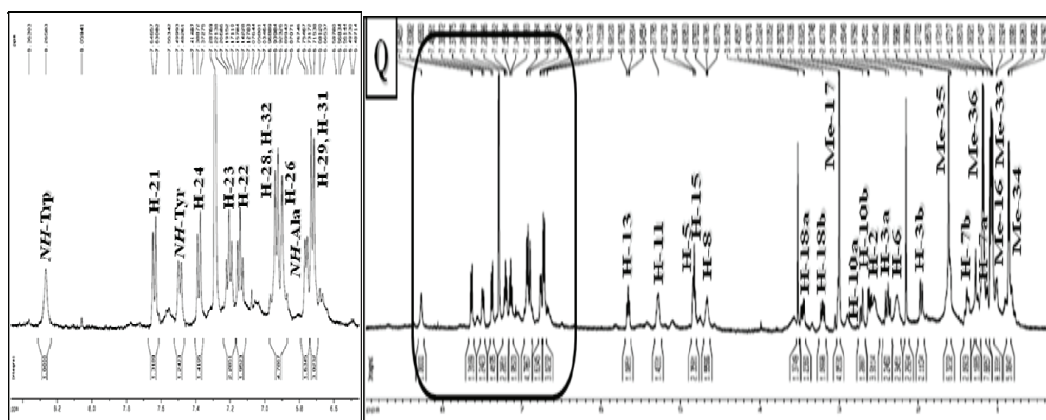


Attachments

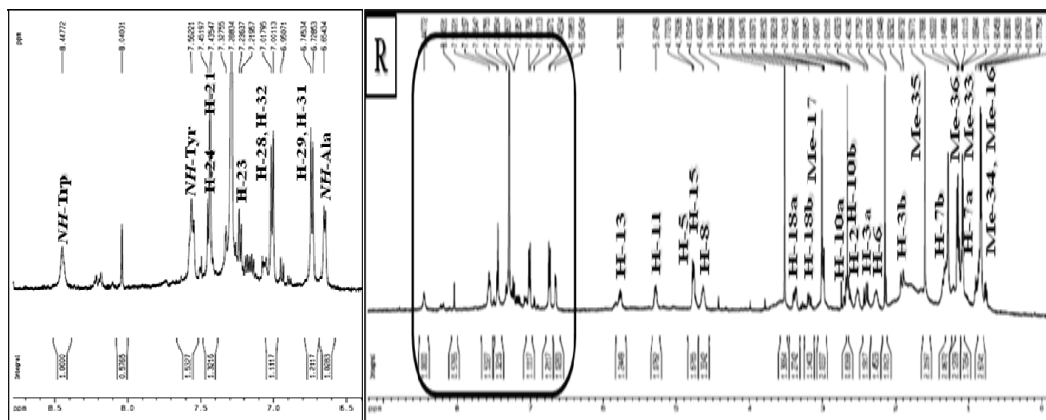
Attachment 44. ^1H NMR spectrum of jaspamide (37).



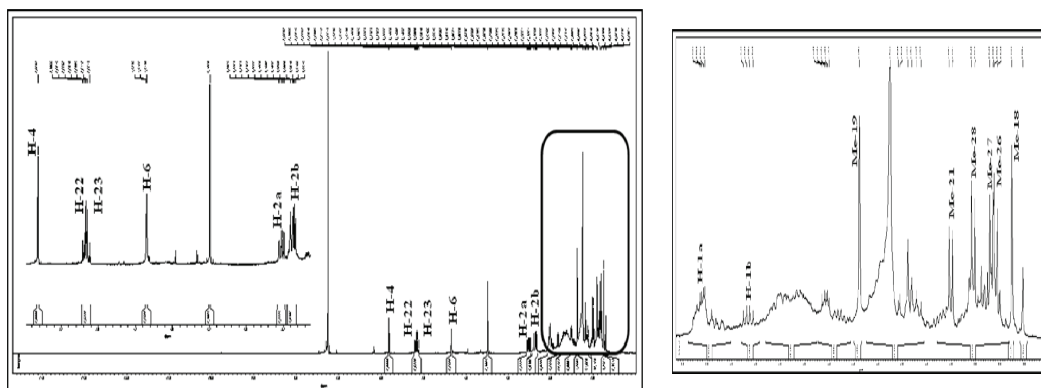
Attachment 45. ^1H NMR spectrum of jaspamide Q (38).



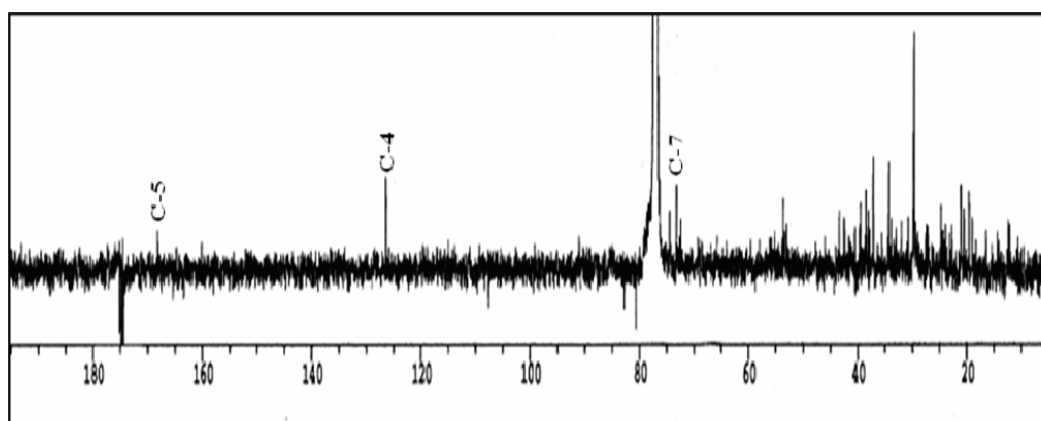
Attachment 46. ^1H NMR spectrum of jaspamide R (39).



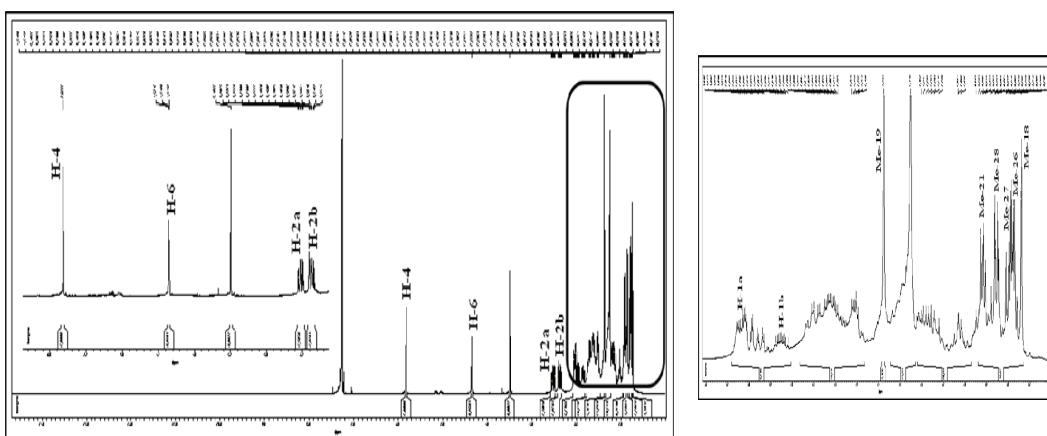
Attachment 47. ^1H NMR spectrum of 6β -hydroxy-24-methylcholesta-4,22-dien-3-one (40).



Attachment 48. ^{13}C NMR spectrum of 6β -hydroxy-24-methylcholesta-4,22-dien-3-one (40).

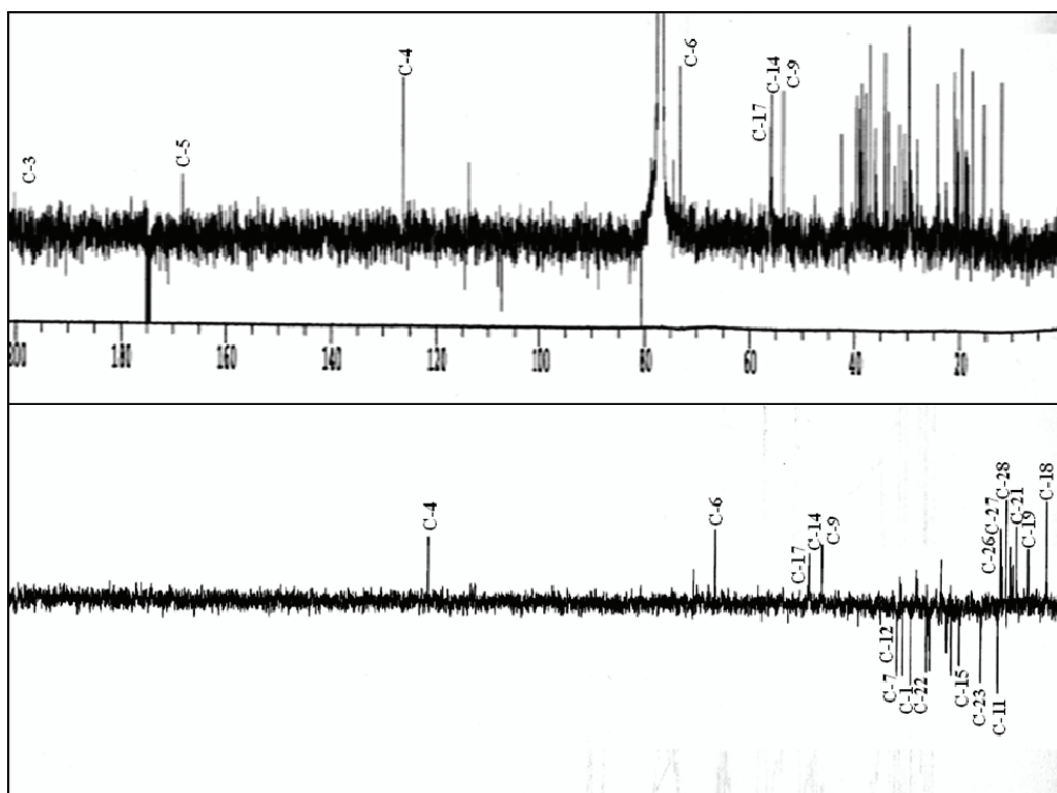


Attachment 49. ^1H NMR spectrum of 6β -hydroxy-24-methylcholesta-4-en-3-one (41).

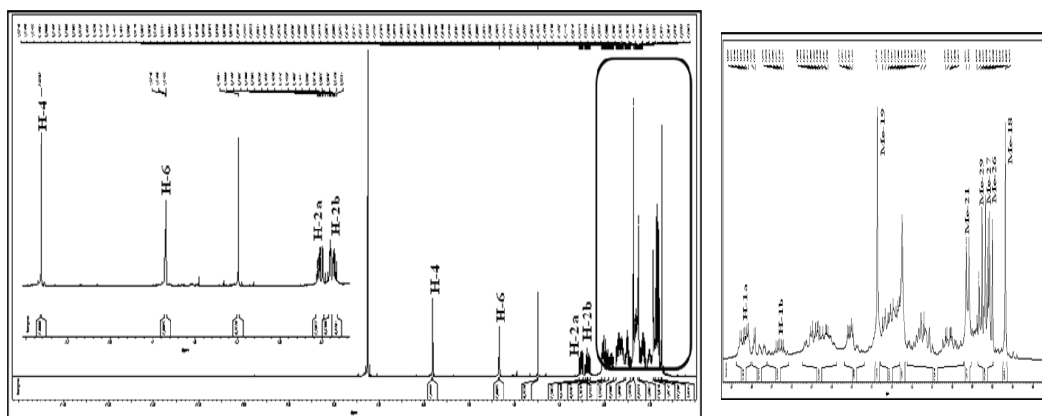


Attachments

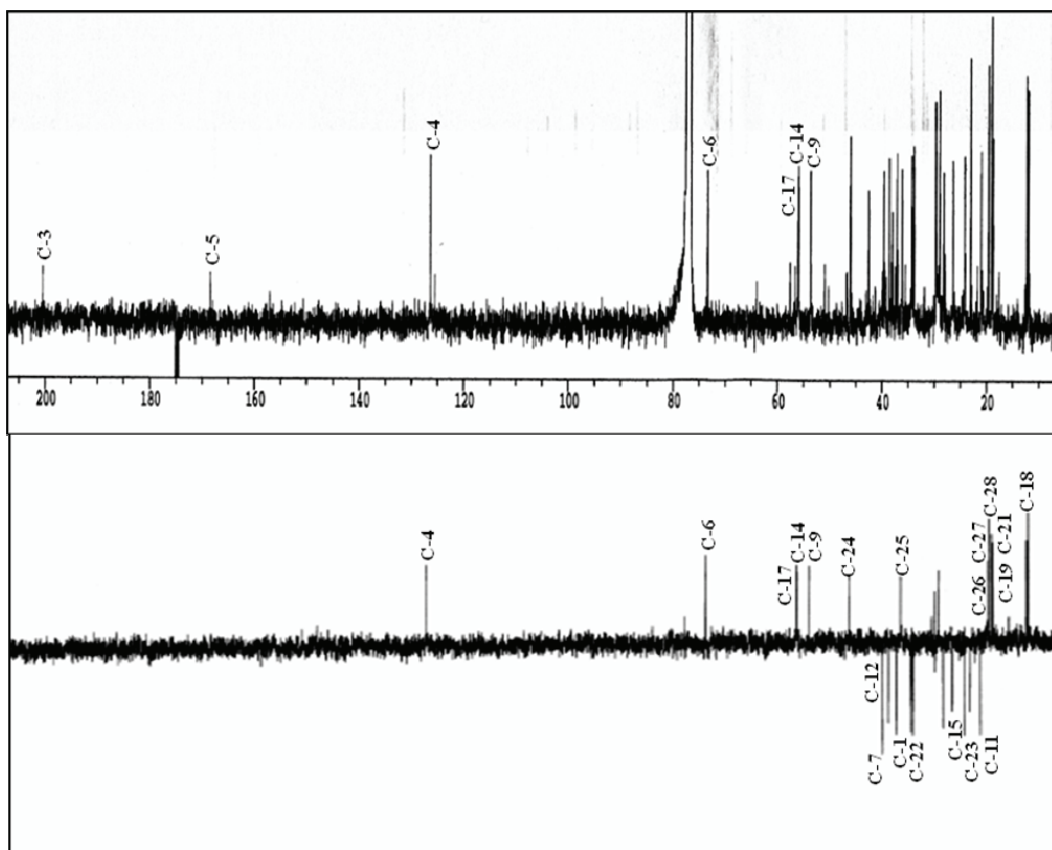
Attachment 50. ^{13}C NMR and DEPT spectra of 6β -hydroxy-24-methylcholesta-4-en-3-one (**41**).



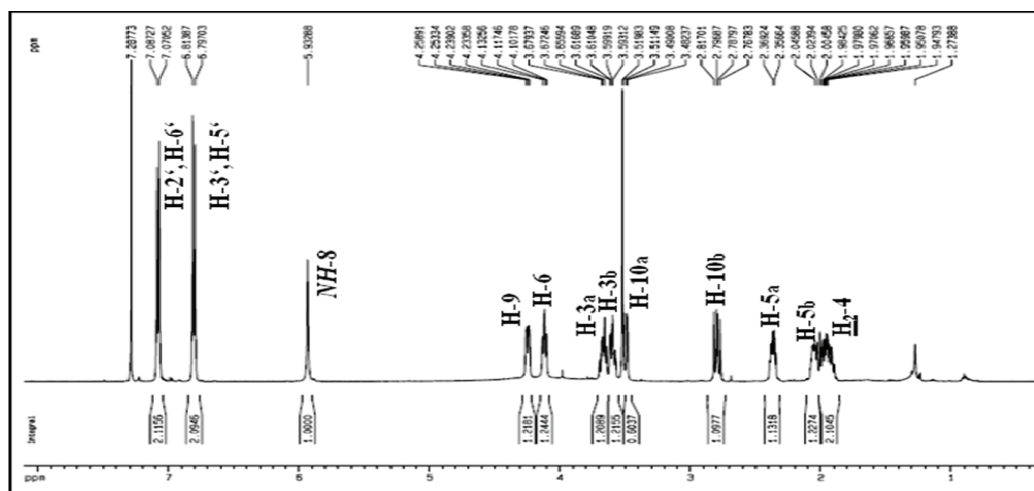
Attachment 51. ^1H NMR spectrum of 6β -hydroxy-24-ethylcholesta-4-en-3-one (**42**).



Attachment 52. ^{13}C NMR and DEPT spectra of 6β -hydroxy-24-ethylcholesta-4-en-3-one (42).

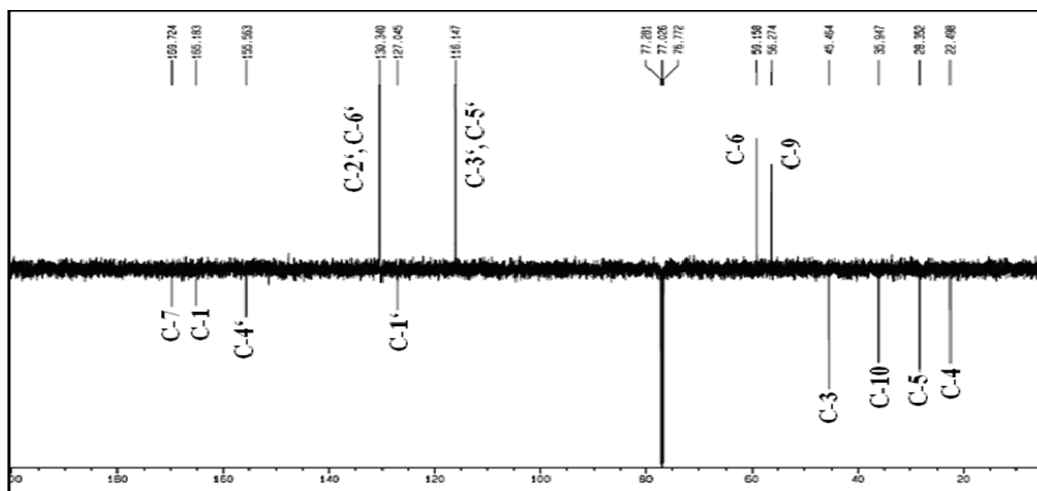


Attachment 53. ^1H NMR spectrum of maculosin-1 (*cyclo*-L-Pro-L-Tyr) (43).

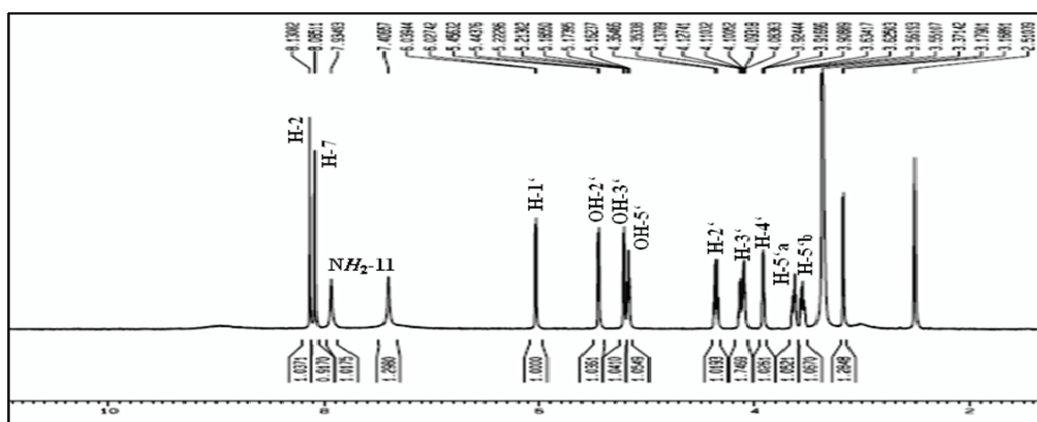


Attachments

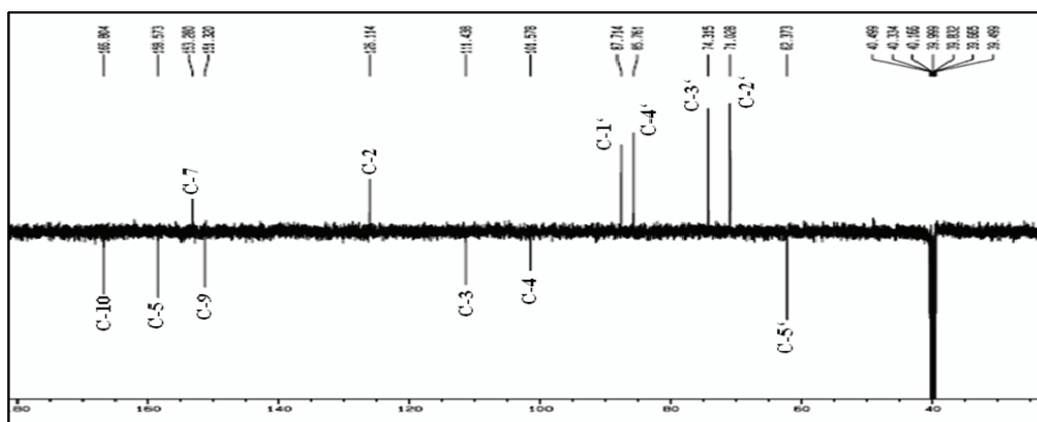
Attachment 54. APT spectrum of maculosin-1 (*cyclo*-L-Pro-L-Tyr) (43).



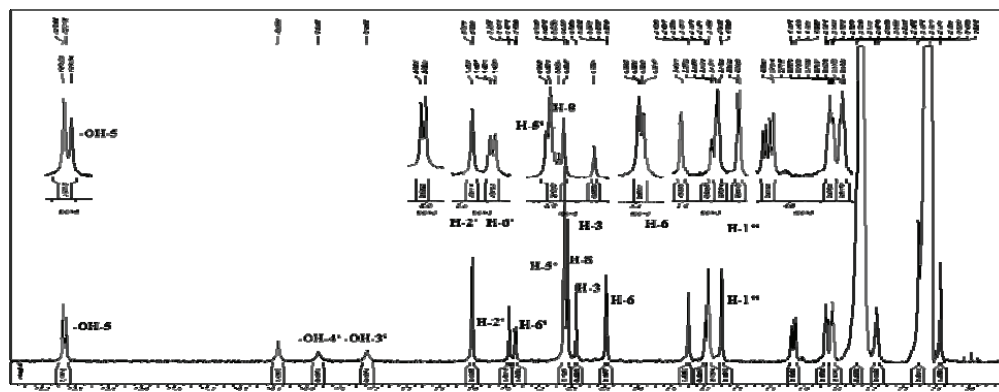
Attachment 55. ¹H NMR spectrum of sangivamycin (44).



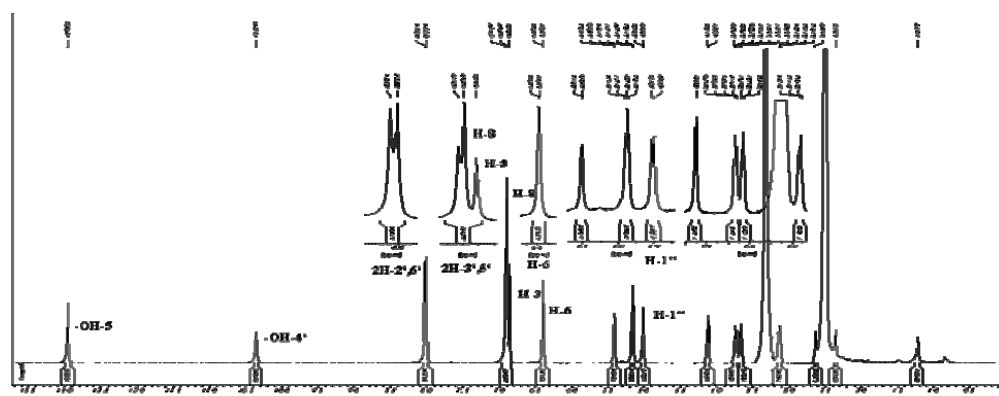
Attachment 56. APT spectrum of sangivamycin (44).



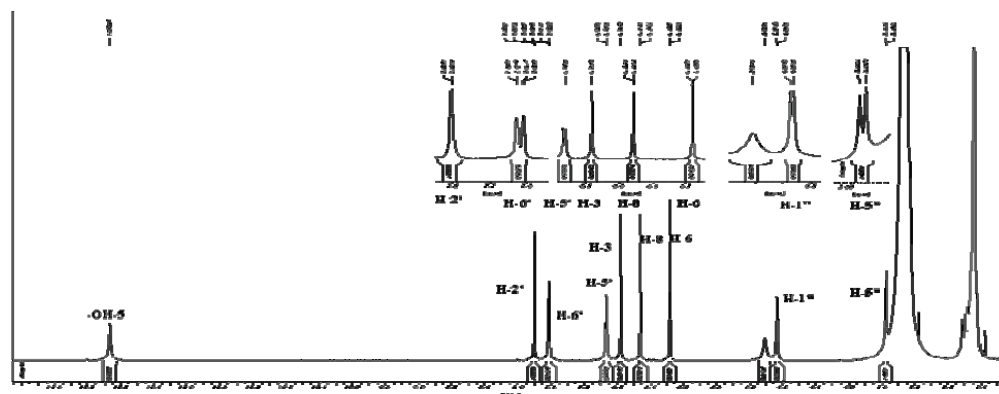
Attachment 57. ^1H NMR spectrum of thalassiolin A(45).



Attachment 58. ^1H NMR spectrum of thalassiolin C (46).

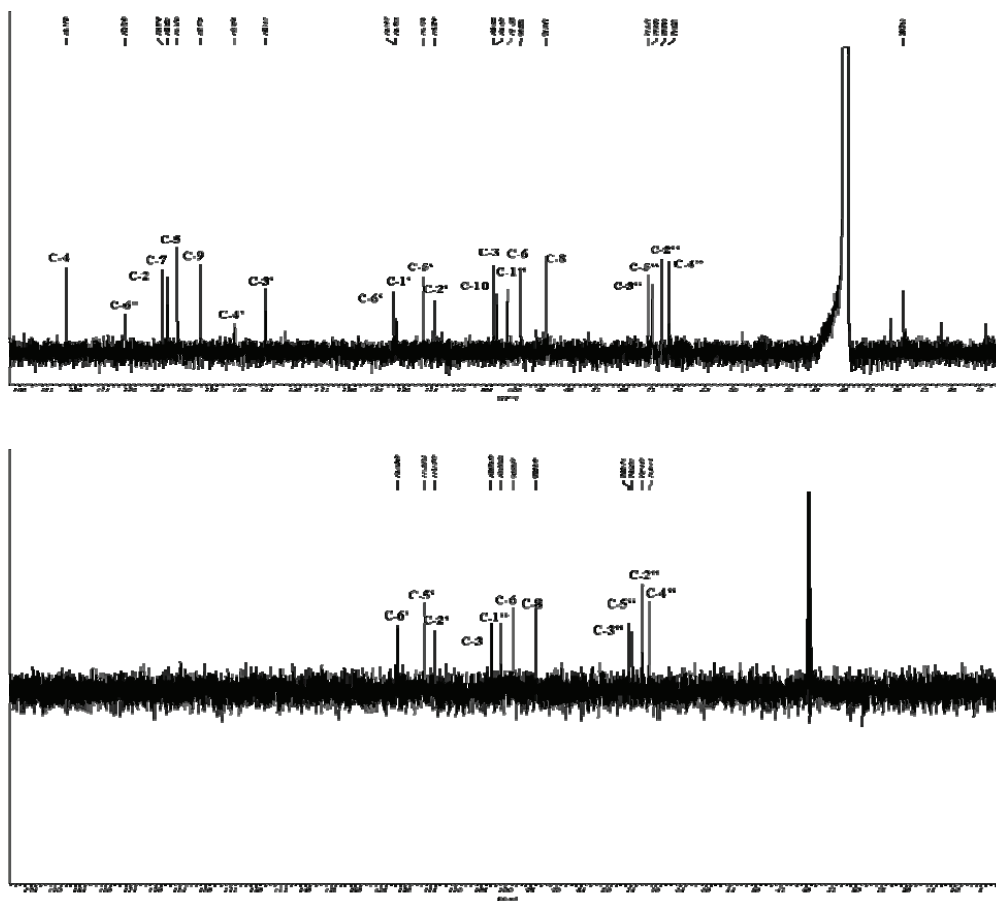


Attachment 59. ^1H NMR spectrum of luteolin 3'-O-glucuronide (47).

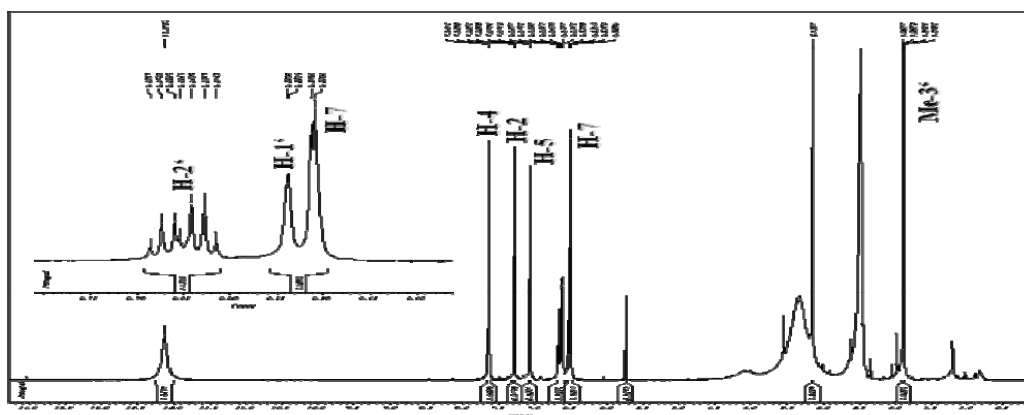


Attachments

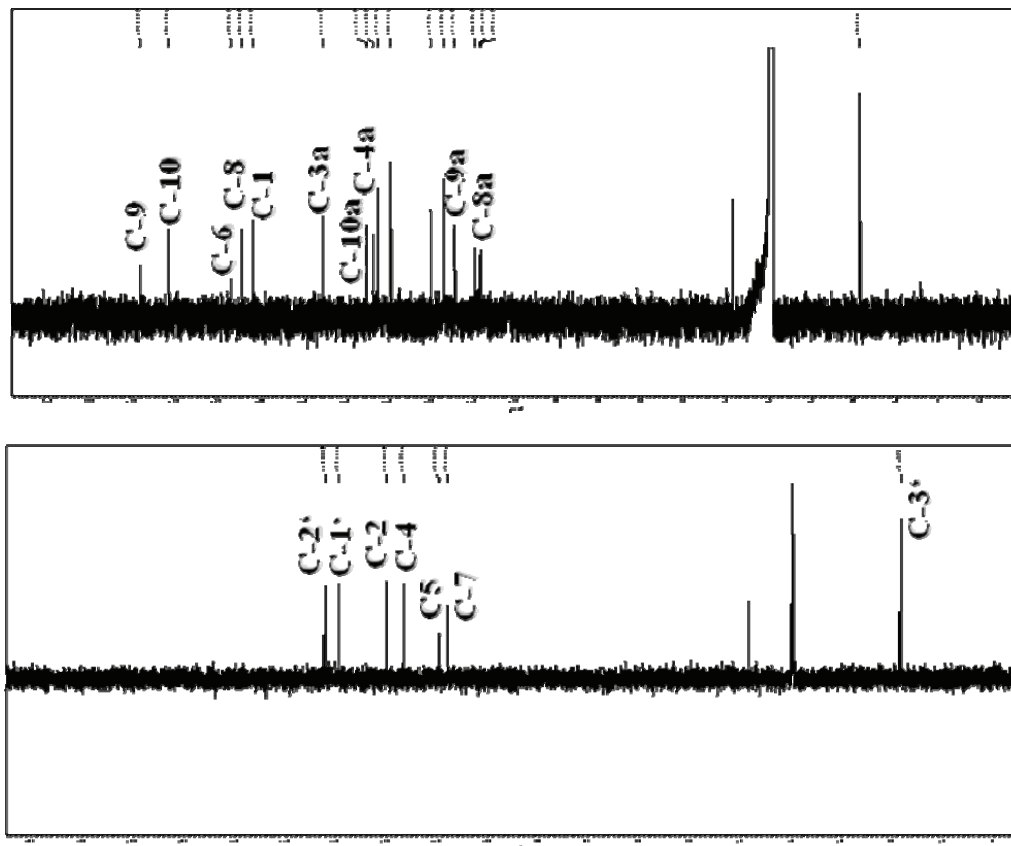
Attachment 60. ^{13}C NMR and DEPT spectra of luteolin 3'-*O*-glucuronide (47).



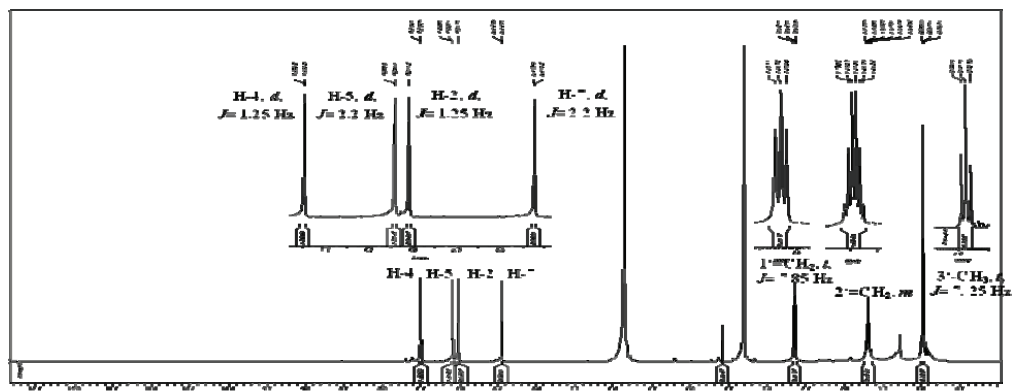
Attachment 61. ^1H NMR spectrum of 1'-deoxyrhodoptilometrene (48).



Attachment 62. ^{13}C NMR and DEPT spectra of 1'-deoxyrhodoptilometrene (48).

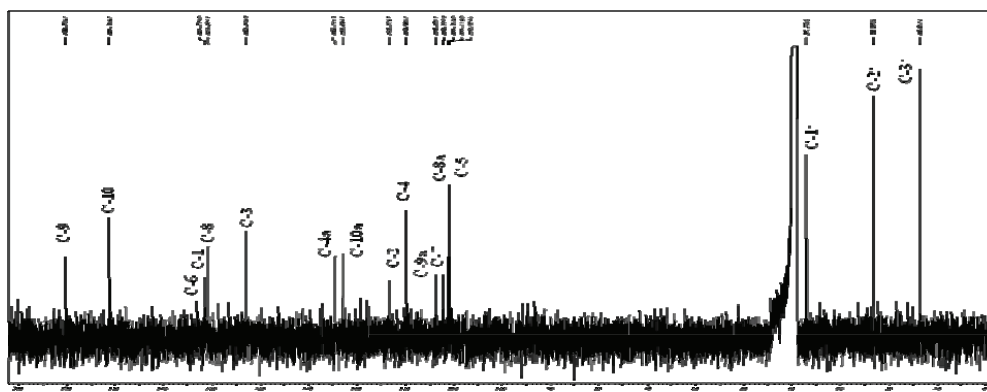


Attachment 63. ^1H NMR spectrum of 1'-deoxyrhodoptilometrin (49).

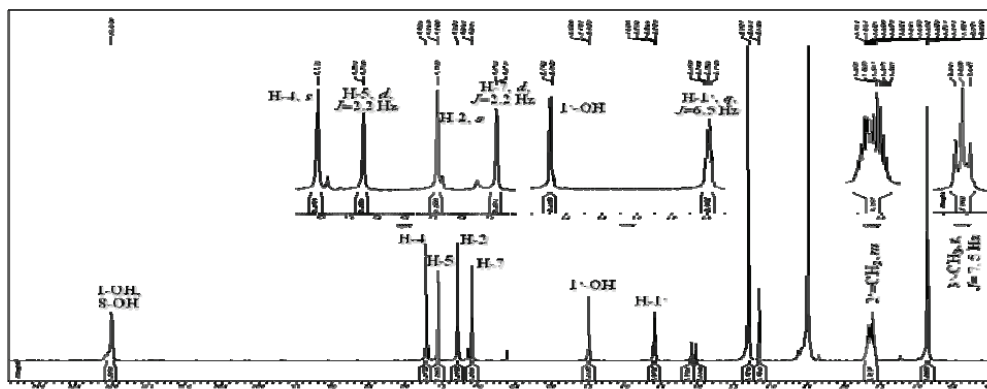


Attachments

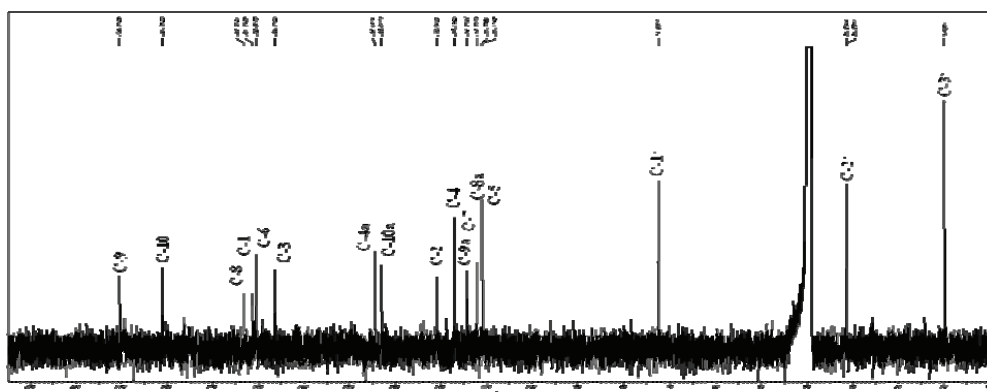
Attachment 68. ^{13}C NMR spectrum of 1'-deoxyrhodoptilometrin-6-*O*-sulfate (51).



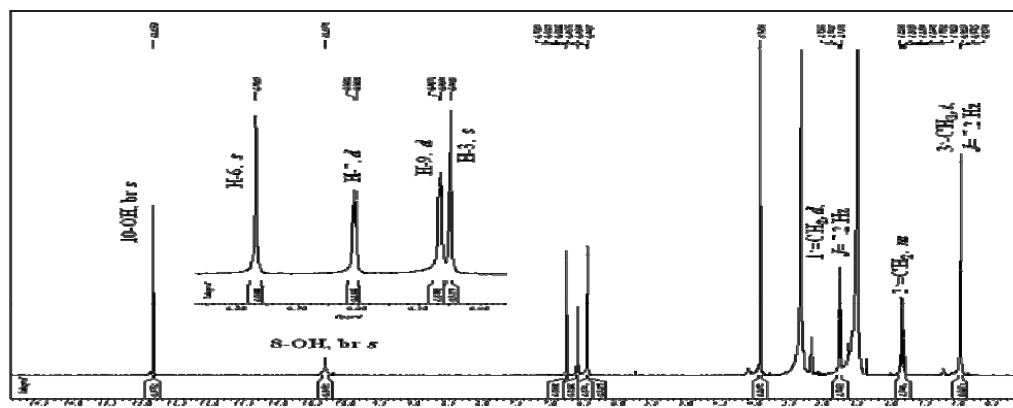
Attachment 69. ^1H NMR spectrum of (*S*)-(-)-rhodoptilometrin-6-*O*-sulfate (52).



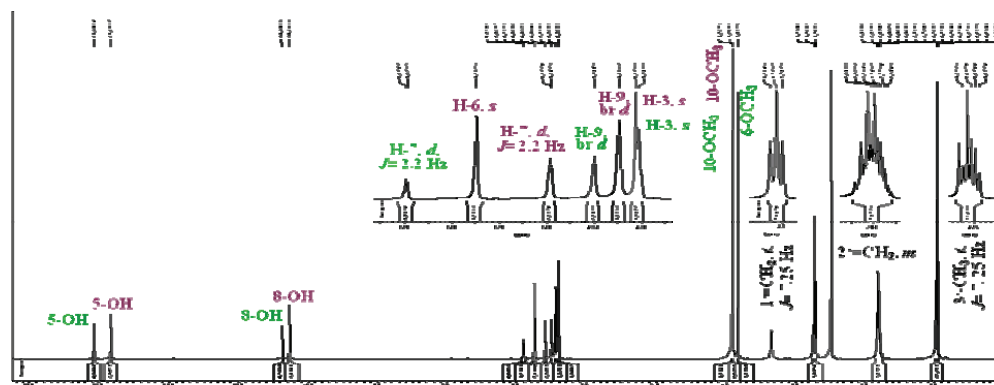
Attachment 70. ^{13}C NMR spectrum of (*S*)-(-)-rhodoptilometrin-6-*O*-sulfate (52).



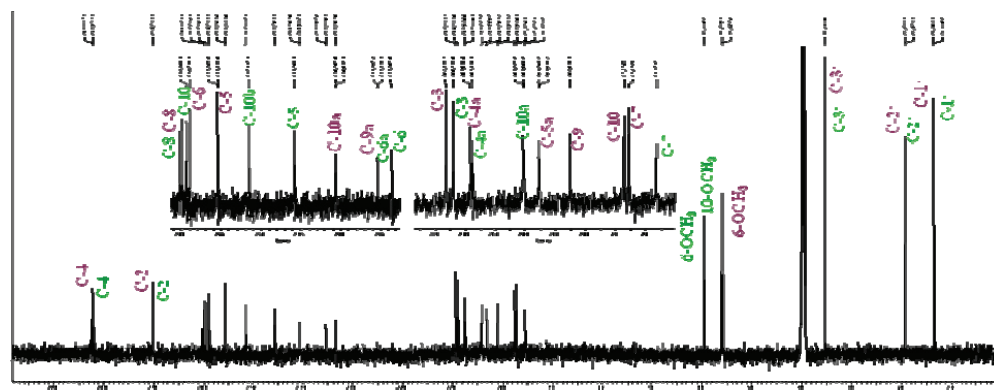
Attachment 71. ^1H NMR spectrum of comaparvin (53).



Attachment 72. ^1H NMR spectrum of comaparvin (53) / 6-methoxycomaparvin (54).

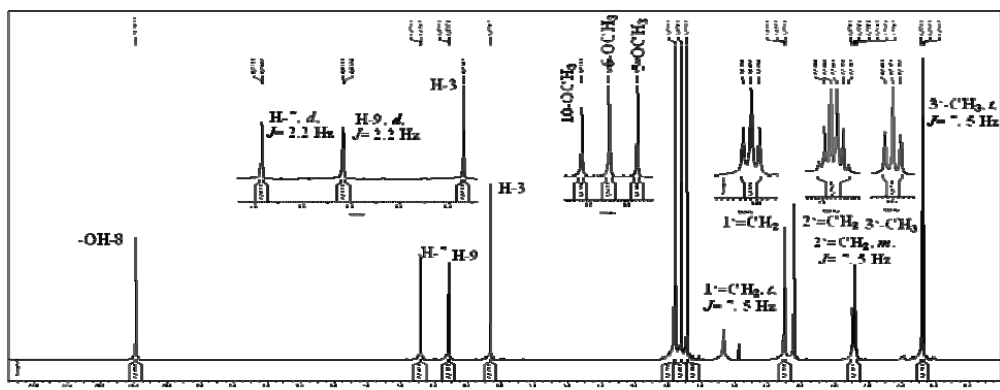


Attachment 73. ^{13}C NMR spectrum of comaparvin (53) / 6-methoxycomaparvin (54).

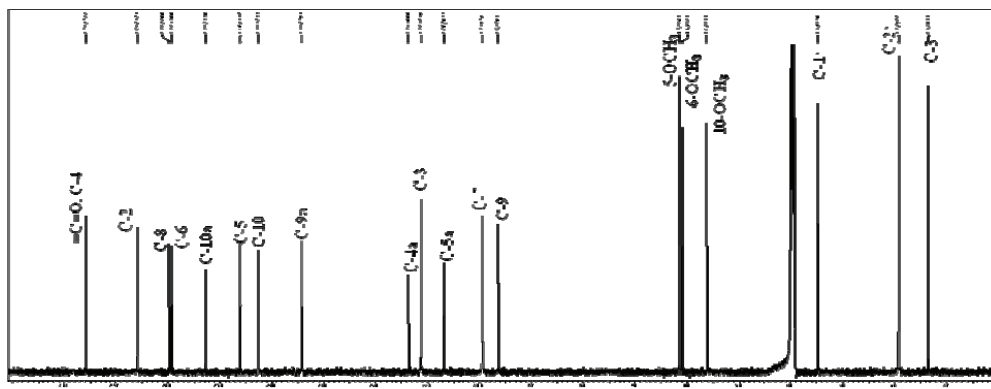


Attachments

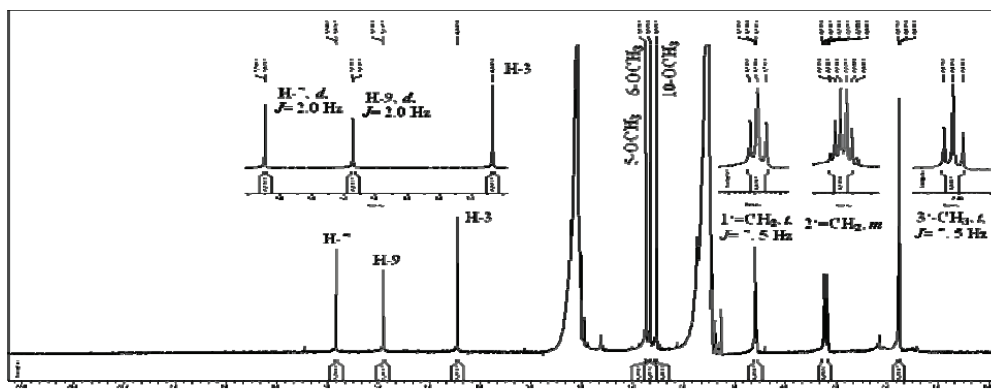
Attachment 74. ^1H NMR spectrum of 6-methoxycomaparvin-5-methyl ether (55).



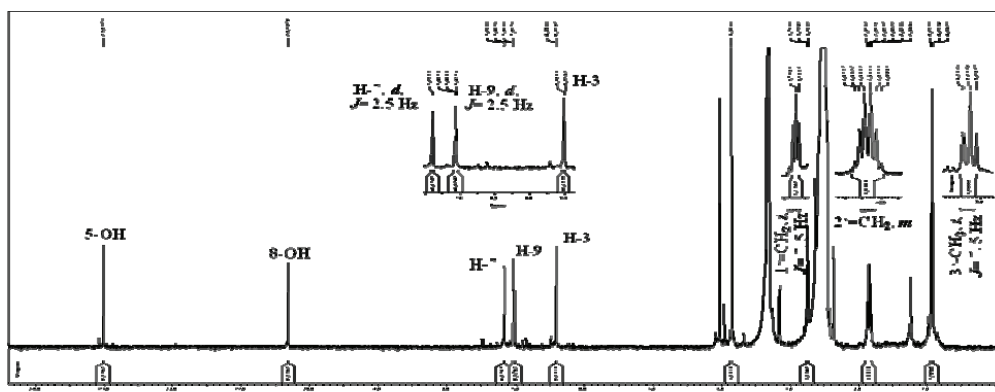
Attachment 75. ^{13}C NMR spectrum of 6-methoxycomaparvin-5-methyl ether (55).



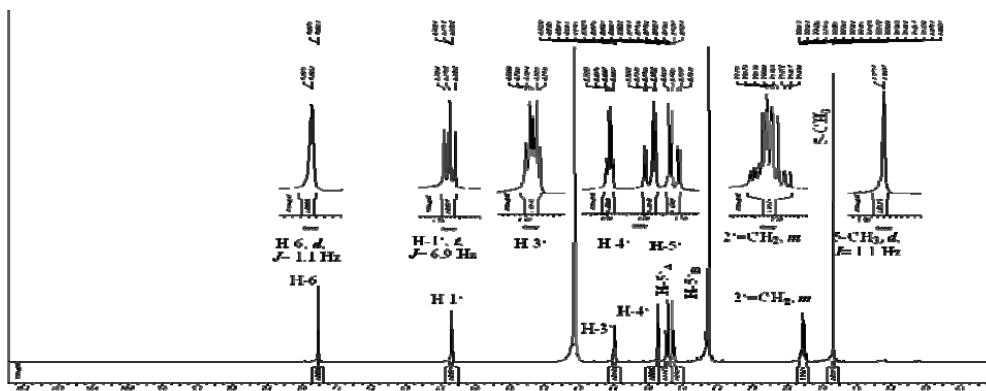
Attachment 76. ^1H NMR spectrum of 6-methoxycomaparvin-5-methyl ether-8-O-sulfate (56).



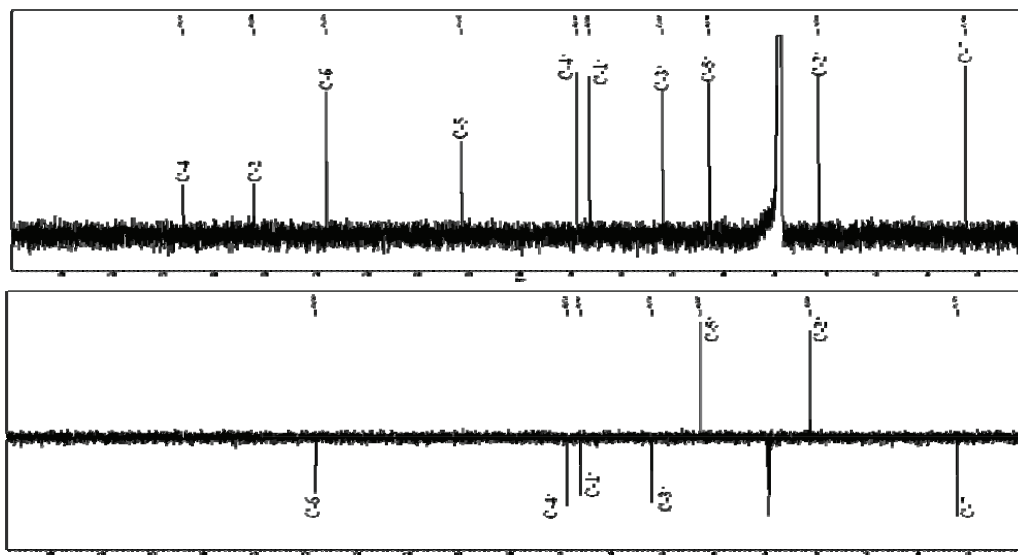
Attachment 77. ^1H NMR spectrum of 6-hydroxycomaparvin-8-*O*-sulfate (57).



Attachment 78. ^1H NMR spectrum of 2'-deoxythymidine (58).



Attachment 79. ^{13}C NMR and DEPT spectra of 2'-deoxythymidine (58).



Resume

Resume

Name: Sherif Saeed Ebada Elsayed
Date of birth: September 1st, 1978 in Cairo, Egypt.
Nationality: Egyptian.
Work address: Institut für Pharmazeutische Biologie und Biotechnologie,
Universitätsstrasse 1, Geb. 26.23, D-40225, Düsseldorf, Deutschland
Tel.: 0049-211-81-14187, Fax.: 0049-211-81-11923
Permanent address: Department of Pharmacognosy and Phytochemistry, Faculty of
Pharmacy, Ain-Shams University, Organization of African Unity
Street 1, 11566, Cairo, Egypt. E-mail: sss3ebada@yahoo.com

Education Course:

- Predocotoral studies at Institute of Pharmaceutical Biology and Biotechnology, Heinrich-Heine University, Duesseldorf, Germany, since January, 2007.
- Receiving the M.Sc. degree in Pharmaceutical Sciences (Pharmacognosy and Phytochemistry) at Department of Pharmacognosy, Faculty of Pharmacy, Ain-Shams University, Cairo, Egypt, in May, 2006. The research project was entitled "Phytochemical and Biological study on *Peltophorum africanum* Sond., family Fabaceae".
- Premaster studies at Department of Pharmacognosy, Faculty of Pharmacy, Ain-Shams University, Cairo, Egypt, since April, 2002.
- General and special preparatory courses of the M. Sc. in Pharmaceutical Sciences (Pharmacognosy) at Faculty of Pharmacy, Ain-Shams University, Cairo, Egypt, grade distinction, in 2001.
- Receiving the Bachelor degree in Pharmaceutical Sciences at Faculty of pharmacy, Ain-Shams University, Cairo, Egypt, in May, 2000.
- Graduate study in Pharmaceutical Sciences at Faculty of Pharmacy, Ain-Shams University, Cairo, Egypt, since Septemtber, 1995.
- Graduating in Al-Tawfikia Secondary School, Cairo, Egypt, in May, 1995.

Scientific Experience:

- Ph.D. student at the Institute of Pharmaceutical Biology and Biotechnology, Heinrich-Heine University, Duesseldorf, Germany, since January, 2007.

- Assistant lecturer at Department of Pharmacognosy, Faculty of Pharmacy, Ain-Shams University, Cairo, Egypt, from 2006–2007.
- Supervising and teaching the graduate practical courses of pharmacognosy and Phytochemistry for 3rd–7th semester students at Department of Pharmacognosy, Faculty of Pharmacy, Ain-Shams University, Cairo, Egypt, from 2004–2006.
- Supervising and teaching the graduate practical courses of Pharmacognosy and Phytochemistry for 4th–6th semester students at Department of Natural Products and Alternative Medicine, Faculty of Pharmacy, King AbdulAziz University, Jeddah, Saudi Arabia, from 2003–2004.
- Teaching Assistant at Department of Natural Products and Alternative Medicine, Faculty of Pharmacy, King AbdulAziz University, Jeddah, Saudi Arabia, from 2003–2004.
- Demonstrator at Department of Pharmacognosy, Faculty of Pharmacy, Ain-Shams University, Cairo, Egypt, in October, 2000.

Publications

- 1) Ebada S.S., Proksch P. (2010). Marine organisms and their prospective use in therapy of human diseases. In Melhorn, H. (ed) Nature helps... (Springer Verlag) (*Submitted*)
- 2) Ebada S.S., Proksch P. (2010). Chemistry and biology of guanidine alkaloids from marine invertebrates. *MiniRev. Med. Chem.* (*Submitted*).
- 3) Ebada S.S., Duong T.N., Li-Weber M., Proksch P. Chemistry and biology of rocaglamides (= flavaglines) and related derivatives from *Aglaia* species (Meliaceae). In Falk H. (ed) Progress Chem. Org. Nat. Prod. (Springer Verlag) (*Submitted*).
- 4) Ebada S.S., Proksch P. Chemistry of marine sponges–Alkaloids, peptides, and terpenoids. In Taglialatela-Scafati O., Fattorusso, E. (ed) Marine Natural Products (Springer Verlag) (*Accepted*).
- 5) Chovolou Y., Ebada S.S., Wätjen W., Proksch P. (2010). Angular naphthopyrones from the Philippine echinoderm *Comanthus* sp. inhibit TNF-alpha-induced NF-κB activation. *Eur. J. Pharmacol.* (*Accepted*).
- 6) Xu J., Ebada S.S., Proksch P. (2010). *Pestalotiopsis* a highly creative genus: chemistry and bioactivity of secondary metabolites. *Fungal Diversity*, **44**, 15–31.
- 7) Ebada S.S., Lin W., Proksch P. (2010). Bioactive sesterterpenes and triterpenes from marine sponges: occurrence and pharmacological significance. *Mar. Drugs.*, **8**, 313–346.

Resume

- 8) Ebada S.S., Wray V., de Voogd N.J., Deng Z., Lin W., Proksch P. (2009). Two new jaspamide derivatives from the marine sponge *Jaspis splendens*. *Mar. Drugs.*, **7**, 435–444.
- 9) Orfali S.S., Ebada S.S., El-Shafae A.M., Al-Taweel A.M., Lin W.H., Wray V., Proksch P. (2009). 3-*O*-*trans*-Caffeoylisomyricadiol: A new triterpenoid from *Tamarix nilotica* growing in Saudi Arabia. *Z. Naturforsch.*, **64c**, 637–643.
- 10) Ebada S.S., Edrada-Ebel R.A., de Voogd N.J., Wray V., Proksch P. (2009). Dibromopyrrole alkaloids from the Marine Sponge *Acanthostylorella* sp. *Nat. Prod. Comm.*, **4**, 47–52.
- 11) Ebada S.S., Edrada-Ebel R.A., Lin W., Proksch P. (2008). Methods for isolation, purification and structural elucidation of bioactive secondary metabolites from marine invertebrates. *Nat. Protcols*, **3**, 1820–1831.
- 12) Ebada S.S., Ayoub N.A., Singab A.B., Al-Azizi M.A. (2008). Phytophenolics from *Peltophorum africanum* Sond. (Fabaceae) with promising hepatoprotective activity. *Pharm. Mag.*, **4**, 286–292.

Conferences

- 1) Ebada S.S., Chovolou Y., Wätjen W., Wray V., Edrada-Ebel R.A., Kubbutat M.H.G., Proksch P. (2010). Protein kinase inhibiting anthraquinones and NF- κ B inhibiting naphthopyrones from the Phillipine echinoderm *Comanthus* sp. *Planta Medica*, **76**. Poster presentation at the 58th international congress and annual meeting of the society for medicinal plants and natural product research, August 16th–September 2nd, Berlin, Germany.
- 2) Ebada S.S., de Voogd N.J., Müller W.E.G., Meijer L., Proksch P. (2010). Kinase inhibiting bromopyrrole alkaloids from the Indonesian sponge *Stylissa massa*. *Planta Medica*, **76**. Poster presentation at the 58th international congress and annual meeting of the society for medicinal plants and natural product research, August 16th–September 2nd, Berlin, Germany.
- 3) Ebada S.S., Lin W., de Voogd N., Proksch P. (2009). New jaspamide derivatives from the marine sponge *Jaspis* sp. *Planta Medica*, **75**. Poster presentation at the 57th international congress and annual meeting of the society for medicinal plants and natural product research, August 16th–20th, Geneva, Switzerland.
- 4) Ebada S.S., Wray V., Edrada-Ebel R.A., Proksch P. (2009). Anthraquinones and naphthopyrones from the marine echinoderm *Comanthus* sp. *Planta Medica*, **75**. Poster presentation at the 57th international congress and annual meeting of the society for medicinal plants and natural product research, August 16th–20th, Geneva, Switzerland.